Th-PM-D7

A CALORIMETRIC STUDY OF LINKAGE IN SPECIFIC PROTEIN-DNA INTERACTIONS. ((Knut Langsetmo and Robert T. Sauer)) Dept. of Biology, MIT, Cambridge, MA 02139. (Spon. by Peter Kim)

Two aspects of linkage are addressed. The energetic contribution of a hydrogen bond network in λ repressor N-terminal domain to binding of O_L1 was examined using thermodynamic 'mutant cycles'. The contribution of N-terminal domain dimerization to binding was also assessed.

Binding of λ repressor N-terminal domain was examined by calorimetric titration with the synthetic O_L1 operator. At 28 °C the total binding reaction is enthalpy driven, with a slightly unfavorable entropy. The co-crystal structure of N-terminal domain and O_L1 shows a hydrogen bonding network between residues Q33, Q44, and the phosphate and base of adenine 2 of the operator. Mutation of either Q33 or Q44 to alanine results in a less favorable binding enthalpy. Changes in binding energetics resulting from mutation of both of these residues are not additive, but rather linked, indicating an interaction between these residues

The overall reaction includes a dimerization component. At 28 °C dimerization is entropy driven. The thermodynamic parameters for the binding component of the reaction were determined by subtracting the values obtained in the dimerization experiments from the results for the total binding reaction.

Both the total reaction and dimerization are strongly temperature dependent. This indicates hydrophobic interactions are important in both dimerization and specific protein-DNA binding.

Th-PM-D8

CHROMATIN NUCLEOPROTEIN POLYMERASE COMPLEXES CONTAINING ONCOGENES AND SUPPRESSER GENES: THEIR POTENTIAL REGULATORY CONTRIBUTION TO METASTASIS ((Nancy L. Rosenberg-Nicolson and Garth L. Nicolson)) Rhodon Foundation for Biomedical Research and The University of Texas M. D. Anderson Cancer Center, Houston, TX 77030. (Spons. by G. Nicolson)

Intact nuclei from metastatic variants of the murine RAW117 large-cell lymphoma cell line were subjected to direct digestion with *Msp*-I by a previously described method designed to fractionate the nucleus into ~6 Nucleoprotein (NP) fractions containing specific polymerase-containing NP complexes. Individual NP constituents of the *Msp*-I-derived subnuclear complexes were purified by two-dimensional isofocusing reducing SDS-polyacrylamide electrophoresis followed by gel excision, electroelution, and removal of SDS by extractigel chromotography. The purified NPs were either dot- or slot-blotted onto a solid support and screened for the presence of a panel of genes (*p53*, *abl*, β-casein, μ chain immunoglobulin, etc.) by hybridization. Analyses were performed on NPs obtained from metastatic variant lines of RAW117. Reproducible differences in NP distribution in the SDS gels and presence of tightly bound genes were noted amongst the metastatic variants, particularly in the presence of *p53* and *abl* genes. We speculate that a specific chromatin NP-gene organization exists in metastatic RAW117 cells. Supported by NCI grant CA44352 to G.L.N.

Th-PM-D9

ZUOTIN, A YEAST Z-DNA BINDING PROTEIN, MAY BE INVOLVED IN DNA REPAIR. ((A. Yu, S. Zhang, Y. Xing, A. Rich, and M. Mitas)) Dept. of Biochemistry and Molecular Biology, 246 Noble Research Center, Oklahoma State University, Stillwater, OK. 74078. Dept. of Biology, Massachusetts Institute of Technology, Cambridge, MA 02139. (Spon. by A. Rich).

ZUO1 encodes a putative yeast Z-DNA binding protein, named Zuotin. In order to understand better the function of Zuotin, and the function of the DNA to which it binds, we constructed a yeast cell line (LNZ14) containing a deletion in the Zuotin gene. Absorbance studies indicated that the wild-type yeast cells grew twice as fast as LNZ14 in rich liquid medium. The ratios of single cells:budding cells in wild-type and LNZ14 were 1:1.1 and 1:1.9, respectively, suggesting that LNZ14 remained longer at the unsegregated phase. These observations suggest that *ZUO1* might be important in maintaining some of the normal events in the yeast cell cycle. To determine whether a mechanism involving DNA repair might be responsible for the differences observed between wild-type yeast and LNZ14 cells, both were subjected to varying doses of mutagenic agents, and the numbers of surviving colonies were determined. The number of LNZ14 cells that survived exposure to low concentrations of *N*-methyl-*N'*-nitro-*N*-nitrosoguanidine (MNNG), *N*-methyl-*N*-nitrosourea (NMU), 4-nitro N-oxide (4NQO), or dimethyl sulfate (DMS), were 1.3 to 13-fold reduced with respect to wild-type cells. However, no differences in survival between the two cell lines were observed in response to various doses of UV irradiation. These data indicate that the yeast Z-DNA binding protein Zoutin may be involved in DNA repair, possibly in DNA base excision repair.

Th-PM-D10

A DIRECT MEASURE OF THE CONTRIBUTION OF SOLVATION TO THE THERMODYNAMICS OF BINDING. (M. C. Chervenak and E. J. Toone*, Department of Chemistry, Duke University, Durham, NC 27708-0346)

The nature of the forces contributing to ligand binding in aqueous solution is still obscure. We have calorimetrically evaluated the thermodynamics of binding of a variety of systems, including protein-carbohydrate, protein-nucleoside, and small molecule-small molecule interactions in both light and heavy water. In each case, the enthalpy of binding was less negative in D_2O than in H_2O, with a compensating change in entropy. For the systems evaluated, the change in molar heat capacity on binding was not affected by solvent isotopic substitution. A plot of the difference in enthalpy between light and heavy water processes, $\Delta\Delta H$, against ΔC_p gives a straight line that passes through the origin with a slope of 5°. We interpret these results in terms of solvent reorganization during binding. We have used a thermodynamic cycle to estimate the magnitude of the contribution of solvent reorganization to the net ethalpy of binding. Our analysis shows 4-18 kcal mol^{-1} of binding enthalpy, representing 25-100% of the total, can be accounted for by the return of water surrounding solutes to bulk solvent during binding.

HEME PROTEINS II

Th-Pos1

PRESSURE MODULATION PERTURBATION OF PROTEIN MOTIONS ((R.M. Ernst, R. Philipp, G.U. Nienhaus, R. Noble, R.D. Young, H. Frauenfelder)) Department of Physics, University of Illinois, 1110 W. Green St., Urbana, IL 61801.

We present results which show that it is possible to couple to functionally important motions of proteins with the application of time-dependent pressure. This pressure modulation technique consists of monitoring the transient visible absorption of the protein while applying isotropic pressure with amplitudes of up to 10 atm at frequencies from 2 Hz to 2 kHz. We have studied sperm whale myoglobin and carp hemoglobin in both the R and T states, and find that pressure modulation dramatically increases the rate at which the CO ligand passes from the protein interior to the solvent for both the myoglobin and T state samples. These results suggest that the myoglobin and T state proteins are more susceptible than the R state hemoglobin to motions induced by the oscillating pressure; this is consistent with a relaxation model of rebinding in these proteins. The pressure modulation technique presents a new method of probing the correlation between protein motions and function, which is key to understanding the structure/function relationship in proteins. (This work supported by the NIH and the ONR.)

Th-Pos2

HEME RELAXATION MODEL OF PROTEIN REBINDING ((Y. Abadan, K. Chu, R.M. Ernst, R. Philipp, G.U. Nienhaus, R. Noble, R.D. Young, H. Frauenfelder)) Department of Physics, University of Illinois 1110 W. Green St., Urbana, IL 61801.

We discuss a model of ligand binding to heme proteins in which the reaction rate is controlled by the heme out-of-plane distance. To support this model, we present IR absorption and visible flash photolysis data from carp R and T state hemoglobin and sperm whale myoglobin. The IR measurements probe the structure of the heme group, while flash photolysis reveals the rebinding function of the protein; the two techniques yield results consistent with a model in which the heme relaxes in discrete steps following ligand dissociation. Ligand concentration studies using flash photolysis, and a novel pressure modulation perturbation method further indicate that the T state matrix is more susceptible than the R state to motions that enable the heme to relax. (This work supported by the NIH.)

Th-Pos3

STRUCTURAL HETEROGENEITY AND GLASSY BEHAVIOR OF PROTEINS ((K. Chu, H. Frauenfelder, G.U. Nienhaus, R. Philipp and R.D. Young)) Department of Physics, University of Illinois, 1110 W. Green St., Urbana, IL 61801.

The infrared CO stretch frequencies of carbonmonoxymyoglobin provide some of the strongest evidence for the hierarchy of conformational substates (CS). The *A* bands ($\approx$1950 cm^{-1}) indicate the existence of three taxonomic substates (CS0), and a multitude of substates within each CS0, called CS1. We use temperature derivative spectroscopy and isothermal kinetics with an FTIR spectrometer to probe the effects of cooling rate on recombination following photolysis. Quickly (cooling rate $\approx$100 K/sec) and slowly (cooling rate $\approx$0.03 K/sec) frozen samples reveal that large changes occur among the CS0, and the CS1 remain relatively unperturbed when the cooling rate is varied by more than four orders of magnitude. The *A* band populations are different because fluctuations between CS0 are frozen out earlier by the cooling-rate dependent glass transition temperature, T_g. The rebinding enthalpy distributions within each individual *A* band remain relatively unchanged.

Th-Pos4

INFRARED STUDIES OF PROXIMAL-SIDE MUTANTS OF MYGLOBIN. ((Y. Abadan, K. Chu, E. Chien, H. Frauenfelder, G. U. Nienhaus, S. G. Sligar and R. D. Young)) Departments of Physics, Biophysics and Chemistry, University of Illinois at Urbana-Champaign (Spon. by NIH)

In recent years, the influence of specific amino acid residues on ligand binding to heme proteins has been investigated through the use of site-directed mutagenesis. These studies have concentrated on residues on the distal side. Since much of the control of ligand binding comes from the proximal side, we studied the proximal mutants H97F and L89I of swMbCO. Temperature derivative spectroscopy (TDS) of the CO stretch bands was used to obtain spectroscopic and kinetic information on the CO binding reaction at temperatures below 160K. The pH dependence of the relative populations of the A substates in these mutants is similar to the wild type, confirming that His E7 predominantly determines the substate ratios. The enthalpy distributions within the A substates are known to be modified by extended illumination, an effect we call light-induced relaxation. The barrier distributions of proximal mutants differ markedly from native sperm whale MbCO upon extended illumination. This result shows that the conformational energy landscape is changed significantly by the alterations on the proximal side and points to a crucial involvement of proximal residues in the control of ligand binding.

Th-Pos5

HEME COORDINATION AND STRUCTURE OF THE CATALYTIC SITE IN NITRIC OXIDE SYNTHASE ((Jianling Wang*, Dennis J. Stuehr#$, Mesao Ikeda-Saito$, and Denis L. Rousseau*)) *AT&T Bell Laboratories, Murray Hill, NJ 07974; #The Cleveland Clinic, Cleveland, OH 44195; $ Case Western Reserve Univ., Cleveland, OH 44106.

Resonance Raman spectra of the resting, reduced, CO- and NO-bound forms of nitric oxide synthase(NOS) have been obtained and found to be consistent with those of the P-450 class of enzymes. Ferric NOS has a five-coordinate high-spin heme indicating that the sixth ligand binding site on the heme is restricted by steric or hydrophobic interactions. The electron density marker ν_4 for NOS(+2) is located at 1347 cm^{-1} characteristic of a thiolate axial ligand on the heme. In the CO-bound enzyme, $\nu_{Fe\text{-}CO}$ is broad and may be resolved into two components of equal intensity, suggesting either heterogeneous interactions in the heme pocket or a different environment for each heme within the two subunits. Addition of arginine shifts both components of $\nu_{Fe\text{-}CO}$ up by 17cm^{-1}. NO reversibly binds to the ferric and ferrous forms of the enzyme ($\nu_{Fe\text{-}NO}$ at 540 and 550cm^{-1}, respectively). In the absence of biopterin, the protein becomes unstable, showing a mixture of different spin states in the ferric and ferrous forms and exchanging the thiolate ligand to hisidine in the CO form, typical of the P-420 derivatives.

Th-Pos6

INTERACTIONS OF PARTIALLY DEOXYGENATED MYOGLOBIN WITH ISOLATED CARDIAC MITOCHONDRIA. ((J.B. Wittenberg)) Department of Physiology and Biophysics, Albert Einstein College of Medicine, Bronx, N. Y. 10461.

Myoglobin (Mb), at the oxygen Pressure (near 2 torr) prevailing in myocytes of the working heart, interacts with isolated cardiac mitochondria to restore the oxygen-limited rate (43% of maximal) of tightly coupled oxidative phosphorylation to the rate achieved when oxygen pressure is not limiting. The effect is maximal at 200 μM Mb and large at 10 μM, showing that it may not be attributed to Mb-facilitated oxygen diffusion, which is negligible at 10μM and increases with Mb concentration to 7000μM. It may be identified with Mb-mediated oxidative phosphorylation (MMOP;Proc. Natl. Acad. Sci. 84, 7503-7507, 1987), a process hitherto demonstrated only in isolated ventricular myocytes, in which Mb-ligated oxygen supports oxidative phosphorylation independent of dissolved oxygen. Partially oxygenated myoglobin, preincubated with isolated cardiac mitochondria, causes the mitochondria, after an induction period, to increase their internally controlled rate of oxidative phosphorylation from a low value to the rate achieved when oxygen pressure is not limiting. This implies regulation of the rate of mitochondrial oxidative phosphorylation by the fractional oxygenation of sarcoplasmic myoglobin.

Th-Pos7

CONTINUED STUDIES OF THE SPECTRAL AND PHYSICAL PROPERTIES OF COHBA DISSOLVED IN THE SOLVENT DMSO. **((Kim K.S. Burnham, Bryan S. Wicks, Eric W. Findsen)) Department of Chemistry, The University of Toledo, Toledo, OH 43606**

The results of studies of stability and photolytic behavior of COHbA in the solvent dimethyl sulfoxide will be presented. A previous report presented results of the study of the solubilization of lyophilized COHbA in the organic solvent DMSO. Resonance Raman studies show that within ~30 ps of excitation the CO ligand is lost and that the Raman spectrum is very similar to that observed with 10 ns pulse width excitation. Results of time-resolved studies from 50 to 2000 ps will also be presented.

Results of protein stability studies where the mole fraction of water is varied and the spectral parameters of the heme are monitored will also be presented. The protein appears most stable in pure water and pure DMSO, and is increasingly destabilized as the mole fractions approach 0.5.

Th-Pos8

REACTION OF NITROBLUE-TETRAZOLIUM WITH HEMOGLOBIN. ((O. Abugo and J.M. Rifkind))NIH/NIA Gerontology Research Center, Baltimore, Maryland 21224.

The reduction of nitroblue tetrazolium (NBT) by superoxide has been used to quantitate superoxide production. We have found that in the presence of hemoglobin there is also a direct NBT reaction with hemoglobin. At low oxygen pressure both oxidation of hemoglobin and the reduction of NBT are spectroscopically observed. However, at high pO_2 the one electron reduced NBT is reoxidized by oxygen and very little NBT reduction is observed. A comparison of hemoglobin oxidation with and without NBT does, however, indicate that oxyhemoglobin also reacts with NBT. For both oxyhemoglobin and deoxyhemoglobin an analysis of the kinetics for both the oxidation of hemoglobin and the reduction of NBT indicate a two-step reaction. The one electron reduction of NBT to the NBT· radical is readily reversible. This reaction is followed by the oxidation of a second heme with the formation of the two electron reduced monoformazan. The overall enhancement of hemoglobin oxidation is similar for both oxyhemoglobin and deoxyhemoglobin, although the rate for the first step in the oxidation process is much faster for deoxyhemoglobin than oxyhemoglobin. The binding of deoxyhemoglobin to the erythrocyte membrane produces a dramatic enhancement of the reaction. This phenomenon is associated with a local increase in the reactants on the membrane surface caused by the interactions of both NBT and deoxyhemoglobin with the membrane. These studies indicate that the reduction of NBT by heme containing proteins needs to be considered in any attempt to use NBT to quantitate superoxide production.

Th-Pos9

FUNCTIONAL CHARACTERIZATIONS OF A POLYMERIZED, CROSS-LINKED HUMAN HEMOGLOBIN. ((M.S. Rogers, B.A. Brockner-Ryan and A.I. Alayash)) Center for Biologics Evaluation and Research, Food and Drug Administration, Bethesda, MD 20892.

Polyethylene glycol-based polymerization of diaspirin cross-linked hemoglobin (DCLHb), an oxygen-carrying red-cell substitute, offers the benefits of reduced renal clearance and increased retention in the vascular circulation. Oxygen equilibrium curves for Poly-DCLHb were slightly left shifted from those of DCLHb with a P50 of 20 mmHg at pH 7.4 and 37°C, a diminished coopretivity (Hill coefficient n =1.7) and a reduced Bohr effect. In rapid mixing experiments (oxygen dissociation and carbon monoxide combination), Poly-DCLHb exhibited a several fold increase in the overall rate of deoxygenation and carbon monoxide binding kinetics over its cross-linked counterpart. Nitric oxide binding to the oxidized forms of modified and unmodified hemoglobin (HbA_0) is biphasic, due to the differing reactivities of the α and β subunits. The binding of NO occurred at faster rates for the modified hemoglobins. Both proteins exhibited similar propensity for autoxidation and oxidative damage by hydrogen peroxide. The functional and redox properties of Poly-DCLHb are qualitatively similar to those of DCLHb. The reduced Bohr effect can be accounted for on the basis of the blockage of the Bohr residues of DCLHb as result of the polymerization process.

Th-Pos10

ROLE OF MONOVALENT/DIVALENT CATIONS ON MULTIMERIC LUMBRICUS HEMOGLOBIN STABILIZATION. ((John P. Harrington)) Department of Chemistry, University of South Alabama, Mobile, Al. 36688.

The large extracellular hemoglobin($3.8x10^6$ Da) isolated from the earthworm, Lumbricus terrestris, has been shown from scanning electron microscopy to form a bilayered hexagonal structure incorporating linker chains for structural integrity (Kapp et al,1987). This hemoglobin has been shown to be constructed of more than 200 globin chains with a subunit stoichiometry of $24(abcd)_2$ chains and 24 linker chains with hemes on chains a,b,c,d, and on one linker chain(Ownby et al,1993). At the functional level, the role of monovalent and divalent cations have been implicated in regulating oxygen binding by this protein. M^{+2} ions were found to exhibit a larger effect on oxygen binding than the M^{+1} ions(Fushitani et al,1986). These effects are partially dependent on ionic radius rather than on ionic strength. To further explore the role of M^{+2} and M^{+1} ions on the structure-function relationships operative in this hemoglobin, studies of the effect of M^{+2} and M^{+1} ions on the rates of autoxidation, resistance to thermal unfolding, and the conversion of the metHb form to the hemichrome state have been carried out. Initial results indicate that 1)M^{+2} ions decrease the rate of autoxidation of LtHb more than M^{+1} ions at pH 7; 2) the order of effectiveness at 25 mM in decreasing the rate of autoxidation is $Ba^{+2} = Ca^{+2}$, Sr^{+2}, and Mg^{+2}; 3)resistance to thermal unfolding(25-65°C) is increased in the presence of Ca^{+2} and Ba^{+2}; 4)M^{+1} ions at higher temperatures (>55°C) enhance thermal unfolding; and 5)reduced hemichrome formation was evident in the presence of Ba^{+2} or Ca^{+2}. Increased effectiveness of Ca^{+2} in reducing autoxidation, increasing resistance to thermal unfolding, and stabilizing the metHb state is consistent with other reports showing Ca^{+2} at low concentration prevents subunit dissociation of this molecule.

Th-Pos11

FLUORESCENCE LINE NARROWING SPECTROSCOPY EMPLOYED TO STUDY THE CONFORMATIONS OF α AND β CHAINS IN HEMOGLOBIN. ((K. Sudhakar, S. Loe, T. Yonetani, and J. M. Vanderkooi)) Dept. of Biochemistry & Biophysics, School of Medicine, University of Pennsylvania, Philadelphia, PA 19104. (Spon. by J. M. Vanderkooi).

Conformational stabilities of protoporphyrin-protoheme hybrid hemoglobins (Hb), in which the protoheme (Fe) in either or both the α- or β - subunits were substituted with protoporphyrin IX (P) (i.e., $\alpha(P)_2\beta(Fe)_2$, $\alpha(Fe)_2\beta(P)_2$ and $\alpha(P)_2\beta(P)_2$), have been investigated by fluorescence, phosphorescence and fluorescence line narrowing (FLN) spectroscopy. The fluorescence and phosphorescence lifetimes for these hybrids decrease in the order: α, β-PHb > α -PHb > β-PHb at 25° C and 77 K which are interpreted in terms of inter-subunit energy and electron transfer. The vibrational features and the energy distribution functions for these hybrids were further studied by FLN spectroscopy. The shape of the distribution function for the 0, 0 transition is approximated by Gaussian functions, centered at 17250 cm^{-1} for β-PHb and 17380 cm^{-1} for α-PHb. Temperature dependence of the FLN spectra were different with a transition seen at ~50 and 70 K, for porphyrin in α and β chain respectively. In addition, step-wise broadening of the individual vibrational lines are observed, indicating differences in flexibility and different phonon coupling for some vibrations of the porphyrin in the two subunits.
(Supported by NIH PO1 GM 48130).

Th-Pos12

COMPARISON OF HORSE FERROUS CYTOCHROME *c* AND Zn-SUBSTITUTED CYTOCHROME *c* BY NMR SPECTROSCOPY. ((H. Anni, J.M. Vanderkooi and L. Mayne)) University of Pennsylvania, Department of Biochemistry & Biophysics, Philadelphia, PA 19104-6089.

In luminescence studies, Zn-substituted cytochrome *c* (Zncyt *c*) has been routinely used as a structurally equivalent protein to cyt *c*. We have measured the one- and two-dimensional nuclear Overhauser NMR spectra of Zncyt *c* in order to check:
a) the geometry of the axial ligands, Met80 and His18, and of other amino acid residues in the vicinity of the porphyrin,
b) the coordination state of the substituted central metal, Zn,
c) the positions of the amino acids involved in the binding of cyt *c* to its redox partners and especially those in the interfacewith cytochrome *c* peroxidase,
d) the overall conformation of the protein.
Our NMR spectra show that the position of the axial ligands, Met80 and His18, remained strikingly the same in Zncyt *c* as in ferrous cyt *c* under the same experimental conditions. This finding could be interpreted as Zn probably being six-coordinated in cyt *c*, in agreement to results in model Zn-porphyrin systems. Moreover, the positions of other amino acid residues in Zncyt *c* are similar to those in ferrous cyt *c*. Our data demonstrate that Zncyt *c* is an adequate structural model for cyt *c*.

(Supported by NIH P01-GM48130)

Th-Pos13

SITE DIRECTED MUTAGENESIS OF PROPOSED CUA LIGANDS HIS-161, CYS-196, CYS-200, HIS-204 AND OF GLU-198, IMPLICATED IN CYTOCHROME *C* BINDING TO CYTOCHROME *C* OXIDASE. ((Henry S. Speno, M. Reza Taheri, Craig T. Martin)) Department of Chemistry and Program in Molecular & Cellular Biology, University of Massachusetts, Amherst 01003. (Sponsored by C. Martin)

Of the four redox active metal centers in cytochrome *c* oxidase, Cu_A has proved most unusual and controversial in its proposed structure and function. ENDOR spectroscopy has defined at least one His and at least one Cys in subunit II as ligands to Cu_A, and spectroscopic studies suggest a dithiolate coordination for Cu_A. Site directed mutagenesis of the highly conserved residues His-161, Cys-196, Cys-200 and His-204 in subunit II provides tests of various models. A variety of single and double substitutions at these locations do not allow cellular respiration in the yeast, *S. cerevisiae*. Furthermore, the absorption at 600nm, characteristic of reduced cytochrome *a*, is not present *in vivo*, suggesting a critical role for these internal residues. The highly conserved Glu-198, located immediately between the two Cys residues and implicated in cytochrome *c* binding, has also been mutated, with less perturbing results, consistent with its role as an external amino acid contributing to the cytochrome *c* binding site. While substitutions of negative and neutral polar amino acids allow for respiration, the replacement of Glu by Lys disrupts oxidase function *in vivo* (but still allows folding of the protein). Mutant enzymes are currently being isolated to allow *in vitro* comparisons with the native enzyme.

Th-Pos14

EFFECTS OF LONG AND DOUBLE CROSSLINKING OF HEMOGLOBIN ((Qunying Zhang)) Department of Chemistry, Loyola University of Chicago, Chicago, IL 60626

Two different length diaspirin intramolecular crosslinking reagents, bis(3,5-dibromosalicyl) fumarate(DBSF) and bis(3,5-dibromosalicyl) sebacate(DBSS), were reacted with human hemoglobin. The double crosslinked hemoglobin, β,α-XLHbA, was crosslinked between both α99 lysines and β82 lysines by the short reagent DBSF. β,α-XLHbA had over 95% of inter-chain crosslinking as measured by SDS electrophoresis. The thermal denaturation temperature (T_m) of β,α-XLHbA was 20.2°C higher than the native hemoglobin and 4.3°C higher than either singly crosslinked hemoglobin, α99XLHbA and β82XLHbA. The oxygen affinity of β,α-XLHbA was the same as the α99XLHbA, and significantly lower than HbA and β82XLHbA. It retained oxygen binding cooperativity. The autoxidation rate of β,α-XLHbA was similar to HbA and β82XLHbA and slower than α99XLHbA. The major product of the reaction of oxyhemoglobin with long diaspirin reagent DBSS was crosslinked between two β chains. This crosslinked species produced from oxyhemoglobin had a considerably lower oxygen affinity than HbA and β82XLHbA. The P_{50} value was not effected by inositol hexaphosphate. The thermal denaturation temperature was higher than HbA, but about 2.1°C lower than α99XLHbA and β82XLHbA. (Supported in part by Research Corporation grant to K. W. Olsen.)

Th-Pos15

OXIDATION OF NITROSYLHEMOGLOBIN BY OXYGEN AND OXYHEMOGLOBIN BY NITROPRUSSIDE WITHOUT PEROXIDATIVE INTERMEDIATES. **((V.W. Macdonald, B.A. Brockner-Ryan, C. Gomez and A.I. Alayash))** Center for Biologics Evaluation and Research, FDA, Bethesda, MD 20892 and US Army Blood Research Detachment, WRAIR, Washington, D.C. 20307. (Spon. by A. Shrake)

Hemoglobin (Hb) interaction with endothelium-derived nitric oxide (NO) is likely responsible for the hemodynamic changes induced by cell-free Hb *in vivo*. Exposure of nitrosylHb to oxygen or oxyHb to NO may induce Hb oxidation with consequent peroxidative damage to the protein and surrounding tissue. The nitrosyl derivatives of unmodified Hb (HbA_0), diaspirin cross-linked Hb ($\alpha\alpha$Hb), and polyethylene glycol polymerized $\alpha\alpha$Hb (Poly$\alpha\alpha$Hb) were each exposed to oxygen in 0.05 M phosphate buffer at pH 7.2. Oxidations were monitored at 27°C in a wavelength scanning spectrophotometer (450-700 nm). Analysis of the spectral data by singular value decomposition (SVD) showed only two components: nitrosylHb and metHb. Multicomponent analysis showed the oxidations to be biphasic, possibly due to differences in the α and β chains, with faster rates for the modified Hb's. Nitroprusside (NTP) oxidations of oxyHb were carried out under similar conditions. Again, only two components were detected, oxyHb and cyanometHb, and the reactions were biphasic and faster for the modified Hb's. NTP oxidation did not produce detectable nitrosylHb. Peroxidative Hb intermediates were not detected in any of the experiments. NO-mediated oxidation of the ferrous heme moiety in Hb may be a normal process that can take place without inducing peroxidative damage.

Th-Pos16

DIFFERENTIATION OF STERIC AND ELECTRONIC EFFECTS IN HEMOGLOBINS AND MYOGLOBINS. ((Kevin Faulkner, Celia Bonaventura and Alvin L. Crumbliss)) Duke University Department of Chemistry, Durham, NC 27708 and Duke University School of the Environment Marine Laboratory. Beaufort, NC 28516

Oxygen binding curves and spectroelectrochemical techniques were used to compare oxygenation and oxidation curves for hemoglobins and myoglobins under equivalent experimental conditions. We use $Ru(NH_3)_6Cl_3$ as a redox mediator, which exchanges electrons with heme iron through an outer-sphere mechanism. Nernst plots for hemoglobins show evidence of cooperative interactions, with redox potentials that are sensitive to functional modulation by pH and anionic effectors. Differences in the anionic effects observed in the Nernst and Hill plots for Hb A and HbCPA indicate significant differences in the electron and oxygen binding processes. These results allow for a more complete differentiation between steric and electronic effects in anionic control of hemoglobin function than has been previously possible.

Th-Pos17

CAN THE KINETICS OF HEMOGLOBIN BE EXPLAINED BY A TWO-STATE ALLOSTERIC MODEL? ((C. M. Jones, E. R. Henry, A. Ansari, J. Hofrichter and W. A. Eaton)) Laboratory of Chemical Physics, NIDDK, NIH, Bethesda, MD 20892.

We have measured the ligand rebinding and conformational relaxation kinetics of human hemoglobin following photodissociation of the heme-carbon monoxide complex from a few nanoseconds to the completion of rebinding at about 10 milliseconds (Jones et al., *Biochemistry 31*, 6692 (1992)). Time-resolved spectra in the Soret region were measured at different degrees of photolysis to vary the number of ligands bound per tetramer. The kinetics are complex, exhibiting non-exponential geminate rebinding and tertiary conformational relaxation, and multiphasic bimolecular ligand rebinding resulting from quaternary conformational changes. Nevertheless, singular value decomposition of the time-resolved spectra shows that there are only two linearly-independent deoxyheme spectra, suggesting only two conformations for deoxyheme-containing subunits. We are exploring the possibility that the kinetics can be explained by a generalization of the two-state allosteric model in which there is incomplete coupling between the tertiary and quaternary conformations. In this model there are only two conformations for each subunit, *r* and *t*, corresponding to high and low affinity states. The relative populations of these two conformations are determined by their ligation state and the quaternary structure of the tetramer, ligation and the *R* quaternary structure favoring *r*, and deligation and *T* favoring *t*.

Th-Pos18

IN SEARCH OF A MODEL FOR MYOGLOBIN KINETICS. ((A. Ansari, C. M. Jones, E. R. Henry, J. Hofrichter and W. A. Eaton)) Laboratory of Chemical Physics, NIDDK, NIH, Bethesda, MD 20892.

Following photodissociation of its carbon monoxide complex myoglobin exhibits deoxyheme spectral changes on the same time scale as geminate rebinding. We have carried out extensive kinetic modelling to establish the relation between these spectral changes and the kinetics of ligand rebinding (T = 268 - 308 K and η = 1 - 300 cP). Two limiting cases can be ruled out: one in which all of the spectral changes arise from "kinetic hole burning", and a second in which the spectral changes have no effect on the geminate rebinding rate. The spectral changes are therefore due at least in part to conformational relaxation of the protein that slows down the rate of geminate rebinding. The data can be qualitatively explained by a "minimal model" in which there is a fast and slow rebinding conformation and two geminate states for each conformation. The differences between the spectra of the two conformations generated from the fits are similar to the differences between those of the *R* and *T* conformations of hemoglobin. In modelling the data, the dependence of the rates on temperature and viscosity was parametrized using a modification of Kramers theory which includes the contributions of both protein and solvent to the friction (Ansari et al., *Science* **256**, 1796 (1992)). The rate of the transition from the fast to the slow rebinding conformation is found to be inversely proportional to the viscosity when the viscosity exceeds about 30 cP, and nearly viscosity-independent at low viscosity.

Th-Pos19

PROTEIN DYNAMICS COUPLED TO CO PHOTODISSOCIATION FROM CARBONMONOXYMYOGLOBIN PROBED BY TIME-RESOLVED INFRARED SPECTROSCOPY ((T. P. Causgrove and R. B. Dyer)) CLS-4, M.S. J567, Los Alamos National Laboratory, Los Alamos, NM 87545

A critical feature of the biological function of heme proteins is the direct coupling of protein motion to the process of binding exogenous ligands to the heme. In carbonmonoxymyoglobin (MbCO), a substantial, specific conformational relaxation is associated with the transition from the ligated to the unligated form of the protein. We have studied these processes on all relevant timescales, from picoseconds to milliseconds, using time-resolved infrared (TRIR) spectroscopy. The amide I region of the IR spectrum is particularly sensitive to changes in the conformation of the polypeptide backbone. We have used this spectral region to probe the global protein relaxation associated with loss of the CO and subsequent displacement of the heme Fe and coupled relaxation of the proximal helices of the protein. The 100 ns difference spectrum (Mb - MbCO) in the amide I region is identical within experimental error to the static FTIR difference spectrum; hence we conclude that the protein relaxation to the deoxyMb conformation is complete on this timescale. We have resolved the dynamics of the global relaxation using picosecond TRIR techniques. The bulk of the relaxation occurs within 10 ps and is complete by 54 ps. The protein relaxation appears to occur in phase with the movement of the Fe out of the plane of the porphyrin (the rate of the latter process has been determined by others using time-resolved resonance Raman and transient near-infrared absorbance of band III). The ultrafast nature of the changes in secondary structure has important implications regarding the mechanism of protein relaxation.

Th-Pos20

COPOLYMERIZATION OF SICKLE AND NON-SICKLE HEMOGLOBINS UNDER CROWDED CONDITIONS. ((Thomas L. Madden, Jining Han, and Judith Herzfeld)) Department of Chemistry, Brandeis University, Waltham, MA, 02254-9110

By extending a successful model for crowded solutions of pure sickle Hb,[1] we studied the behavior of mixtures of sickle and non-sickle Hb. As in the original model, the extended model takes account of excluded volume, soft repulsions, cooperativity in polymerization, and variable polymer hydration. The only new parameter is $\Delta\phi$, which is the free energy penalty for replacing a sickle Hb monomer with a non-sickle Hb monomer in the polymer. For hybrid monomers, this penalty is incurred in one orientation but not the other. We found that the isotropic phase boundary is insensitive to hybridization in agreement with sedimentation experiments. The nematic phase boundary, however, is sensitive to hybridization. By adjusting $\Delta\phi$, the theory can rationalize the data from both sedimentation and osmotic pressure experiments. The analysis shows $\Delta\phi \approx 2$. This suggests that copolymerization of non-sickle Hb is controlled by the protonation of a group with pK ≈ 6.1. This, in turn, suggests that the β6 glutamic acid of normal Hb is accommodated in the polymer by forming a salt bridge with the β77 histidine of the neighboring Hb molecule.

[1] R. Hentschke and J. Herzfeld, Phys. Rev. **A43**, 7019 (1991).

Th-Pos21

THE GLASS TRANSITION IN MYOGLOBIN

((Peter J. Steinbach and Bernard R. Brooks)) DCRT, NIH, Bethesda, MD 20892

The temperature dependence of protein dynamics has been studied by performing 150-ps molecular dynamics simulations of carboxy-myoglobin (MbCO). Dynamics was simulated from 100 to 300 K at 25-K intervals for MbCO hydrated by 0 and by 350 waters, representing dried and fully hydrated protein, respectively. The simulations reproduce the glass-transition temperature (about 220 K) and the magnitude of anharmonic motion at higher temperatures that have been measured by neutron scattering. Previous simulations have predicted harmonic motion about three times larger than that measured experimentally. Low-temperature starting conformations were prepared for the current simulations by quenched molecular dynamics, resulting in lower energy conformations than energy minimization and reducing the overestimate of harmonic fluctuation by about 20%.

Simulations were also performed in which dihedral transitions were prohibited by large energy barriers. Dihedral interconversion has been correlated to the onset of anharmonic motion that marks the glass transition (1). A glass transition was still simulated in the absence of such interconversion, with anharmonic motion reduced by about a factor of two. Thus, concerted non-local motions contribute significantly to the glass transition.

1. P.J. Steinbach and B.R. Brooks, *Proc. Natl. Acad. Sci. USA 90* (1993), 9135.

Th-Pos22

CHARACTERIZATION OF *ARTHROMYCES RAMOSUS* PEROXIDASE.

((Z. S. Farhangrazi, I. Yamazaki, B. Sinclair, B. Copeland, T. Amachi, L. Powers)) National Center for the Design of Molecular Function, Utah State University, Logan, UT 84322-4630 and Institute for Fundamental Research, Suntory Ltd., Shimamato-cho, Mishima-gun, Osaka 618, Japan.

Arthromyces ramosus peroxidase (ARP), a fungal peroxidase, has been found to give stronger chemiluminescent oxidation of luminol than that produced by horseradish peroxidase (HRP) in assays of glucose and cholesterol (1). To compare the catalytic function of these enzymes we have investigated the redox properties of catalytic intermediates of ARP. Our studies show that the reduction potential of compound II/native couple is higher than the reduction potential for compound I/compound II. These two couples, respectively, are higher than those for HRP. At neutral pH, compound I of ARP was stable, but there was an apparent absence of the formation of compound II. Compound II was seen as an intermediate only at alkaline pH. Compound II of ARP is unusually unstable at neutral pH and is immediately reduced to native compound without apparent accumulation. Our EPR results clearly indicate that both HRP and ARP oxidize hydroquinone through one-electron oxidation mechanisms. In addition we report other characteristics of ARP, such as enzyme activity in oxidizing some typical substrates and the results of X-ray absorption spectroscopy.

Supported in part by NIH grant number 5 P41 RR06030-03

(1) Anal. Biochem. 189, 182-185, 1990

Th-Pos23

RESONANCE RAMAN AND CIRCULAR DICHROISM OF THE 28-kD COBALAMIN-BINDING DOMAIN OF *E. COLI* METHIONINE SYNTHASE.

((James M. Puckett*, Kwok To Yue&, and Luigi G. Marzilli*)) Departments of *Chemistry and &Physics, Emory University, Atlanta, GA 30322.

E. coli cobalamin-dependent methionine synthase is a 136.1 kD monomeric enzyme that catalyzes the transfer of a methyl group from N5-methyltetrahydrofolate to the sulfur atom of L-homocysteine to form L-methionine. This catalysis involves a methylcobalamin intermediate. The large size of this enzyme precludes NMR solution studies of the mode of rate enhancement. Therefore, the 28kD cobalamin-binding domain isolated upon tryptic digestion is being examined as a prelude to such studies. Since activity is no longer observed for the 28kD cobalamin-binding protein, the fidelity of binding is probed using visible circular dichroism and resonance Raman spectroscopies. The spectra of the free methylcobalamin are also measured for comparison. The 28kD domain and the holoenzyme have essentially identical CD and Raman spectra, strongly suggesting conformational integrity of the cobalamin. Furthermore, differences between the bound and the unbound cobalamin Raman spectra indicate structural distortions upon binding. In particular, peak at ca. 1554 cm^{-1} in the Raman spectrum of the holoenzyme may be used as a probe for binding since it is absent in the unbound spectrum. Isotopic substitution experiments involving replacement of the methyl group with CD_3 are underway to assign the Co-methyl stretching frequency. Comparison of this with the known frequency of the free methylcobalamin may provide insight into the possibility of a structural *trans*-effect from the benzimidazole moiety that is modulated by the enzyme to make the Co-methyl bond more labile.

Th-Pos24

Geminate Recombination in Photodissociated Alkylcobalamins.

((Y. Lu, M. Yang, J. M. Friedman, M. R. Chance)) Albert Einstein College of Medicine, Bronx, NY 10461

The nature of the cobalt-carbon (Co-C_α) bond in alkylcobalamins has been the subject of interest because of its important role in enzymatic reactions. Flash photolysis techniques have been undertaken by several investigators, but direct observation of the geminate recombination on a nanosecond timescale has not been reported. We have photo-induced the cleavage of Co-C_α bond in methylcobalamin and adenosylcobalamin by using single pulses of 6.5 mJ at 532-nm from a Nd:YAG laser (40 ps duration). The nanosecond transient absorption spectra from 1 ns to 50 ms clearly show both geminate recombination and diffusional recombination phases in both photodissociated cobalamins. A rapid radical-Co(II) recombination process is observed over a period of ~200ns. Subsequent rebinding kinetics is much slower and with a total of approximately 40% recombination at 50 ms. These reactions are important since cobalamin enzymes act as a geminate "cage" to promote or prevent Co-C_α bond cleavage depending on the reaction conditions. Our results suggest that the decay of the photodissociated products appears to have at least two components: the first rapid partial decay is the contribution from radicals trapped in solvent "cage" and ends within a very short time scale. The onset of the second process is several hundred nanoseconds after photodissociation and is apparently diffusion controlled. The viscosity and temperature dependence of the reactions will be presented. This research is supported by the NRICGP/CSRS/USDA program in Human Nutrients 91-37200-6897.

Th-Pos25

THE EFFECT OF HYDROGEN BONDING TO BOUND DIOXYGEN ON ELECTRON-NUCLEAR COUPLING TO THE AXIAL IMIDAZOLE IN OXY COBALTOUS TETRAPHENYLPORPHYRIN (TPP) IMIDAZOLE COMPLEXES.

((H. Caroline Lee[1], and Jack Peisach[1,2]))Depts. of [1]Molecular Pharmacology, [2]Physiology & Biophysics, Albert Einstein College of Medicine, Bronx, NY 10461.

OxyCo(*o*-R)$_1$TPP-imidazole complexes, where R is an amide, urea or hydroxyl group capable of formimg a hydrogen bond to bound O_2, were used to model the distal histidine•••O_2-Fe-proximal histidine structure found in most O_2-carrying hemoproteins. EPR and electron spin echo envelope modulation (ESEEM) spectroscopy were used to measure hyperfine coupling to Co, and nuclear hyperfine and nuclear quadrupole coupling to the imine nitrogen of the axial imidazole. The presence of a hyperfine-coupled deuteron found for complexes in which the acidic proton on R was deuterated was used as a probe for a hydrogen bond to the bound O_2. An increase in hydrogen bonding to bound O_2 was accompanied by a reduction in hyperfine and quadrupole coupling to the axial imidazole, as was found for oxyCo-substituted hemoproteins. No apparent correlation between deuterium coupling and the magnitude of Co hyperfine coupling was found. Reduction in coupling to axial imidazole was accompanied by an increase in O_2 affinity in the Co complexes and in the corresponding Fe complexes.

Th-Pos26

CHARACTERIZATION OF THE NADH DEHYDROGENASE AND FUMARATE REDUCTASE OF *FIBROBACTER SUCCINOGENES*.

((S.W. Meinhardt and T.L Glass)) Dept. of Biochemistry and Dept. of Vet. and Microbiol. Sci., North Dakota State Univ. Fargo ND 58105.

The obligate anaerobe *Fibrobacter succinogenes* is the major cellulolytic bacteria in the bovine rumen. Previous investigations into the metabolic processes of this organism have established glucose degradation through the Embden-Meyerhof-Parnas pathway with succinate serving as the final electron acceptor. In these studies no NADH dehydrogenase activity could be detected, although a $FMNH_2$ linked fumarate reductase was observed. We have demonstrated the presence of a NADH dehydrogenase that is linked through the quinone pool to the fumarate reductase. The NADH-Q oxidoreductase activity is sensitive to rotenone, $HgCl_2$, and o-phenanthroline, and it exhibits a narrow pH dependence with an optimum at pH 6.0 and apparent pK_a values of 8.5 and < 5 at low ionic strength. Increasing the ionic strength results in the narrowing of the pH dependence without a change in the optimum. The NADH-fumarate oxidoreductase activity is sensitive to HOQNO. At low ionic strength the fumarate reductase exhibits low activity, <0.05 μmoles/min-mg protein, between pH 9 and pH 5.5. The activity increases as the pH is lowered below pH 5.5. In the presence of 50 mM NaCl or KCl, the fumarate reductase has an optimum activity at pH 6.0, 0.25 μmoles/min-mg protein, and apparent pK_a values of 6.7 and 5.2. This complex contains at least one *b*-type cytochrome, α_{max} 563 nm.

Th-Pos27

EVIDENCE FOR PH DEPENDENT ALTERNATIVE PATHWAYS OF NADH AND NADPH OXIDATION BY MITOCHONDRIAL COMPLEX I - AN INHIBITOR STUDY.

((W. M. Anderson and D. Trgovcich-Zacok)) Ind. Univ. Sch. of Med., NWCME, 3400 Broadway, Gary, IN, USA 46408

The Baaker and Albracht model of electron flow through the NADH-ubiquinone reductase portion of the mitochondrial electron transport chain (Biochim. Biophys. Acta 850, 413-422 & 423-428, 1986) predicts a heterodimer of complex I in which protomer 1 (a) is responsible for NADH oxidation at pH 8 (b) is not able to react with NADPH, and (c) contains FMN and Fe-S clusters 1-4 in stiochiometric amounts. Protomer 2 (a) is responsible for NAD(P)H oxidation at pH 6.5 and (b) contains FMN and Fe-S clusters 2-4, but not Fe-S cluster 1. Strict intrepretation of this model would allow only for inhibitors which blocked both NADH oxidase, pH 8.0 and NAD(P)H oxidase, pH 6.5 (category 1); or NADH oxidase, pH 8.0, but not NAD(P)H oxidase, pH 6.5 (category 2). No other category of inhibitors would be allowed. Examination of this model using both recently identified and classical inhibitors of NADH-ubiquinone reductase revealed five different categories of inhibitors, three more than allowed by the Baaker and Albracht model. Our results suggest that (a) NADH oxidase, pH 8.0, NADH oxidase, pH 6.5, and NADPH oxidase, pH 6.5 each utilize different electron flow pathways through complex I; and (b) complex I NADPH oxidase, pH 6.5 bypasses the rotenone-piericidin A inhibitory site. Assuming the heterodimer portion of the model of complex I to be correct, our results indicate that there may be cross-talk in electron flow between the two protomers which further complicates the elucidation of the pathway of electron flow from pyridine nucleotides to ubiquinone within NADH-ubiquinone reductase. Supported by Indiana Heart Assoc.

Th-Pos28

GENE CLONING, SEQUENCING, AND EXPRESSION OF THE SMALL MOLECULAR MASS UBIQUINONE-BINDNG PROTEIN (QPC-9.5 kDa) IN BOVINE HEART MITOCHONDRIAL UBIQUINOL-CYTOCHROME *C* REDUCTASE.

(Linda Yu, Shigeyuki Usui, and Chang-An Yu) Department of Biochemistry and Molecular Biology, Oklahoma State University, Stillwater, OK 74078

Subunit VII of bovine heart mitochondrial ubiquinol-cytochrome *c* reductase has been identified as one of the Q-binding proteins (QPc-9.5 kDa) in this segment of the electron transfer chain. The Q-binding domain has been localized to amino acid residues 48-57 by isolating and sequencing the azido-Q linked peptide from the V-8 digested, [^{3}H]-azido-Q labeled QPc-9.5 kDa. The cDNA encoding QPc-9.5 kDa was recently obtained by immunological screening of a bovine heart cDNA expression library in λgt11 with antibodies against QPc-9.5 kDa. The cDNA insert was 665 bp long with an open reading frame of 246 bp which encoded a mature protein of 81 amino acids. The cDNA insert had a 24 bp 5' non-coding sequence and a 305 bp 3' non-coding sequence containing a poly A tail. The amino acid sequence of QPc-9.5 kDa deduced from the nucleotide sequence is the same as that obtained from protein sequencing except at residue #61, which is tryptophan instead of cysteine. QPc-9.5 kDa was over-expressed in Sf9 insect cells using a baculovirus expression system. Deletion of the 3' non-coding sequence had no effect on the expression of QPc-9.5 kDa in this system. The expressed protein was located in the membrane fraction and could be solubilized by treatment with 1% sodium cholate. This work was partially supported by a grant from NIH (GM 30721).

Th-Pos29

CLONING AND SEQUENCING OF A cDNA ENCODING QPS2 OF BOVINE HEART MITOCHONDRIAL SUCCINATE-UBIQUINONE REDUCTASE.

(Gyesoon Yoon, Linda Yu, and Chang-An Yu), Department of Biochemistry & Molecular Biology, Oklahoma State University, Stillwater, OK 74078

Bovine heart mitochondrial succinate-ubiquinone (Q) reductase is composed of two parts: a water-soluble succinate dehydrogenase and a membrane anchoring protein fraction (QPs). Isolated QPs showed three protein bands (QPs1, QPs2 and QPs3) in high resolution SDS-PAGE with apparent molecular weights of 11, 9.5 and 8.5 kDa, respectively. QPs1 is cytochrome b_{560} with a molecular weight of 14,320, determined from the amino acid sequence deduced from nucleotide sequence, and confirmed by mass spectrometric analysis. Recently pure QPs2 protein was obtained and antibodies against this protein were raised in rabbits and purified. The immunospecificy of anti-QPs2 antibodies was confirmed by ELISA and Western blotting. When anti-QPs2 antibodies were used to screen a beef heart cDNA expression library in λgt11, one cDNA clone encoding QPs2 was obtained. The cDNA insert is 1120 base pairs with an open reading frame of 405 base pairs that coded for 135 amino acid residues. The cDNA insert contains no poly A tail. The molecular weight of QPs2, calculated from the deduced amino acid sequence, is 14,614, suggesting the presence of a leader sequence. QPs2 is a very hydrophobic protein. Four probable membrane-spanning segments were revealed by a hydropathy plot of the sequence. Supported in part from a grant from NIH (GM 30721).

Th-Pos30

DIFFRACTION STUDIES OF HEXAGONAL AND ORTHORHOMBIC CRYSTALS OF UBIQUINOL:CYTOCHROME C OXIDOREDUCTASE.

((Edward A. Berry, Vladimir M. Shulmeister, Li-shar Huang, and Sung-Hou Kim)) Lawrence Berkeley Laboratory, Berkeley, CA 94720.

Ubiquinol:cytochrome c reductase has been crystallized in an orthorhombic space group ($C222_1$) as well as the previously reported ($P6_1(5)22$) crystals. The unit cell parameters of the orthorhombic crystals are a,b,c=384, 118, 177 Å. Systematic extinctions result in less spot overlap than with the hexagonal crystals. The highest resolution spot observed thus far is 3.80 Å (h,k,l=14,-24,-29). This is comparable to our best observation with the hexagonal crystals, 3.86 Å (h,k,l=34,-16,78).

A Hg-containing amide of nitrosalicylic acid has been synthesized and shown to inhibit cytochrome reductase with K_i=3 μM and characteristics of antimycin. Hexagonal crystals have been grown in the presence of saturating concentration of this inhibitor for use as a heavy atom derivative. These crystals diffract as well as the native, with identical cell parameters. Datasets have been collected to 4.7 Å for the native and derivative hexagonal crystals.

To improve the crystalline order we are improving purity and expanding the range of conditions under which crystals can be grown, as well as working with the enzyme from other sources. We have found conditions for growing crystals in a phosphate-free system and with either of 4 different detergents, in the presence or absence of divalent cations. We have grown crystals from pig as well as beef heart enzyme, and other sources are being tested.

Th-Pos31

STUDIES OF *ESCHERICHIA COLI* NADH:UBIQUINONE OXIDOREDUCTASE (NDH-1)

((V.D.Sled', T.Friedrich$^+$, H.Leif$^+$, H.Weiss$^+$, M.W.Calhoun*, R.B.Gennis* and T.Ohnishi)) Univ. of Pennsylvania, Philadelphia, PA 19104, USA; $^+$Inst. of Biochem., Univ.of Düsseldorf, 4000 Düsseldorf 1, Germany; *Dept.of Chem., Univ. of Illinois, Urbana, IL 61801, USA.

The sequence analysis of the *E.coli* NDH-1 gene locus, containing 14 genes, revealed the presence of all polypeptides homologous to the mammalian counterparts which are presumed to bind substrates and the redox groups (FMN and FeS clusters). On the other hand, EPR spectral features of the FeS clusters in *E.coli* NDH-1 differ significantly from those of the mitochondrial system. The EPR analysis of membranes from wild strain and a mutant with genetically deleted succinate dehydrogenase, and of isolated NDH-1 revealed that NDH-1 contains at least 5 EPR-detectable FeS clusters: 3 binuclear {two axial-type ($g_{||,\perp}$= 2.02,1.94) and $E_{m,7} \cong$ -270 and -380 mV; and a rhombic-type ($g_{z,y,x}$= 2.00,1.95,1.92) with an $E_{m,7} \cong$ -240 mV} and 2 tetranuclear {one rhombic-type ($g_{z,y,x}$= 2.09, 1.94,1.89) with $E_{m,7} \cong$ -240 mV, and one axial-type ($g_{||,\perp}$=2.05,1.91) and $E_{m,7} \cong$ -280 mV}. Based on analysis of the EPR spectra of *E.coli* mutants with genetically deleted subunits of NDH-1, we will discuss identity of the FeS clusters in different subunits and correspondence between clusters of NDH-1 in *E.coli* and in mitochondria. {Supported by NIH Grant GM-30736 (T.O.) and GM-35438 (R.B.G.)}

Th-Pos32

ELECTRONIC STRUCTURE OF THE Q_S UBISEMIQUINONE RADICAL IN SUCCINATE-UBIQUINONE REDUCTASE (SQR) PROBED WITH ELECTRON NUCLEAR DOUBLE RESONANCE (ENDOR). ((C-A. Yu[a], L. Yu[a], R. Barnard[b], H. Sun[b], and C. P. Scholes[c])) Dept. of Biochemistry[a], Oklahoma State University, Stillwater, Oklahoma 74078; Depts. of Physics[b] and Chemistry[c], SUNY at Albany, Albany, NY 12222.

The purpose of this work is to obtain unpaired electron spin information at the Q_S radical center in SQR for correlation with the distinct physical and functional characteristics of that center. The Q_S ubisemiquinone radical is highly stabilized with respect to its quinone and quinol forms, and in comparison with protein-bound ubisemiquinones of the bc1 complex (Q_C) [Salerno et al. (1990) *Biochemistry* 29, 6987] and the bacterial reaction centers (Q_a & Q_b) [Lubitz et al. (1985) *BBA* 808, 464], the Q_S radical EPR linewidth is broader (12 Gauss peak-to-peak for Q_S vs 9-10 Gauss for Q_a, Q_b, Q_C). With ENDOR we have observed from Q_S radical a large proton hyperfine coupling of order 20 MHz. The proton(s) which account for this large coupling are not exchangeable with solvent, and their signal disappears in the presence of the specific Q_S inhibitor, thionyl trifluoroacetone (TTFA). There is also evidence for exchangeable protons which have couplings in the 4-8 MHz range; exchangeable proton couplings of this order have been observed from Q_a, Q_b, and Q_C. We are improving resolution of weakly coupled ($\leq$ 4 MHz) protons for further comparison studies.

This work was supported by grants from the National Institutes of Health (GM 30721 to C-A. & L. Yu; GM 35103 to C.P.S.)

Th-Pos33

MUTATIONS AT CONSERVED RESIDUES IN CYTOCHROME *b* SUBUNIT OF *R. SPHAEROIDES* AFFECT QUINONE REDUCTASE SITE. ((B. Hacker, B. Barquera, A. R. Crofts and R. B. Gennis)) School of Chemical Sciences and School of Life Sciences, University of Illinois, Urbana, IL 61801.

The catalytic locus of the quinone reductase site (Q_i) of the bc_1 complex is based on conserved and drug resistant residues in the cytochrome *b* subunit. Previous work has shown that mutant analysis provides information on electron flow through the Q_i site. Highly conserved *b* subunit residues of *R. sphaeroides* (R114,W129,N223) were targeted for mutagenesis to determine their Q_i site role. All mutants assembled a bc_1 complex except for R114A and R114Q. The flash kinetic reoxidation of cytochrome b_H is perturbed only in W129F. Antimycin titrations clearly show Q_i site perturbations in all of the mutants. N223V is an example of a severely impaired Q_i site since it lacks antimycin induced oxidation despite a 150 mV redox peak. Future analysis will help to clarify the role of the semiquinone at the Q_i site.

Th-Pos34

EXPRESSION OF THE IRON-SULFUR CLUSTER BINDING SUBUNITS OF THE ENERGY-TRANSDUCING NADH-UBIQUINONE OXIDOREDUCTASE (NDH-1) OF *PARACOCCUS DENITRIFICANS*

((T. Yano[1], V. Sled[2], T. Ohnishi[2] and T. Yagi[1])) [1]TSRI, La Jolla, CA 92037, [2]University of Pennsylvania, Philadelphia, PA 19104-6089.

Paracoccus denitrificans, a free-living mitochondrion, has an aerobic respiratory chain that appears to be revolutionally related to mitochondrial one. To date *Paracoccus* is believed to contain only energy-transducing NADH-ubiquinone oxidoreductase, NDH-1, but not NDH-2 which does not bear energy coupling site. *Paracoccus* NDH-1 is probably composed of 14 dissimilar subunits and contains 5 EPR-visible FeS clusters. Those are two binuclear (N1a, N1b) and three tetranuclear (N2, N3, N4) clusters similar to composition of FeS clusters of its bovine counterpart. Recently, the complete DNA sequence of a gene cluster encoding the *Paracoccus* NDH-1 has been determined. The *Paracoccus* NDH-1 gene cluster bears 14 structural genes and 6 URFs. On the basis of the deduced primary structures of the *Paracoccus* NDH-1 subunits and results of resolution experiments of bovine Complex I, the NQO1, 2, 3, 6 and 9 subunits have been speculated to bear FeS clusters. In order to directly verify whether these subunits actually ligate the FeS clusters, we have attempted to express these subunits in *E. coli*.

The NQO2 subunit was expressed in the cytoplasmic space but not in the membrane fraction. The expressed NQO2 subunit is associated with the EPR-visible binuclear FeS cluster which exhibits rhombic symmetry.

The NQO3 subunit was expressed in both the cytoplasmic phase and membrane fraction. The expressed NQO3 subunit bears at least two EPR-visible FeS clusters. One is a binuclear (axial symmetry) and the other is a tetranuclear cluster (rhombic symmetry).

Further characterization of the expressed subunits by EPR, RR and MCD is in progress.

Th-Pos35

GENOMIC STRUCTURE OF THE 13.2 kDa (IP) SUBUNIT OF NADH: UBIQUINONE OXIDOREDUCTASE FROM MOUSE AND RAT.

((J.D. Watson, B. Beckett-Jones, R.N. Roy and T.G. Flynn)) Department of Biochemistry, Queen's University at Kingston, ON Can. K7L 3N6. (Spon. by A.S. Mak)

The sequence of a peptide extracted from rat atria was used to construct a 48-mer oligonucleotide based on codon usage with inosine at positions of 4 -fold redundancy. The corresponding cDNA clone was isolated from a rat atrial library and used as a probe of a rat genomic library. Over 3000 nt of the 13.2 kDa (IP) gene was sequenced including the complete coding domain and the 5' and 3' flanks. The gene contains a single 61 nucleotide intron, beginning 50 nucleotides into the mature protein coding domain. The 5' flank sequence contains 10 potential NRF-1 regulatory elements, consistent with the role of this protein as a subunit of complex I. In addition, the gene is surrounded by AT rich tracts and a GT_{36} repeat is present in the distal 3' flank, both representing potential regulatory elements. A portion of the mouse 13.2 kDa (IP) gene was amplified using PCR with primers based on the rat sequence. The mouse sequence does not contain an intron within the sequenced region, unlike the rat gene. The deduced protein sequence from mouse, rat and cow (Walker, J.E. *et. al.*, J.Mol.Biol. **226**:1051-1072. (1992)) are greater than 90% identical, with regions of complete identity occurring in discrete segments, probably indicating functionally significant domains. Supported by the MRC of Canada.

Th-Pos36

THE IR VIBRATIONS OF Q_A IN BACTERIAL REACTION CENTERS RECONSTITUTED WITH ISOTOPICALLY LABELED QUINONES

J. Breton, J.-R. Burie, C. Berthomieu, G. Berger and E. Nabedryk
SBE/DBCM, C.E.N. Saclay, 91191 Gif-sur-Yvette Cedex, France

Photoreduction of the primary electron acceptor Q_A in Q_A-depleted *Rb. sphaeroides* RCs reconstituted with UQ_6 or vitamin K_1 labeled on the carbonyl oxygen atoms and with uniformly ^{13}C-labeled UQ_8 has been characterized by FTIR spectroscopy. Two carbonyl modes of the neutral $^{12}C^{16}O$ Q_A are demasked at 1660 and 1629 cm^{-1} for UQ and 1651 and 1640 cm^{-1} for vitamin K_1, while the C=C modes are found at 1613 and 1590 cm^{-1} for vitamin K_1 and at 1601 cm^{-1} for UQ. Compared with the spectra of the isolated quinones, the different frequency downshifts (≈7 cm^{-1} and 21 cm^{-1}) of the two C=O in the Q_A site underscore the unequivalence of the two carbonyls in providing asymmetrical bonding interactions with the protein. While the admixture of C=O and C=C character is significantly perturbed, the methoxy groups of UQ do not appear to suffer crual strain upon binding. The smaller width of the C=C and C=O bands *in vivo* than *in vitro* indicates precise interactions between the quinone and the protein. The location of the anion bands of vitamin K_1 *in vivo* and *in vitro* demonstrates a considerable downshift (≈90 cm^{-1}) of the C···O mode of Q_A^- upon binding. The absence of a splitting of the C···O mode is interpreted in terms of symmetrical bonding interactions of the two carbonyls after reduction. A similar conclusion is reached for the Q_A^- C···O mode of UQ_6. Comparison of the Q_A^-/Q_A spectra of *Rb. sphaeroides* RCs reconstituted with vitamin K_1 and of *Rp. viridis* RCs containing the native menaquinone demonstrates that the protein contours at the Q_A site of the two species are offering very comparable interactions to these closely related naphtoquinones, although the interactions are not identical at the vibrational level.

Th-Pos37

KINETICS OF $Q_A^-Q_B \Rightarrow Q_AQ_B^-$ ELECTRON TRANSFER AND PROTONATION PROCESSES IN BACTERIAL PHOTOSYNTHETIC REACTION CENTERS: EVIDENCE FROM TIME-RESOLVED IR SPECTROSCOPY

((Rainer Hienerwadel, Christian Fogel, Stefan Grzybek, Werner Mäntele))
Institut für Biophysik, Albertstraße 23, 79104 Freiburg, Germany

Light-induced electron transfer in bacterial photosynthetic reaction centers (RC) proceeds from a primary donor to a primary (Q_A) and a secondary (Q_B) quinone. $Q_A^-Q_B \Rightarrow Q_AQ_B^-$ electron transfer is typically monitored indirectly by measuring the electrochromic shift of a bacteriopheophytin (BPheo) absorbance band at 750 nm. The activation energy for this process is ≈18 kcal/mol, higher than for the typical e^- transfer rates in the RC. We have analyzed the dynamics of $Q_A \Rightarrow Q_B$ electron transfer in *Rb. sphaeroides* RC directly following the rise of the C-O vibrational mode of Q_B^- at 1478 cm^{-1}, previously assigned in FTIR difference spectra. Formation of Q_B^- is considerably faster (100 µsec) than the 750 nm signal (1 msec) at 5° C. Instead, the kinetics of the 750 nm signal matches that of an IR signal at 1725 cm^{-1} arising from H^+ uptake by GLU L212 near Q_B. The temperature dependence for the 1478 cm^{-1} signal reveals a process with low activation energy (<4 kcal/ mol) for $Q_A^-Q_B \Rightarrow Q_AQ_B^-$. Instead, H^+ transfer to GLU L212 and the BPheo shift match over the temperature range from 0-25 °C; both are activated with ≈14-18 kcal/mol. At t=20°C and above, the kinetics of electron transfer matches that of H^+ transfer and of the 750 nm signal. We thus conclude that the 750 nm signal rather arises from protolytic reactions in the RC than from Q_A^- or Q_B^- formation, and fast $Q_A \Rightarrow Q_B$ electron transfer is followed by slower protonation processes.

Th-Pos38

INTERACTION DOMAIN FOR THE REACTION OF CYTOCHROME C WITH THE RADICAL AND THE OXYFERRYL HEME IN CYTOCHROME C PEROXIDASE COMPOUND I. ((L. Geren, M.A. Miller*, S. Hahm, R. Liu, S. Hibdon, J. Kraut*, B. Durham and F. Millett)) Dept. Chem. Biochem., Univ. of Arkansas, Fayetteville, AR, USA, 72701; *Dept. Chem., Univ. of California at San Diego, La Jolla, CA, 92093.

Kinetic studies of the cytochrome c peroxidase mutants D32Q, E33N, D34N, E35N, E290N, D291Q and A193F were carried out in order to characterize the interaction domain used in the electron transfer reaction with both horse and yeast cytochrome c. Stopped-flow experiments in 310 mM ionic strength buffer at pH 7 revealed that yeast iso-1-ferrocytochrome c reduces the radical on the indole group of Trp-191 in compound I (CMPI) with a second-order rate constant $k_a = 2 \times 10^8\ M^{-1}s^{-1}$. A second molecule of iso-1-cytochrome c then reduces the oxyferryl heme Fe(IV) in CMPII with a rate constant $k_b = 5 \times 10^7\ M^{-1}s^{-1}$. The rate constants of both reactions increase significantly with decreasing ionic strength. D34N and E290N have the smallest rate constants: 17-50% of the values of native, while A193F is 25-50% of native, E33N and E35N have intermediate rates, and D32Q and E291Q have the same rate constants as native. Laser flash photolysis at low ionic strength facilitated the measurement of rate constants for intracomplex electron transfer between the heme group of ruthenium labeled cytochrome c and the radical in CMPI. The effects were similar to the results from the stopped-flow data. (Supported by NIH Grant GM20488 and NSF Grant MCB9119292.)

Th-Pos39

RHODOBACTER CAPSULATUS CONTAINS A NOVEL *cb*-TYPE CYTOCHROME C OXIDASE WITHOUT A Cu_A CENTER. ((K. A. Gray, M. Grooms, H. Myllykallio & F. Daldal)) Department of Biology, University of Pennsylvania, Philadelphia, PA 19104.

A *cb*-type cyt *c* oxidase has been purified from aerobically grown cells of the Gram-negative, photosynthetic bacterium *R. capsulatus*. Cyt *cb* is highly active (turnover number of about 600 mol $O_2\ s^{-1}$), inhibited by low concentrations of cyanide (25 μM was sufficient) and consists of three subunits of M_r 45,000, 32,000 and 28,000. The 28 kDa and 32 kDa subunits bind heme C and heme analysis suggests that the enzyme contains 2 heme B per 2 heme C. Neither heme A nor heme O is present. Partial amino acid sequence analysis reveals homology to the deduced amino acid sequences of the *fix*N, O and P genes from *Bradyrhizobium japonicum* and *Rhizobium melioti*. The *fix*NOQP gene cluster appears to encode a cyt *c* oxidase utilized under microaerophillic growth conditions in those organisms. The two *c*-type cyt have different E_m values (265 mV and 320 mV) and the low spin cyt *b* has an E_m value of about 385 mV. Titrations of membranes isolated from a cytochrome oxidase mutant of *R. capsulatus* missing the 32 kDa cyt *c* show that the 28 kDa cyt *c* titrates with an E_m value of about 320 mV, therefore the larger cyt *c* subunit has an E_m value of about 265 mV. The enzyme binds CO and the CO difference spectrum indicates binding to a high spin cyt *b*. X-band EPR spectra of the purified enzyme show resonances due to both high spin and low spin ferricytochromes. However a classical Cu_A-like signal in the g = 2 region is absent. Supported by NIH GM38237 and DOE-ER20052.

Th-Pos40

CONFORMATIONAL ANALYSIS OF NON-ELECTROSTATICALLY MEMBRANE-BOUND FORMS OF CYTOCHROME *c*. ((J.D. Cortese, A.L. Voglino and C.R. Hackenbrock)) Department of Cell Biology and Anatomy, University of North Carolina at Chapel Hill, Chapel Hill, NC 27599-7090.

We have shown that a small portion of endogenous cytochrome *c* (cyt *c*) remains bound to the inner mitochondrial membrane at high, physiological ionic strength *I* (MB-cyt *c*). Isolated inner membranes can be enriched in MB-cyt *c* at high *I* (H*I*-MB-cyt *c*; low electron transport [ET] activity) or low *I* (L*I*-MB-cyt *c*; high ET activity). H*I*-MB-cyt *c* spontaneously converts over time to a membrane-bound form with increased ET activity and then to an electrostatically-bound form (EB-cyt *c*) that is released from membranes. Using circular dichroism (CD) and spectral analysis, we have detected differences in secondary structure between H*I*-MB-cyt *c*, L*I*-MB-cyt *c* and EB-cyt *c* bound to small unilamellar vesicles (SUV). CD spectra were deconvoluted in five secondary structure components by singular value decomposition. Penetration of SUV by cyt *c* as H*I*-MB-cyt *c* substantially alters its α-helical (αH decreases to 9.2 ± 3.1%) and parallel ß-sheet structure, resembling apocyt *c* more than cyt *c*. αH was very similar for L*I*-MB-cyt *c*, EB-cyt *c*, and cyt *c*. Our conformational evidence supports previous kinetic measurements in showing that the overall conformation of H*I*-MB-cyt *c* is different from that of L*I*-MB-cyt *c*, and that L*I*-MB-cyt *c* is a closer conformer of EB-cyt *c* and cyt *c*. It appears that the strong but transient interaction of MB-cyt *c* with membranes occurs when α-helices form ß-like structures. A reversal of this sequence could occur after completion of cyt *c* synthesis by cyt *c* heme lyase; a H*I*-MB-cyt *c*-like form (low αH) could convert, through reorganization of ß-structures, to a EB-cyt *c*-like form that is released into the mitochondrial intermembrane space. Supported by NSF and NIH.

Th-Pos41

ADDITION OF PURIFIED SUBUNIT III (SIII) TO BOVINE HEART CYTOCHROME c OXIDASE DEPLETED IN SIII STIMULATES THE PROTON-PUMPING ACTIVITY OF THE ENZYME. ((L.J. Prochaska, C. Murphy and A. Walter*)) Depts. of Biochem. & Mol. Biol. and Phys. & Biophys.*, Wright State Univ., Dayton, OH 45435.

Our laboratory and others have shown that the removal of subunit III (SIII) from beef heart cytochrome c oxidase (COX) results in a 50-60% decrease in proton-pumping activity without affecting the electron transfer activity of the enzyme. We have isolated SIII by gel filtration in 3% SDS. SIII in low SDS/phospholipid/cholate mixtures exhibited ellipticities at 210 nm and 222 nm in circular dichroism, suggesting that isolated SIII retained some α-helical conformation in the SDS/phospholipid mixtures. Upon addition of purified SIII to SIII-depleted COX and subsequent formation of phospholipid vesicles, a stimulation of proton-pumping activity was observed when compared to SIII-depleted COX in liposomes (COV-III). The maximum stimulation (1.9 fold) of proton-pumping by SIII in COV-III was observed at a 1:1 molar stoichiometry of added SIII to SIII depleted COX. The respiratory control ratios of COV-III were also increased by the addition of SIII. The stimulation of activities induced by purified SIII was not due to a physical change in the properties of the liposomes; all COX-containing (with or without SIII) liposomes exhibited a similar size distribution on gel filtration HPLC and also had similar density distributions on sucrose gradients. The mechanism of how SIII reassociation with SIII-depleted COX modifies COX proton-pumping activity is under investigation. (Supported by NIH HLB 29051 & American Heart Association Ohio Affiliate)

Th-Pos42

IDENTIFICATION OF A CARBOXYLATE RESIDUE CRITICAL FOR PROTON PUMPING ON THE INNER SIDE OF SUBUNIT I OF CYTOCHROME *C* OXIDASE ((J. Fetter, J.W. Thomas*, Y. Kim, R.B. Gennis*, G.T. Babcock and S. Ferguson-Miller)) Departments of Biochemistry and Chemistry, Michigan State University, East Lansing, MI 48824 and *School of Chemical Sciences, University of Illinois, Urbana, IL 61801

Cytochrome aa_3 of *Rb. sphaeroides* is highly homologous to mitochondrial cytochrome *c* oxidases, with the same heme A and copper centers and ability to pump protons. Mutational analysis indicated the location of metal centers in subunit I and suggests residues that might be involved in a proton relay system. Of the three regions in subunit I so far examined, transmembrane helix VII, an external loop between helices IX and X, and an interior loop between helices II and III, the last appears to be most critical. Mutation of Asp 132 to Asn strongly inhibits electron transfer and completely inhibits proton translocation, in a purified, reconstituted system. Successful reconstitution of this mutant is indicated by its ability to respond to uncoupler and ionophore induced changes in the membrane potential and/or pH gradient. But interestingly, it shows an opposite response to these effectors compared to wild-type, suggesting that proton pumping and aspects of regulation are altered in this mutant. No interruption in the catalytic conversion of O_2 to H_2O is observed, as examined by catalase assay and the enzyme exhibits essentially native spectral characteristics, indicating no general disruption of active site structure. The II-III loop region is clearly important in the energy conserving function of cytochrome *c* oxidase.

Th-Pos43

A KINETIC MECHANISM FOR THE OPTICAL CHANGE INDUCED BY FORMATE BINDING TO CYTOCHROME *C* OXIDASE FROM BOVINE HEART. ((S. M. Gullo and G. M. Baker)) Northern Illinois University, Department of Chemistry, DeKalb, IL 60115 .

The addition of buffered formate to cytochrome *c* oxidase at pH 8.8 induced a 430 → 414 nm conversion in the a_3-Cu_B site. Formate binding, measured at 414 nm, was monophasic at 1.0 mM (5.0 μM heme *a*) but biphasic at ≥ 5.0 mM, despite the occurrence of a clear isosbestic wavelength. Weighted linear regressions of k_{obs} vs. [formate] suggested a two step mechanism involving a rapid 430 ⇌ 414 and a slower 430′ ⇌ 414′ conversion. The kinetic plot gave equilibrium dissociation constants, K_D^{fast} and K_D^{slow}, of 3.1 mM and 28 mM, respectively, although standard error bars made it difficult to establish whether the slower phase was weakly dependent or independent of [formate]. This was resolved by making equilibrium measurements of the total absorbance change for binding of formate. A curve fit of these data gave $K_D^{app} = 0.3$ mM. This was inconsistent with the above mechanism which predicts $K_D^{fast} \leq K_D^{app} \leq K_D^{slow}$. An alternative two step mechanism was therefore proposed: a rapid 430 ⇌ 414, as before, and a slower, formate-independent 414 ⇌ 414′ conversion. This predicts $K_D^{app} \leq K_D^{fast}$, in accord with observation. Simulation of the time dependent changes in the 430, 414, and 414′ forms by numerical integration were consistent with the observed kinetic changes.

Th-Pos44

MOLECULAR STRUCTURE OF THE HEME-COPPER BINUCLEAR CENTER OF THE *E. COLI* CYTOCHROME *BO* COMPLEX. ((T. Mogi, T. Hirano, M. Tsubaki[1], H. Hori[2], T. Uno[3], Y. Nishimura[4], H. Nakamura[5] and Y. Anraku)) Dept. Plant Sciences, Grad. Sch. Science, Univ. Tokyo, Hongo, Bunkyo-ku, Tokyo 113, [1]Fac. Science, Himeji Inst. Tech., Hyogo 678-12, [2]Fac. Eng. Science, Univ. Osaka, Osaka 560, [3]Fac. Pharm. Sciences, Univ. Tokushima, Tokushima, 770, [4]Grad. Sch. Integr. Sciences, Yokohama City Univ., Yokohama 236, and [5]Protein Eng. Research Inst, Osaka 565, Japan.

Roles of conserved aromatic amino acid residues in subunit I of the *E. coli* cytochrome *bo* complex were studied using the purified mutant oxidases. W280L mutation slightly reduced the enzymatic activity that was accompanied by minor spectroscopic perturbations. Y288L, W331L and F348L mutant oxidases were found to be defective in the Q_1H_2 oxidation and showed perturbations in the 77K redox difference spectra of the low-spin heme B and also in the reduced CO-bound and air-oxidized CN-bound difference spectra that are attributable to changes in the high-spin heme. Y288L mutation resulted in conversion of the oxidase to the heme-BB type and severely reduced the binding activity of exogenous ligands, indicating that Tyr288 in helix VI is essential for binding specificity of hemes and for catalytic functions at the binuclear center. W331L mutation perturbed CO-binding without loosing the Cu_B center, whereas F348L mutant oxidase exhibited an enhanced g=6 high-spin signal and altered the CO-binding FTIR and RR spectra as in the Cu_B-deficient mutant oxidase (H333A). Phe348 in helix VIII seems to provide the Cu_B binding site. Based on a three dimensional model of the redox metal centers, we discuss the possible structural and functional roles of aromatic amino acid residues at the heme-copper binuclear center.

Th-Pos45

DEMONSTRATION OF A HEME-HEME BINUCLEAR CENTER IN THE CYTOCHROME BD COMPLEX OF E. COLI BY FT-IR SPECTROSCOPY AT LOW TEMPERATURES. ((J.J. Hill, R.B. Gennis, and J.O. Alben)) University of Illinois, Urbana, IL 61801, and Ohio State University, Columbus, OH 43210.

The cytochrome bd complex is a terminal ubiquinol oxidase, which is part of the aerobic respiratory chain of *E. coli*. The enzyme contains a low spin heme, heme b_{558} and two high spin hemes, b_{595} and heme d (a chlorin), but no copper as in the cytochrome c oxidases. Heme b_{558} is involved in quinol oxidation, and heme d is the site where O_2 or CO bind, and where water is produced. The FT-IR absorbance difference spectrum of the CO complex (continuous photolysis minus dark at 10 Kelvin) shows two bands centered at 1984 cm^{-1} ($\Delta\nu_{1/2}$ 3.9 cm^{-1}) and 2133 cm^{-1} ($\Delta\nu_{1/2}$ 2.0 cm^{-1}), corresponding to CO bound to heme d and the heme-pocket surface, respectively. Relaxation of the carbonyl in the dark partitions between the heme d site and a new site seen as a band centered at 1974 cm^{-1} ($\Delta\nu_{1/2}$ 3.5 cm^{-1}). Photolysis with light of wavelengths longer than 700 nm dissociates the heme d adduct, but not the new site adduct.The data show that the new site is a kinetically trapped CO-heme b_{595} adduct. The single narrow IR absorbance band associated with each site indicate the CO binding pocket is non-polar and highly ordered, and that the protein is frozen into only one major conformational substate. Temperature dependent relaxation of the carbonyl to the two heme sites is similar to that reported for simple heme proteins.

This work was supported in part by grants from the National Institutes of Health (to RBG) and the National Science Foundation (to JOA).

Th-Pos46

IDENTIFICATION OF THE SUBSTRATE BINDING SITE IN *ESCHERICHIA COLI* CYTOCHROME *bo* -UBIQUINOL OXIDASE. (Ryan Welter, Lian-Quan Gu, and Chang-An Yu), Dept. of Biochemistry and Molecular Biology, Oklahoma State University, Stillwater, OK 74078, and (Jon Rumbley, and Robert B. Gennis), Dept. of Chemistry and Biochemistry, University of Illinois, Urbana, IL 61801

Cytochrome *bo*-ubiquinol oxidase, one of two ubiquinol oxidases in *E. coli*, contains four protein subunits with molecular weights of 58K, 33K, 22K, and 17K. The complex catalyzes the two electron oxidation of ubiquinol-8 and the reduction of molecular oxygen to water. The primary sequences of all four subunits have been determined, but the substrate binding site has not been investigated. The photoreactive, radiolabeled azido-ubiquinone derivative, [^{3}H]-3-azido-2-methyl-3-methoxy-6-geranyl-1,4-benzoquinone, (azido-Q), which has been widely used in locating ubiquinone binding sites in other proteins, was used to identify the binding site of this enzyme. When reduced by dithioerythritol, the azido-Q functions as substrate with partial effectiveness, suggesting that azido-Q binds to the substrate binding site of this oxidase. When cytochrome *bo* ubiquinol oxidase is incubated with an eight fold molar excess of azido-Q, ten minutes of illumination with UV yields a 50% loss of activity. Uptake of the radiolabeled azido-Q correlates with the photoinactivation. Analysis of the distribution of radioactivity among subunits after separation by SDS-PAGE shows subunit II is heavily labeled, but not the other subunits. This suggests that the ubiquinone binding site of this complex is on subunit II. HQNO and ubiquinol-1 decrease the azido-Q labelling upon illumination demonstrating competition for the binding site as would be expected. This work was partially supported by a grant from NIH (GM 30721 to CAY) and DOE (DOE DEFG 02-87ER13716 to RBG).

Th-Pos47

SPECTROSCOPIC STUDIES ON "MONOMERIC" CYTOCHROME *c* OXIDASES FROM SHARKS ((Jim Peterson, David E. Holm, Linda L. Pearce, Gerald Godette, Celia Bonaventura and Joseph Bonaventura)) The University of Alabama, University of Alabama at Birmingham, Duke University Marine Laboratory (Spon. by L.L. Pearce)

Cytochrome *c* oxidases isolated from sharks have the same fundamental functional and structural properties as the enzyme isolated from mammalian sources, except that they do not show any tendency to aggregate in solution. This makes them a better experimental system than the commonly employed beef heart enzyme with which to study the general characteristics of cytochrome *c* oxidases. The enzyme purified from the Atlantic sharpnose shark exhibits electronic spectral features which show a complicated dependence on pH, type of detergent present and ionic strength. These results will be discussed in relation to plausible mechanisms of proton translocation in cytochrome *c* oxidase

Th-Pos48

ELECTRON TRANSFER BETWEEN THE OXYFERRYL HEME Fe(IV) AND Trp 191 IN CYTOCHROME c PEROXIDASE COMPOUND II. ((R.Liu[1],S.Hahm[1],M.Miller[2],L.Geren[1],S.Hibdon[1],J.Kraut[2], B.Durham[1], and F.Millett[1])) [1]Department of Chemistry and Biochemistry,University of Arkansas,Fayetteville, AR72701 and [2]Department of Chemistry, University of California,San Diego,La Jolla,CA92093.

The pH dependence of the reaction of yeast cyt c peroxidase with horse cyt c derivatives labeled at specific lysine amino groups with(dicarboxybipyridine)(bisbipyridine) ruthenium(II) was studied by flash photolysis. The rate constant of intramolecular electron transfer from the indole ring of Trp-191 to the oxyferryl heme was 1100s^{-1} at pH5,and was decreased with increasing pH. Stopped-flow spectroscopy studies showed that yeast cyt c reduces the radical in compound I with a rate constant of 2 x 10^8 $M^{-1}s^{-1}$ at pH 6 and 400 mM ionic strength. A second molecule of cyt c then reduces the oxyferryl heme in compound II (CPMII) with a rate constant of 3.0 x 10^7 $M^{-1}s^{-1}$. The role of Met-230 in cyt c peroxidase was also studied by using M230I Mutant. The results are consistent with a mechanism in which cyt c first reduces the radical on Trp-191 to form CMPII (IV,R),followed by conversion to CMPII(III,R·). (This work was supported in part by NIH Grant NIH GM20488).

Th-Pos49

CRYSTAL STRUCTURE OF THE CHLOROPLAST CYTOCHROME f REVEALS A NOVEL CYTOCHROME FOLD AND UNEXPECTED HEME LIGATION ((Sergio E. Martinez, Deru Huang, Andrzej Szczepaniak, William A. Cramer, and Janet L. Smith)) Dept. of Biological Sciences, Purdue University, West Lafayette, IN 47907

The cytochrome b_6f complex connects the two reaction center complexes in oxygenic photosynthesis. The crystal structure of the reduced redox-active 252 residue lumen-side domain of the 285 residue cytochrome *f* of the b_6f complex has been solved by multiple isomorphous replacement and anomalous scattering to a resolution of 2.3 Å. In addition to being the first polypeptide of the b_6f or bc_1 complexes to be solved crystallographically, the structure has unique aspects and major features: (i) Unlike all other *c*-type cytochrome structures that consist of one predominantly alpha helical domain, cyt *f* contains two domains in an elongate (75 Å x 35 Å x 24 Å) structure whose defined secondary structure is mostly beta sheet. (ii) The covalently bound heme lies within the larger domain near the interface between the two domains, its iron 45 Å from the C-terminal residue that is connected to the trans-membrane alpha-helix. (iii) The smaller domain (residues 169 - 231) contains a positively charged region that includes Lys 187, 28 Å from the heme Fe, which was previously shown to cross-link to plastocyanin. (iv) The axial sixth heme ligand is the alpha amino group of the N-terminal tyrosine residue. This implies that the redox center cannot be assembled until translocation of cyt *f* has proceeded sufficiently through the thylakoid membrane for the signal peptide to be cleaved. (v) The larger domain has the fibronectin type III domain fold found in many animal proteins. This fold has not been previously found in a plant protein.

Th-Pos50

NEAR-INFRARED SPECTRAL CHANGES OF CYTOCHROME aa_3 DURING POTENTIOMETRIC TITRATIONS.

((R.W. Hendler[a], P.A. Harmon[b], and I.W. Levin[b]))
[a]Laboratory of Cell Biology, NHLBI and [b]Laboratory of Chemical Physics NIDDK, NIH, Bethesda, MD. 20892.

Optical absorbance at 830 nm is often taken as a measure of the amount of Cu_A present in preparations of cytochrome aa_3. Although it is known that some of the signal is due to cytochrome a_3, the percent of spectral contamination is considered minimal. Our results confirm that a difference spectrum with a broad absorbance feature near 830 nm does arise during oxidation, and that it displays Nernst-like titration behavior with an apparent E_m near 250 mV. To obtain a clearer picture of the extent of overlap of spectra in the near-infrared region, singular value decomposition (SVD) has been applied to potentiometric titrations. We find significant spectral contributions from both cytochromes a and a_3, the former contributing to a trough near 750 nm and the latter to a trough near 705 nm and a peak near 775 nm in the difference spectra. A titratable species with a unique spectrum having a peak absorbance at 830 nm was not resolved by SVD. On the basis of the current results, it is concluded that in the absence of other independent information, it is risky to attribute the absorbance at 830 nm solely (or even mostly) to Cu_A.

Th-Pos51

CHARACTERIZATION OF CYTOCHROME *b*-c_1 COMPLEX SUBUNIT IV DEFICIENT MUTANTS OF RHODOBACTER SPHAEROIDES.

(Yeong-Renn Chen, Shigeyuki Usui, Chang-An Yu, and Linda Yu), Department of Biochemistry & Molecular Biology, Oklahoma State University, Stillwater, OK 74078.

Rhodobacter sphaeroides mutants lacking subunit IV (Mr=14,384) of the cytochrome *b*-c_1 complex (*b*-c_1) have been constructed by site-specific recombination between the wild-type genomic subunit IV structural gene (*fbc*Q) and a suicide plasmid containing a deletion in *fbc*Q. Southern blot analysis confirmed that the wild-type *fbc*Q gene was exchanged for the defective *fbc*Q gene. Isolates with the *fbc*Q deletion (representative strain: RSΔIV-2) give rise to a photosynthetically competent phenotype after an adaptation time of 34 to 52 hours. The chemical compositions, spectral properties, and ubiquinol-cytochrome *c* reductase activities in chromatophores prepared from wild-type and adapted RSΔIV-2 cells were similar. However, the apparent K_m for Q_2H_2 of ubiquinol-cytochrome *c* reductase in chromatophores from adapted RSΔIV-2 cells was ten times higher than that in chromatophores from wild-type cells. Although the *b*-c_1 activity in chromatophores of adapted RSΔIV-2 cells is more labile to detergent treatment than that in wild-type chromatophores, it can be purified by the methods developed for the wild-type cells. The purified *b*-c_1 complex (three-subunits) from RSΔIV-2 had a specific activity only one-fourth of that measured for the wild-type *b*-c_1 complex (four-subunits). The low activity is accompanied by an increase of the apparent K_m for Q_2H_2 from 4 μM to 10 μM, suggesting that subunit IV may play a role in quinone binding. This work was partially supported by a grant from NIH (GM 30721).

DNA REPLICATION/CHROMATIN

Th-Pos52

THE EFFECTS OF UNPAIRED BASES IN AN OLIGO DEOXY(A)•DEOXY(T) TRACT ON DNA BENDING

((Vasavi Malineni, Darryl A. LeBlanc and Kathleen M. Morden))
Dept. of Biochemistry, Louisiana State University, Baton Rouge, LA 70803

Other investigators have studied DNA bending in oligonucleotides based on anomalous gel migration of DNA sequences containing oligo d(A)•d(T) tracts and unpaired bases. These studies have shown that the presence of a d(A)•d(T) tract that is in phase with the helical repeat causes additive bending in DNA. Bending is also caused by the presence of unpaired bases in DNA. We are using gel electrophoresis to investigate bending in a series of oligonucleotides containing unpaired bases surrounded by an oligo d(A)•d(T) tract. The local structure of unpaired bases in related oligonucleotides has been determined using NMR. Shown below is the monomer unit that is ligated to construct the multimer repeats, where X=G, Z=C or X=G, Z=no base or X=no base, Z=G:

```
5′      ATGTGCAAXAAGCGACTCGGC 3′
3′ GCCGTACACGTTZTTCGCTGA      5′
```

Thus, we are able to compare the migration of oligonucleotides containing unpaired bases with the migration of a sequence which contains an (A)4•(T)4 tract or an interrupted (A)4•(T)4 tract. The results of these studies will be discussed and compared to the local structures as determined by NMR.

Supported by NIH grant GM38137 & a fellowship from the Howard Hughes Medical Institute to V.M.

Th-Pos53

TEMPERATURE-DEPENDENT SMALL ANGLE X-RAY SCATTERING OF A 45-MER DUPLEX WITH A-TRACTS IN SOLUTION

((S.S. Chan[a], D. Kergil[b], J. Trewhella[b], R.H. Austin[c], K. J. Breslauer [a] and M.E. Hogan[d])) [a]Dept Chem., Rutgers University, Piscataway, NJ 08855; [b]Los Alamos Nat. Lab., Los Alamos, NM 87545; [c]Dept. Physics, Princeton U, Princeton, NJ 08544, [d]Center Biotech., Baylor Coll. of Med., Woodlands, TX 77381

Phased A-tracts are one of the more extreme examples of how DNA sequence influences the large-scale structure of the double helix: it is believed that the presence of A-tracts phased to the helix repeat of 10.4 bp/turn results in a bent DNA molecule. However, there is strong evidence that there is a premelting structural transition in sequences with phased A-tracts which could be responsible for the bending of the helical duplexes: above the transition, with a mid-point temperature centered at about 37°C, DNA duplex with A-tracts is not bent. To test this we have completed temperature-dependent **solution small angle X-ray scattering** (SAXS) of a 45 bp duplex containing four phased segments of $(dA)_5$-tract comparing with a randomized sequence isomeric duplex. There is no change of the SAXS data for the randomized duplex, but there is a definite change for the phased duplex between 15°C and 55°C. Modeling calculations are underway which should reveal the detailed nature of the structural transition.

Th-Pos54

DYNAMIC LIGHT SCATTERING FROM MONODISPERSE CIRCULAR DNA: IONIC STRENGTH DEPENDENCE.

((Jay Newman†, John Tracy††, and Robert Pecora††)) †Department of Physics, Union College, Schenectady, NY 12308 †† Department of Chemistry, Stanford University, Palo Alto, CA 94305

Monodisperse 2311 base pair circular DNA was studied over a range of ionic strengths from 0.01 to 1 M using dynamic light scattering techniques. Autocorrelation functions were analyzed using the inverse Laplace transform method (CONTIN). Above the lowest scattering angle studied (33°), generally two peaks were seen in the distribution of decay rates. The translational diffusion coefficient, corresponding to the slower of the peaks, at a DNA concentration of 100 μM was found to be 4.52 ± 0.07, nearly independent of added NaCl, using a buffer of 10 mM Tris, 1 mM EDTA, at pH 8.0. The mean relaxation frequency of the first internal mode decreases by a factor of two with decreasing ionic strength. The amplitude of this mode, when plotted as a function of the square of the reduced scattering vector length, $q^2R_g^2$, lies on the same curve at all ionic strengths studied. Calculation of the radius of gyration as a function of ionic strength is based on a scaling argument (J. Seils and R. Pecora, Macromolecules 25:354-362, 1992) and shows a 25% increase from 65 nm as the ionic strength is decreased over the range of study. (This work was supported by National Science Foundation grant CHE-9119676 to R.P. and DMB 8905906 to J.N.)

Th-Pos55

THE EFFECT OF pH ON REACTIONS CATALYZED BY REVERSE TRANSCRIPTASE FROM HIV-1.

((T. Fujimori and K.A. Johnson)) Dept. of Mol. and Cell Biology, The Pennsylvania State University, University Park, PA 16802

The rates of incorporation of dTMP onto a 25mer primer/36mer template by reverse transcriptase and of the reverse reaction, pyrophosphorolysis, were measured in single turnover experiments at various pH. The rate of polymerization increased with increasing pH: a plot of log k_{ss} versus pH has a slope of 1 in the pH range of 7-9 and a slope of 0 at pH>9. A plot of log k_{ss}/K_{ss} versus pH for the pyrophosphorolysis reaction was bell-shaped with a maximum rate at pH 7. Analogous experiments at saturating concentrations of inorganic pyrophosphate were hampered by the low solubility of Mg·PPi; however, a similar bell-shaped curve was also observed at high concentrations of PPi (10 mM).

In the forward reaction, the 3′ hydroxyl of the primer strand of DNA acts as a nucleophile toward the α-phosphate of dTTP. This nucleophilic attack should be base catalyzed because the protonated 3′ oxygen is a poor nucleophile. In the reverse reaction, PPi acts as a nucleophile toward the phosphate of the 5′ dTMP at the 26th position of the primer strand of DNA. This nucleophilic attack should be acid catalyzed because the unprotonated 3′ oxygen is a poor leaving group. Our observations support these predictions between pH 7-9: the rate of the polymerization reaction increases with increasing pH, which is consistent with base catalysis, while the rate of the reverse reaction decreases with increasing pH, which is consistent with acid catalysis. These data suggest that deprotonation of the 3′ hydroxyl is associated with the rate limiting step for the polymerization reaction; the protonation of this 3′ oxygen is associated with the rate limiting step for the reverse reaction. Supported by Grants GM44613 and GM14590 from NIH.

Th-Pos56

INHIBITION PATTERN OF REVERSE TRANSCRIPTASE BY NON-NUCLEOSIDE INHIBITORS. ((R. A. Spence[1], W. M. Kati[2], and K. A. Johnson[1])) [1]Pennsylvania State University, University Park, PA, 16802, and [2]Abbott Laboratories, Abbott Park, IL 60064.

The mechanism of inhibition of Reverse Transcriptase (RT) by three non-nucleoside compounds was determined by applying rapid chemical quench techniques to observe the incorporation of dNMP into DNA. The K_d values for the interaction of the RT•DNA complex with O-TIBO, Cl-TIBO, and Nevirapine were determined to be 3.2 μM, 0.3 μM, and 20 nM. The rates for the binding of these inhibitors were determined to be slow (~10^4 $M^{-1}s^{-1}$). In the presence of 10 mM Mg^{2+} the RT•DNA complex showed a decreased affinity for these non-nucleoside inhibitors. A decrease in the association rates was observed in the presence of Mg^{2+} whereas, the dissociation rates were not affected. This observation is consistent with an interaction between the metal and inhibitor binding sites. We attribute the observed polymerization rate in the presence of saturating amounts of inhibitor to slow turnover of the inhibited RT•DNA complex. The overall catalytic pathway of RT in the presence of these non-nucleoside inhibitors will be presented. (Supported by NIH grant GM 44613).

Th-Pos57

KINETIC ANALYSIS OF PORCINE LIVER DNA POLYMERASE γ. ((S. W. Graves and K.A. Johnson,)) Dept. of Molecular &Cell Biology, 106 Althouse Laboratory, Pennsylvania State University, University Park, PA. 16802.

Porcine liver mitochondrial DNA polymerase (DNA polymerase γ) exists in native form as an enzyme with a mass of 160kD and is thought to consist of two subunits with masses of 48kD and 120kD. This enzyme has both polymerase and 3'-5' exonuclease functions (Kunkel, *et al.*,1989, *Biochemistry* **28**, 988-995) although the enzyme is strongly inhibited by chain terminating nucleotide analogs. (Mosbaugh, 1988, *Nucleic Acids Research* **16**, 5645-5659). Inhibition of DNA polymerase γ is thought to be an important factor in contributing to the toxicity of AZT in AIDS treatment. Utilizing pre-steady state kinetics, we have begun investigations into subunit composition and function of DNA polymerase γ. Assays based on single nucleotide incorporation of dNMPs into a synthetic primer-template suggest that both a small (48kD) and large subunit (120kD) are required for tight binding of DNA polymerase γ to DNA. Incorporation of dTMP into the primer-template occurs with a burst followed by a slower linear phase. Further investigations will be directed to understand the specific functions of each subunit, to elucidate the kinetic mechanism of the correct nucleotide incorporation, and to study the inhibition of the enzyme by nucleotide analogs. (Supported by Grants GM44613 and GM08358-03)

Th-Pos58

MOLECULAR DETERMINANTS OF THE POL-EXO TRANSITION IN THE COMPLEX OF DNA WITH KLENOW FRAGMENT.
((D. P. Millar and T.E. Carver)) Department of Molecular Biology, The Scripps Research Institute, 10666 North Torrey Pines Road, La Jolla, CA 92037.

The Klenow fragment of DNA pol I contains a 5'-3' polymerase and a 3'-5' exonuclease in the same polypeptide chain. The latter activity is involved in proofreading bases misincorporated by the polymerase. We have examined the distribution of DNA between the polymerase and exonuclease sites using time-resolved fluorescence spectroscopy of dansyl probes covalently attached to DNA seven bases from the primer terminus. Although the structure of DNA bound at the exo site has been determined, the inter- and intra-molecular mechanisms of shuttling between the pol and exo sites remain unclear, and the effects of protein and DNA structure upon the tendency of DNA to occupy a particular site have not been resolved. Since the protein's DNA footprint shifts as DNA termini move from the pol site to the exo site, altering the environment of the dansyl probe, we can resolve the contributions of various factors to this aspect of proofreading discrimination. We examined the effects of different divalent ions, nucleotide mono- and tri-phosphates, varying DNA sequence and structure, mismatched base-pairs and site-specific mutations in Klenow fragment upon the distribution of DNA between the pol and exo sites. These studies help to clarify the nature of the protein-DNA interactions in each site and the mismatch recognition mechanisms that control the pol-exo transition.

Supported by NIH grant GM44060 and NRSA fellowship GM15729.

Th-Pos59

PARTITIONING OF T4 POLYMERASE BOUND DNA BETWEEN POLYMERASE AND EXONUCLEASE SITES: A STOPPED FLOW KINETIC AND TIME RESOLVED FLUORESCENCE DYNAMICS STUDY. ((M.R. Otto[1], L.B. Bloom[2], R. Eritja[3], L. Reha-Krantz[4], M.F. Goodman[2], J.M. Beechem[1])) [1]Vanderbilt University, Nashville, TN, [2]University of Southern California, Los Angeles, CA, [3]CID-CSIC, Barcelona, Spain, [4]University of Alberta, Edmonton, Alberta.

Do polymerases with exonuclease and polymerase activities in a single domain bind preferentially to DNA at a single functional site or does an equilibrium exist? What physical states exist during the process of binding and subsequent polymerization and/or excision? We are investigating these questions with bacteriophage T4 DNA polymerase(T4) and primer/template(P/T) DNA with the fluorescent nucleotide 2-aminopurine monophosphate (dAPMP) at the 3' primer end. Studies were conducted using mispaired and correctly paired DNA as well as single site T4 polymerase mutants with mutations in proposed polymerase or exonuclease active sites. Time-resolved experiments of various bound complexes were performed to determine primer base psec/nsec mobilities. Fluorescence of dAPMP in DNA is quenched, allowing stopped flow kinetic experiments of dAPMP excision to be performed by monitoring changes in dAPMP fluorescence. Results showed complex multiphasic kinetics. The stalled *wt* T4-DNA complex with dAPMP at the 3' position of the P/T (Mg^{2+} absent) is very nearly as fluorescent as free dAPMP. Placing dAPMP in the penultimate 3' position nearly abolishes this enhancement, suggesting the terminal dAPMP is singly sequestered within one of the two binding sites. Bound complexes containing exonuclease site mutant T4 have decreased dAPMP fluorescence intensity whereas a polymerase site mutant T4 does not. Addition of the next nucleotide triphosphate significantly decreases fluorescence of the polymerase mutant T4-DNA complex. These results suggest 3' dAPMP is preferentially bound at the exonuclease site.

Th-Pos60

FLUORESCENCE SPECTROSCOPIC STUDIES OF NUCLEOTIDE BINDING SITES OF *E. coli* PRIMARY REPLICATIVE HELICASE DnaB PROTEIN.
((Wlodzimierz Bujalowski and Malgorzata Maria Klonowska)) Department of Human Biological Chemistry & Genetics, The University of Texas Medical Branch Galveston, Galveston, Texas 77555-0653

Nucleotide binding sites on *E. coli* primary replicative helicase DnaB protein are key elements in the mechanism of the enzyme's functioning in DNA replication. The nature of the environment near the base, and the ribose binding regions has been studied using nucleotide analogs bearing fluorescence modification at two different locations, the base (1,N^6-ethenoadenosine diphosphate (εADP)) and 2'- and 3' hydroxyls of the ribose ring, (2'(3')-O-(2,4,6-trinitrophenyl)adenosine 5'-diphosphate (TNP-ADP) and 3'-O-(N-Methylantraniloyl)-5'-diphosphate (MANT-ADP)).
Steady-state fluorescence and emission-polarization studies indicate that the base has a substantial mobility when bound to the proteins and is located in relatively polar environments. The fluorescence of εA is characterized by single lifetime of 24.8 ns which is not changed upon binding.
In contrast, fluorescence anisotropy of the labels (TNP and MANT) attached to the ribose is very close to the theoretical one for a completely immobilized chromophore, indicating that the ribose is held very rigidly. The fluorescence intensity of bound TNP and MANT groups is increased several times and the fluorescence emission spectra are blue shifted, compared to the free nucleotides in solution, indicating that the ribose ring is located in a hydrophobic environment.
Fluorescence quenching studies, using external collisional quenchers, indicate substantial burial of both base and ribose binding sites within the protein matrix; however, the ribose binding site has significantly less accessibility to the solvent when compared to the base binding region. A functional significance of these studies for the free energy transduction by the DnaB helicase is discussed.

Th-Pos61

THE BACTERIOPHAGE T4 DNA REPLICATION PRIMOSOME: STOICHIOMETRY, STRUCTURE, AND MOLECULAR INTERACTIONS
((F. Dong[1], E. P. Gogol[2], and P. H. von Hippel[1])) [1] Inst. of Mol. Biol., Univ. of Oregon, Eugene, OR 97403; and [2]Prog. in Mol. and Cell Biol., Univ. of Texas at Dallas, Richardson, TX 75083.

The T4 DNA replication system can be used to examine coordinated interactions between and within functional macromolecular complexes. In this system two subassemblies, the "holoenzyme" (comprising the DNA polymerase and a three protein processivity complex), and the "primosome" (comprising the replication helicase and primase), interact with the single-stranded DNA binding protein to accomplish both leading and lagging strand DNA synthesis at physiological rates and fidelities.

The primosome catalyzes the unwinding of the double-stranded DNA ahead of the replication complex to expose the templating strands, and also lays down RNA primers for lagging strand DNA synthesis. We have applied physical biochemical and cryoelectron microscopic techniques to study the stoichiometry, the association states, and the structural properties of the complexes formed by the helicase and the primase on various DNA template constructs. Results from these studies (in combination with our previous data on the association states and structures of the helicase protein) demonstrate that each complex formed by these two proteins on DNA templates consists of one primase and six helicase molecules. The conformations of these complexes and the molecular interactions involved in assembling the protein and DNA components into a working primosome will be discussed.

Th-Pos62

TRYPTOPHAN RADICALS FORMED BY IRON/OXYGEN REACTION WITH *E. COLI* RIBONUCLEOTIDE REDUCTASE PROTEIN R2 MUTANT Y122F. ((M. Sahlin[a], G. Lassmann[b], S. Pötsch[b], A. Slaby[a], B.-M. Sjöberg[a] and A. Gräslund[c])) [a]Dept. of Molecular Biology, [c]Dept. of Biophysics, Stockholm University, S-106 91 Stockholm, Sweden, and [b]Max-Delbrück-Center of Molecular Medicine, D-13122 Berlin-Buch, Germany.

Ribonucleotide reductase catalyses the reduction of ribonucleotides to the corresponding deoxyribonucleotides, necessary for DNA synthesis. The small subunit of iron-containing ribonucleotide reductases, protein R2, contains a diferric iron center and a stable free radical on a tyrosine residue (Y122) in its native state. The iron/radical site is formed in apoprotein R2 by a redox reaction with ferrous iron and oxygen. The present study concerns the corresponding reaction in a mutant apoprotein R2, Y122F, which lacks the essential Y122. The normal iron center is formed, but the reduction equivalent from Y122 now must be supplied elsewhere. We have followed the reaction by low temperature EPR and room temperature stopped flow EPR and have observed several para-magnetic transients on the < sec to minute time scale. Using incorporated deuterium-labeled tryptophan we have found at least two species which can be assigned to oxidized tryptophan radicals. The results show that tryptophans are easily oxidizable in a protein when a strong oxidation potential is created in its interior. The oxidized states exist on the minute time scale in the absence of external reductants. Their sites may represent potential participants in electron transport pathways needed for the enzymatic function.

Th-Pos63

COMPLEX FACTORS INVOLVED IN THE TURBIDITY OF SUSPENSIONS OF ISOLATED NUCLEI. ((A. Prado, C. Puyo, J. Arlucea, F.M. Goñi and J. Aréchaga)) Departaments of Cell Biology and Biochemistry, University of the Basque Country, P.O. Box 644, E-48080 Bilbao, Spain. (Spon. by E. Padrós).

The turbidity of a suspension of isolated nuclei from tissue homogenates is a complex case of non-Rayleigh scattering. Among the factors that may contribute to an increase in turbidity we have characterized: cation-dependent chromatin condensation, thermal denaturation of chromatin, nuclear shrinking, and changes in the optical properties of the membrane bilayer. Chromatin condensation increases particle in-homogeneity, thus increasing the scattering. Nuclear size decreases concomitantly with an increase in turbidity, in the presence of magnesium ions; this effect does not appear to be osmotic in origin, but will contribute to the observed magnesium-dependent increase in turbidity. Finally, both magnesium ions and sucrose appear to have non-osmotic effects on the turbidity of membrane suspensions, probably consisting of changes in phospholipid conformation within the bilayer, in one case because of electrostatic binding to polar headgroups, in the other because of changes in the environmental polarity.

Th-Pos64

A MODEL FOR DNA ARRANGEMENT IN MULTIVALENT CATION TOROIDAL CONDENSATES. ((N.V. Hud, K.H. Downing and R. Balhorn)) Biology and Biotechnology Research Program, Lawrence Livermore National Laboratory, Livermore, CA 94550, Life Science Division, Lawrence Berkeley Laboratory, Berkeley, CA 94720

When DNA is condensed by multivalent cations such as spermidine, hexammine cobalt (III) or protamine, toroidal and rod-like condensates are frequently observed. Toroids typically measure 900Å in outer diameter with a 200Å diameter hole. The rod-like structures are usually 1800Å long and 300Å wide. These dimensions are relatively independent of the length of DNA being condensed. EM images have revealed that some toroids are not perfectly circular, but appear kinked with oval holes. If the DNA in such toroids was wound in a spool-like fashion, the local radius of curvature near the center would be significantly less than the radius of curvature of free DNA in solution, indicating a localized energy requirement for DNA bending during condensation. We present a novel model for toroid generation, that accounts for the ratio of outer to inner toroid diameter and describes the origin of kinks. Furthermore, no DNA within these model toroids is expected to experience high bending energies. The model toroid is generated by assuming that the DNA with in a toroid can be depicted as a series of 400bp loops, these loops pack together in a fashion such that they process about a central axis, which is the center of the toroid hole. This model also suggests a reason why the rod-like structures are more favored over toroids for shorter pieces of DNA.

This work was conducted under the auspices of the U.S. Department of Energy Contract W-7450-ENG-48

GENE REGULATION AND TRANSCRIPTION

Th-Pos65

CONTEXT DEPENDENCE OF INTERACTIONS IN *LAC* REPRESSOR-OPERATOR COMPLEXES

Diane E. Frank and M. Thomas Record, Departments of Biochemistry and Chemistry, University of Wisconsin, Madison, WI 53706

The thermodynamic properties of the molecular interactions contributing to specificity in *lac* repressor-operator complexes are being examined in a series of symmetrical *lac* operator variants differing at one or more symmetrical positions. The equilibrium binding constants for the variant operators span the entire 10^7-fold range between specific and nonspecific binding of *lac* repressor (0.15M KCl, 24°C). An energetic penalty ($\Delta\Delta G$) of 3-5 kcal/mol results from the introduction of a single symmetric base pair substitution into the ideal symmetric *lac* operator contained on a 40 base pair synthetic DNA fragment. However, if introduced in the context of a second substitution, the energetic penalty is not as severe ("non-additive") and is dependent on the nature of the second substitution, in aggrement with the observations of Lesser, *et al.* (1) for the EcoRI system. Mossing and Record (2) and Lesser, *et al.* (1) proposed that such non-additive free energy effects resulted from adaption at the protein-DNA interface to optimize complementarity of contacts between functional groups of the nucleotide bases of variant DNA sequences and the corresponding amino acid residues. We are investigating the dependences of these interactions on univalent salt concentration and temperature to assess the roles of the polyelectrolyte and hydrophobic effects in adaptability and context dependence from protein-DNA interactions.

1. Lesser, D.R., Kurpiewski, M.R., and Jen-Jacobson, L. (1990) *Science* **25**, 776-786.
2. M.C. Mossing and M.T. Record (1985) *J.Mol.Biol.* **186** 295-305.

Th-Pos66

HYDRATION EFFECTS ON DNA-PROTEIN INTERACTIONS

((D.C. Rau[1] and M.M. Gamer[2])) [1]NIDDK and [2]NICHD, NIH, Bethesda, MD 20892

The binding of a gene regulatory protein to DNA brings together two complementary surfaces. When the two macromolecules bind, some interactions with the milieu are lost, and new interactions with the complementary surface formed. In addition, DNA-mediated protein-protein interactions (*e.g.* DNA looping), are an important part of the biological activity of most transcriptional regulators. Varying the solution osmotic pressure (by adding high concentrations of a small molecule solute) allows one to determine the the total number of water molecules released upon prtoein-DNA complex formation. Association equilibrium constants for either the *gal* repressor-operator interaction or the Catabolite Activator Protein (CAP)-*gal* promoter interaction were measured by titration of a fixed concentration of an end-labelled DNA fragment (containing one or two binding sites) and varying protein concentration with increasing osmotic pressure. The amounts of both free and complexed DNA are quantitated by electrophoresis on non-denaturing gels. Molar concentrations of several different neutral solutes drastically increases the extent of binding of the *gal* repressor protein to a DNA fragment containing two *gal* operator sites. Quantitative analysis shows that the binding of the first protein molecule is accompanied by the release of approximately 80-120 water molecules from the complex on formation. The binding of the second repressor is highly cooperative in the presence of an osmolyte. When the second protein molecule binds, another 150-200 water molecules are released.. This extr a water release strongly suggests that either a protein mediated loop structure, which has been predicted to occur based on genetic evidence, but has never been observed before *in vitro*, is induced by the addition of osmolyte. When the CAP protein binds to its site in the *gal* promoter, approximately 55 waters are released: this is consistent with its smaller size (MW 45,000 as opposed to MW 65,000 for the gal repressor), and correspondingly smaller DNA binding site.

Th-Pos67

RAPID-REACTION KINETICS STUDIES OF THE INTERACTION OF GAL AND LAC REPRESSORS WITH DNA. ((M. Hsieh and M.D. Brenowitz)) Department of Biochemistry, Albert Einstein College of Medicine, Bronx, NY 10461.

Transcriptional regulation in both prokaryotes and eukaryotes requires the binding of regulatory proteins to specific DNA sequences. DNA-binding involves a multi-step process whereby a protein binds non-specifically to DNA and translocates to a specific site by one-dimensional diffusion via intra- and inter-segmental transfer mechanisms [O.G. Berg, R.B. Winter & P.H. von Hippel, *Biochemistry 20*, 6929-6948, 1981]. This facilitated translocation enables the protein to bind its target at faster than a diffusion-determined rate.

Kinetics studies using the *E. coli* Lac repressor and a dimeric mutant of the protein have provided evidence for the facilitated translocation mechanisms [R.B. Winter, O.G. Berg & P.H. von Hippel, *Biochemistry 20*, 6961-6977, 1981; T. Ruusala & D.M. Crothers, *PNAS 89*, 4903-4907, 1992]. However, questions remain as to the relative contribution of the various modes of facilitated translocation. In order to study the kinetics of association between DNA-binding protein and DNA, we have developed a method that combines rapid-reaction kinetics with a DNase I footprint assay. Using this method, we are able to measure the association rate at individual sites when multiple sites are present. The low dead-time ($\approx$ 100 msec) of the method allows analysis of interactions over a wider range of protein concentrations than previously possible.

Using this method, *E. coli* Gal repressor exhibits association rate enhancement at lower salt concentrations, suggestive of underlying salt-dependent facilitated mechanism [$k = (1.2 \pm 0.4) \times 10^8$ M^{-1} sec^{-1} (50 mM KCl) and $(4.2 \pm 1.5) \times 10^7$ M^{-1} sec^{-1} (100 mM KCl)]. We compare the kinetics of association of Gal repressor, Lac repressor and a Lac repressor dimeric mutant to single- and multiple-operator DNAs in order to resolve the contributions of various modes of facilitated translocation. (Supported by grants from the Hirshl-Weill Caulier Trust, American Cancer Society and NIH training grant F31-GM13850.)

Th-Pos68

SELF-ASSOCIATION AND DNA BINDING IN λ cI REPRESSOR N-TERMINAL DOMAINS. ((David L. Bain and Gary K. Ackers)) Department of Biochemistry and Molecular Biophysics, Washington University School of Medicine, St. Louis, MO 63110.

A research program of this laboratory has focused on thermodynamic studies of the interactions of cI repressor with the right operator region of bacteriophage λ (see Koblan, K.S., & Ackers, G.K. (1992) *Biochem. 31*, 57-65 and references therein). To understand better the nature of cooperativity and site-specificity in the various protein-DNA assemblies of this system, the interactions of cI amino terminus (the DNA binding domain) with O_R were studied as a function of temperature, pH, and salt. This study has included: (a) quantitating the binding and cooperative free energies, and (b) determining the states of protein aggregation. Self-assembly of N-terminal domains was studied using sedimentation equilibrium. Self-assembly was modelled best as a monomer-dimer-tetramer reaction. N-terminal domains undergo a monomer-dimer transition that is independent of pH and KCl. The enthalpy of dimerization was large and positive, in sharp contrast to that of intact repressor (Koblan, K.S., & Ackers, G. K. (1991) *Biochem. 30*, 7817-7821). The energetics of N-terminal domains binding to O_R were determined using quantitative DNase I footprint titration (Brenowitz, M., *et al.* (1986) *PNAS 83*, 8462-8466). Binding was found to be non-cooperative under all conditions. Binding to all three sites was accompanied by negative enthalpies (large at site 1, small at sites 2 and 3), by release of ions, and by differential absorption of protons. The origins of these effects will be discussed. (Supported by NIH Grant GM 39343.)

Th-Pos69

MUTATIONS IN THE C-TERMINAL DOMAIN OF λ cI REPRESSOR REDUCE OR ELIMINATE COOPERATIVE INTERACTIONS. ((David S. Burz and Gary K. Ackers)) Department of Biochemistry and Molecular Biophysics, Washington University School of Medicine, St. Louis, MO 63110.

Lambda cI repressor dimers bind with 2.5-3 kcal/mol of cooperative free energy to the tripartite right operator (O_R) [Johnson *et al.*, (1981) *Nature* **294**, 217; Brenowitz *et al.*, (1986) *Methods Enzymol.* **130**, 132]. Quantitative modeling has suggested that cooperativity is required for maintenance of the lysogenic state and for efficient switching to lytic growth [Ackers *et al.*, (1982) *PNAS* **79**, 1129; Shea and Ackers, (1985) *J. Mol. Biol.* **181**, 211]. Cooperativity and self-association involve protein-protein contacts between C-terminal domains of the repressor molecule [Pabo *et al.*, (1979) *PNAS* **76**, 1608]. To address the role of C-terminal domains in mediating oligomeric properties, a genetic screen was used to select repressor mutants defective in these interactions [Beckett *et al.*, (1993) *Biochemistry* **32**, 9073]. Repressor dimerization constants were determined along with free energies of O_R binding and cooperativity. This was done for eight mutant repressors, each containing an amino acid substitution in the C-terminal domain or in the linking segment between domains. The majority of mutants were found to dimerize with similar energetics to wild type. DNAse I footprint titrations of binding to wild type and reduced valency O_R DNA [Koblan *et al.*, (1992) *Methods Enzymol.* **201**, 405] indicated that the intrinsic free energies of binding for the mutants are similar to wild type. Cooperative energies span a range of values from fully cooperative to complete elimination of pairwise cooperativity. (Supported by NIH grant GM-39343.)

Th-Pos70

CALORIMETRIC ANALYSIS OF λ cI REPRESSOR BINDING TO DNA OPERATOR SITES. ((Eddine Merabet and Gary K. Ackers)) Dept. of Biochemistry and Molecular Biophysics, Washington University School of Medicine, St. Louis, MO 63110.

The enthalpies of binding cI repressor to bacteriophage λ right operator DNA have been measured using Isothermal Titration Calorimetry. At 20°C, the association of wild type cI with single-site (21bp) synthetic operator DNA containing specific sequences O_R1, O_R2, or O_R3 is characterized by $\Delta H_1 = -21.8 \pm 1.6$ kcal/mol, $\Delta H_2 = -15.9 \pm 1.5$ kcal/mol and $\Delta H_3 = -18.1 \pm 1.7$ kcal/mol, respectively. By comparison, non-specific binding yields an enthalpy of only -2.0 ± 0.6 kcal/mol. These values are in good agreement with the van't Hoff enthalpies determined by quantitative footprint titrations (Koblan, K.S., & Ackers, G.K. (1992) *Biochem.* **31**, 57-65). Additionally, GD147, a mutant containing a single amino acid change (Gly to Asp) in the C-terminal domain of cI repressor and defective in cooperative interactions was studied. This mutant binds to operator sites with similar intrinsic affinities as wild type (Beckett, D. et al. (1993) *Biochem.* **32**, 9073-9079). The temperature dependence of ΔH yielded negative heat capacities for all three sites. However, the large negative enthalpies of interaction cause the net thermodynamic driving force for cI repressor-DNA association to be enthalpic in the physiological temperature range. For instance, extrapolation of the enthalpy-entropy compensation plot shows that, for O_R1, $\Delta H=0$ at $T_H = -26.0$°C. Measurements of the heat of binding of cI with synthetic fragments containing various combinations of multiple specific sites (O_R1, O_R2, and O_R3) show that the enthalpies of cooperative interactions between repressor dimers bound to adjacent sites are temperature dependent. (Supported by NIH grant GM 39343.)

Th-Pos71

THE EFFECT OF THE DNA SEQUENCE ON THE THERMODYNAMIC PROPERTIES OF CRP-DNA INTERACTIONS. ((Erica A. Pyles and James C. Lee)) Department of Human Biological Chemistry & Genetics, University of Texas Medical Branch, Galveston, TX 77555.

The binding affinity of *E. coli* cyclic AMP receptor protein (CRP) for DNA has been shown to be cAMP and DNA sequence dependent. The apparent equilibrium constants were quantitatively measured by monitoring the change in anisotropy of fluorescently labeled synthetic promoter sites upon binding to CRP. As is true for the lac-CRP interaction (Heyduk, T. and Lee, J. C. (1990) *Proc. Natl. Acad. Sci. USA 87*, 1744-1748), it appears that the monoligated CRP-(cAMP) complex is the conformational form of CRP that binds with high affinity to the *gal* and *crp* promoter sites. It was found that the affinity of CRP for the promoter sites increased in the following manner; *crp* < *gal* < *lac*. No specific interaction was observed between CRP and a nonspecific oligodeoxynucleotide under high salt conditions. In addition the apparent equilibrium constant of CRP bound to a synthetic gal promoter which contains the lac inverted repeat, was greater than the apparent equilibrium constant for CRP bound to the *lac* promoter. These results indicate that the conserved motif and the inverted repeat are minimal structural requirements for CRP to recognize its binding sites on DNA. However, the entire binding site sequence should be examined to elucidate the mechanism(s) of how CRP-DNA interactions regulate the transcription of many bacterial genes.

Th-Pos72

CHARACTERIZATION OF THE POLYMERIC FORM OF ELONGATION FACTOR TU FROM *E. COLI*
((Michael K. Helms)) Univ. of Hawaii, Honolulu, HI 96822.
(Spon. by D.Jameson)

Elongation factor Tu (EF-Tu) from *E. coli* is a 43 kDa protein best known for its role in prokaryotic protein biosynthesis, where it carries aminoacyl-tRNAs to the elongating ribosome. The state of aggregation of EF-Tu is relevant not only to its role in protein biosynthesis, but also to a possible role as a structural protein. It is shown here that EF-Tu polymerizes to form complex, highly branched species under conditions of low ionic strength and slightly acidic pH. Fluorescence micrographs of EF-Tu labeled with tetramethylrhodamine isothiocyanate (TRITC) reveal the branching and large size (>4μm) of the polymers. Dynamic light scattering studies demostrate that on a polymer with an approximate radius of 115 nm, the ratio of the radius of hydration to the radius of gyration is 0.93, which closely resembles the expected value for a hard sphere. The model of a hard sphere is not inconsistent with the structures observed under the fluorescence microscope. Time resolved phosphorescence anisotropy of erythrosin isothiocyanate labeled EF-Tu revealed fast motions on the order of a few microseconds when placed in glycerol. The fast motions may represent local flexibility of the polymers. This work was funded by the National Science Foundation.

Th-Pos73

ROLES OF SUBUNIT INTERFACE IN THE TRANSMISSION OF SIGNAL IN CAMP RECEPTOR PROTEIN. ((Xiaodong Cheng and James C. Lee)) Department Human Biological Chemistry and Genetics, The University of Texas Medical Branch. Galveston, TX 77555.

Escherichia coli cAMP receptor protein (CRP), a homodimer which contains two interacting domains, is a key regulatory transcriptional factor. The proposed mechanism of CRP involves activation of CRP by the binding of cAMP. The singly liganded CRP-cAMP complex binds to specific DNA sequences. the binding sites of cAMP and DNA are located in different domains. To facilitate our understanding of the allosteric pathway of CRP activation, Ser 128 at the subunit interface and also cAMP binding pocket was mutated to either alanine or proline by site-directed mutagenesis. Both mutants show a crp$^-$ phenotype *in vivo*. The biochemical and biophysical properties of S128P were studied. The CD spectrum of S128P is identical to that of the wild type indicating no major secondary structural changes have occurred even though a proline was placed in the middle of the C-helix. However, results from proteolytic digestion study imply that the alignment of subunits or the protein dynamic of the S128P mutant is different. Results from cAMP binding studies indicate that the binding affinity of the first cAMP is similar for both mutant and wild type proteins, but the mutant exhibits an even higher degree of negative cooperativity in of the second cAMP molecule binding. Results from the DNA binding study suggest that S128P has a much weaker affinity for DNA than the wild type. We, therefore, propose that Ser 128 plays an important role in mediating all reactions executed by CRP subsequent to the binding of the first cAMP molecule. Hence, Ser 128 must be involved in intra- and intersubunit signal transmission.

Th-Pos74

Mn^{2+} BINDING TO WILD-TYPE AND MUTANT T7 RNA POLYMERASES BY EPR. ((A-Young Moon Woody[1], Sandra S. Eaton[2], Gareth R. Eaton[2], Patricia A. Osumi-Davis[1], and Robert W. Woody[1])) [1]Dept. of Biochem. & Mol. Biol., Colorado State Univ., Ft. Collins, CO 80525 and [2]Dept. of Chemistry, University of Denver, Denver, CO 80208.

Asp537 and Asp812 are essential in the catalytic mechanism of T7 RNA polymerase (T7RNAP), as the mutants D537N and D812N have no detectable activity. The hypothesis that these two amino acids act as metal-binding sites has been tested using EPR with Mn^{2+} as the metal ion. Mn^{2+} is able to substitute for Mg^{2+} in transcription by T7RNAP on templates containing the T7 promoter. Mn^{2+} binding to the wild-type enzyme and the mutants D537N and D812N was measured over the concentration range of 25 μM to 1.5 mM. Scatchard plots show a straight line, suggestive of a single intrinsic dissociation constant, and give approximately two Mn^{2+}-binding sites in all three cases. The data were also analyzed by non-linear least-square fits to the binding isotherms. The K_d values are *ca.* 400, 1700 and 800 μM for wild-type, D537N and D812N, respectively. The concerted change in K_d values on mutation of either Asp 537 or 812 suggests that both Asp side chains participate in binding both Mn^{2+}. Mutants D537E and D812E have been produced and are enzymatically active. Data on Mn^{2+} binding to these mutants will also be presented. (Supported by GM23697 and a BRSG grant (CSU).)

Th-Pos75

Mn^{2+} BINDING TO WILD-TYPE AND MUTANT T7 RNA POLYMERASES BY EPR. ((A-Young Moon Woody[1], Sandra S. Eaton[2], Gareth R. Eaton[2], Patricia A. Osumi-Davis[1], and Robert W. Woody[1])) [1]Dept. of Biochem. & Mol. Biol., Colorado State Univ., Ft. Collins, CO 80525 and [2]Dept. of Chemistry, University of Denver, Denver, CO 80208.

Asp537 and Asp812 are essential in the catalytic mechanism of T7 RNA polymerase (T7RNAP), as the mutants D537N and D812N have no detectable activity. The hypothesis that these two amino acids act as metal-binding sites has been tested using EPR with Mn^{2+} as the metal ion. Mn^{2+} is able to substitute for Mg^{2+} in transcription by T7RNAP on templates containing the T7 promoter. Mn^{2+} binding to the wild-type enzyme and the mutants D537N and D812N was measured over the concentration range of 25 μM to 1.5 mM. Scatchard plots show a straight line, suggestive of a single intrinsic dissociation constant, and give approximately two Mn^{2+}-binding sites in all three cases. The data were also analyzed by non-linear least-square fits to the binding isotherms. The K_d values are *ca.* 400, 1700 and 800 μM for wild-type, D537N and D812N, respectively. The concerted change in K_d values on mutation of either Asp 537 or 812 suggests that both Asp side chains participate in binding both Mn^{2+}. Mutants D537E and D812E have been produced and are enzymatically active. Data on Mn^{2+} binding to these mutants will also be presented. (Supported by GM23697).

Th-Pos76

EFFECTS OF SEQUENCE VARIATIONS IN THE -10 HEXAMER ON THE STRUCTURES OF OPEN COMPLEXES BETWEEN *ESCHERICHIA COLI* $E\sigma^{70}$ RNA POLYMERASE AND A SYNTHETIC PROMOTER ((M.L. Craig and M.T. Record, Jr.)) Department of Biochemistry, University of Wisconsin-Madison, Madison, WI 53706.

Key steps on the pathway to the formation of the initiation-competent open complex (RP_{O2}) at the λP_R promoter include:

$$R + P \underset{k_{-1}}{\overset{k_1}{\rightleftarrows}} RP_{C1} \underset{k_{-2}}{\overset{k_2}{\rightleftarrows}} RP_{C2} \underset{k_{-3}}{\overset{k_3}{\rightleftarrows}} RP_{O1} \underset{k_{-4}}{\overset{k_4}{\rightleftarrows}} RP_{O2}$$

The open complexes, RP_{O1} and RP_{O2}, have been characterized kinetically by fluorescence-detected abortive initiation and filter binding (1,2) and structurally by DNA footprinting (3,4). Similar studies are in progress for a set of synthetic promoter variants in order to compare the properties of the synthetic promoter to those of λP_R and to investigate the role of the locally-denatured -10 base pairs in the formation of the open complexes. Single and double thymine to adenine transversions were introduced into the synthetic consensus promoter at positions -7 and -12 (-10 sequences AATAAa, aATAAT, and aATAAa). Located at opposite ends of the -10 region, these highly conserved positions are observed by $KMnO_4$ footprinting to be single-stranded in RP_{O1} and RP_{O2} of our consensus promoter. Results of $KMnO_4$ and other footprinting studies will be presented.

1. J.-H. Roe, M. T. Record, Jr., *Biochemistry* **24**, 4721-4726 (1985).
2. W. C. Suh, S. Leirmo, M. T. Record Jr., *Biochemistry* **31**, 7815-7825 (1992).
3. W. C. Suh, W. Ross, M. T. Record Jr., *Science* **259**, 358-361 (1992).
4. W. C. Suh, M.T. Record, Jr., unpublished.

Th-Pos77

ON THE MECHANISM OF FIDELITY IN RNA SYNTHESIS. ((L. Lee, J.J. Butzow, E. Tarien, T. Frazier and G. L. Eichhorn))
NIH, Gerontology Research Center, Laboratory of Cellular & Molecular Biology, Baltimore, MD 21224

We have been studying a model for assuring fidelity in RNA synthesis that depends on the ability of E. coli RNA polymerase to assume two conformations, one to place a correct NTP substrate into bond-forming position and the other to prevent an incorrect substrate from assuming such a position. Studies in other laboratories had suggested that an NTPase activity associated with the polymerase also contributes to fidelity through preferential cleavage of the incorrect substrate. We had confirmed such preferential cleavage, and incorporated it into our fidelity mechanism. Nevertheless, our preferential cleavage was not the all-or-nothing effect previously reported, and we have now determined that the extent of the NTP cleavage we observe can be interpreted by competition for the correct substrate between RNA synthesis and substrate cleavage, while cleavage is the only option for the incorrect substrate. Some evidence that indicates the NTPase may still affect fidelity, but perhaps not through preferential cleavage. Our studies are consistent with those of Erie et al (Science, in press), that show an incorrect NTP leading to an inactivated state of the polymerase that interacts preferentially with protein factor GreA. We have begun studies with yeast RNA polymerase to determine whether fidelity may be assured by a similar mechanism in a eukaryotic system.

Th-Pos78

DIFFERENTIAL EXPRESSION OF PHOSPHOLAMBAN GENE TRANSCRIPTS IN MURINE ATRIUM AND VENTRICLE ((Koss, K.L.†, Ponniah, S.‡, Jones, K.W.§, and Kranias, E.G.‡))
Departments of †Physiology & Biophysics, ‡Pharmacology & Cell Biophysics, and §Division of Cardiovascular Biology, University of Cincinnati, College of Medicine, Cincinnati, OH 45267-0575.

Phospholamban (PLB), a sarcoplasmic reticular phosphoprotein, is physiologically important in the regulation of cardiac contractility, and alterations in PLB mRNA levels appear to be associated with deterioration of cardiac function in cardiomyopathic disease. The present study was designed to test the hypothesis that PLB gene transcripts are differentially expressed between murine atrial and ventricular tissues. Quantitation of PLB mRNA copies in atrial and ventricular RNA extracts from the FVB/N and B6D2-F1 mouse strains was performed by mRNA dot blot analysis, using an end-labelled DNA oligonucleotide, antisense to a portion of the PLB coding region, as a probe. Linearized PLB cDNA was used as a standard and the obtained copy numbers/μg RNA were normalized to total 18s RNA. Our findings indicate that the PLB mRNA copy number is higher in the mouse ventricle than in the atrium. There is a 2-fold difference in PLB transcript abundance between the atrium and ventricle of FVB mice ($1.2E^7 \pm 0.4E^7$ mRNAs vs. $2.8E^7 \pm 0.3E^7$ mRNAs) (mean ± S.D.) and a 3-fold difference ($1.8E^7 \pm 0.7E^7$ vs. $5.8E^7 \pm 2.3E^7$) between the atrium and ventricle of B6D2 mice. These findings were confirmed by in situ oligonucleotide hybridization of sectioned hearts.

This study was supported by AHA-SW9331-F, AHA-SW9213-I, and HL26057.

Th-Pos79

DRUG INDUCED CHANGES OF PURKINJE CELLS WITHIN THE CEREBELLAR CORTEX OF RAT BRAINS: A VIBRATIONAL IMAGING MICROSCOPIC STUDY.

((E. Neil Lewis[§], David S. Lester[#] and Ira W. Levin[§])) [§]NIDDK, NIH, Bethesda MD 20892. [#]FDA/CDER/DRT, Laurel MD 20708.

The cerebellar cortex plays a major role in controlling motor and sensory responses and is made up of three cell layers. The central portion is the Purkinje region consisting of a single layer of cells parallel to the outer surface of the cerebellar lobes. These cells have large (50 μm in diameter) flask shape bodies with an elaborate dendrite tree extending into the molecular layer. Treatment of rats with two drugs, Ibogaine and Cytarabine, anti-addiction and anti-cancer drugs, respectively, has been shown to destroy specifically a large number of Purkinje cells.

While both conventional Raman and infrared spectroscopies have been used extensively for examining molecular reorganizations of biological materials, a recent development, **vibrational spectroscopic imaging microscopy**, has provided an even more effective technique for the study of biological systems at both the cellular and molecular levels. The technique provides the ability to probe the spectroscopic and chemical characteristics of a sample at the molecular level, while simultaneously providing images at spatial resolutions approaching 1 μm. Since the method can readily record images with 65,536 (256x256) pixels and since for each pixel there is a measured Raman or near-infrared spectrum, any of the experimental observables, frequencies, intensities or linewidths, can be used to construct new image presentations which emphasize different domains of chemically and/or structurally distinct species.

Using this new imaging technique, we present for the first time high fidelity vibrational images of a native biological material; namely, brain slices from control and drug treated animals. In addition, the technique will be used to monitor changes in the distribution and chemical composition of Purkinje cells as a function of drug treatment.

Th-Pos80

DIRECT TEST OF THE "SQUEEZE-OUT" HYPOTHESIS OF PULMONARY SURFACTANT FUNCTION IN SITU AT THE A/W INTERFACE. ((B. Pastrana-Rios,*, C.R. Flach,* J.W. Brauner,* A.J. Mautone,# and R. Mendelsohn*)) Dept. of Chemistry, Rutgers University,* Newark, NJ 07102 and Dept. of Anesthesiology, UMDNJ, Newark, NJ 07102.#

Lung surfactant is a mixture of lipids and proteins that functions, perhaps as a monolayer film, by lowering surface tension at the air-alveolar interface to near zero. DPPC is the main component of the surfactant system, and unlike the other surfactant components, has the ability to substantially lower the surface tension. It has thus been proposed that at high surface pressures, non DPPC components are "squeezed out" from the surface. We have used external reflection FT-IR under physiologically relevant pressures of 40-70 dynes/cm in situ at the A/W interface to test this hypothesis. Surface films of DPPC-d_{62}/DOPG and DPPC-d_{62}/POPG at compositions mimicking those of the surfactant lipids were spread as insoluble monolayers at the A/W interface. The films were examined under conditions of controlled surface pressure. The proportions of the deuterated (DPPC-d_{62}) and proteated (DOPG or POPG) components at the surface were monitored by the integrated areas of the CD_2 and CH_2 stretching bands, respectively. At mole ratios of 7:1 (DPPC-d_{62}/DOPG or DPPC-d_{62}/POPG), substantial squeeze-out was observed at high surface pressures and at fast rates of film compression. For the saturated pair of phospholipids DPPC-d_{62}/DPPG, squeeze-out was much less effective. The phenomenon appears to require unsaturation in the acyl chains and high rates of compression.

Th-Pos81

EXTERNAL REFLECTANCE INFRARED SPECTROSCOPY: INSTRUMENT DESIGN AND CONFORMATIONAL STUDIES OF PHOSPHOLIPID MIXTURES AND PEPTIDES IN SITU AT THE AIR/WATER INTERFACE.((C.R. Flach, J.W. Brauner and R. Mendelsohn))Dept. of Chemistry, Newark College of Arts and Sciences, Rutgers University, Newark, NJ 07102.

External reflectance FT-IR has been used to study phospholipid mixtures and peptides in situ at the air/water interface. An FT-IR spectrophotometer interfaced to a miniaturized surface film balance permitted the study of binary phospholipid monolayers as a function of surface pressure and the presence of Ca^{2+} ion. Acyl chain perdeuterated 1,2-dipalmitoylphosphatidylcholine in equimolar mixtures with 1,2-dipalmitoylphosphatidylserine allowed observation of CD_2 and CH_2 stretching frequencies. The data, treated according to a two-state model, suggested miscibility of the lipids in the presence and absence of Ca^{2+}. Modification of the instrument design to compensate for the presence of water vapor has permitted peptide conformation and amide hydrogen exchange studies of the air/water and air/deuterium oxide interface. The frequency and lineshape of the amide I band and presence of the amide II band for model amphiphilic β-sheet and α-helical peptides were studied. Deuterium exchange in the β-sheet peptide is indicated by a downward shift in the amide I frequency, whereas it is unclear whether the frequency shift of the amide I band in the α-helical peptide indicates deuterium exchange or a conformational change to random coil.

Th-Pos82

THE CONFORMATIONAL BASIS OF A. LAIDLAWII B ADAPTATION TO ALTERED GROWTH TEMPERATURES: FT-IR STUDIES OF MEMBRANE ORDER ((D.J.Moore and R.Mendelsohn)) Dept. of Chemistry, Newark College, Rutgers University, Newark NJ 17102.

Coupled CH_2 wagging mode progressions can be detected in the infrared spectra of live A.laidlawii B cell membranes enriched in saturated fatty acids. Using these modes as probes of acyl chain conformational order, the extent of the all-trans chain conformation present in live cells grown at several temperatures has been quantitated. Cells enriched in myristic acid were grown at 25°C and 37°C, while cells enriched in pentadecanoic acid were grown at 30°C and 37°C. From the intensity of the CH_2 wagging progression components and the suggestion that at low temperatures (≈-60°C) the acyl chains are in the all-trans conformation we have been able to quantitate the amount of disorder (at the growth temperature) in the membranes of cells grown at different temperatures. Our data indicate that A.laidlawii B cells maintain 1.3 - 1.8 gauche bonds per acyl chain at their growth temperature. Furthermore, the ability of cells highly enriched in a single fatty acid to maintain a relatively constant degree of disorder (when grown at temperatures up to 12 degrees apart) supports the hypothesis that these cells have a mechanism by which they can control the overall fluidity of their membranes.

Th-Pos83

TWO DIMENSIONAL INFRARED SPECTROSCOPY (2D IR) ON HYDRATED POLY(L-LYSINE) FILMS.

((R. Buchet[1], M. Müller[2] and U. P. Fringeli[2,3]))[1]Phys.Chem.Biol. Univ. Lyon I,69622 Villeurbanne France.[2]ETH Technopark, CH-8005 Zürich Switzerland.[3]Phys. Chem., Univ. Vienna, A-1091 Vienna, Austria.

Temperature modulated infrared spectra of poly(L-lysine) films hydrated with ^2H_2O (80 % relative humidity) were measured. The temperature was varied periodically with an amplitude of +/- 2 °C around 28 °C , the α helix to β pleated sheets phase transition temperature. The structural changes are fully reversible at these conditions. The modulated infrared spectra of poly(L-lysine) permit to resolve component bands in amide I' and in amide II' regions that are not easily detected on the stationary infrared spectra.The modulated infrared spectra were analysed by using curve fitting analysis of phases and 2D IR cross correlation methods. Both approaches are consitant to each other and provide more insight into the assignment of component bands. For example, by etablishing correlation between component bands of the very well known amide I' region and other components of the less known amide II' region , it is possible to assign without any ambiguity the components of the amide II' region.The 1469 cm^{-1} and 1449 cm^{-1} are assigned respectively to α helix and β pleatted sheets.

Th-Pos84

PROTEIN NORMAL MODES: CALCULATION OF SPECTROSCOPICALLY RELIABLE INFRARED AMIDE BANDS. ((W.C. Reisdorf, Jr. and S. Krimm)) Biophysics Research Division, University of Michigan, Ann Arbor, MI 48109

Confident interpretations of the vibrational spectrum of a protein in terms of its structure ultimately rest on our ability to correctly predict the normal modes of the molecule. This depends on having appropriate vibrational force fields, which are now becoming available (Krimm and Bandekar, Adv. Protein Chem. 38, 181 (1986)), and suitable programs for solving the eigenvalue problem. We have developed programs, based on POLYPEP (Tasumi et al, Biopolymers 21, 711 (1982); Ataka and Tasumi, J. Mol. Struct. 143, 445 (1986)), that permit the calculation of the frequencies and infrared intensities of the amide I, II, III and V bands of polypeptides and proteins. These programs incorporate transition dipole coupling for obtaining frequency shifts in amide I and II modes and *ab initio* dipole derivatives for computing intensities. This capability makes it possible, for example, to analyze in detail the effects of structural modifications on the vibrational spectrum of the α-helix. The present studies have concentrated on α-helical polypeptides and proteins, with myoglobin and hemerythrin presented as examples of the latter.

Th-Pos85

SEPARATION OF OVERLAPPING BANDS IN THE IR CARBONYL SPECTRA OF A FRESHLY PREPARED MULTILAYER OF CHLOROPHYLL *A*

G. Petit, M. Trudel and C. Chapados, Département de chimie-biologie, Université du Québec à Trois-Rivières, Trois-Rivières, QC, Canada G9A 5H7

Six consecutive infrared spectra of a freshly prepared multilayer of chlorophyll *a* were obtained in the carbonyl region. The spectra show three broad bands assigned to the ester carbonyls, to the free ketone carbonyl, and to the associated ketone carbonyl. The intensity of the ketone bands vary with time. The second derivative and the Fourier self-deconvolution techniques were applied to the spectra to enhance them in order to determine the number of components and their positions. With the fifteen components observed, the band simulation technique was applied to all the spectra to evaluate the intensity of the components. From the results, a model for the multilayer of Chl *a* is built which consist, for the fresh multilayer, of two Chl *a* molecules linked together and two water molecules for the unit organization. One water molecule is attached to the Mg of one Chl, the other water molecule is H-bonded to the first water on one side and H-bonded to the π electron network of the second Chl on the other side. With time the water molecules leave the Chl layers causing a disruption of the organization which reorganize later on. This process goes on until the multilayer is stabilized.

Th-Pos86

RE-EVALUATION OF AMIDE I BAND ASSIGNMENTS OF FTIR OF PROTEINS FOR GLOBAL SECONDARY STRUCTURAL ANALYSIS. ((J.J. Unruh, H.M. Farrell, Jr. and T.F. Kumosinski)) ERRC, USDA, Philadelphia, PA 19118 (Spon. by H.M. Farrell)

To alleviate the confusion among the scientific community regarding the global secondary structural assignments of amide I FTIR bands of proteins, a comparative analysis of 15 to 20 proteins was initiated. Theoretical FTIR amide I envelopes by Torii and Tasumi (J. Chem. Phys. (1992), 96:3379-3387), experimental FTIR envelopes in water, and previously reported spectra in D_2O by Susi and Byler were evaluated. Qualitative comparisons were performed using calculated second derivative spectra while quantitation was effected using non-linear regression analysis to resolve all spectra into component Gaussian bands. Calculated percent areas were then utilized for obtaining band frequency assignments. The results demonstrate that in water, the 1667 and 1951 cm^{-1} bands arise, in part, from the carboxyl stretch and the amide deformation of aspargine and glutamine, respectively. In D_2O, only the carboxyl stretch is observable at 1660 cm^{-1}. Comparison of experimental global secondary structures with values calculated from X-ray crystal structures using 3D Ramachandran plots shows agreement within 4% between the water data and theoretical spectra. The D_2O results were not as precise due to increased hydrogen bonding of D_2O which competes for protein sites, possibly causing conformational changes due to increased hydrophobic interactions.

Th-Pos87

CONFORMATIONAL INFRARED BAND ASSIGNMENTS FROM POLY-L-LYSINE AND POLY-L-GLUTAMIC ACID: SECONDARY STRUCTURE BY PARTICLE BEAM/FT-IR SPECTROMETRY. ((V.E. Turula Jr. and J.A. de Haseth)) University of Georgia, Chemistry Dept., Athens, GA 30602-2556. (Spon. by R.A. Dluhy)

Infrared spectrometry can be used to estimate secondary structure content of proteins in aqueous media. Spectra acquired from liquid solution are complex; the conformationally sensitive amide absorption bands which are intrinsically overlapped must be extracted from underneath water absorptions as well as from each other. Rigorous experimental requirements and mathematical manipulations make reproducibility difficult. We have developed a technique, with the use of the particle beam apparatus that rapidly evaporates the water surrounding a protein, and deposits it onto an IR-substrate so that a spectrum may be obtained. The conformation of poly amino acids such as poly-L-lysine and poly-L-glutamic acid can be manipulated by solution pH, temperature, and solvent composition such that a specific structural order (e.g. α-helix, β-sheet) is energetically favored and forms. With an entire polypeptide chain conformed to a specific structure, the infrared spectrum is simplified so exact band assignments, that are useful in conformational elucidation of globular proteins, can be made. It is shown how these structures and transient conformations affect infrared spectral results from solution spectra, liquid films, and deposits made by particle beam. Not only were the data of these poly amino acids collected from particle beam deposits free of the masking water absorptions, but by forcing the dominance of a single type of secondary structure their IR band assignments were directly transferable to other unperturbed biopolymers which possess a mixture of structure types.

Th-Pos88

STRUCTURAL CHARACTERIZATION OF IRON-BLEOMYCIN BY RESONANCE RAMAN SPECTROSCOPY ((Satoshi Takahashi*, Joseph W. Sam#, Jack Peisach# and Denis L. Rousseau*)) *AT&T Bell Laboratories, Murray Hill, NJ 07974, #Albert Einstein College of Medicine, Bronx, New York 10461

Bleomycins (BLMs) constitute a family of structurally related glycopeptide antibiotics currently used in the treatment of various tumors. Although it is the iron complex of BLM which is believed to be responsible for the drug's DNA cleavage activity, there has been little information concerning the structure of Fe-BLM. We present the first report of resonance Raman scattering from Fe-BLM in the Fe^{3+}, Fe^{2+} and $Fe^{2+}CO$ states. Experiments were performed on purified and freshly complexed samples at moderate laser power (407nm, 10~30mW). These three states have a line (1608, 1595 and 1607cm^{-1}, respectively) assignable to the amide I mode of the deprotonated amide group coordinated to iron. Several other lines show redox state dependent intensity and frequency changes. The Fe^{3+} complex has a line located at 561cm^{-1}, whose isotope shifts in $H_2{}^{18}O$ and D_2O are best explained by a Fe-OH stretching mode. This result establishes the coordination of hydroxide to the ferric complex. The CO stretching frequency of the $Fe^{2+}CO$ complex appears at 1980cm^{-1}.

Th-Pos89

Heme-Ligand Vibrations in Cytochrome Oxidase, Structural Implications and Model and Computational Results.

E. Schmidt[1], H. Zhang[1], Y. Kim[1], Y. Liang[1], C.K. Chang[1], G.T. Babcock[1], J. Hosler[2], S. Ferguson-Miller[2]
Departments of [1]Chemistry, [2]Biochemistry and the LASER Laboratory, Mich. State Univ., E. Lansing,MI

In wild-type sphaeroides cytochrome oxidase, the ν(Fe-His) vibration occurs at 214 cm^{-1} in the ferrous enzyme; in the carbonmonoxy form the ν(Fe-CO) vibration is at 516 cm^{-1}. On the D412N mutant, the ν(Fe-CO) vibration is unchanged, whereas the ν(Fe-His) mode shifts to 218 cm^{-1}. Conversely, in H333N ν(Fe-His) occurs at its wild type frequency but ν(Fe-CO) shifts down to 500 cm^{-1}. These results support the structural model for cytochrome oxidase advanced recently (Hosler, et al. J. Bioenerget. Biomembranes 25,121(1993). To rationalize these data on intermediates in dioxygen reduction by cytochrome oxidase, both model compounds and computational strategies are being used. The model compound approach is based on the Naphthoic Kemp's acid porphyrin that allows characterization of the effects of intramolecular hydrogen bonds to ligands bound at the metal. Carbon monoxy, oxy, and peroxy ligands are being studied. The computational approach relies on semi-empirical methods and is directed at oxy and peroxy ligated heme cations. The electronic properties of these species have been calculated, the location of the charge transfer state has been determined, and the photoactivity of various excited electronics has been studied.

Th-Pos90

TIME-RESOLVED RESONANCE RAMAN STUDIES OF S_1 EXCITED STATES OF METALLOPORPHYRINS

((Douglas H. Kreszowski, Geurt Deinum, and Gerald T. Babcock))
Department of Chemistry and the LASER Laboratory, Michigan State University, East Lansing, MI 48824.

In photosynthesis, absorption of light leads to electronically excited chlorophylls in the light harvesting antenna. Energy transfer of the excitation energy can ultimately result in oxidation of the special pair in the reaction center. Porphyrins can be used as simplified models of these reaction centers. Vibrational spectroscopy is a particularly informative technique useful in analyzing conformational changes of molecules in excited states. Therefore, pump/probe picnosecond time-resolved Resonance Raman spectroscopy is frequently applied to characterize excited electronic states of metalloporphyrins. Previous applications of time-resolved Raman techniques to T_1 states indicate a Jahn-Teller distortion present in metalloporphyrins with D_{4h} symmetry. This distortion is absent in free base porphyrins with the lower D_{2h} symmetry. Time-resolved Resonance Raman spectra of ZnOEP in the S_1 state shows modes at 1570, 1449, 1359, and 1259 cm^{-1}. The spectra of this species, as well as of its triplet and of the corresponding states in ZnTPP are presented and are interpreted in terms of molecular structures. (Supported by NIH grant GM25480).

Th-Pos91

INTERACTION OF ARSENIC SPECIES WITH SULFHYDRYL-CONTAINING BIOLOGICAL MOLECULES: A RAMAN SPECTROSCOPY STUDY. ((J.A. Centeno)) Dept. of Environmental and Toxicologic Pathology, Armed Forces Institute of Pathology, Washington, D.C. 20306-6000

Arsenic (As) toxicity in living systems has been postulated to be mediated through two different mechanisms: by As binding to sulfhydryl-containing enzymes, especially to the dihydrolipoic acid moiety inhibiting the decarboxylation of α-ketoglutarate, or by the substitution of the phosphate moiety in enzyme-catalyzed reactions. The first mechanism is due to the presence of trivalent arsenic (As^{3+}) while pentavalent (As^{5+}) arsenic may be the active arsenic specie in the latter case. In addition, in living organism inorganic arsenic can be methylated to form monomethylarsonic (MMA) and dimethylarsenic (DMA) which are two forms of As^{5+} and that are believed to be less acutely toxic than As^{3+} species. Although several studies have been dedicated to study the toxicity of As^{3+}, the molecular mechanism is still unclear. Accordingly, in order to understand the role of arsenic redox and methylation reactions with biological systems we have investigated the reactions of arsenic species with sulfhydryl-containing system including glutathione (GSH) and L-cysteine by employing Raman spectroscopy. The binding of As^{3+} to the cysteinyl thiolate group was confirmed by the disappearance of the sulfhydryl group (-S-H) stretching mode at 2530 (for GSH) and at 2569 cm^{-1} (for L-cysteine), respectively. Raman frequencies arising from the methylene ($-CH_2$) group bonded to the sulfhydryl group of the cysteinyl residue were also affected by arsenite binding. Mixtures of arsenate (As^{5+}) species with GSH and L-cysteine in D_2O showed oxidation of the S-H moiety to form the dimer structure as evidenced by the appearance of a new Raman line at 501 cm^{-1} assigned to the disulphide (S-S) stretching frequency.

Th-Pos92

VIBRATIONAL AND UV CD STUDIES OF THE BINDING OF THE HIV-1 mRNA TAR REGION WITH THE TAT-PEPTIDE ((T. Xiang, M. Diem and D.J. Goss)) Dept. of Chemistry, Hunter College of CUNY, New York, NY 10021.

A short peptide (11 amino acids) that contains the basic region of the HIV-1 Tat protein binds specifically to an RNA stem-loop structure, ΔTAR, which is located in the HIV long terminal repeat. Our VCD and CD experiments show that both ΔTAR and Tat-peptide have stable secondary structures and, after forming 1:1 (molar ratio) complex, the binding induced conformational change can be seen from the VCD and CD spectra of the complex. In addition, the Tat-peptide's CD spectrum shows it has a random coil secondary structure, and its VCD spectrum, which is stable with the temperature and concentration, shows it may have a special loop conformation. Grant support:NSF MCB - 9303661 (D.J.G.), NIH GM 28619 (M.D.).

Th-Pos93

RAMAN DIFFERENCE SPECTROSCOPY AND ELECTROSTATICS CALCULATIONS OF THE ACTIVE SITE INTERACTIONS OF NADH WITH VARIOUS DEHYDROGENASES ((J.B. van Beek, M.R. Gunner and R.H. Callender)) Dept. of Physics, City College of CUNY, New York, NY 10031.

We have investigated the molecular interactions and structural properties of NADH bound to glycerol-3-phosphate dehydrogenase, a B-side enzyme, by Raman Difference spectroscopy. The position of the $-NH_2$ rocking mode of the carboxamide group of NADH is not affected by binding to the enzyme, indicating no change in hydrogen bond strength to the $-NH_2$ group. Furthermore, the measured frequencies and bandwidths of the C-D stretch of the C4 *pro-R* and *pro-S* deuterated hydrogens suggest that no large change in conformation of the nicotinamide head group occurs in the binary complex. Electrostatics (DELPHI) calculations of NADH binding to lactate, malate, and glyceraldehyde-3-phosphate dehydrogenase shows that significant polarization of the cofactor has to occur to explain strong binding of the nicotinamide head group. Regardless, the electrostatic interaction between the α2F helix dipole and the carbonyl oxygen of NADH does not appear to be the main source of binding of this carbonyl oxygen to the enzyme, as has been proposed. Significantly, this favorable interaction is largely negated by the unfavorable interaction with the residues next to the N-terminus of the α2F helix. A large favorable electrostatic interaction calculated for the carbonyl oxygen with the protonated active site histidine explains the experimentally observed change in histidine pKa upon binding of NADH. Implications of these results for the mechanism of the stereospecific hydride transfer catalyzed by these enzymes will be discussed.

OTHER SPECTROSCOPIES

Th-Pos94

NANOSECOND TIME-RESOLVED MAGNETIC CIRCULAR DICHROISM SPECTROSCOPY OF CYTOCHROME c_3.
((D. B. O'Connor,[1] R. A. Goldbeck,[1] J. H. Hazzard,[2] D. S. Kliger[1] and M. A. Cusanovich[2])) [1]Chem. & Biochem. Dept., Univ. of California, Santa Cruz, CA 95064; [2]Biochem. Dept., Univ. of Arizona, Tucson, AZ 85721.

The UV-vis magnetic circular dichroism (MCD) spectra of the ns kinetic photolysis intermediates of the tetraheme electron-transfer protein cytochrome c_3 (Cc3) are reported. CO replaces histidine as the axial sixth ligand at each heme site, forming a low-spin complex with an MCD spectrum similar to that of myoglobin-CO. Photodissociation of Cc3-CO produces a transient 5-coordinate, high-spin (S=2) species with an MCD spectrum similar to deoxymyoglobin. The recombination kinetics of CO with heme Fe appear to involve at least 5 first-order or pseudo first-order rate processes, corresponding to time constants of 5.7 μs, 62 μs, 425 μs, 2.9 msec, and a time constant greater than 1 s. The insensitivity of observed rate constants to variation of the actinic photon flux suggests non-cooperative heme-CO rebinding. The growing in of an MCD signal characteristic of bis-histidine axial ligation within tens of microseconds after photodissociation shows that, although heme-CO binding is thermodynamically favored at 1 atm CO, binding of histidine to the sixth axial site competes kinetically with CO rebinding.

Th-Pos95

CHARACTERIZATION OF A PEPTIDE SEQUENCE WHICH FORMS A STABLE ß-STRUCTURE IN A VARIETY OF SOLVENTS ((D.V. Waterhous and W.C. Johnson, Jr.)) Dept. of Biochemistry and Biophysics, Oregon State University, Corvallis, OR 97331-7305.

We have recently identified and synthesized a peptide sequence from a protein that has a high propensity for ß-strand formation, as predicted by the Chou -Fasman algorithm. We have studied its secondary structure by circular dichroism (CD) in a series of solvents that enhance α-helices (alcoholic solvents including TFE), or ß-strands (detergents such as octyl-ß-glucoside, nonmicellar SDS, and digitonin/cholate), or random coils (sodium phosphate buffer, pH 7.2). Several peptides that we have recently studied adopt all three of these conformations, dependent only on the bulk solvent environment. Our new peptide sequence has proved to be a stable ß-strand under all the solvent conditions we have studied, even in buffer at room temperature. (This work is supported by NIH grant GM 21479).

Th-Pos96

LEFT-HANDED POLY(PRO)II STRUCTURE IN GLOBULAR PROTEINS - IDENTIFICATION AND CD ANALYSIS. ((N. Sreerama and R.W. Woody)) Department of Biochemistry and Molecular Biology, Colorado State University, Fort Collins, CO 80523.

It has been shown that the left-handed poly(Pro)II type structure (PII) is an important element of secondary structure in globular proteins. The PII structure has been also invoked in explaining the CD spectra of unordered polypeptides. We have developed an algorithm to identify the PII structure from the x-ray structures of proteins and incorporated the resulting PII fractions in the analyses of CD spectra. Our algorithm utilizes virtual bond angle C_{i-1}^{α}-C_i^{α}-C_{i+1}^{α} and virtual dihedral angles C_{i-1}^{α}-C_i^{α}-C_{i+1}^{α}-C_{i+2}^{α} and O_{i-1}=C_{i-1}-C_i=O_i, and identifies PII structure among residues not assigned to α-helix or β-sheet by the Kabsch & Sander method. The fraction of PII structure was considered in the secondary structure analysis from CD using the self-consistent method. Among the proteins in our basis set, approximately 10% residues were assigned the PII structure and a negative correlation was found between the fractions of α and PII. The CD spectrum of PII deconvoluted from the analysis was almost identical to the experimental spectrum of poly(Pro)II, and that of the unordered fraction was unlike any known CD spectrum. Inclusion of isolated residues in the PII fraction has little effect on the calculated PII spectrum but improves the analysis for the PII and turn fraction. (Supported by GM 22994)

Th-Pos97

TRYPTOPHAN CIRCULAR DICHROISM OF HEN, TURKEY AND HUMAN LYSOZYMES. ((Irina Grishina and Robert W. Woody)) Department of Biochemistry & Molecular Biology, Colorado State University, Fort Collins, CO 80523.

The B_b absorption band of Trp side chains, located near 225 nm, is the most intense absorption band in the Trp spectrum with $\epsilon_{max} \sim 5*10^4$. Pairs of nearby Trp residues can give rise to exciton couplets which may be detectable against the background provided by amide groups. Trp may be responsible for anomalous features in the far-uv circular dichroism (CD) of proteins, which can interfere with secondary structural analysis by CD. Calculations of the exciton CD of Trp were performed on the basis of Trp coordinates in various lysozyme structures from the Brookhaven Protein Data Bank using the origin-independent version of the matrix method (Goux and Hooker, 1980, JACS 102, 7080). The mixing of six electronic transitions in Trp was considered. Significant CD was predicted for hen and turkey lysozymes in the far uv. The calculated near-uv CD for hen lysozyme matches the experimental amplitude. Trp62 in hen and turkey lysozymes was found to be sensitive to disturbances on the protein surface due to binding of substrate, antibodies and intermolecular contacts in the crystal. Conformational changes of Trp62 are predicted to have a strong effect on the overall Trp CD. Differences in the CD of hen and human lysozymes are attributed mostly to the W62Y substitution. (Supported by USPH GM22994).

Th-Pos98

CHIRAL TEMPLATES BUILT IN THE DYE BINDING SITE OF PROTEINS: INTERPRETATION OF CD AND HYPOCHROMISM IN TERMS OF WELL DEFINED LOCAL INTERACTIONS ((K. Ajtai, E. Klimtchuk and T.P. Burghardt)) Department of Biochemistry, Mayo Foundation, Rochester, MN 55905

Iodoacetamido fluorescein was used to probe the dye binding pocket of S1 near to SH1. A characteristic large CD signal was observed in the lowest energy absorption band of the fluorescein upon the covalent binding of the probe. Perturbation of the native protein structure (pH, proteolysis, temperature) eliminated the signal indicating it originates from the specific interaction of the probe with the protein. To clarify the mechanism of protein induced dye chirality, model systems of optically active aromatic chiral amines and amino acids complexed with fluorescein were constructed. From the CD and extinction coefficient spectra, we measured the rotary and dipole strength of the complex and performed calculations, based on well known methods employing the coupling of transition dipole moments, to estimate the orientation of the probe relative to the chiral template. Similar calculations were also performed on the probe-protein complex to estimate the orientation of the probe relative to the 3-D structure of S1. Supported by NIH (R01 AR 39288), AHA (GIA 930 06610), and the Mayo Foundation.

Th-Pos99

AN INSTRUMENT FOR SIMULTANEOUSLY MONITORING CD AND FLUORESCENCE AS A FUNCTION OF TITRANT CONCENTRATION: APPLICATION TO THE UREA UNFOLDING OF *trp* APOREPRESSOR. ((G.D. Ramsay and Maurice R. Eftink)) Department of Chemistry, Univ. of Mississippi, University, MS 38677.

In the past we have reported on the use of a modified Aviv 62DS CD spectrophotometer to make CD, fluorescence, light scattering, and absorbance measurements during a single thermal melt. This experimental approach allows savings in time and material and reduces errors due to sample variations. Here we report on the addition of a programmable Hamilton syringe pump to perform ligand and denaturant titrations. The syringe pump is synchronized with the spectrophotometer by a "master" PC computer that issues commands to make injections and start data collection. This setup is capable of measuring a variety of spectroscopic parameters during a single titration. The urea denaturation of the *trp* aporepressor at a variety of pHs is presented as an example. Global data analysis was used to more accurately determine thermodynamic parameters. At pH 5.5 denaturation is multi-state, with an intermediate appearing maximally at ~4 M urea. The data were well described by the model of D_2=2M=2U, where the dimer dissociates into two monomers, which then are denatured. Supported by NSF DMB 91-06377.

Th-Pos100

MULTICHANNEL INSTRUMENT FOR OPTICAL TOMOGRAPHY IN THE NEAR INFRARED. ((S.A. Walker, S. Fantini, M.A. Franceschini and E. Gratton)) Laboratory for Fluorescence Dynamics, Department of Physics, Univ. of Illinois at U-C, 1110 West Green, Urbana, IL 61801.

There is a growing medical interest in locating tumors in the human body by means of a method which utilizes non-ionizing radiation and is more cost effective than current options (i.e. Magnetic Resonance Imaging, X-ray techniques). Optical imaging is a good candidate for this method since near infrared light, which penetrates several centimeters into tissues, is non-ionizing radiation. Using a diffusion model it is possible to independently measure the scattering (μ_s') and absorption (μ_a) coefficients in tissues. In frequency domain spectroscopy, intensity modulated light sources such as light emitting diodes (LEDs) can be used, making the instrument particularly practical. We have designed a portable, multichannel, multidetector instrument which can produce tomographic images in real time. We use a number of LEDs as light sources and two detector optical fibers, separated by 2 cm, all mounted onto a measuring probe. The LEDs emit light with a peak wavelength at 710 nm, and are turned on one at a time. In order to reconstruct the values of the optical parameters of the sample volume, we assign a value of μ_a and μ_s' to each source-detector ray. This assignment is made possible by processing the data relative to different source-detector separations, whose values range from 2 to 4 cm. We then consider a weighted linear superposition of the values of μ_s' and μ_a relative to each source-detector ray, which yields an optical map of the region considered. Results from measurements on a phantom in a highly scattering medium will be shown. Supported by National Institutes of Health grant RR03155.

Th-Pos101

100kHz OPTICAL MULTI-CHANNEL ANALYZER. ((P.D. Smith, J. Cole, W.S. Friauf, H. Frederickson and R.W. Hendler)) NCRR, DCRT, and NHLBI, NIH, Bethesda, MD 20892.

An optical multi-channel analyzer capable of recording spectra at sampling rates up to 100kHz has been designed, constructed, and applied to studying the kinetic reaction mechanisms associated with cytochrome oxidase and bacteriorhodopsin. The instrument features a massively parallel approach in which each photosensing element of the detector has a dedicated amplifier, integrator, and data buffer. 92 such elements are divided in two separate arrays, each of which sits at the focal plane of a 1/4m Ebert monochromator. Both monochromators may be tuned to cover independent, 130nm wide, regions of the spectrum from 350nm to 900nm with a dispersion of 2.6nm per element. Each element has 12 bit resolution with an electronic dark count of +/-1 count. A total of 1024 reads from a single experiment can be made with intervals from 10us to several seconds. Custom software provides a number of computer driven features: entry of run parameters; transfer of data from temporary buffers to permanent files; real time display; sample averaging; and control and synchronization of associated experimental hardware. Optical fibers or lenses provide coupling from a parabolic reflector Xenon arc source, through the sample chamber, to the entry slit of the monochromator.

Th-Pos102

PROTEIN DYNAMICS STUDIED BY TIME RESOLVED TRIPLET-TRIPLET ABSORPTION FROM TRYPTOPHAN RESIDUES

((Anne Gershenson, Duncan G. Steel, Ari Gafni)) Institute of Gerontology, University of Michigan, Ann Arbor, MI 48109.

Triplet state spectroscopies are exquisitely sensitive to protein conformation and can be applied to probe structure and conformational transitions. We employ steady state, time resolved and circularly polarized phosphorescence techniques and are developing a transient absorption system. Absorption techniques allow investigation of nonemissive triplet states and triplet state photochemistry. Our system uses a CW argon laser as a probe beam. The focusability of both the probe and the excitation (frequency doubled dye laser) beams yields better overlap between the two beams than would a flash lamp probe. The low (<2%) signal strength of transient absorption on optically thin samples necessitates the use of a low noise probe beam. Our approach incorporates feedback control of the argon laser and a balanced detection system which results in a noise reduction of 32 dB. Initial experiments compare the phosphorescence decay kinetics to those observed using time resolved triplet-triplet absorption of E. coli alkaline phosphatase (AP) and rabbit phosphoglycerate kinase (PGK). AP contains 3 tryptophan residues per monomer only one of which, Trp109, phosphoresces in deoxygenated solution at room temperature. Phosphorescence measurements of AP show nonexponential kinetics with discrete lifetimes of order 1.8 and 0.5 seconds. Transient absorption experiments show the presence of decay kinetics not observed in phosphorescence. PGK displays negligible room temperature phosphorescence but has a transient absorption signal in both deoxygenated and aerated solutions indicating the presence of an absorbing species other than the tryptophan triplet. Supported by NIA grant AG09761 and ONR.

Th-Pos103

PHOSPHORESCENCE OF KERATIN FIBERS

Chandra M. Pande, *Clairol Inc. Stamford, Ct. 06922.*

Hair fibers are comprised of proteins belonging to the keratin family. The fiber structure is rather complex. The outer cuticle cells surround the inner cortical cells. The latter consist of crystalline fibrillar structures embedded in an amorphous matrix. Almost 95 % of the dry hair mass is proteinaceous.

We had previously reported on our fluorescence studies on hair fibers [1]. We have now measured the room temperature phosphorescence spectra from human hair. Excitation of hair at 285 nm results in the phosphorescence emission maximum at ca. 440 nm. The steady state spectra are generally similar for wool, yak hair, and human hair, although subtle differences exist. Time resolved experiments for the human hair reveal that at room temperature, at least two exponentials are needed to adequately fit the data with life times, τ, of 0.04 and 0.5 ms, respectively. Both components contribute almost equally. Interestingly, steady-state experiments reveal that addition of water, which is known to swell the hair fibers, increases the fluorescence emission at the expense of phosphorescence. Time-resolved experiments show that, under these conditions, the long lived (τ = 0.5 ms) component almost disappears. These data may provide an insight into the mechanistic aspects of the luminescence of keratin fibers and, perhaps, proteins in general.

1. C. Pande, *Biophys J.* (1991), 59, 40a.

Th-Pos104

Localization and characterization of signals for phosphorescence and fluorescence-lifetime-based sensing in tissues ((C.L. Burch, L. F. Suddeath, and E.M. Sevick)) Departments of Chemical and Biomedical Engineering, Vanderbilt University, Nashville, TN 37235.

Quantitative and non-invasive monitoring in the clinic may be possible with the development of near-infrared fluorescent and phosphorescent probes whose lifetimes, τ, are sensitive to changes in metabolic conditions. However, the utility of lifetime-based sensing depends upon (i) deconvoluting τ from time-dependent measurements of photon migration times and (ii) determining the tissue depth from which the phosphorescent or fluorescent signal originates. In this study, a computational finite element scheme was employed to show that quantitative determination of the τ may be recovered from properly referenced frequency-domain measurements. However, our results suggest that signals from fluorophores with long-lived lifetimes ($\tau \geq 50$ ns) cannot originate from significant tissue depths. Even when the fluorophore is concentrated at tissue regions far from the surface, the concentration of excited fluorophore may be maximum just beneath the tissue surface due to the preponderance of excitation fluence from the source. When a fluorescent probe is used for contrast in optical imaging, the apparent location of the predominant fluorescent signal will depend upon the selectivity and τ of the probe. The conclusions suggest that probes be developed with (i) minimal lifetimes for sensing deep tissue regions and with (ii) the greatest selectivity for diseased tissues for optical imaging. Supported by the Whitaker Foundation and the NSF Young Investigator Program (EMS).

Th-Pos105

TIME-RESOLVED ROOM TEMPERATURE PHOSPHORESCENCE OF THE SINGLE BURIED TRYPTOPHAN OF *Bacillus stearothermophilius* PHOSPHOFRUCTOSE KINASE.

((Bruce D. Schlyer‡, Duncan G. Steel‡§, Ari Gafni‡*))
Institute of Gerontology‡, Department of Biological Chemistry*, and Department of Physics and Electrical Engineering§, University of Michigan, Ann Arbor, MI.

The phosphorescence of the single tryptophan (Trp179) in *Bacillus stearothermophilius* phosphofructose kinase (PFK) shows distinctly nonexponential kinetics at room temperature with an average lifetime of 200 milliseconds. This complex decay behavior reflects heterogeneity in the Trp179 environment which exists on a time scale which is large with respect to the triplet state lifetime. Previous fluorescence measurements have shown that the heterogeneous decay of PFK arises from two micro-conformational states of Trp179 (Kim et al., Biophys. J. (1993) 63 215-226). This conclusion, based on extensive elimination of all other possible origins of heterogeneity, implies that the putative ground-state conformers interconvert on times scales which are slower than the nanosecond fluorescence lifetime. Our preliminary phosphorescence kinetics suggest that the ground-state heterogeneity reported by the fluorescence experiments involves conformers which exist on an extended time scale. Addition of the allosteric inhibitor phosphophenolpyruvate quenches the phosphorescence yet has little effect on the fluorescence. Data includes kinetic experiments involving temperature, externally added quenchers, excitation wavelength dependence, and circularly polarized phosphorescence.
Supported by NIA grant #AG09761 and ONR contract #N00014-91-J-1938.

Th-Pos106

MAGNETIC FIELD EFFECTS ON METAL-CATALYZED FREE RADICAL REACTIONS: LUMINOL RADICAL RECOMBINATION IN SOLUTION.

((Albert Zacarias, Bruce Simon* and Aruni Bhatnagar)). Department of Physiology and Biophysics, University of Texas Medical Branch, Galveston TX 77555 and *Electro-Biology Inc. Parsippany NJ 07054-1079.

Magnetic field dependence of chemiluminescent reactions of luminol (5-amino-2,3-dihydrophthalhydrazine 1,4-dione) was studied using a phase detection method. Luminol was mixed with an oxidant and made to flow through a flow cell surrounded by a pair of Helmholtz coils. The emitted light was measured using a photon counter which recorded light intensity in phase with a pulsed magnetic field (10 to 100 msec in duration). When potassium ferricyanide, $CuSO_4$, or hemin and hydrogen peroxide was used as the oxidant in protic solutions, the emitted light intensity increased, in phase with the external magnetic field. The increase in light intensity saturated at 30 Gauss with a $B_{1/2}$ value of 15 Gauss. The maximal increase in light intensity was 0.25 to 0.35 %. Under the present experimental conditions, recombination of the superoxide-generated peroxy radicals in aprotic media was insensitive to the external magnetic fields (< 300 Gauss). On the basis of these results it is hypothesized that external magnetic fields affect the recombination of nitrogen centered luminol and not the recombination rates of luminol semidione or its peroxy radical. External magnetic field-induced increase in light intensity can be explained by the ability of external magnetic fields to remove degeneracy from the triplet state of the radical pair and decrease the rate of radical recombination through a hyperfine effect. Similar hyperfine effects of low magnetic fields could affect the reaction yields of analogous biochemical reactions. (Supported by EBI grant and NIH grant HL 44675)

Th-Pos107

AFFINITY LABELING OF CYSTEINE-121 IN B-LACTOGLOBULIN WITH ALL-TRANS-4-BROMORETINAL.

((J.M.Chapman, B.M. Chapman, D.W. Brake, E.S. Hazard, K.L. Schey, and R.K. Crouch)) MUSC, Charleston,SC 29425.

Beta-Lactoglobulin (BLG) was chosen to investigate the possibility of covalently modifying a cysteine residue in a retinoid binding protein with an affinity label because of the amount of information that is known about its structure and binding properties. BLG commonly exists as two genetic variants A and B which differ in their amino acid sequence at positions 64 and 118. Both forms contain two disulfide bridges (66-160 and 106-119) and a free cysteine (121). The complex of BLG-retinol has a hydrophobic binding pocket that is limited by Phe 136, and by the following amino acid residues: 139 to 143 (Ala-Leu-Lys-Ala-Leu), 3 to 5 (Val-Thr-Gln), 105 to 106 (Phe-Cys), 117 to 119 (Leu-Val-Cys), and by Leu 95. It is the proximity of cysteine residue 121 to the binding pocket that made the study of affinity labeling BLG with 4-bromoretinal feasible. The uptake of all-trans-4-bromoretinal was studied by the quenching of protein fluorescence and binding was studied by incubating protein samples with 3H-11,12-4-bromoretinal. The quenching of protein fluorescence is equal to that of all-trans-retinal which has been previously shown to occupy the same binding pocket as all-trans-retinol. Protein was enzymatically digested and peptide fragments separated and collected by reverse phase HPLC. Both 214nm (amide bond) and 370nm (retinal) wavelengths were monitored and the peptide fragment that possessed covalently bound ligand was subjected to matrix assisted laser desorption time of flight spectroscopy. The molecular ion corresponded to a mass of 3899.36 daltons which was in close agreement of the predicted mass of 3901.8 daltons for the peptide containing residues 102-135 and the free cysteine residue 121. Partial Edman sequencing confirmed the identity of the peptide.

Th-Pos108

A FREQUENCY-DOMAIN MEASUREMENT OF THE SPECTRAL PROPERTIES OF A MULTIPLY SCATTERING MEDIUM CONTAINING METHEMOGLOBIN. ((J. B. Fishkin, P.T. C. So, A. Cerussi, S. Fantini, M.A. Franceschini, and E. Gratton)) Laboratory for Fluorescence Dynamics, Dept. of Physics, Univ. of Illinois at Urbana-Champaign, 1110 West Green, Urbana 61801.

We have measured the optical absorption and scattering coefficient spectra of a multiply scattering medium containing methemoglobin using frequency-domain techniques. The methemoglobin absorption spectrum determined in the multiply scattering medium is in excellent agreement with a corrected methemoglobin absorption spectrum obtained from a steady-state spectrophotometer measurement of the optical density of a minimally scattering medium. Frequency-domain techniques allow for the separation of the light absorbing from the light scattering properties of the medium, including the scattering due to the methemoglobin molecules distributed in the medium. Thus, frequency-domain techniques provide an absolute measurement of optical absorption spectra. The phase shift (Φ) and demodulation (M) of a light-intensity wave are the measured parameters typically used in the frequency-domain to determine optical properties. For multiply scattering media, these quantities can be written in terms of the optical parameters of the medium using diffusion theory. The methemoglobin absorption spectrum is accurately determined by fitting Φ and AC (or Φ and DC) data to diffusion theory, but inaccurately determined by fitting Φ and M data to diffusion theory ($M \equiv AC/DC$). Possible reasons for the inaccuracy of the methemoglobin absorption spectrum obtained from Φ and M data are discussed. Support: National Institutes of Health grants RR03155 & CA57032 .

Th-Pos109

FUNCTIONALITY OF PROTEINS AT WELL DEFINED SURFACES: MEASUREMENTS OF LIGHT INDUCED ELECTROGENIC EVENTS COMBINED WITH THE QUARTZ CRYSTAL MICROBALANCE E. Höök, M. Rodahl* and P Brzezinski, Dept. of Biochemistry and Biophysics and Dept. of Applied Physics*, Chalmers Univ. of Technology, S-41296 Göteborg, Sweden, Fax (+46)-31 7722811.

We have constructed an experimental set-up for studies of protein adsorption to well-defined surfaces and the properties of the adsorbed proteins. One part of the set-up is a quartz crystal microbalance (QCM) which consists of a quartz slab with a pair of gold electrodes deposited by evaporation on each side of the slab. An oscillator drives the quartz plate at its resonance frequency in gaseous or liquid environments. The frequency is sensitive to any mass adsorbed to the electrodes of the QCM and mass changes of approx. ~1 ng/cm^2 were resolved. Another parameter of the QCM is the quality (Q) factor, which is a measure of the dissipative losses in the adsorbed material. For example, a flexible adsorbed protein film induces more dissipative losses than does a rigid film of the same mass. In our set-up changes in 1/Q of ~10^{-8} were resolved. Consequently, the set-up is suitable for measurements of structural changes in the adsorbed protein film.

As a model system we chose reaction centers (RCs) from the photosynthetic bacterium *Rb. sphaeroides*. To simultaneously use the QCM technique and measure light-induced charge-transfer reactions (electrogenic events) in the RCs a gold surface was modified with an ~12 nm octadecylmercaptan (ODM) monolayer (hydrophobic insulator) and an RC-containing lipid monolayer was adsorbed to the ODM monolayer. Upon pulsed illumination we observed voltage changes associated with electrogenic events in the RCs. This shows that the techniques can be combined to in real time measure the monolayer adsorption, structural changes and light-induced electrogenic events in e.g. RCs.

Th-Pos110

DIELECTRIC SPECTROSCOPY OF A COMPLEX BIOLOGICAL SYSTEM. ((M. Egger and E. Donath*)) Physiologisches Institut, Universität Zürich, Winterthurerstr. 190, CH - 8057 Zürich, Switzerland; * Institut für Biophysik, FB Biologie, Humboldt-Universität zu Berlin, Invalidenstr. 42,D-O-1040 Berlin, Germany.

We demonstrated previously that it platelet activation can be assessed by means of "electrorotation" (Egger et al. Biochim. Biophys. Acta 972:265-276,1988). Upon activation the rotation decreased, and with strong activators completely disappeared. It was not clear how and at which step the activation process was coupled to the dielectric parameter change of the cell. Now, we investigated by means of comparing the capability of different activators to induce the rotation change in presence of diamide whether the electrorotation change is a primary membrane event or whether it depended on the more complex interplay of metabolic and cytoskeleton involved processes. We expected diamide to inhibit significantly protein dependent processes. It was shown that it is possible to quantify morphological changes and changes in the dielectric properties of the platelet membrane with dielectric spectroscopic measurements of "electrorotation" in the low and high frequency range. For the interpretation of the experimental results we used a model describing the electrorotation behavior of a large number of aggregated small particles as a function of the intensity of aggregation, of the dielectric parameters of the gap between the particles, and of the particle membrane.

Th-Pos111

TIME-RESOLVED X-RAY SPECTROSCOPY OF B-12 COENZYMES. ((W. Clavin, E. Scheuring, M. Wirt, L. Miller, N. Mahoney, J. Wu, Y. Lu, M. R. Chance)) Albert Einstein College of Medicine, Bronx, N.Y.

Methylcobalamin dependent enzymes catalyze methylation reactions which are accompanied by cyclization of the cofactor between Co(I) and Co(III)-methyl states. We chose to study the structure of the five coordinate "base-off" species, where the 5,6-dimethylbenzimidazole ligand in the fifth position is detached. Our earlier time-resolved optical studies imply the existence of a transient, four coordinate (square planar) complex subsequent to the photolysis of "base-off" alkylcobalamins. Such four coordinate Co(II) species are expected to be unstable but, their relevance to B-12 enzyme mechanisms is highlighted by our recent discovery of a four coordinate Co(II) species in the corrinoid protein of *C. thermoaceticum*. We utilized the time-multiplexed laser-photolysis system coupled to a rapid flow cell in order to characterize the structure of the initial photoproduct. The X-ray pre-edge spectrum of a 5-coordinate species has a significant peak, corresponding to a 1s-3d transition at about 10 eV below the edge. The 4-coordinate species lacks this feature but has a 1s-4p + SD peak at higher energy. We used this "fingerprint" to monitor the structural change upon photolysis. Since the quantum yield of the "base-off" species is 0.4, the production of a square planar photoproduct should reduce the intensity of the 1s-3d transition by 40% coincident with the laser flash. The photoproduct of the "base-off" methylcobalamin shows a significant decrease in the 1s-3d peak and the appearance of the 1s-4p + SD peak indicating a 4-coordinate species. This work was supported by the NSF grant #BIR-9303830.

Th-Pos112

A NEW METHOD FOR EXAMINING DYNAMICS :TIME RESOLVED X-RAY SPECTROSCOPY STUDIES OF TRIGGERED REACTIONS USING SOLID STATE DETECTORS ((M.R. Chance, E. Scheuring, A. Xie, L.M. Miller, Y. Lu, W. Clavin, J. Wu.)) Albert Einstein College of Medicine, Bronx, NY

The dynamics of metal sites in proteins are important to understanding the functional properties of enzyme reactions and ligand binding. A number of time-resolved spectroscopic techniques (especially optical and Raman studies) have greatly advanced our understanding of protein reactions. X-ray absorption spectroscopy is a well established technique for examining site geometry and bond distances in metalloproteins and has particular advantages in that data can be obtained in solution. We report a high signal-noise technique with microsecond time resolution to examine the structure of evolving metal centers after a laser trigger. This technique can be applied to any repetitively triggerable reaction of interest.

A solid state Canberra germanium detector produces current pulses related to the energy of the incoming x-ray photons. We used the unipolar outputs from spectroscopy amplifiers linked to a 13-element x-ray detector at beamline X-9 at the National Synchrotron Light Source. The amplifier pulses were input to a multi-channel discriminator/time-base circuit. Discriminated pulses are partitioned into 2048 time bins with user specified width from 5 μs to 300 ms per bin under software control. This work was supported by NSF-BIR-#9303830.

Th-Pos113

BOUNDARY CONDITIONS FOR THE DIFFUSION EQUATION IN RADIATIVE TRANSFER ((R. C. Haskell, B. J. Tromberg, L. O. Svaasand, T.-T. Tsay, T.-C. Feng, and M. S. McAdams)) Harvey Mudd College, Claremont, CA 91711; Beckman Laser Institute, U. of CA, Irvine, CA 92715; U. of Trondheim, 7000 Trondheim, Norway

Using the method of images, we examine the three boundary conditions commonly applied to the surface of a semi-infinite turbid medium. We find that the image charge configurations of the "partial current" and "extrapolated boundary" conditions have the same dipole and quadrupole moments, and that the two corresponding solutions to the diffusion equation are approximately equal. In applying diffusion theory to frequency-domain photon migration (FDPM) data, these two approaches yield values for the scattering and absorption coefficients that are equal to within 3%. Moreover, the two boundary conditions can be combined to yield a remarkably simple, accurate, and computationally fast method for extracting values for optical parameters from FDPM data.

FDPM data was taken both at the surface and deep inside tissue phantoms, and the difference in data between the two geometries is striking. Neglect of the boundary in analyzing surface data results in errors of 50% or more in values deduced for the optical coefficients. As expected, aluminum foil placed on the surface of a tissue phantom resulted in phase and modulation data closer to that of an infinite medium geometry. Raising the reflectivity of a tissue surface can, in principle, eliminate the effect of the boundary. However, we find that phase and modulation data are very sensitive to the reflectivity in the range 80% to 100%, and a minimum value of 98% is needed to reliably mimic an infinite medium geometry. We conclude that non-invasive measurements of optically thick tissue require a rigorous treatment of the tissue boundary, and we suggest a unified partial current - extrapolated boundary approach.

Th-Pos114

TWO-PHOTON SCANNING PHOTOCHEMICAL MICROSCOPY: MAPPING LIGAND GATED ION CHANNELS. ((Winfried Denk and Jürgen A. Steyer)), AT&T Bell Laboratories, Murray Hill, NJ 07479.)

We report the imaging of the acetylcholine receptor (AchR) distribution on cultured BC3H1 cells by localized two-photon-absorption induced photochemical release of the nicotinic agonist carbamoylcholine from an inactive or "caged" precursor, (N-((α-2-carboxy)-2-nitrobenzyl)carbamoylcholine). The location of the laser focus is raster scanned across the specimen while the transmembrane current is recorded using a patch clamp electrode in whole-cell mode. By using the detected current magnitude to control the pixel intensity an "induced-current" image is generated that reflects the receptor distribution at a resolution approaching the size of the diffraction limited focal spot. This method specifically detects receptors on that cell that was selected for patch-clamp recording, a property expected to be invaluable for elucidating connectivities in the intertwined network of cells in the central nervous system. The highly nonlinear two-photon excitation probability affords optical section properties equivalent to those of confocal imaging. Excitation light came from a colliding pulse mode locked (CPM) dye laser which produces pulses with a repetition rate of 150 MHz and a pulse width of below 100 fs. Both rhodamine 6G and B were used alternatively as gain dyes, yielding wavelengths of around 620 and 640 nm respectively, both of which are effective at uncaging but photodamage, as assessed by the increase in the baseline holding current, was much reduced at the longer wavelength. The response time of the whole cell current limits the achievable scan speed so that an image of a single focal slice is acquired in ≈ 100 s. In our case the background current noise limiting the sensitivity, which may reach single receptor levels for better caged compounds, is dominated by channel gating due to activation of some fraction of the nicotinic current by the caged compound. Preliminary results indicate that this activation is due to the caged compound itself rather than to contamination by free carbamoylcholine. We expect this method to be easily extendible to other caged neurotransmitters as well as to caged intracellular messenger substances.

Th-Pos115

CALCIUM-ION MICRODOMAINS AT SINGLE PRESYNAPTIC ACTIVE ZONES IMAGED BY FLUORESCENCE CONFOCAL MICROSCOPY. ((Naoum P. Issa and A. J. Hudspeth)) Howard Hughes Medical Institute and Center for Basic Neuroscience Research, University of Texas Southwestern Medical Center, Dallas, TX 75235-9117.

Exocytosis of neurotransmitter molecules is triggered by the influx of Ca^{2+} at a presynaptic terminal. Recent measurements have demonstrated that the Ca^{2+} concentration at presynaptic active zones in frog hair cells can transiently reach 1 mM (Roberts *et al., J. Neurosci.* 10:3664, 1990). In an effort to measure the time course of changes in Ca^{2+} concentration at presynaptic active zones, we used tight-seal, whole-cell recording pipettes to load hair cells with the Ca^{2+}-sensitive dye, fluo-3. We observed approximately 20 fluorescent spots, each about 0.5 μm in diameter, along a cell's basolateral surface. Because the distribution of these spots resembled that of presynaptic active zones, we compared the pattern of fluo-3 fluorescence with transmission electron micrographs of serial sections from the same four hair cells. At least 84% of the bright spots in confocal images corresponded to presynaptic active zones. The intensity of the bright spots increased in response to cellular depolarization that caused Ca^{2+} influx, and decreased with hyperpolarization. Tight-seal, cell-attached recordings from the membrane patches at active zones verified the colocalization of voltage-gated Ca^{2+} channels and Ca^{2+}-activated K^+ channels at the hair cell's afferent synapse. The results confirm that most of a hair cell's Ca^{2+} channels congregate at some 20 active zones, and indicate that depolarization creates microdomains of high Ca^{2+} concentration immediately adjacent to presynaptic membranes.

Th-Pos116

ATOMIC FORCE SCANNING MICROSCOPY LOCALIZATION OF CALCIUM CHANNELS AT A CHOLINERGIC PRESYNAPTIC NERVE TERMINAL TRANSMITTER RELEASE FACE. ((E.F. Stanley*, V. Parpura+ and P.G. Haydon+)). *Synaptic Mechanisms Section NINDS NIH; +Signal Transduction Training Group ISU.

We applied Atomic Force Scanning Microscopy (AFM) to the calyx-type presynaptic nerve terminals of the chick ciliary ganglion to examine surface topography and to localize the calcium channels associated with transmitter release. Calyces were identified by dye staining (J. Neurosci.11:985; Neuron 7:585) and were then fixed and scanned with the AFM. We used ω-conotoxin GVIA (ω-CTX), which blocks transmitter release and calcium influx in this synapse (PNAS 87:9683) to locate the presynaptic calcium channels. The terminals were treated with biotinilated ω-CTX, fixed and scanned. The same terminal regions were then re-scanned after treatment with streptavidin-30 nm gold to tag the toxin and the calcium channels. Clusters of particles were noted that reflect the location of the presynaptic calcium channels since neighboring non-terminal structures and treminals pre-blocked with untagged ω-CTX were virtually particle free. Within each cluster the gold particles were distributed in arrays suggestive of a discrete organization of the release face calcium channels.

Th-Pos117

CYCLOTHIAZIDE ENHANCES EPILEPTIFORM DISCHARGES IN RAT NEOCORTICAL NEURONS. ((M. R. Pelletier and J. J. Hablitz)) Neurobiology Research Center, Univ. of Alabama at Birmingham, Birmingham, AL 35294.

Cyclothiazide (CYZ) inhibits the rapid desensitization characteristic of AMPA receptors and prolongs AMPA mediated synaptic currents. We investigated the role of AMPA receptor desensitization in control of synaptic responses in rat neocortex. Intracellular recordings were obtained from layer II/III pyramidal neurons in in vitro brain slices. AMPA mediated responses were isolated by recording in the presence of 3 mM Mg^{++} and 20-50 μM APV and 10 μM bicuculline to block NMDA and $GABA_A$ receptors. Under these conditions stimulation in layer IV/V evoked an epileptiform discharge consisting of a membrane depolarization with superimposed action potentials (PDS). Bath application of CYZ did not affect input resistance, resting potential or repetitive firing. An increase in PDS amplitude and duration was observed. These effects were quantified from measurements of the PDS integral. After 15 min of exposure, CYZ produced 28.7% (n=5) and 37.4% (n=4) increases in the PDS integral at concentrations of 20 and 100 μM, respectively. These effects were not reversible during a wash period of 15 min. The effect of 100 μM CYZ increased during the wash period. PDS integrals were increased by 73.4% at the end of the wash relative to control while responses in neurons exposed to 20 μM CYZ remained enhanced by 31.4%. These results suggest that AMPA receptor desensitization may contribute to regulation of synaptic responses in adult neocortical neurons in vitro.

Th-Pos118

MODELING AND SIMULATION OF SINGLE NMDA-ACTIVATED ION CHANNELS. ((N. W. Kleckner and B. S. Pallotta)) Dept. of Pharmacology, University of North Carolina at Chapel Hill, Chapel Hill NC 27599.

N-Methyl-D-aspartate (NMDA) receptor linked ion channels are a subset of excitatory amino acid receptors found throughout the brain. Although much is known about the functions and macroscopic activity of these channels, no kinetic models have been proposed that accurately describe their single-channel kinetic behavior. Based on a detailed kinetic analysis of recordings from NMDA/glycine-activated single channels, we have generated a model that describes the single-channel behavior of NMDA channels at one concentration of NMDA and glycine. NMDA/glycine-activated currents were recorded from cell-attached patches of rat brain cortical neurons maintained in culture. To control the membrane potential using this patch configuration the cells were depolarized by external application of a high K^+ containing solution (110 mM), and the patch potential was adjusted to -70 mV. NMDA (1 μM) and glycine (10 μM) were present in the patch pipette. The kinetic model proposed below was generated as the result of a series of kinetic analyses of single-channel data. The number of kinetic states in the model was determined by the fit of open and shut interval histograms with the sum of 2 and 5 components, respectively. Transitions between kinetic states were determined by burst/cluster analysis, adjacent states, gateway analysis, and autocorrelation. Simulated data based on this model were analyzed by the same methods described above for actual data. Simulated data gave open and shut interval distributions with time constants and relative areas that are similar to actual data. The model accurately predicts channel bursting behavior, including the proportions of short and long openings in single and multiple opening bursts, clusters and superclusters. This model will be expanded to account for the dependence of channel kinetics on NMDA and glycine concentration. Supported by NIH NS29881.

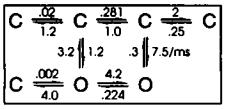

Th-Pos119

PROPERTIES OF NMDA-ACTIVATED CHANNELS TREATED WITH THE HISTIDINE MODIFIER DIETHYLPYROCARBONATE (DEP): BURST PROPERTIES, INHIBITION BY ZINC, AND REVERSAL BY HYDROXYLAMINE. ((J.L. Donnelly and B.S. Pallotta.)) Dept. of Pharmacology, University of North Carolina at Chapel Hill, Chapel Hill, NC 27599.

We previously reported (Biophys.J (1993) 64:A324) that the open probability of NMDA channels in outside-out patches from rat cortical neurons is increased 2-5-fold after treatment with DEP. We have continued to study this effect so that a kinetic description of the modified channel might be derived and to further examine the characteristics of the modification.

Kinetic analysis of DEP-modified channels shows an increase in number of openings per burst as well as an increase in burst duration. Adjacent states and autocorrelation analyses indicate that the connectivity between closed and open states has not been disturbed by the modification. These results are consistent with our previously proposed model.

In whole-cell studies, DEP reduces the sensitivity of NMDA-activated channels to voltage-independent high-affinity zinc inhibition (Traynelis and Cull-Candy (1991) J. Physiol. 433:727). In our studies of outside-out patches however, DEP modification does not affect sensitivity to zinc (IC_{50} ~ 0.1 μM). This discrepancy might indicate that the effects of DEP depend on the time of exposure: 30 sec in our experiments compared to 1-10 min. in the whole-cell work.

The effects of DEP appear to arise from histidine(s) modification. Treatment of outside-out patches with TNBS, a lysine modifier and N-acetylimidazole, a tyrosine modifier, did not reproduce the effects of DEP. In addition, the effect can be reversed by treatment with 10 mM hydroxylamine, which specifically reverses the modification of histidine and tyrosine residues. In some patches, hydroxylamine irreversibly increased the open probability of DEP-modified channels. As hydroxylamine treatment of unmodified channels had no effect, this increase was probably due to cleavage of di-modified rings, further evidence that a histidine is reponsible for the effect. Supported by NS 29881.

Th-Pos120

DENDRITIC RECORDINGS OF SINGLE VOLTAGE-GATED Na^+ AND Ca^{2+} CHANNELS IN CA1 PYRAMIDAL NEURONS

((J.C. Magee & D. Johnston)), Division of Neuroscience, Baylor College of Medicine, Houston, TX 77030

Many central neurons possess extensive dendritic arborizations that act to integrate synaptic activity recieved from the thousands of synapses located on the dendrites. Historically, dendrites have been considered to be passive membrane structures. However, substantial evidence continues to accumulate suggesting that active processes do exist within dendrites. Cell-attached patch techniques in hippocampal slices were used to record single Na^+ and Ca^{2+} channel activity in the proximal dendrites (20 to 120 μm from soma) of CA1 pyramids. Na^+ channel activity could be identified by inward current polarity, voltage-dependent gating and unitary current amplitude (-1.6 pA at -40 mV). Addition of QX-314 to the cell interior and TTX to pipette solution reduced channel activity. Na^+ channels were found in every patch examined and more than a single channel was usually present. Mean slope condutance was 15 pS and extrapolated reversal potential was +60 mV. Ca^{2+} Channel activity was also recorded using a pipette solution containing mainly BaCl2. Ca^{2+} channel openings were found in about every third patch examined and patches containing only a single channel were often encountered. Addition of Cd to pipette solution eliminated channel openings. In 3 of 16 patches, channels possessing a large unitary current amplitude (-1.5 pA at 0 mV), slope conductance (approx. 30 pS) and a sensitivity to BAYK 8644 were found. In 13 of 16 patches we recorded activity from channels that had lower slope conductances (12 to19 pS). These channels could be further subdivided on the basis of channel behavior. One set showed transient openings and reopenings and a unitary current of -0.8 pA at -10 mV and the second displayed prolonged channel openings and a smaller unitary current (-0.5 pA at -10 mV). Thus there are multiple types of Ca^{2+} channels and a single type of Na^+ channel present in the proximal dendrites of CA1 pyramidal cells, (NS09482-01).

Th-Pos121

COVALENT DERIVATIZATION AND SEQUENCING OF MEMBRANE PROTEINS USING MASS SPECTROMETRY.

((G.H. Addona, T.A. Davis, D.F. Hunt and D.S. Cafiso)). Department of Chemistry, University of Virginia, Charlottesville, VA 22901.

In an effort to examine the structure of the nicotinic acetylcholine receptor(nAChR) and other large membrane proteins, we have developed a rapid, highly sensitive method to identify lysine residues accessible to covalent derivatization. The AChR was purified from *T. Californica* by affinity chromatography and reconstituted into egg phosphatidylcholine at lipid to protein ratios of 400:1. Accessible lysines in the reconstituted AChR were modified with water soluble sulfosuccinimidobiotin. The labeled AChR was fragmented with *Staphylococcus aureus* V8 and water soluble biotinylated fragments isolated with avidin affinity chromatography. Derivatized peptides were identified with a matrix-assisted laser desorption time of flight mass spectrometer and/or electrospray ionization tandem mass spectrometer. Many regions of the AChR were derivatized, including the N-terminal region and the region between putative α-helices M3 and M4. Derivatization of the native AChR structure in well-sealed systems is currently underway. This work is relevant to studying the transmembrane topology of membrane proteins as well as their tertiary structure. Methods are being explored using bifunctional reagents and amide-proton exchange with mass spectrometry to provide tertiary structural information on membrane proteins.

Th-Pos122

CALCIUM INFLUX THROUGH CLUSTERS OF RECOMBINANT GLUTAMATE RECEPTOR CHANNELS EXPRESSED IN XENOPUS OOCYTES

((D. Gremmels, M. Hollmann*, S. Heinemann*, A. Konnerth+ and B.U. Keller)) MPI für biophys. Chemie, 37077 Göttingen, +Universität des Saarlandes, Homburg, Germany *Salk Institute, La Jolla, CA 92037. (Spon. by B.U. Keller)

The functional properties of recombinant glutamate receptor channels of the AMPA/KA receptor type were studied after expression in *Xenopus* oocytes. Recombinant channels composed of subunits $GluR_1$ - $GluR_6$ were studied by simultaneous electrophysiological measurements and video calcium imaging using the fluorometric dye fura-2. Application of glutamate receptor agonists induced monovalent cation currents as well as calcium influx through AMPA/KA receptor channels for all subunit combinations investigated. Calcium influx induced significant elevations of intracellular calcium in spatially distinct membrane sites ("membrane hot spots"), which correlated with the sites of maximum current response to GluR agonists. A significant calcium influx was observed for subunit combinations $GluR_{1,2}$ and $GluR_{2,3}$, which form channels with linear I-V relations. Under comparable conditions, linearly conducting channels induced intracellular calcium elevations which were one order of magnitude smaller compared to those induced by inwardly rectifying AMPA/KA receptor channels $GluR_1$, $GluR_3$ or $GluR_{1,3}$. Video imaging analysis showed that the elevations in intracellular calcium concentrations depended significantly on the density of channels in the oocyte. For clusters of linearly conducting AMPA/KA receptor channels, local calcium concentrations reached maximum values of several hundred nanomolars, suggesting that calcium influx through clusters of these channels is a significant factor in the regulation of cytosolic calcium levels.

Th-Pos123

EXPRESSION CLONING OF A NOVEL GLUTAMATE-GATED CHLORIDE CHANNEL FROM *CAENORHABDITIS ELEGANS*.

((D.F. Cully, D.K. Vassilatis, P.S. Paress, K.K. Liu, and J.P. Arena)) Merck Research Laboratories, Rahway, N.J. 07065 (Spon. by M. Leibowitz)

The soil nematode *Caenorhabditis elegans* has been used extensively as a model for neurobiology and development. We have used *C. elegans* to study the mode of action of the family of compounds called avermectins, which have potent anthelmintic and insecticide activity. To clone the target of avermectin action we have used the surrogate expression system of the *Xenopus laevis* oocyte. *C. elegans* RNA injected into oocytes encodes a chloride channel that is sensitive to both avermectin and the neurotransmitter glutamate[1,2]. An *in vitro* RNA expression library was synthesized from size fractionated *C. elegans* RNA and a pool of 5000 clones was identified that encoded a glutamate and avermectin-sensitive current. Subfractionation of the pool of 5000 into smaller pools indicated that two subunits were present in the 5000 pool that were necessary for recovering both the avermectin and glutamate responses. By a process involving the reconstitution of these responses through the complementation of the subfractionated pool with RNA from a second pool we have isolated two different clones; pGluClα and pGluClβ. RNA from pGluClα elicits a current sensitive to avermectin but not to glutamate while pGluClβ RNA elicits a glutamate-sensitive but avermectin-insensitive current. (See Arena et. al., this session, for details of electrophysiology.) The DNA sequences of these clones predict proteins that share approximately 38% identity with the GABA and glycine-gated chloride channel subunits. Phylogenetic analyses show that GluClα and GluClβ are members of a novel subclass of ligand-gated chloride channels.

1. Arena, J. P. et. al. Mol. Pharm. 40: 368-374, 1991
2. Arena, J. P. et. al. Mol. Brain Res. 15: 339-348, 1992

Th-Pos124

PROPERTIES OF A NOVEL GLUTAMATE-GATED CHLORIDE CHANNEL FROM *CAENORHABDITIS ELEGANS*.

((J.P. Arena, K.K. Liu, D.K. Vassilatis, P.S. Paress and D.F. Cully)) Merck Research Laboratories, Rahway, N.J. 07065.

Poly (A^+) RNA isolated from the soil nematode *Caenorhabditis elegans* encodes for a glutamate- and avermectin-sensitive chloride channel in *Xenopus* oocytes[1,2]. Using an expression cloning approach we isolated two clones, pGluClα and pGluClβ, that upon coexpression in oocytes reconstituted many of the properties observed after injection of poly (A^+) RNA (See Cully, et. al., this session for cloning). After coexpression of the two clones, avermectin directly activated a membrane current (EC_{50}=189 ± 7 nM(SEM)), that was blocked with picrotoxin (50 μM). The EC_{50} for activation of current with L-glutamate was 1.36 ± 0.05 mM. Current was also activated with a structural analog of glutamate, ibotenic acid, but not with NMDA, quisqualate, kainate, AMPA, GABA, or glycine. The response to submaximal glutamate concentrations was potentiated 5-fold in the presence of avermectin. The reversal potential for either glutamate- or avermectin-sensitive current was -35 ± 1 mV in 122 mM $[Cl]_O$, and shifted to 29 ± 3 mV in 7.6 mM $[Cl]_O$. The current/voltage relationship (I/V) outwardly rectified in a manner predicted by the Goldman-Hodgkin-Katz equation (GHK). When mRNA from pGluClα was injected, oocytes expressed a chloride channel that was sensitive to ivermectin (EC_{50}=142 ± 15 nM), but not glutamate. Conversely, injection of RNA from pGluClβ encoded a chloride channel that was activated by glutamate (EC_{50}=378 ± 20 μM) but not avermectin. Moreover, the glutamate response in oocytes expressing homomeric GluClβ channels was not potentiated by avermectin. The I/V for homomeric GluClα was more linear than predicted by GHK, while the I/V for homomeric GluClβ was more outwardly rectifying than the GHK prediction. We conclude that GluClα and GluClβ associate upon expression to form heteromeric chloride channels. They represent subunits of a novel subclass of chloride channels gated by glutamate and modulated by avermectins.

1. Arena, J.P. et. al. Mol. Pharmacol. 40: 368-374, 1991
2. Arena, J.P. et. al. Mol. Brain Res. 15: 339-348, 1992

Th-Pos125

SYNAPTOTAGMIN AND SYNTAXIN ARE NOT PRIMARY TARGETS OF LAMBERT-EATON MYASTHENIC SYNDROME AUTOANTIBODY.

((Ravindra K. Hajela and William D. Atchison)), Department of Pharmacology and Toxicology and Neuroscience Program, Michigan State University, East Lansing, MI 48824-1317, USA.

Lambert-Eaton Myasthenic Syndrome (LEMS) is an autoimmune neuromuscular disease in which impaired Ca^{2+} entry into the nerve ending and release of acetylcholine results in muscle weakness. The identity of the primary antigenic target molecule(s) of the autoantibodies is uncertain, but is believed to be the Ca^{2+} channel complex at the motor nerve terminal. Some recent studies however, suggest more indirect impedance caused by autoantibodies binding to synaptotagmin or syntaxin, molecules presumed to be involved in docking and/or coupling the synaptic vesicles to the Ca^{2+} channels in the active zone. Western blot analyses of rat and human brain synaptosomal proteins and pure recombinant synaptotagmin and syntaxin were used to test directly the hypothesis that LEMS autoantibodies are directed against either synaptotagmin or syntaxin. We find no reactive component against either peptide in IgG of five LEMS patients, whereas both human and rat brain contain proteins recognized by antibodies directed against synaptotagmin or syntaxin. This suggests that these proteins are not the primary targets of LEMS antibodies. Supported by NIH grant ES05822 and a BRSG Grant from the College of Veterinary Medicine at Michigan State University.

Th-Pos126

CHARACTERIZATION OF A HIGH-VOLTAGE ACTIVATED CALCIUM CURRENT IN ISOLATED PEPTIDERGIC TERMINALS FROM THE CRAB, *CARDISOMA CARNIFEX*.
((J.E. Richmond and R.Penner)) University of Hawaii, Honolulu, HI 96822. (Spon. by I.M. Cooke)

The properties of calcium channels underlying peptide release have been described in very few neuronal preparations due to the inaccessibility of the secretory terminals. The X-organ - sinus gland, a major peptidergic neurosecretory system in Crustacea analagous to the vertebrate neurohypophysis, has large nerve endings (up to 25 µm diameter) which can be isolated and voltage-clamped. Using these terminals, we have examined calcium currents in the whole-cell voltage-clamp configuration. There appears to be only one type of calcium current based on current-voltage relationships from holding potentials (V_h) of -90 mV and -50 mV. This current is high-voltage activated, starting at -40 mV and reaching peak current amplitude at +10 mV. Peak currents for terminals in 52 mM external calcium are -45.1 ± 14.4 pA (mean and S.D), with an average current density of 12.9 µA/cm^2. The $V_{1/2}$ for activation is -5.3 mV, with a slope conductance of 3.8 *e*. In 52 mM calcium the current totally inactivates within 200 msec at prepulse potentials around +10 mV. Replacement of calcium with isotonic barium removes this inactivation suggesting that inactivation over this time range is calcium-dependent. A comparison of the terminal calcium current with that of the isolated neuronal somata from which the terminals project, suggests that the calcium currents in these two regions are identical. Although these currents resemble the L-type calcium currents of vertebrate neurons, they show no dihydropyridine-sensitivity. We are currently examining other high-voltage activated calcium channel blockers to further define the pharmacological profile of this calcium current. These results demonstrate that, unlike the rat neurohypophyseal terminals which possess both low- and high-voltage activated calcium channels, the terminals of crab X organ neurons have a single population of high-voltage activated channels. Supported by NIH Grant RO1 NS15453 to I. M. Cooke.

Th-Pos127

SODIUM/CALCIUM EXCHANGER GENE EXPRESSION IN AGING RAT BRAIN
((V.Janapati and R.A.Colvin)) Department of Biological Sciences, Ohio University College of Osteopathic Medicine, Athens, OH 45701, USA.

The sodium/calcium exchanger is a transmembrane protein ubiquitously present in most excitable cells. It plays an important role in the maintenance of intracellular Ca^{2+} ion concentration. Chronic elevation of cytoplasmic calcium ion concentration is toxic and may be responsible for neuronal degeneration and death associated with aging and in certain neurodegenerative disorders. To study age dependent changes in the expression of the sodium/calcium exchanger gene in rat brain a 300bp probe was generated by RT-PCR of human brain total RNA. Primers for the PCR were designed based on the published cDNA sequence for the human heart exchanger. The PCR amplified fragment was subcloned and ^{32}P-labeled cRNA or cDNA probes were generated. Northern analysis was performed on total RNA isolated from different brain regions of 3 months (young) and 24 months (old) Fischer 344 rats. The results showed at least two transcripts for the exchanger corresponding to sizes 7kb and 15kb. The two transcripts are present in the three brain regions analyzed - cerebral cortex, cerebellum and hippocampus. The 15kb transcript was most prevalent in cerebral cortex whereas the 7kb transcript was predominant in cerebellum and hippocampus. Comparison of the age dependent expression of these two transcripts showed a significant decline in the levels of both the transcripts only in cerebral cortex. The results suggest that the aging process may alter the gene expression of the exchanger in the rat cerebral cortex. Recently, Ian Furman and colleagues (FEBS 319:105-109) have isolated two isoform cDNAs for the exchanger from a rat brain cDNA library. We have developed a probe to measure the levels of these two isoforms in rat brain by RNase protection assay. This probe will be used to study how the isoform levels are altered during aging in rat cerebral cortex.

Th-Pos128

ELECTROGENIC SEROTONIN TRANSPORT IN STABLE CELL LINES ((S. Risso, L.J. DeFelice, B.J. Duke, F. Laezza, R.D. Blakely)) Dept of Anatomy and Cell Biology, Emory University School of Medicine, Atlanta, GA 30322.

Na and Cl ions co-transport with serotonin (5HT), but uptake is reported as electroneutral. Our results show that 5HT transport generates current. We have investigated the electrophysiological properties of human 5HT transporter (hSERT) with whole cell voltage-clamp techniques. The experiments are performed at room temperature. The pipette contains an intracellular-like solution (KCl 120 mM; $CaCl_2$ 0.1 µM) and the cells are bathed in physiological solution (NaCl 130 mM). Patching 293 cells stably transfected with the hSERT cDNA, we recorded 5HT-induced currents. The figure shows the current response to a seven sec voltage ramp. The endogenous current is the control. The induced inward current increases with the concentration of 5HT and reaches a saturation at 0.5 µM 5HT. With 1µM 5HT, the induced current is 40 pA at -120 mV. The current does not reverse. A highly specific antagonist of the hSERT, paroxetine (1 µM), reduces the current to control (cf. Bruns et al., Neuron 10:559-572, 1993). The figure in the insert shows the normalized average current from 5 cells at V= -80 mV as a function of the 5HT concentration. The current fits the Hill equation: $I=Io[S]^n/([S]^n+Km^n)$; n=1.44+/-0.17; Km=0.24+/-0.03 µM, which agrees with radioactive flux studies. (NIH 1-PO1-HL27385 and NIH DA-07390)

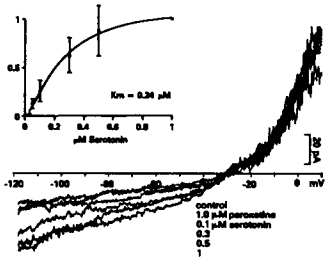

Th-Pos129

TYROSINE KINASE ACTIVATION PREVENTS CHANNEL MODULATION BY PROTEIN KINASE C DURING SYNAPSE FORMATION.
((S. Catarsi and P. Drapeau)) Centre for Research in Neuroscience, McGill University and MGH Research Institute, Montreal, Quebec, Canada H3G 1A4.

We have examined the signals regulating extrasynaptic channel modulation by transmitter during synapse formation between identified leech neurons. An early event during innervation of the P neuron by the R neuron is the loss at sites of cell contact of extrasynaptic, depolarizing cation channel modulation by protein kinase C (PKC), which is activated by the R cell transmitter, serotonin (5-HT). This response to 5-HT was lost within an hour at sites of contact with neurites of the P cell. The selective tyrosine kinase inhibitor lavendustin A (but not the inactive B form) prevented the loss of the extrasynaptic response and blocked synapse formation. Single cation channel recordings revealed that the channels lost their sensitivity to PKC activation by the phorbol ester PMA and that this could be prevented by tyrosine kinase inhibitors.
We conclude that R cell-specific contact activates a P cell tyrosine kinase that renders extrasynaptic channels insensitive to modulation by PKC as a necessary functional event during synapse formation.
Supported by the MRC, FRSQ and FCAR of Canada & HFSP.

Th-Pos130

Computer simulation of Voltage-dependent Sodium Channels (NaCs) Clustering in Neuron Membrane.
((L. P. Savtchenko & S. M. Korogod)) lab of biophysics & bioelectronics, State Univ., 320625, Dniepropetrovsk, Ukraine.
It is know that a decisive role of cell-cell connections belong of plasmic membrane. In a neuronal plasmic membranes the spatial distribution of NaCs, of transmembrane potential and Na^+-ion inner concentration may play a impotent role in function neuronal cells. We was observed in a mathematical model of cylinder-shaped cell creation of the spatial distribution of open NaCs in the form of steady state spatially non-uniform, in particular spatially periodical, longitudinal distributions. The resulting spatial distribution is suggested as a kind of dissipative structure appearing far from equilibrium maintained due to consuming the energy of dephosphorylation of the ATP molecules. In our view, two principal physiological aspects of the results obtained could be emphasized. First, maintained non-uniform distribution of the membrane potential could be a factor which controls the state (and probably weight) of synapses located on the membrane. Second, maintained non-uniform distribution of the surface density of NaCs (and probably other membrane proteins) could underlie morphogenetic events (e.g. shaping, process outgrowth etc.). The crucial point is that these distributions, being dissipative structures, depend on the intrinsic system parameters (process diameter, mean channel density, the length and time constants etc.), and also external influences.

Th-Pos131

PREPARATION OF EXTRUDED LIPOSOMES WITH INORGANIC MICROPOROUS MEMBRANES.

((David G. Rhodes and Chengjiu Hu)) Pharmaceutics Division College of Pharmacy, U. of Texas at Austin, Austin, TX 78712-1074

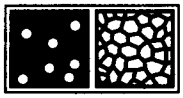

Extrusion methods provide a facile method of manufacturing unilamellar liposomes. These liposomes have been used in a wide variety research applications and for drug encapsulation. Most published protocols use Nucleopore® filters, but the pore area of these filters (2.35% of total area for 100 nm pores) is very small. Whatman® Anopore™ membranes are rigid aluminum oxide, with a 'honeycomb' structure which leaves approximately 40% of the total filter area open. Liposomes of several compositions have been produced using both filters, and compared. Electron microscopy and laser light scattering particle size analysis have been used to evaluate the quality and reproducibility of liposomes prepared by extrusion with Anopore™ membranes. Fluorescence and radiotracer methods have been used to evaluate retention and encapsulation efficiency. These filters provide a rapid, efficient means of producing liposomes with well defined size distribution and superior retention efficiency. The principal disadvantage appears to be the limited number of available sizes compared to the Nucleopore® membranes.

Th-Pos132

QUALITY CONTROL OF LIPID VESICLE MORPHOLOGY: A PRACTICE-ORIENTED SET OF ASSAY METHODS.

((H.J.Gruber, Th.Schmidt, A.Pilger, and H.Schindler)) Institute for Biophysics, J. Kepler University, A-4040 Linz, Austria

Three methods are presented for the determination of external surface of lipid vesicles with 2 % absolute accuracy. These methods (referred to as ESR, NBD and TNBS assays) use different marker lipids (a spin-labeled lipid analogue, NBD-PE, or aminolipids in general, respectively). Spectroscopic signal from the external fraction of marker lipids change upon addition of "impermeable" external reagents (ascorbate, dithionite, or TNBS, respectively), allowing to calculate the fraction of membrane surface accessible to external reagent. External surface data for identical batches of vesicles matched for the three assays within 2 %, but only after appropriate redesign or adaptation of so far published procedures. Main improvements related to slow influx of reagents (TNBS and NBD assays) or to redistribution of marker lipids (ESR assay), obscuring determination of outer vesicle surface from fast reaction between reagent and readily accessible marker lipids. Furthermore, suitable stategies were found to obtain accurate 100 % values (reaction of all marker lipids present). This included corrections for light scattering (NBD assay) and for turbidity (TNBS assay).

For the determination of inaccessible volume trapped chloride was chosen as a convenient marker because its ubiquity eliminates the need for prelabeling. As in the case of external surface assays a number of pitfalls had to be eliminated from conventional procedures in order to obtain reliable data under widely differing circumstances.

Th-Pos133

RAPID SEPARATION OF CONTAMINANTING SUVS FROM EXTRUDED DMPC LUVS AS CHARACTERIZED USING CYTOCHROME B5.

((Robert Doebler and Peter W. Holloway)) Dept. of Biochemistry, Univ. of Virginia Sch. Med., Charlottesville, VA.

Cytochrome b_5 (b_5) binds spontaneously to lipid vesicles via a 43 amino acid membrane-binding domain. The degree of binding of b_5 is known to be sensitive to vesicle size, with the protein having a higher affinity for small unilamellar vesicles (SUVs) than for large unilamellar vesicles (LUVs). Dimyristoylphosphatidylcholine (DMPC) LUVs prepared by the hand-held extrusion method contain contaminating smaller vesicles which compete for b_5, and so lower the amount of protein bound to the actual LUVs. Partial separation of contaminating small vesicles from extruded LUVs is achieved by centrifugation through minicolumns of Sephacryl S-500 with greater than 50% recovery of lipid. The resulting vesicles (S-500 LUVs), when analyzed by gel filtration, are seen to have less of a trail of contaminating smaller vesicles, as compared to the crude LUVs. Gel filtration studies of b_5 added at a lipid to protein ratio of 1000:1 to both the crude LUVs and S-500 LUVs show that binding to the actual large vesicles in the solutions is occurring at approximate ratios of 2000:1 and 1200:1, respectively; since SUVs compete for b_5 more effectively than do LUVs, the results indicate that the crude LUVs indeed contain more contaminating small vesicles than do S-500 LUVs. The pattern of b_5 binding to crude LUVs is similar to that of S-500 LUVs which are intentionally contaminated with sonicated SUVs (1:1); the majority of the protein binds to the SUVs, causing a high lipid to protein ratio of about 3000:1 in the S-500 LUVs. Supported by a Grant-in-Aid from the American Heart Association, Virginia Affiliate, Inc.

Th-Pos134

PERMEABILITY OF H_2O/D_2O EXCHANGE ACROSS MODEL MEMBRANE VESICLES AND PROTEOLIPOSOMES

((Sudarsan Jagannathan and Gary L. Powell)) Department of Biological Sciences, Clemson University, Clemson SC 29634-1903.

The permeability of H_2O/D_2O exchange across large unilamellar vesicles can be measured in the absence of a probe. Addition of D_2O to vesicles made in the presence of H_2O buffer, change the scatter of light as a result of changes in refractive indices as H_2O mixes with D_2O within the vesicles (Engelbert H.P. *et.al* Ber. Bunsenges Phys. Chem *89*, 1985). The permeability of H_2O/D_2O exchange, can be studied by monitoring the decrease in light scattering with a fluorescence spectrophotometer. Using this technique the permeability of H_2O/D_2O exchange across dioleoylphosphatidylcholine (DOPC), vesicles was determined to be 1.92×10^{-5} cm/s. The permeability of H_2O/D_2O exchange across dimyristoylphosphatidylcholine vesicles is significantly lower at temperatures below the phase transition. The presence of 10 mol % bovine cardiolipin in DOPC vesicles lowers the permeability of H_2O/D_2O exchange while 10 mol % of dioleoylphosphatidylglycerol does not. It is also shown that the presence of 10 mol % cardiolipin in DOPC vesicles reconstituted with cytochrome *c* oxidase exhibits significantly lower permeability of H_2O/D_2O exchange. These results indicate the the possibility that the presence of cardiolipin in the inner mitochondrial membrane might serve to make the inner mitochondrial membrane a tighter barrier thereby increasing the efficiency of ATP synthesis. (This work was partially supported by a grant from the Public Health Service- HL 38190.)

Th-Pos135

EFFECTS OF TEMPERATURE AND VESICLE DIAMETER ON E/M DIPS IN PYRENE-PC/DMPC BINARY MIXTURES.

((D. Tang, and P. L.-G. Chong)) Dept. of Biochemistry, Temple University, Philadelphia, PA 19140.

In a previous study, we observed a series of dips in the plot of E/M (the ratio of the excimer to monomer fluorescence intensity) vs. the mole fraction of 1-palmitoyl-2-(10-pyrenyl)decanoyl-*sn*-glycerol-3-phosphatidylcholine (Pyr-PC) in Pyr-PC/DMPC binary mixtures at 30 °C. (Biophys. J. 65:903-910). In the present study, temperature and vesicle diameter have been employed to characterize the physical nature of the E/M dips in Pyr-PC/DMPC binary mixtures. An E/M dip at 66.7 mol% Pyr-PC in DMPC is discernible at 30-43 °C. At higher temperatures somewhere between 52-62 °C, the depth of the dip drops abruptly and the dip becomes a kink. This result is consistent with the hypothesis that the existence of an E/M dip relies on the balance between the entropy-driven randomization and the energy minimization due to the maximal separation of the bulky pyrene rings. Similar results were obtained for the E/M dip at 71.4 mol% Pyr-PC. The effect of vesicle diameter on the E/M dip was studied by using large unilamellar vesicles prepared by the extrusion method. The depth of the E/M dip at 66.7 mol% Pyr-PC, measured at 30 °C, is found to decrease with decreasing vesicle diameter. As the diameter is reduced to 40-64 nm, the dip becomes a kink. These results are consistent with the theory that the long-range repulsive interaction between Pyr-PCs is the main physical origin for maximal separation of Pyr-PC molecules in lipid membranes.

Th-Pos136

MASS-ACTION LAWS DESCRIBING LAURIC ACID MESOPHASE FORMATION.

((S.W. Smith[1], and B. D. Anderson[2])) [1]Glaxo, Inc., RTP, NC 27709. [2] Univ. of Utah, Salt Lake City, UT 84112. (Spon. by S.W. Smith)

Lauric acid (LA), dodecanoic acid, has previously been reported to form mesomorphic aggregates in solution; however, quantitative mass-action laws describing aggregate formation remain elusive. In this study, LA concentrations in filtered or ultrafiltered samples collected from suspensions of LA or potassium hydrogen dilaurate which varied in KCl concentration ($0<[KCl]<0.2$M), pH ($3<pH<8.5$), and temperature ($25°C<T<32°C$) were measured. At 32°C, suspensions were turbid over a narrow pH region that depended on [KCl] indicating the presence of large colloidal aggregates. In these turbid regions, LA concentrations in filtered samples were significantly higher than in ultrafiltered samples. Ultrafiltrate concentration-pH profiles were consistent with a monomer-solid phase equilibrium in solution indicating the usefulness of ultrafiltration to measure monomer concentrations in the presence of large colloidal aggregates. Light scattering and mannitol trapping experiments demonstrated the presence of vesicles in the mesophase region. A mass-action law for LA mesophase formation was derived from the monomer-mesophase concentration relationships and accounts for the observed cooperativity, composition, and pH-dependence of LA mesophase formation. The mass-action law supports the hypothesis that a domain of the intact vesicle is the unit in equilibrium with the LA monomer in solution. The concept of unit domains may have general application to lipid bilayer self-assembly.

Th-Pos137

PARTITION OF FREE FATTY ACIDS INTO PHOSPHATIDYLCHOLINE AND PHOSPHATIDYLETHANOLAMINE BILAYERS.((M. Langner, T. Isac and S.W. Hui))Biophysics Department, Roswell Park Cancer Institute, Buffalo, NY 14263.

The partition of free fatty acids (FFA) to egg-phophatidylcholine (egg-PC) and egg-phosphatidylethanolamine (egg-PE) vesicles was studied. The alteration of pH of the aqueous media in vesicles suspensions, caused by the addition of FFA, depends on the chain length and degree of saturation of FFA and on vesicle composition. Media pH decreases more in egg-PE than in egg-PC vesicle suspensions when FFA was added. The fluorescence free fatty acid indicator (ADIFAB) was used to measure the amount of FFA remaining in the aqueous phase. More FFA was found in the media of egg-PE vesicle suspensions, whereas little FFA was detected in the presence of egg-PC vesicles. Therefore the partition of FFA was a cause for the "buffering effect" of egg-PC vesicles. The amount of FFA incorporated into phospholipid bilayers was also estimated by measuring the changes of the pH at the bilayer surface, by means of fluorescence of the fluorescein attached to the head-group of PE. The surface pH measurement was more sensitive to FFA partition than the bulk pH measurement of the media. The amount of incorporated FFA in egg-PE was found to be much less than that in egg-PC vesicles. The high surface concentration of FFA, in the case of strong partition, causes the protonation of FFA, and renders further partition undetectable.

Th-Pos138

SPECTRAL CHANGES OF THE LIPID FLUORESCENT PROBE, LAURDAN, DURING THE SOLUBILIZATION OF LIPOSOMES BY OCTYL GLUCOSIDE. ((G.O.D Meyer, M.Ollivon and M.Paternostre)), URA CNRS 1218, Univ. Paris XI, 92296 Châtenay M., France.

Laurdan (6-dodecanoyl-2-dimethylaminonaphtalene) is a fluore--scent probe highly sensitive to physico-chemical properties of its environment (polarity, viscosity, conductivity, etc..). The emission spectra of this molecule, present two maxima and the variations of the intensity ratio of these two peaks have been correlated to the gel-liquid crystalline phase transition occuring in lipidic membranes (1). The sensitivity of this technique is extremely high and only a Laurdan/lipid molar ratio of 0.15% is necessary to detect this phase transition. We have followed the spectral changes of Laurdan incorporated in the membranes of small and large unilamellar liposomes during the vesicular to micellar transition induced by a non ionic detergent Octyl Glucoside. The evolution of the fluorescence intensity ratio of the two maxima has been correlated to the turbidity changes induced during the solubilization process of the same vesicles. The limits of the vesicle saturation by the detergent and of their solubilization into mixed micelles as deduced from the two techniques, are in good agreement, indicating that Laurdan is also sensitive to this transition.
(1):Parasassi T. et al, Biophys. J., (1991), 60, 179-189

Th-Pos139

RAPID PHOSPHATIDYLETHANOL TRANSFER ACROSS PHOSPHOLIPID BILAYERS
((A.V.Victorov, N.Janes, G.Moehren, E.Rubin, T.F.Taraschi and J.B.Hoek)) Dept. Pathol. and Cell Biol., Thomas Jefferson Univ., Philadelphia, PA 19107.

Phosphatidylethanol (PEth) is an anionic phospholipid formed in vivo or in vitro in the presence of ethanol via a transphosphatidylation reaction catalyzed by phospholipase D. The transbilayer distribution of low (0.5-2%) levels of PEth in small and large unilamellar phosphatidylcholine (PC) vesicles (SUV and LUV, respectively) was monitored by ^{13}C NMR of PEth ^{13}C-labeled at its headgroup methylene. Discrimination of interleaflet sites was based on a difference in chemical shifts of the outer and inner ^{13}C-PEth signals induced either by different lipid packing (in SUV) or by application of the shift reagent (in LUV). PEth is shown to undergo a rapid transbilayer redistribution ($t_{1/2}$ < 1 hour at 23°C, pH 6.7) in response to external administration of multivalent cations (Ca^{2+}, Pr^{3+}, Mn^{2+}, Yb^{3+}) or to changes in temperature. Addition of EGTA to Ca^{2+}-treated SUV returned the PEth distribution to the initial state. The pK of PEth was 1.43, as determined from the pH dependence of the chemical shift of the ^{13}C-labeled signal in LUV. Thus, at the pH of these experiments the protonated form of PEth constitutes a vanishingly small fraction of this phospholipid. This suggests that PEth transbilayer transfer is facilitated by its small hydrophobic headgroup. The rate of transbilayer transfer of PEth greatly exceeds, by 1-3 orders of magnitude, that reported for other natural phospholipids near physiological pH. Supported by US PHS Grants AA07186, AA00088, AA07215, AA07463 and AA08714.

Th-Pos140

VERIFICATION OF DIELECTRIC SHELL THEORIES BY DIELECTROPHORETIC AND ELECTROROTATIONAL STUDIES OF SYNTHETIC VESICLES. (Ka Lok Chan[1,2]) [1]University of Texas M. D. Anderson Cancer Center, Department of Molecular Pathology, Box 089, 1515 Holcombe Boulevard, Houston, TX 77030, USA; [2]University of Wales, Institute of Molecular and Biomolecular Electronics, Dean Street, Bangor, UK.

Dielectrophoresis and electrorotation are receiving increasing attention as useful phenomena for the characterization and manipulation of cells. In order to interpret dielectrophoretic and electrorotational data, however, an appropriate dielectric model is required. Most often, shell models have been applied for deriving cellular dielectric properties from such data. In this study, unilamellar, obligolamellar, and multilamellar vesicles and multi-vesicular liposome of varying phospholipid/cholesterol compositions and of different sizes have been synthesized and investigated by electrorotation. A general purpose, recursive alogarithm has been developed and was used to analyze the dielectric properties of the various types of vesicles in terms of dielectric shell theory. Fluorescence microscopy, flow cytometry and electron spin resonance of spin probes have been employed to characterize the vesicle morphology and membrane properties. The dielectric data deduced from the electrorotation data by the shell model alogarithm agreed with the observed morphology of each vesicle. This validates the application of dielectric shell theory for analysis of simple cellular systems.

Th-Pos141

CAN ETHER LIPOSOMES BE USED FOR ORAL VACCINES?
((E. L. Chang)) Center for Bio/Molecular Science and Engineering, Code 6900, Washington, D. C. 20375-5348.

Lipid vesicles have the potential to be ideal carriers for the oral delivery of vaccines. The liposomes, however, must overcome several obstacles to be successful. The most immediate requirement is preservation of membrane integrity during their passage through the harsh environments of the GI tract. Lipid vesicles generally show good stability against low pH, while the incorporation of cholesterol has been effective against destabilization by bile salts. However, the combined effects of bile salts and lipases have proven to be more intractable (1).
Since ether bonds in lipids are known to be stable against most chemical and enzymatic lipase actions, we have studied the stability of ether liposomes to determine whether they can potentially be effective as carriers for oral immunogens. The effects of detergents and lipases, both singly and in combination, on membrane integrity of vesicles made with ether lipids (either diether or tetraether lipids) were determined. Liposomes made with 1,2-O,O-dioctadecyl-rac-glycero-3-phosphocholine and cholesterol showed essentially no leakage over 24 h at 37°C in buffer or 10 mM octyl-β-glucoside (OBG). Incubation with pancreatin or pancreatin with OBG produced leakage rates with half-lifetimes of 42 and 21 hours respectively. 10 mM sodium taurocholate with pancreatin yielded a half-life of 11 hours. Dihexadecyl PC /cholesterol vesicles were less stable while egg PC/cholesterol liposomes showed no stability in detergent.
(1) Chiang, C.-M. and Weiner, N. (1987) International Journal of Pharmaceutics 37, 75-85.

Th-Pos142

PREPARATION AND CHARACTERIZATION OF LIPOSOME BASED SYNTHETIC THROMBOPLASTINS. ((Roberta A. Parente, Utpal R. Chakraborty, Brenda Pollick-Andrews, Joan Riley and Bryant M. Moore)). Ortho Diagnostic Systems, Raritan, NJ 08807

The prothrombin time (PT) test is used to determine deficiencies of clotting factor activity in the extrinsic coagulation pathway. Until recently, commercially available thromboplastins were derived from animal sources (rabbit, bovine, human). We have prepared and characterized synthetic thromboplastins from highly purified phospholipids and recombinant human tissue factor. The resulting PT reagents contain the tissue factor protein reconstituted into liposomes composed of phosphatidylcholine, phosphatidylglycerol, phosphatidylethanolamine and phosphatidylserine. Liposomes were prepared by standard detergent solubilization / removal techniques. We have investigated lipid acyl chain length, degree of unsaturation and presence of cholesterol in the liposomes with respect to stability and performance of these proteoliposomes in a PT assay. Liposome size was measured by dynamic light scattering. Dimyristoyl and dipalmitoyl acyl chains gave rise to the largest and most heterogeneous samples at 200-250 nm in diameter as compared to 130-150 nm for unsaturated lipids. Mixed chain palmitoyl-oleoyl liposomes were intermediate in size. Samples prepared from unsaturated lipids have been studied by electron microscopy and are mostly unilamellar. Clotting times of control plasmas were prolonged when using saturated lipids or cholesterol in the presence of dioleoyl lipids to prepare the liposomes. Our results suggest that unsaturated lipids are necessary to support activity of the tissue factor protein in initiating the extrinsic clotting cascade. The development of synthetic thromboplastins provides an alternative to animal based thromboplastins and affords us the opportunity to understand the role of lipids in thromboplastin reagent activity.

Th-Pos143

ELECTROPHORETIC STUDIES OF STERICALLY STABILIZED LIPOSOMES COMPARED TO RED BLOOD CELLS.

((Joel A. Cohen[1], Bhagya Puntambekar[2] and Martin C. Woodle[2]))
[1]University of the Pacific, San Francisco, CA 94115 and
[2]Liposome Technology, Inc., Menlo Park, CA 94025.

The blood circulation times of intravenous drug-containing liposomes can be greatly enhanced by the grafting of polyethylene glycol (PEG) to the liposome surfaces. The mechanism for this improved evasion of macrophages is unknown but may be related to a liposome surface "brush" that bears some similarity to the red blood cell (RBC) glycocalyx. It is therefore of interest to determine whether PEG-grafted liposomes share other physical properties with RBCs. Particle electrophoresis reveals 2 features of RBCs that differ from normal liposomes of similar charge: (1) the negative RBC zeta potential in univalent electrolytes cannot be reversed by the addition of Ca^{++}, (2) the RBC electrophoretic mobility is significantly lower than expected from its surface charge. In both respects, the electrophoretic behavior of PEG-modified liposomes varies continuously from that of unmodified liposomes to that of RBCs as the PEG molecular weight is increased. Both electrophoretic effects appear to result from an increasingly thick surface brush. The hydrodynamic brush thickness can be determined from the zeta potentials as a function of PEG molecular weight and PEG mole fraction in the membrane. The brush thickness, in turn, can be correlated with biological blood circulation times.

Th-Pos144

LIPID BINDING AND INSERTION BY FULL-LENGTH AND TRUNCATED ALZHEIMER'S β-AMYLOID PEPTIDES. ((M. A. Moore and M. P. McCarthy)) CABM/ RWJMS-UMDNJ, Piscataway, NJ, 08854.

Alzheimer's disease (AD) is a progressive form of senile dementia characterized pathologically by proteinaceous aggregates called amyloid plaques. A major component of the amyloid plaque is the β-amyloid protein (βAP), a peptide of 39-42 amino acids. In addition to forming amyloid plaques, the βAP has been shown to have both neurotrophic and neurotoxic effects, to disrupt calcium homoestasis, and to form cation channels in lipid bilayers. We have recently demonstrated, by three separate criteria, that both full-length and truncated forms of the βAP bind to, or insert within, lipid bilayers. βAP peptides were reconstituted into defined lipid vesicles by dialysis, or mixed with pre-formed vesicles. In the presence of lipid, both full -length (βAP_{1-40}) or a more hydrophilic truncated form (βAP_{1-28}), cosedimented with membranes by centrifugation. In addition, these βAP peptides were strongly labeled by the hydrophobic photolabel (trifluoromethyl)- 3-(*m*-[^{125}I]iodophenyl)diazirine ([^{125}I]TID) in the presence of lipids, but only weakly labeled (if at all) in the absence of lipids. [^{125}I]TID is a probe which has been used to identify membrane-spanning regions of intrinsic membrane proteins. Finally, both βAP_{1-40} and βAP_{1-28} partitioned into the hydrophobic, detergent-rich phase when solubilized in Triton X-114. Partitioning into the detergent-rich phase of Triton X-114 is a characteristic of hydrophobic, intrinsic membrane proteins. In combination, these results strongly suggest that βAP peptides interact directly with lipid bilayers. Conditions which alter the distribution of βAP peptides between membrane-associated and free states could regulate some of the physiological effects of the βAP peptides.

Th-Pos145

pH-Dependent Interaction of Chromogranin A with Integral Membrane Proteins of The Secretory Vesicle Including A 260 kDa Protein Reactive to The Inositol 1,4,5-Trisphosphate Receptor Antibody Seung Hyun Yoo Laboratory of Cellular Biology, National Institute on Deafness and other Communication Disorders, National Institutes of Health,Bethesda, MD 20892

Chromogranin A is a high capacity, low affinity Ca^{2+} binding protein suggested to be responsible for the Ca^{2+} storage function of the secretory vesicle, which has been identified as a major inositol 1,4,5-trisphosphate (IP_3)-sensitive intracellular Ca^{2+} store of adrenal medullary chromaffin cells. Moreover, chromogranin A has recently been shown to interact with the vesicle membrane at the intravesicular pH of 5.5 and to be released from it at a near physiological pH of 7.5 (Yoo, S. H. (1993) Biochemistry 32, 8213-8219).

In the present study, chromogranin A is shown to interact with several integral membrane proteins of secretory vesicles at pH 5.5, but not at pH 7.5. One of the chromogranin A interacting membrane proteins had a size of 260 kDa and reacted with the IP_3 receptor antibody. This result suggested not only the existence of the IP_3 receptor in the vesicle membrane but also the existence of direct communication between chromogranin A and the IP_3 receptor. In addition, the pH-dependent interaction of chromogranin A with integral membrane proteins implies an important role for chromogranin A in the sorting process of the vesicle membrane proteins during vesicle biogenesis in the trans-Golgi network.

Th-Pos146

MOLECULAR PROPERTIES AND pH STABILITY OF STRATUM CORNEUM LIPID LARGE UNILAMELLAR VESICLES

((Rita M. Hatfield*+, Robert Harper++, Priscilla Walling+ & Leslie W-M Fung*)) *Dept. of Chemistry, Loyola University of Chicago, Chicago, IL 60626; +Helene Curtis Industries, Inc., Chicago, IL; ++Hilltop Research Inc., Cincinnati, OH.

The uppermost layer of mammalian skin, the stratum corneum, provides the barrier between skin and the external environment. The unique lipid composition of the stratum corneum has been shown to form lipid bilayers *in vitro*. In order to study the molecular properties of these stratum corneum lipids, we prepared large unilamellar vesicles (LUVs) by extrusion methods using commercially-available lipids. The percentages of lipids used to make the LUVs were based on the weight percentages of each lipid found in the stratum corneum: 55% ceramides, 25% cholesterol, 5% cholesteryl sulfate, and 15% free fatty acids (Wertz *et al.* (1987) *J. Invest. Dermatol.* 89, 419-425; Abraham, W. (1992) *Sem. in Dermatol.* 11:2, 121-128). The composition of ceramides (bovine brain types III and IV) and free fatty acids (palmitic, lignoceric, and octacosanoic acids) was specifically chosen to reflect the distribution in mammalian stratum corneum. Quasi-elastic light scattering (QELS) revealed an effective diameter of about 120 nm with a narrow size distribution for these LUVs. Changes in the effective diameter and polydispersity of the LUVs were followed as a function of time and pH, over the pH range 5-9. QELS data showed that these vesicles were more stable at basic pH. Spin label electron paramagnetic resonance and differential scanning calorimetry were used to study the physical properties of the lipids in the LUVs as a function of temperature. Our results showed that the stratum corneum LUVs prepared from commercially-available lipids have properties similar to stratum corneum lipids. These vesicles may be used to study the functional properties of the stratum corneum. (Supported by Helene Curtis Ind.)

LIPIDS

Th-Pos147

STUDY OF THE INTERDIGITATION OF C26:0 CEREBROSIDE SULFATE IN A MATRIX OF DEUTERATED DIMYRISTOYL-PHOSPHATIDYLCHOLINE OR DEUTERATED DIPALMITOYL-PHOSPHATIDYLCHOLINE BY INFRARED SPECTROSCOPY.

((A. Nabet and M. Pézolet)) CERSIM, Département de chimie, Université Laval, G1K 7P4 Québec, Canada, ((J.M. Boggs)) The Hospital for Sick Children, M5G 1X8 Toronto, Canada

The C26:0-cerebroside sulfate (C26-CBS) is a sphingolipid with a long chain of 26 methylene groups and a short chain of which, 14 methylene groups penetrate into the bilayer. Sphingolipids are abundant in brain membranes and are known to be involved in the demyelinating disease adrenoleukodystrophy. Since the C26:0 CBS is an asymmetric lipid, it can give rise to two types of interdigitation: mixed or partially interdigitated structures. In order to understand how CBS packs with other lipids in membranes, we have studied the interdigitation of C26:0 CBS into matrices of either deuterated dimyristoylphosphatidylcholine (DMPC-d_{54}) or deuterated dipalmitoylphosphatidylcholine (DPPC-d_{62}) using transmission and attenuated total reflectance (ATR) infrared spectroscopy. Our results on the frequency of the CH_2 stretching modes and on the orientation of the CBS acyl chains show that in both DMPC-d_{54} and DPPC-d_{62}, the long acyl chain of C26-CBS interdigitates across the PC bilayer center in the gel phase.

Th-Pos148

PALMITOYL CoA BILAYER INTERACTION: A DSC AND X-RAY STUDY ((D.W. Chester[ββ†], Schnayder[†], B.E.)) BSAC[ββ] and Department of Biochemistry[†], University of Connecticut Health Center, Farmington, CT.

We have examined the structure and thermotropic behavior for the interaction of the Δ^9-desaturase substrate, palmitoyl CoA, with DMPC, DPPC, and POPC unilamellar and multilamellar vesicles as well as partially hydrated [98 % relative humidity] multilayers. Based on small molecule effects on bilayer thermotropic behavior, Jain and Wu [1977] and Bach [1979] suggest that the membrane region being perturbed can be *inferred* from DSC data. The main chain ΔH_c for both vesicles and multilayers is essentially unaffected by acyl CoA partitioning. In contrast, significant changes were observed in t_m and $\Delta t_{½}$ [measure of transition cooperativity] as a function of acyl CoA incorporation. In POPC vesicles and multilayers, both $\Delta t_{½}$ and t_m were increased as a function of acyl CoA content. The affect of acyl CoA partitioning into DPPC vesicles and multilayers differs slightly. The $\Delta t_{½}$ and t_m both increase for both for vesicles in solution while for multilayers, $\Delta t_{½}$ increases and t_m remains essentially unchanged. The DPPC pretransition enthalpy was significantly effected by acyl CoA incorporation yet continued to persist even at high [1:26] ligand concentrations. Assuming validity of the Jain and Wu (1977) and Bach (1979) algorithms, these data suggest a type A† effect indicative of acyl CoA perturbation of the upper acyl chain region [C_1-C_9] of the bilayer.

Small angle x-ray scattering results on fully hydrated POPC multilayers [98 % relative humidity] in the presence and absence of acyl CoA at 37°C demonstrate a small separation in the headgroup spacing across the bilayer and increase in the full width at half maximum of the phospholipid headgroup peak. These data suggest that the moiety giving rise to the increased electron density [CoA] resides in the headgroup region. One curious finding in the low temperature POPC x-ray studies below the thermal phase transition [-8.4°C] was the observation of a ~300 Å repeat period similar to that observed for the $P_{\beta'}$ in DPPC. This work was supported by NIH-GM-15924.

Th-Pos149

SHAPE OF THE HYDROPHOBIC BARRIER OF A PHOSPHOLIPID BILAYER: EFFECTS OF CHOLESTEROL, ALKYL CHAIN LENGTH AND UNSATURATION. ((W.K. Subczynski, A. Wisniewska, J.-J.Yin, J. S. Hyde, and A. Kusumi)) Inst. of Molecular Biology, Jagiellonian Univ. Krakow, Poland. Biophysics Research Inst. Medical College of Wisconsin, Dept. of Biophysics, Kyoto Univ. Japan. (Spon. by C.-S. Lai)

The value of A_z obtained at x-band from stearic acid and tempocholine dipalmitoylphosphatidic acid ester spin labels in frozen suspensions of phosphatidylcholine membranes has been used as a hydrophobicity parameter. By measuring A_z using probes with the nitroxide moiety at various depths in the membrane, the shape of the barrier to water transport has been estimated. It was found that the length of the alkyl chain does not influence the height of the barrier, while unsaturatiion significantly increases the hydrophobicity of the central region of the bilayer. Addition of 20-30 mol% of cholesterol to saturated lipids increases water penetration in and near the polar headgroup region to a depth of 7 to 9 carbons. At concentration over 30 mol%, the depth of water penetration increases. In all investigated membranes, cholesterol abruptly decreases water penetration, which results in a very high hydrophobicity of membrane center that is comparable to that of the membrane center equal to the hydrophobicity of the pure hydrocarbon solvents. It was also found that cholesterol (30 mol%) significantly increases the accessibility of polar molecules ($K_3Fe(CN)_6$) to a depth of 7 to 9 carbons. However, it does not influence penetration to the membrane center.

Th-Pos150

DIFFERENT EFFECTS OF POLAR CAROTENOID AND CHOLESTEROL ON ALKYL CHAIN BENDING IN LIPID BILAYERS: A PULSE ESR SPIN LABELING STUDY. ((J.-J.Yin and W.K. Subczynski)) Biophysics Research Inst. Medical College of Wisconsin, Milwaukee, WI 53226 & Biophysics Dept., Inst. of Molecular Biology, Jagiellonian Univ. Poland.

Short pulse saturation recovery (SR) electron spin resonance (ESR) technique has been used to study the effects of polar carotenoid-lutein and cholesterol on interactions of ^{14}N, ^{15}N stearic acid spin label pairs in phosphatidylcholine (PC) membranes in the fluid phase. Bimolecular collisions for pairs consisting of various combinations of ^{14}N-16-; -10-; -7-, or -5-doxylstearate and ^{15}N-16-doxylstearate in dimyristoyl-PC (DMPC) or egg yolk PC (EYPC) membranes were measured. In the absence and presence of lutein or cholesterol for both lipid systems, the collision rates were ordered as 16:5 < 16:7 < 16:10 < 16:16. For all spin-label pairs studied, interaction frequencies were greater in DMPC than in EYPC. Polar carotenoid-lutein reduces the collision frequency for all spin-label pairs, while cholesterol reduces the collision frequency for 16:5 and 16:7 pairs and increases the collision frequency for 16:10 and 16:16 pairs. Effects of both modifiers are more pronounced in DMPC than in EYPC. The observed differences in the effects of carotenoid and cholesterol on alkyl chain bending result from differences in the structure of cholesterol and polar carotenoid and from their different localization within the membrane.

Th-Pos151

SPECTROSCOPIC STUDIES OF THE INTERACTION OF PRIMAQUINE WITH MODEL MEMBRANES: ((Janice R. Perussi, Victor E. Yushmanov, Shirley E. Monte, Hidetake Imasato, Marcel Tabak)). Instituto de Física e Química de São Carlos-USP, C.P. 369, 13560-970, São Carlos, SP, Brazil.

Primaquine (PQ) possess a wide range of antimalarial activity, being considered one of the most effective antimalarial drugs. In order to study its effect in biological systems it is important to know the sites of protonation as well as the pK_a value and the association constants K_A for the PQ membrane-complex. In this study, the micellar systems were formed by surfactants with different charge of headgroups:cationic cetyltrimethylammonium chloride (CTAC) and anionic sodium docecylsulfate (SDS) were used as model of lipid aggregates. PQ has charged aliphatic side chain and the solubility is high enough in the whole physiological pH range. We obtained the following values of pK for PQ: 3.0, 6.7 and 10.3. The intermediate value is not described in the literature and maybe it is originated by a decomposition product which, even at low concentration can be detected if it has a high extinction coefficient. This supposition is supported by the binding constants obtained. K is $5x10^2$, $4x10^3$ and $2.5x10^3$ M^{-1} for SDS and 5, 24.7 and 18.7 M^{-1} for CTAC at pH 4.5, 7.0 and 8.0 respectively. PQ in the protonated state interacts quite strongly with anionic micelles.

Financial Support: FAPESP, CNPq, FINEP

Th-Pos152

CONTRIBUTIONS OF THE HYDROPHOBIC APOPROTEINS TO THE INTERFACIAL ACTIVITY OF PULMONARY SURFACTANT. ((S.B. Hall, Z. Wang, and R.H. Notter)) Internal Medicine, Oregon Health Sciences Univ., Portland, OR 97201, and Depts of Pediatrics and Environmental Medicine, University of Rochester, Rochester, NY 14642. (Spon. by J.A. Schellman).

Pulmonary surfactant includes small amounts of hydrophobic proteins as well as its phospholipids. Previous studies of hydrophobic apoprotein function have focused on their ability to accelerate phospholipid adsorption. To determine apoprotein contributions in the surface film itself, we compared solvent-spread films of calf surfactant phospholipids, with and without apoproteins, obtained by column chromatography . Films of purified phospholipids (PPL) and of surfactant proteins and phospholipids (SP&PL) were compressed to pressures above equilibrium spreading values on a Wilhelmy balance. PPL mimicked the surface behavior of the parent calf surfactant in some respects, and also reached slightly higher maximum surface pressures than SP&PL during a single compression from low initial concentrations. However, the presence of SP improved other aspects of film behavior compared to PPL. For films at initial concentrations sufficient to reach the equilibrium pressure limit, the maximum pressure for PPL during compression became constant, independent of the extent of initial surface excess. SP&PL films had maximum dynamic pressures that increased as surface excess increased, and which surpassed the level achieved by PPL. During continuous compression-expansion cycling, SP&PL films also maintained high surface pressures through more cycles, with smaller hysteresis loops, suggesting better respreading. These results suggest that along with surfactant phospholipids, the hydrophobic SP also have significant effects on the interfacial film, in addition to their role in facilitating adsorption.

Th-Pos153

THE ADSORPTION OF WATER BY PHOSPHATIDIC ACID. ((G.L. Jendrasiak and R.L. Smith)) East Carolina University School of Medicine, Greenville, NC 27858. (Spon. by Bela Kuemmel-Karvaly)

We have obtained the water adsorption isotherm for the monosodium form of egg phosphatidic acid (PA). The isotherm is very similar to that previously acquired for egg phosphatidylcholine (EPC), both qualitatively and quantitatively. The nature of the PA isotherm indicates strong water binding by this phospholipid. We were unable to calculate BET parameters from the first isotherm obtained for a given PA sample; rehydration of the sample, however, allowed a BET analysis to be carried out. Such hysteresis suggests a rearrangement of the PA film with hydration.

Concomitant with the hydration measurement, the D.C. electrical conductivity was observed. The conductivity increased very rapidly (orders of magnitude) with adsorption of the first few water molecules and then leveled off. We also obtained the activation energy for this conductivity process so as to provide further information on the initial binding of water molecules by PA.

Th-Pos154

^2H NMR STUDIES OF L_α-PHASE CEREBROSIDE BILAYERS PROVIDE A SELF-CONSISTENT MODEL OF MEMBRANE DYNAMICS AND ACTIVATION ENERGIES
((J.R. Long, S.K. DasGupta, R.G. Griffin)) MIT, Cambridge, MA 02139. (Spon. by R.G. Griffin)

^2H NMR inversion recovery experiments of the cerebroside N-palmitoylgalactosylsphingosine (NPGS) in the L_α phase have demonstrated significant anisotropy in the spin-lattice relaxation spectra of the acyl chain CD_2 groups.[1] Both the form of the anisotropy and the splittings between the perpendicular edges of the powder pattern can be simulated by employing a simple motional model comprised of discrete hops between nine sites, which result from the coupling of long-axis diffusion and gauche-trans isomerization. Using this model, site populations and motional rates may be quantitatively assigned. Specifically, the temperature dependence of motional rates and site populations have been determined for several methylene groups along the acyl chain, providing self-consistent measurements of gauche-trans isomerization and long-axis rotational diffusion rates. An overall picture of lipid dynamics and activation energies for various motions emerge from these values.

1. J.B. Speyer, R.T. Weber, S.K. DasGupta and R.G. Griffin, Biochemistry 28, 9569 (1989).

Th-Pos155

DIRECT NMR EVIDENCE FOR SURFACE BINDING OF ETHANOL TO LIPID BILAYERS.

((Judith A. Barry & Klaus Gawrisch)) NIAAA, NIH, Rockville, MD 20852

The mechanisms behind the membrane-mediated effects of alcohol were examined via the interaction of ethanol with phospholipid bilayers at sub-maximal hydration levels. ^{2}H and ^{31}P NMR spectroscopy was used to monitor deuterated water, ethanol, and the headgroups and acyl chains of neutral phospholipids. Ethanol interacted strongly with both phosphatidylcholine and phosphatidylethanolamine bilayers, as indicated by large quadrupolar splittings of 6 to 9 kHz for CH_3CD_2OH. Ethanol binding most likely results from H-bonding and hydrophobic interactions between lipid and ethanol at the lipid-water interface. This conclusion is based on the observation that ethanol binding: 1) is not altered significantly by the lipid L_α-to-gel phase transition, and 2) triggers a significant change in the headgroup orientation. Binding increases the area per lipid, resulting in a pronounced disordering of the acyl chains. The lipid-ethanol interaction reported here may serve as a model for the binding of ethanol in the aqueous interface regions of a variety of macromolecules, including membrane proteins and carbohydrates.

Th-Pos156

INTERACTION OF THE CYTOLYTIC δ-ENDOTOXIN CytA FROM *Bacillus thuringiensis* var. *israelensis* WITH PHOSPHOLIPID MEMBRANES.

((P. Butko, F. Huang, M. Pusztai-Carey and W.K. Surewicz)) Institute for Biological Sciences, National Research Council, Ottawa, Ontario K1A 0R6, Canada.

A 27 kDa protein CytA is a major component of the mosquitocidal crystals in *B. thuringiensis* var. *israelensis*. We have used fluorescence and FTIR spectroscopies, and differential scanning calorimetry to explore the toxin-membrane interaction. Our data indicate that the toxin binds to phospholipid vesicles with the association constant of 5×10^{5} M^{-1} with respect to a "binding site" comprised of approximately 150 lipid molecules. The protein-membrane binding is driven largely by hydrophobic interaction. Only few, if any, of the bound toxin molecules actually penetrate into the bilayer core. Approximately 300 toxin molecules must bind to the surface of the vesicle membrane before the latter's permeability barrier breaks down. Both small ions and large molecules, such as 10 kDa dextrans, are released from the lipid vesicles as a consequence of the toxin action. The data suggest that the cytolytic action of cytA is due to general perturbation of the lipid membrane rather than creation of small, well-defined, proteinaceous channels.

Th-Pos157

FTIR STUDIES OF ANTIMICROBIAL PEPTIDE CONFORMATION AND ORIENTATION AT THE LIPID-WATER INTERFACE.

((W. David Braddock[a], Brad Kaufman[b] and Paul H. Axelsen[b]))
[a]Mayo Clinic, Rochester MN; [b]University of Pennsylvania, Philadelphia PA

Antimicrobial peptides, as a component of the host-defense mechanism against infection, are being found in creatures as diverse as mammals, amphibians, and insects. Their mechanism of action is unknown, but it is remarkably specific, and may generally involve membrane perforation or disruption. To examine the structural details of the interaction between these peptides and membranes surfaces, an FTIR spectrometer, coupled to a Langmuir-Blodgett lipid film deposition system, has been specially designed and assembled to obtain polarized IR spectra of soluble peptides which adsorb to and/or penetrate a supported lipid monolayer. Spectra may be collected in either H_2O or D_2O, using various lipids, and at various lipid surface pressures. Preliminary results for cecropin A and sarcotoxin 1A suggest that (a) the peptides have a high affinity for POPC monolayers; (b) a conformational change (random→helix) may occur as these peptides insert into the monolayer; (c) if helical, their helix axis is sharply tilted with respect to the plane of the membrane surface.

WDB supported by the Keck-Mayo Training Program in Molecular Biophysics
PHA supported by a Biomedical Scholar Award from the L. P. Markey Charitable Trust

Th-Pos158

MOLECULAR DYNAMIC SIMULATIONS OF DRUGS, PEPTIDES AND PROTEINS IN LIPID BILAYERS.

((L. Herbette 1, S. Gallion 2, D. Rhodes 3, M. Hibert 4, J. Hoflack 4, S. Trumpp-Kallmeyer 4, D. Jenkins 5 and M. Trumbore 1)) Biomolecular Structure Analysis Center, Univ. of Conn. Health Center, Farmington, CT 06030-2017, (1). Marion Merrell Dow Research Inst., Cincinnati, OH (2). Univ. of Texas, College of Pharmacy, Austin, TX (3), Marion Merrell Dow Research Inst., Strasbourg, France (4), Visionary Systems and Molecular Visions Inc., New Haven CT (5).

A fully hydrated lipid bilayer structure with different fatty acyl chain lengths and varying numbers of lipids per monolayer has been successfully established and run under the AMBER force field using three dimensional periodic boundary conditions. These equilibrated lipid bilayer structures have been used to study the interactions of different hydrophobic and amphiphilic drugs, peptides and proteins. Work with two different drugs indicate that for lacidipine a 1-4 dihydropyridine calcium channel antagonist shown by x-ray diffraction to be located deep within the membrane hydrocarbon core, a stable bilayer drug system can be established and simulated. Drugs which are located at the hydrocarbon core/water interface, such as propranolol, an antagonist to the β_1 adrenoceptor, can cause some instability in the bilayer model due to perturbations in the packing of lipids in the glycerol backbone region. Other studies to date involve the interactions of putative membrane active peptides, such as Substance P, and the interactions of G protein coupled receptors, such as bacteriorhodopsin, with the model lipid bilayer. Results from these latter cases will be presented. This work is funded by Marion Merrell Dow, Cincinnati, OH, NIH postdoctoral fellowship #1 F32 DE05612-01A1 (M. Trumbore) and Glaxo SpA, Verona, Italy.

Th-Pos159

ASSOCIATION AND LOCALIZATION OF PYRIDINE IN PHOSPHOLIPID BILAYERS: DSC & ^{13}C-MAS, ^{31}P & ^{2}H NMR.

((J. M. Henderson and M. Petersheim)) Chemistry Dept., Seton Hall University, South Orange, NJ 07079.

Pyridine is found in tobacco smoke, a wide variety of foods, petroleum products and is a common industrial pollutant. It may have both beneficial and detrimental pharmacological activities: inhibiting oxidation of substances like benzene in vivo (Harper, B.L. & M.S. Legator. 1987. *Mutat. Res.* 179:23-31), reducing stress ulcers as an antiplatelet aggregator (Kumashiro, R. et al. 1985. *Eur. Surg. Res.*. 17:44-55), but also inducing a variety of oxidases (Park, K.S. et al.1992. *Biochim. Biophys. Res. Commun.*.185:676-682.; Kim, H. et al.1992. *Biochim. Biophys. Res. Commun.* 186:846-853) There is also evidence that pyridine may directly affect membrane processes (Lukashev, E.P., et al. 1991. *Biol. Membr.* 8:161-171). The work presented demonstrates that pyridine associates with the glycerol and choline moieties in dimyristoyl-phosphatidylcholine (DMPC) liposomes (C-13 MAS NMR). Pyridine has little effect on the head group conformation (P-31 NMR powder patterns) but causes large changes in the lipid thermal transitions (DSC): drop in T_m and cooperativity with an increase in magnitude of the enthalpy for the gel to liquid crystal transition. Pyridine does not appear to displace a significant amount of water from the lipid interface (H-2 NMR powder pattern for D_2O). The effect of pyridine on the membrane will be compared with other simple aromatic species such as the general anesthetic, benzyl alcohol.

Th-Pos160

CATIONIC LIPID MONOLAYERS AND THEIR INTERACTION WITH ANIONIC POLYMERS

Y. Xu[1], M. Levy[1], J. Goerke[2], F. C. Szoka Jr.[1],
[1] School of Pharmacy, University of California, San Francisco, CA 94143
[2] Cardiovascular Research Institute, University of California, San Francisco, CA 94143

We have examined the correlation of surface pressure [π] and surface potential [ΔV] with molecular area [A] for four synthetic cationic lipids ([2,3-(dioleoyloxy)propyl]-N,N,N-trimethylammonium [DOTMA], 1,2-bis(oleoyloxy)-3-(trimethylammonio)propane [DOTAP], Dioctadecylamidoglycylspermine [DOGS] and 2,3-dioleyloxy-N-[2(spermine carboxamido)ethyl]-N,N-dimethyl-1-propanaminium trifluoroacetate [DOSPA]) using surface monolayer techniques (Table). These lipids and their mixtures with dioleoylphosphatidylethamolamine [DOPE] are used to transfect DNA into cells. They exhibit non-ideal mixing with DOPE due to an electrostatic interaction between the cationic headgroup and DOPE that condenses the monolayer. Anionic water soluble polymers such as Dextran Sulfate or DNA strongly interact with the monolayer mainly through electrostatic forces. Such interaction results in changes in the molecular arrangement and packing of the monolayer. This work is supported by NIH DK 46052 (FCS) and NIH HL24075 (JG).

Table: Monolayer parameters of cationic lipids and their mixtures with DOPE(PE)

	DOPE	DOTMA	DOTAP	DOGS	DOTMA/PE (1:1 wt.)	DOTAP/PE (1:1 wt.)	DOSPA/PE (3:1 wt.)
Mean molecular area $\bar{A}$ (Å²)	80	83	72	83	73	70	98
Collapse molecular area A_C (Å²)	51	52	48	37	50	46	47
Collapse surface pressure π_C (mN/m)	47	45	46	67	48	46	46
Collapse surface potential ΔV (mV)	460	520	555	635	555	560	520

Th-Pos161

NEUROMODULIN PEPTIDE ON THE MEMBRANE SURFACE
((Stacey Leigh Wertz and David S. Cafiso)) Department of Chemistry, University of Virginia, Charlottesville, VA, 22901.

Neuromodulin is a 25 kDa calmodulin-binding protein kinase C substrate found in axonal growth cone membranes. It appears to bind membranes electrostatically at a positively charged region of the protein located near the N-terminus. One basic 17 residue segment of neuromodulin contains the calmodulin binding site and the PKC phosphorylation site.(Apel, ED, Byford, MF, Au, D, Walsh, KA, and Storm, DA. (1990) *Biochemistry* **29**, 2330-2335.). Two spin-labeled mutants of this peptide have been made with one and two cysteines substituted. Spin labels were attached via disulfide linkages using a methanethiosulfonate nitroxide at the cysteine residues, and the binding of these peptides to membranes with various phosphatidylserine content were measured using electron paramagnetic resonance. In SDS micelles, the peptides exhibited an ionic strength dependent aggregation. High resolution nuclear magnetic resonance techniques are being used to obtain structures for the solution and membrane associated peptide. In methanol, the peptide appears to be α-helical based on the Cα chemical shifts. In aqueous solution and in micelles, the peptide is more extended. This structural information is being used to calculate the electrostatic contribution to the binding by solving the non-linear, three dimensional Poisson-Boltzmann equation.

MEMBRANES - CELLULAR

Th-Pos162

DUAL-WAVELENGTH RATIOMETRIC FLUORESCENCE MEASUREMENT OF THE MEMBRANE DIPOLE POTENTIAL. ((E. Gross, R. S. Bedlack, Jr. and L. M. Loew)) Physiology, U. Conn. Health Center, Farmington, CT 06030.

The electrostatic potentials associated with cell membranes include the transmembrane potential ($\Delta\Psi$), the surface potential (Ψ_s) and the dipole potential (Ψ_D). Ψ_D, which originates from oriented dipoles at the surface of the membrane, rises steeply just within the membrane to ~ 300 mV. Here we show that the potential-sensitive fluorescent dye di-8-ANEPPS can be used to measure changes in the intra-membrane dipole potential. Increasing the content of cholesterol and 6-ketocholestanol (KC), which are known to increase Ψ_D in the bilayer, results in an increase in the ratio, R, of the dye fluorescence excited at 440 nm and 530 nm in a lipid vesicle suspension; increasing the content of phloretin, which lowers Ψ_D, decreases R. Control experiments show that the ratio is insensitive to changes in the membrane's microviscosity. The lack of an isosbestic point in the fluorescence excitation and emission spectra of the dye at various concentrations of KC and phloretin, argues against 1:1 chemical complexation between the dye and KC or phloretin. The sensitivity of R to Ψ_D is 10-fold larger than to $\Delta\Psi$, while it is insensitive to changes in Ψ_s. This can be understood in terms of the location of the dye chromophore with respect to the electric field profile associated with each of these potentials. (supported by USPHS grant GM35063)

Th-Pos163

ENDOGENOUS ELECTRIC FIELDS WITHIN THE NEURONAL PLASMALEMMA: NON-UNIFORMITIES SUGGESTING DIFFERENTIAL VOLTAGE DEPENDENCE ((R.S. Bedlack Jr., M.-d. Wei, S. Fox, E. Gross and L.M. Loew)) U. Conn. Health Center, Physiology, Farmington, CT 06030

Within the plasmalemma, voltage-gated ion channels and other signal transducing structures are influenced by electric fields. We used a fluorescent, ratiometric potential-sensitive dye (di-8-ANEPPS) and digital imaging microscopy to make the first measurements of endogenous "intramembrane" electric fields (IEF's) in differentiated N1E-115 neuroblastoma cells. Surprisingly, we found that IEF's associated with neurites were consistently more positive than IEF's associated with somas. Chemically clamping the transmembrane potential with valinomycin or the outer surface potential with high [Ca^{2+}] produced changes in the IEF in all cellular regions but did not change its spatial non-uniformity. A compelling explanation is that IEF asymmetries were created by differences between the dipole potential (i.e. the lipid composition) of the neurites' plasmalemmae compared to that of the the somas'. (Based on model membrane studies, di-8-ANEPPS displays great sensitivity to electric fields associated with the dipole potential.) Regardless of their origin, the measured IEF asymmetries might impart an enhanced voltage sensitivity to neurites relative to their somas. (supported by USPHS grant GM35063)

Th-Pos164

TREHALOSE SUPPRESSES THE PHASE TRANSITION TEMPERATURE IN DRY YEAST. ((S. B. Leslie, S. A. Teter, L. M. Crowe, and J. H. Crowe)) University of California, Davis, CA 95616

Recent work has clearly demonstrated a direct correlation between the amount of trehalose present in the yeast *Saccharomyces cerevisiae* and its ability to tolerate dehydration, but has failed to elucidate the specific role played by trehalose. Using Fourier transform infrared spectroscopy (FTIR) we measured the dry gel to liquid crystal phase transition temperature (T_m) of phospholipids in both intact *S. cerevisiae* and isolated plasma membranes dried in the presence and absence of trehalose. Trehalose lowers the dry T_m in yeast from 58°C to 40°C, thus allowing yeast rehydrated above 40° to avoid the damaging effects of passing through a phase transition. The asymmetric PO_2^- stretch was used to determine T_m in intact cells because the large neutral lipid content of yeast made it impossible to determine a T_m using the CH_2 vibrations. The T_m of both intact cells and isolated membrane determined using PO_2^- was consistently lower than that determined using CH_2 stretches, indicating that there is a change in headgroup conformation prior to acyl chain melting. Use of the asymmetric PO_2^- vibration makes it possible to determine the T_m in systems where the phospholipid CH_2 vibrations are masked by large neutral lipid concentrations. (Supported by NSF grants DCB89-18822 and IBN93-08581)

Th-Pos165

TREHALOSE INHIBITS ETHANOL EFFECTS ON INTACT CELLS AND LIPOSOMES. ((J.J.Mansure[1], A.D.Panek[1], L.M.Crowe[2] and J.H.Crowe[2])) [1]Universidade Federal do Rio de Janeiro, Brazil, [2]University of California, Davis.

The effect of ethanol on stability of intact yeast cells has been investigated. Several strains with differences in trehalose metabolism were examined for their ability to survive in the presence of 10% (v/v) ethanol. A linear correlation was observed between cell viability and trehalose concentration. When leakage of electrolytes from the cells was recorded by observing changes in conductivity of the medium, we found that ethanol increases leakage, but the presence of trehalose reverses that effect. Similar studies were done with liposomes of similar composition to those seen in intact cells in log and stationary phases. In the presence of ethanol, carboxyfluorescein trapped in the liposomes leaked to the medium. When trehalose was added inside, outside or on both sides of the membrane, the ethanol-induced leakage was strongly inhibited. More leakage was observed in liposomes in gel phase state than liquid crystalline suggesting that the thermotropic behavior of the lipids in the plasma membrane, together with trehalose, plays a role in enhancing ethanol tolerance. (This work was supported by CNPq.)

Th-Pos166

EFFECT OF CHOLESTEROL ON RETINAL ROD OUTER SEGMENT DISK MEMBRANES.

((Arlene D. Albert, Philip L. Yeagle, Clare Whiteway, Anthony Watts and Richard Epand)) Departments of Biochemistry and Ophthalmology, University at Buffalo, Buffalo, NY 14214, Department of Biochemistry, Oxford University, Oxford, UK, Department of Biochemistry, McMaster University, Hamilton, Onterio, Canada

The cholesterol content of retinal rod outer segment (ROS) membranes varies considerably. In the ROS plasma membrane it is high, while in the disk membranes it is high in nascent disks but decreases as the disks mature and are apically displaced. The function of the photoreceptor, rhodopsin can be modulated by membrane cholesterol. The mechanism of cholesterol effect in the membrane has therefore been investigated in disk membranes. Because cholesterol readily equilibrates between membranes, the disk membrane cholesterol can be altered by incubation with cholesterol/phospholipid vesicles. In a similar manner, labeled cholesterol derivatives can also be transferred into disk membranes. Membrane cholesterol was investigated using three independent techniques: (1) Fluorescence energy transfer between the fluorescent cholesterol derivative, cholestatrienol and the protein indicated some interaction, but the data do not support a direct, specific, sterol-protein interaction. (2) ^{13}C NMR of ^{13}C-labeled cholesterol supports the hypothesis that cholesterol alters the lipid bilayer in which the receptor resides. (3) Differential scanning calorimetry (DSC) indicates that the protein is stabilized by cholesterol in that the T_m is increased in response to higher membrane cholesterol. Additional DSC experiments indicate a sensitivity of the rhodopsin to hydrocarbon chain length and saturation. (National Eye Institute EY03328)

Th-Pos167

MEMBRANE PROPERTIES THAT INFLUENCE BOVINE RETINAL ROS MEMBRANE FUSION.

((K. Boesze-Battaglia)), Dept. Cell Biology, New Jersey School of Medicine and Dentistry, Osteopathic Medicine, 2 Medical Center Dr. Stratford, NJ 08084.

The formation of packets of membranous material in the ROS is postulated to involve a ROS membrane fusion event. The role of protein phosphorylation and changes in membrane composition in ROS membrane fusion was determined. The R_{18} lipid mixing assay was used to study the effect of protein phosphorylation, cholesterol and phospholipase treatment on intact ROS membrane fusion and disk-plasma membrane fusion. IEF experiments were performed to determine changes in disk membrane protein phosphorylation as a function of disk membrane age and spatial distribution. Phospholipase C and A_2 treatment resulted in a 4 and 5 fold increase in the initial rates of disk membrane-plasma membrane fusion respectively. This increase in fusion rates was dose dependent. Light induced membrane protein phosphorylation resulted in a 2 fold increase in the initial rates of disk-R_{18} labeled plasma membrane fusion. Cholesterol had no effect on the initial rates of disk-plasma membrane fusion. Disk-plasma membrane fusion was followed using R_{18} labeled intact ROS membranes, with fusion initiated upon ROS lysis. This newly described fusion assay has qualitatively the same calcium dependence as that described previously for isolated disk membrane-plasma membrane fusion. Isoelectric focusing of endogeneously phosphorylated rhodopsin suggests that there are slight differences in the number of phosphates per rhodopsin as a function of disk membrane position in the outer segment. When approximately 85-90 % of the total rhodopsin in the disk membranes is bleached, greater than 50 % of the rhodopsin isolated from the newly formed disks is composed of phosphorylated species containing less than three phosphates per rhodopsin. Phosphorylated rhodopsin isolated from older disks contains less than 35 % of rhodopsin molecules with 3 or less phosphates per rhodopsin.

Th-Pos168

RESTORATION OF MEMBRANE STRUCTURE, COMPOSITION AND FUNCTION IN ATHEROSCLEROTIC ARTERIAL SMOOTH MUSCLE CELLS (SMC) BY HUMAN HDL.

M Chen, RP Mason & TN Tulenko, Medical College of Penna, Phila., PA and †University of Connecticut, Farmington, CT

We have demonstrated that dietary atherogenesis in rabbits is accompanied by excess membrane cholesterol content, increased membrane bilayer width, suppressed Na^+/K^+ATPase activity and increased cytosolic Ca^{++} ($[Ca^{++}]_i$) levels. The objective of the present study was to determine if biological cholesterol acceptor particles could remove excess membrane cholesterol and restore membrane composition, structure, function and cellular $[Ca^{++}]_i$. SMC isolated from atherosclerotic aorta were incubated with apoprotein-A1, apoHDL, HDL_2 or HDL_3 at various concentrations and for various durations. We found that apoprotein-A1 and apoHDL had no effect while HDL_2 and HDL_3 reduced membrane cholesterol, with HDL_3 being the most effective particle. Further studies demonstrated that HDL_3 (500μg prot./ml for 24 hours) restored membrane cholesterol (C/PL molar ratio) by 95% (0.415 to 0.333; $p<.01$), restored bilayer width by 100% (58Å-56Å) and restored Na^+/K^+ATPase activity by 79% (0.016 to 0.023 μmole/mg p/min; $p<.01$) back toward values obtained in control SMC. This reversal of membrane parameters was also accompanied by a complete restoration of $[Ca^{++}]_i$ levels (248 to 111 nmoles/L; $p<.001$) to control. Taken together, these findings demonstrate that removal of excess membrane cholesterol by HDL_3 in atherosclerotic SMC corrects membrane and cell function back to normal, healthy SMC. Thus, human HDL initiates "reverse cholesterol transport" at the cellular level in atherosclerotic SMC and restores abnormalities in SMC function. These results are consistent with the hypothesis that HDL contributes to arterial wall protection in vivo by protecting membrane cholesterol levels.

Th-Pos169

DIRECT MEASUREMENT OF FUSION PORE CONDUCTANCE DURING VIRUS-INDUCED CELL-CELL FUSION

((I. PLONSKY, and J. ZIMMERBERG)) LTPB, NICHD, NIH Bethesda, MD 20892 (Spon. by H. Pant)

The fusion of biological membranes was investigated by a double whole-cell recording technique. Intercellular conductance was measured during baculovirus-induced syncytia formation of insect cells. Acidic perfusion of cell pairs under double whole-cell recording induced abrupt, symmetrical currents in both cells. Currents indicated the appearance of junctional conductance (G). After stabilization of conductance at the level of several nS, G continued to grow slowly and sometimes jumped to greater than 100 nS. Junctional conductance never developed without perfusion of the cells with acid solution. In experiments designed for optimal time resolution, the rise-time of the pore conductance was in the range of 100-400 μs. In a few experiments, the second pore appeared soon after the first current transients. Surprisingly, pore flickering was never seen. Fusion pores showed a broad distribution of conductances in the range of 200-2000 pS, with a predominant value around 1 nS. To compare double whole-cell data with the conventional approach to calculating G, time-resolved admittance measurements were done. The amplitude and time course of fusion pore development were similiar to those obtained with double whole-cell technique. This confirms the original models for fusion pore conductance calculations and extends the time-resolution of continuous fusion pore measurements to the submillisecond domain.

Th-Pos170

CLASSICAL AND CORRALLED LIPID MODELING OF APOCYTOCHROME C BINDING TO ERYTHROCYTES.

((G. Krishnan, R. D. MacGregor, S. B. Shohet, and C. A. Hunt)) School of Pharmacy, University of California, San Francisco, CA 94143.

Classical modeling of apocytochrome c binding to human erythrocytes indicates the presence of 3 classes of sites having dissociation constants of $2x10^{-9}$, 10^{-7} and $7x10^{-7}$ M. These affinities, and the number of sites per μm^2 for each, are remarkably similar to values reported for apo c binding to its target, mitochondria. Because erythrocytes lack mitochondrial proteins, we suggest apo c binds primarily lipid in both membranes. Erythrocyte binding of apo c is positively cooperative (Hill coef. >2), but mitochondrial binding is noncooperative, possibly reflecting better apo c solvation by mitochondrial lipids. However, it is difficult to rationalize why there are 3 different apo c-lipid affinities, or why erythrocytes bind <9% of the apo c anticipated from its binding to liposomes. Therefore, we analyzed the binding data using a corralled lipid model. In this model the 3 classes of sites arise from 3 different corral areas delineated by the membrane skeleton, and the cooperativity of corralled lipid explains the reduced erythrocyte binding of apo c without postulating 3 different lipid-apo c interactions.

Th-Pos171

PHOSPHATIDYLETHANOL FORMED IN CELLS EXPOSED TO ETHANOL IS A STRONG PROMOTER OF NONBILAYER STRUCTURES

((Y.-C. Lee, G. Moehren, N. Janes, E. Rubin, J.B. Hoek and T.F. Taraschi)) Department of Pathology and Cell Biology, Thomas Jefferson University, Philadelphia, PA 19107.

In the presence of ethanol, phospholipase D catalyzes a transphosphatidylation reaction that leads to the formation of the rare phospholipid, phosphatidylethanol (PtdEth). PtdEth was determined to have unusual properties, being the only anionic phospholipid that forms a non-bilayer, hexagonal (H_{II}) phase in the absence of divalent cations and at physiological pH. We examined the ability of dioleoyl lipid species to promote formation of the H_{II} phase in a liposomal matrix of 1-palmitoyl-2-oleoyl-phosphatidylethanolamine (POPE). Potency is shown to correlate with headgroup volume as predicted by shape theories. PtdEth, however, promotes the H_{II} phase with a potency far in excess of other phospholipids (1). To investigate the effect of acyl chain composition on this potency, dilute concentrations (5 mole%) of PtdEth with various fatty acid compositions, e.g. DM (14:0/14:0), MO (14:0/18:1), PO (16:0/18:1), EGG, SA (18:0/20:4) and DO (18:1/18:1) were incorporated into a liposomal matrix consisting of POPE and the effect on the $L_\alpha \rightarrow H_{II}$ transition was studied by ^{31}P NMR. The ability to promote the H_{II} phase is shown to correlate with the degree of acyl chain unsaturation (DM < MO ≈ PO < EGG < SA < DO). DOPtdEth in trace amounts (1 mole%) induces the formation of the H_{II} phase in liposomes that mimic the phospholipid composition of an inner plasma membrane leaflet. The membrane destabilizing properties of PtdEth may play a role in alcohol-induced cell injury. Supported by PHS AA07215, AA07463, AA07186, AA00088. 1. Lee et al. *Biophys.J.* 65,1429-1432(1993).

Th-Pos172

MEMBRANE TOLERANCE DETECTED BY SPIN-COUNTING METHOD OF ESR SPECTROSCOPY

((D.C. Wang*, E. Rubin and T.F. Taraschi)) *Columbia University, Department of Medicine, 630 West 168th Street, New York, NY 10032; Department of Pathology & Cell Biology, Thomas Jefferson University, Philadelphia, PA 19107

It is well known that lipids from different tissues of alcohol-fed animal requires more ethanol to reach fluidity in its bilayer structure (membrane tolerance). A spin-counting method of ESR spectroscopy quantitatively measuring the partitioning of spin probe, TEMPO, has been applied to distinguish the lipids from liver microsomes of control animals (control) and the lipids from liver microsomes of ethanol-fed animals (alcoholic). This method treats the lipid structure as a whole and measures TEMPO distributions between the aqueous and lipid phases. Originally, the tolerance was measured by the order parameters of ESR spectra, which monitors ethanol influence on the motion of lipid molecules at specific position in the lipid bilayer. Both methods yield equivalent results. Conventional, TEMPO partitioning is measured by the peak heights of aqueous and lipid phases in a spectrum. Our method is more accurate and sensitive, because the lipids are in liquid-crystalline phase at the experimental conditions. Results revealed that lipids from controls & alcoholics showed temperature dependent partition coefficients of TEMPO (Kp/°C) and a transition of 37-39°C. Below and above this transition, the Kp/°C could be treated as linear with different slopes. The relationship of Kp and temperature from alcoholic samples can be fit in two states with different Kp/°C emerged together as a single transition. However, the control sample showed a more complicated transition. The slope of control Kp/°C was about 20% greater than the slope of alcoholic Kp/°C in the temperature range below the transition. These Findings can be used to study the tolerance. Grant: AA07186, AA00088.

Th-Pos173

POLYLYSINE BINDING INHIBITS THE PROTON PUMPING OF PLANT TONOPLAST H+-ATPASE.

((Shu-I Tu, Deidre Patterson, David Brauer, and An-Fei Hsu)) USDA/ARS/NAA, Eastern Regional Research Center, 600 E. Mermaid Lane, Philadelphia, PA 19118

Polylysine of various sizes was used to decrease the negative charges on the cytoplasmic surface of tonoplast vesicles obtained from corn roots. The interaction between polylysine and the membrane led to an increase in the light scattering of the vesicles, suggesting a volume increase. The binding of polylysine did not significantly affected the fluidity of the lipid domain of the membrane as judging from the insensitivity of DPH polarization to the presence of polylysine. With added polylysine (ave MW 9,870) up to 300 µg per mg of membrane protein, the ATP hydrolysis activity of the ATPase was slightly increased (less than 20%). However, the proton pumping activity was already decreased more than 50% with added polylysine as 100 µg per mg of protein. Under the applied conditions, the membrane proton leakage remained relatively unchanged. Thus, the neutralization of membrane surface negative charges by polylysine appeared to decoupled the proton pumping from ATP hydrolysis of the tonoplast H+-ATPase.

COMPUTER SIMULATIONS

Th-Pos174

IN THE SEARCH OF THE OPTIMAL SEQUENCE.

((Adam Godzik and Jeff Skolnick)) TSRI, La Jolla, CA 92037

Inverse folding algorithms are capable of recognizing the correct sequence to match a protein structure. But is it possible to design a sequence to fit a given structure without the help of a sequence databank? To answer this, we start from the simplified description of the protein structure in the form of a topology fingerprint and search for the global minimum of the energy in the sequence space. MC and GA minimization methods are utilized.

It is possible to find sequences with energies of hundreds of kT lower than native, but more detailed analysis casts severe doubts, whether they are better than the native sequence. A number of constraints are violated for these low energy sequences, including composition (they are built from only two to three different aminoacids), volume (they could not possibly fit into the desired structure) and specificity (the same sequence has the lowest energy in different structures). Also different sequences are obtained for slightly different energy parameters. These results tell more about the model's deficiencies, than about the question of ideal sequences.

It is only after introducing volume constraints that reasonable sequences are obtained. After restricting the total volume of interacting triplets, which in itself is not enough to recover the native sequence, minimization can produce sequences which could not be dismissed as artificial by any simple test. Moreover, the sequence similarity between the low energy sequences and the native one was on the level of 35% of identical aminoacids, and the predicted sequences could be easily recognized by any sequence analysis package as belonging to the correct family.

Th-Pos175

Ca^{2+}-BOUND CONFORMATIONS OF MET-ENKEPHALIN AND MORPHINE ARE SIMILAR.

((B.S. Zhorov and V.S. Ananthanarayanan)) Biochemistry Dept., McMaster Univ., Hamilton, Ont., Canada L8N 3Z5.

The conformationally rigid alkaloid morphine and the flexible pentapeptide hormone Met-enkephalin (Met-enk) act on the μ-opioid receptor. In spite of much effort it has not been possible to demonstrate any substantial conformational similarity between these two ligands by experimental or theoretical approaches. Based on a proposal on the importance of Ca^{2+} in the bioactive structures of hormones and drugs (Biochem. Cell Biol. 1991, *69*:93), we calculated the conformations of free and Ca^{2+}-bound forms of Met-enk and morphine. A Monte Carlo with energy minimization and ECEPP/2 force field was used to obtain minimum-energy conformers (MECs). Lowest-energy MECs of Met-enk did not resemble that of morphine. However, one of the lowest MECs of the Met-enk:Ca^{2+} complex showed a remarkable structural match to the MEC of morphine:Ca^{2+} complex. Both were compact and had the polar and nonpolar moieties identically disposed. In both, the distance between the positive charges on the Ca^{2+} and NH_3^+ was 8-9Å. Both fit a conical bottom of a channel-like receptor with Phe and Met residues of Met-enk extending toward the channel mouth. Similar MECs were found in several other μ-opiate but not in δ-opiate peptides. Thus, incorporation of Ca^{2+} provides a structural basis for opioid structure and selectivity. (Sponsored by CHF and MRC Canada).

Th-Pos176

MODELING OF THE COMBINING SITE OF AN ANTI-SWEET TASTE LIGAND ANTIBODY

((M. Viswanathan[1], J.M. Anchin[2], D.S.Linthicum[2] and S.Subramanium[1])) [1]Beckman Institute, Center for Biophysics and Computational Biology, University of Illinois, Urbana, IL 61801 , [2] Dept of Veterinary Pathobiology,Texas A&M University,College Station, TX 77843

Antibody proteins display a high degree of sequence and structural homology and are easy targets for homology modeling. The three dimensional structure of the antigen combining sites of the monoclonal antibody NC6.8e raised against the high potency sweetener, (N-(p-cyanophenyl)-N'-diphenyl-methyl) guanidineacetic acid has been modeled. The heavy and light chains were found to be sequence homologous to anti-hen egg lysozyme antibody, HyHel-5 and anti-fluorescin antibody, FAB respectively and the hybrid scaffold constructed from these two chains was used as a starting point for modeling the 6.8e fragment. Residue replacements that were consistent with the rotamer library of side chains from proteins were carried out and each of the hypervariable loops was independently subject to molecular mechanics refinement. The entire structure was subject to further refinement through high temperature molecular dynamics. The best energy structure obtained from this refinement was highly consistent with the experimental binding affinity and fluorescence measurements carried out with model ligands. This structure also had an rms deviation of about 2 A as compared to the high resolution structure obtained by Guddat et al . (Supported by NIH /NIGMS GM 46535)

Th-Pos177

COMPUTER SIMULATION OF ANESTHETIC QUANTUM EFFECTS ON BACTERIAL LUCIFERASE

((D.E. Louria, D.L. Koruga, R. Lahoz-Beltra and S.R. Hameroff)) Departments of Anesthesiology and Physiological Sciences, University of Arizona, Tuscon, AZ 85724 USA, Department of Mathematics, Complutense University of Madrid, Madrid 28040 Spain.

A unitary theory of anesthesia is supported by anesthetic inhibition of photoemission from bacterial and firefly luciferase. In a hydrophobic pocket within bacterial luciferase (BL), electron transfer from a flavin to an aldehyde substrate results in the excited photoemitting state. Anesthetics compete with aldehyde for binding in this hydrophobic pocket, a region presumably similar to anesthetic sites within neural proteins essential for consciousness. The active, region of BL was computer simulated using "Hyperchem" software (Autodesk Inc., Sausalito, CA) in quantum mechanics mode. Electrostatic potential contours were mapped and energy gradients calculated with and without aldehyde, eleven different anesthetics and the convulsant indoklon. With aldehyde and indoklon present, large electrostatic potential differences and energy gradients were observed between the electron donating flavin and acceptor; directional electron movement is thus favored. With no aldehyde and with each anesthetic studied, electrostatic potential differences and energy gradients were minimal; directional electron movement is not favored. Computer simulation of BL offers precise localization of anesthetic effect (the aldehyde site) and probability of electron movement. Inhibition of such movement may account for anesthesia.

Th-Pos178

FACTORS INFLUENCING ACCURACY OF COMPUTER-BUILT MODELS: A STUDY BASED ON THE LEUCINE ZIPPER GCN4 X RAY STRUCTURE.
((L. Shen, R. E. Bruccoleri, S. Krystek, J. Novotny)), Department of Macromolecular Modeling, Bristol-Myers Squibb, Princeton NJ 08543-4000

Krystek et al. (*Int. J. Protein Peptide Res.* 38 (1991), 229-236) reported on a three-dimensional model of the leucine zipper GCN4 built from its amino acid sequence. When the X-ray structure of the GCN4 dimer became available, the r.m.s. shift between the model and the structure was determined as 2.7 Å on all atoms, 1.1 Å on the backbones. Pilot experiments with the CONGEN conformational search algorithm were run, aimed at improving the accurancy of GCN4 modeling. With a judicious choice of CONGEN search parameters, the backbone r.m.s. improved to 0.8 Å, 2.5 Å on all atoms. Side chain conformations of Val and Leu at the helical interface were well reproduced (1.2 Å r.m.s.) and serious side chain misplacements occured with only a small number of charged amino acids and a tyrosine. Use of the X-ray backbone as the template for side chain construction leads to a significant improvement in their placement (2.1 Å r.m.s., 0.7 Å on the Val and Leu residues at the interface). Inclusion of the crystal environment, as a passive background, into the backbone and side chain conformational search further improved accurancy of the model to an 1.6 Å on all side chains except Arg, Lys, Asp, Glu, His, Tyr). Analysis of the GCN4 crystal packing revealed that 70% of the surface of the dimer was involved in crystal contacts with other dimers, and that charged residues often interacted with immobilized water molecules. Thus, occassional large r.m.s. deviations between the model and the X-ray side chains were due to conditions that do not occur in solution where surface side chains sample multiple conformations (cf., e.g., NMR spectroscopy).

Th-Pos179

MOLECULAR DYNAMICS STUDY OF BACTERIORHODOPSIN M INTERMEDIATE
((D. Xu, M. Sheves and K. Schulten)) Beckman Institute, UIUC, Urbana, IL, 61801.

Starting from a refined structure of bacteriorhodopsin with added inter-helical loops and sixteen water molecules in the L state of the pump cycle, we employed a simulated annealing schedule to describe the M intermediate. The simulations resulted in a very heterogeneous M intermediate, with a sequence of conformations which describe the transition of the Schiff base from pointing to the extracellular site to pointing to the intracelluar site. The transition involves a change in retinal's geometry as well as overall conformational changes which are in agreement with recent observations. The simulations also indicate an important role of water bound inside the protein. Water molecules involved in interactions with the Schiff base counter ion in BR_{568} alter their hydrogen bonding pattern to facilitate proton release to the extracellular side and to isolate Asp-85 from the Schiff base through formation of a hydrogen bridge network between retinal and Asp-96.

Th-Pos180

Analysis of Actin Rotational Dynamics by Time-resolved Phosphorescence Anisotropy ((Q. Zhang, E. Prochniewicz, and D. D. Thomas)) Dept. of Biochemistry, University of Minnesota Medical School, Minneapolis, MN 55455.

Rotational dynamics of F-actin labeled at Cys 374 with erythrosin iodoacetamide (ErIA) was studied using time-resolved phosphorescence anisotropy (TPA). Data were analyzed in terms of three models: (1) Rigid body diffusion about the filament axis. (2) Wobbling of monomer or subdomain-1 in a cone of restricted angular amplitude. (3) Twisting of the whole actin filament regarded as a flexible rod. In a refinement of previous analyses, non-parallel emission and absorption dipoles were considered. Theoretical TPA decays were simulated for each of the 3 models and compared with the experimental data. The results show that model 1 can be ruled out, implying that intrafilament motions exist. The length dependence of the experimental decay indicate that the intrafilament motions can not be simply explained by model 3. We suggest that the observed length dependence is due to either (1) a combination of models or (2) cooperative interaction among actin monomers along the filament.

Th-Pos181

COMPUTATIONAL STUDY OF THE PROTON WIRE IN A HYDROGEN-BONDED WATER CHAIN.
((R. Pomès and B. Roux)) Department of Chemistry, University of Montréal, Montréal, Québec, Canada H3C 3J7

The transfer of protons across membranes is an important step in numerous physiological processes. The gramicidin A channel constitutes a model system to elucidate some fundamental aspects of proton transfer. In this channel, the rapid translocation of protons is attributed to a hydrogen-bonded chain mechanism made possible by the linear arrangement of water molecules, or *proton wire*.

The transfer of protons across the gramicidin channel and the hydrogen-bonded chain mechanism are investigated by means of computer models. The flexibility and dissociation of water molecules are accounted for by an empirical energy function, the "Polarization Model" of Stillinger and David. Quantum mechanical effects are included by treating the protons of the water molecules with the discretized Feynmann path integral method.

The properties of the linear hydrogen-bonded network are studied with molecular dynamics simulations in the channel and in a continuous cylindrical tube to assess the effects due to the presence of the protein backbone atoms.

Th-Pos182

MACROSCOPIC HYSTERESIS ARISING FROM A POPULATION OF ELEMENTARY UNITS WITH "ON/OFF" STATES. EXAMPLE: LUNG PRESSURE-VOLUME HYSTERESIS. ((Gunter N. Franz and David G. Frazer)) W. Va. Univ. Sch. of Med., Dept. of Physiology, Morgantown, WV 26506 and NIOSH, Physiology Sect., Morgantown, WV 26505.

Elementary units for which the threshold for the "off-to-on" transition differs from that for the "on-to-off" transition have a "toggle" characteristic or hysteresis described by two step functions. If all elementary units have the same thresholds for the "on" and the "off" transitions, respectively, then the macroscopic behavior as a sum of unit behaviors exhibits hysteresis that is a scaled replica of the unit "toggle" characteristic. If the respective unit thresholds, however, are described by discrete density functions, then the macroscopic hysteresis differs from the scaled "toggle" characteristic and consist of segments of the integrals of the threshold densities (distribution functions). The shape of the "down" segment of the macroscopic hysteresis changes further if the unit behavior in the "on" state is described not by a constant but by a monotonic function for inputs beyond the "on" threshold and back down to the "off" threshold. This poster demonstrates the application of this hysteresis model to pressure-volume hysteresis in lungs. Frazer *et al.* have presented experimental evidence (Respiration Physiol. *43*: 237-246, 1981 and *61*: 277-288, 1985.) that the hysteresis present in quasistatic volume-pressure curves of excised rat lungs, for the most part, depends on (1) the opening (recruitment or "on" transition) of closed lung units during inflation from low end-expiratory pressures, (2) the subsequent monotonic expansion of open lung units during continued inflation, (3) monotonic contraction of open lung units with deflation, and (4) closing (derecruitment or "off" transition) of open lung units with continued deflation to low end-expiratory pressures.

Th-Pos183

APPROXIMATIONS FOR INCORPORATING SOLVENT EFFECTS IN COMPUTER SIMULATIONS OF BIOMOLECULES
((D. Beglov and B. Roux)) Department of Chemistry, University of Montreal, Montreal, Quebec, Canada H3C 3J7

Three different computational approaches, based on approximations made at different levels, have been developed and tested to incorporate the influence of solvation on biomolecules.

In a first approach, the relation of an infinite bulk system to a finite spherical representative is demontrated based on a rigorous statistical mechanical formulation. In this method, the water molecules inside a spherical region around a biomolecular solute are represented explicitly; the influence of the remaining bulk water is taken into account with a mean force potential. The approach is tested with the calculation of solvation free energies of various solutes in water.

In a second approach, the dominant effect of solvation on a biomolecular solute is represented by including only the solvent molecules of the primary hydration shell explicitly. The method is computationally inexpensive and allows an extensive exploration of the configurational space available to a flexible biomolecule. The approach is tested with small polypeptides molecules.

In a third approach, an integral equation developed from statistical mechanical Hypernetted-Chain (HNC) and Mean-Spherical-Approximation (MSA) liquid state theories described the average solvent and ion densities around a macromolecular solute of arbitrary geometry. It is shown that the integral equation reduces to a modified Poisson-Boltzmann integro-differential equation with a space-dependent dielectric constant which depends on the local ionic concentration. Numerical methods based on a cubic lattice to solve the equation are being explored.

Th-Pos184

MAPPING THE POTENTIAL SURFACE OF SUPERCOILED DNA. ((S.C. Pedersen)) Department of Chemistry, Rutgers, the State University of New Jersey, New Brunswick, New Jersey 08903 (Spon. by R.M. Levy)

A new method has been developed that allows the determination of the potential surface of supercoiled DNA taking into account pseudo-sequence effects. The model used for the circular DNA is that of a thin elastic rod composed of a variable number of segments, each possessing unique bending and twisting constants, as well as intrinsic curvature and torsion. The geometry of the DNA is described by piecewise cyclic B-spline curves with the overall length of the DNA and the individual segment lengths held fixed. The potential surface is mapped following a systematic survey of conformational space where each segment is afforded a fixed angle through which it has rotational and bending freedom.
(Research supported by USPHS grant GM-34809; calculations carried out at the Rutgers Center for Computational Chemistry and the Pittsburgh Supercomputer Center)

Th-Pos185

THEORY AND NUMERICAL ANALYSIS OF THE EFFECTS OF LIGAND BINDING AND BASE SEQUENCE ON DNA SUPERCOILING ((T.P. Westcott)) Department of Chemistry, Rutgers, the State University of New Jersey, New Brunswick, New Jersey 08903 (Spon. by W.K. Olson)

A DNA polymer with hundreds or thousands of base pairs can be modeled as a thin elastic rod. Using the elastic theory of rods, the energy of the DNA can be expressed as an integral over the entire arc length. By setting the first variation in the energy to zero, an expression for the equilibrium configuration of the rod is obtained. The resulting differential equations can be simplified to a set of nonlinear algebraic equations by discretizing the rod into a number of small elements with regular shapes. Each element can then have its own physical characteristics; thus, individual base effects can be taken into account. It is possible to study chains containing regions of intrinsic curvature, altered twist, differences in intrinsic bending and twisting stiffness, bound drugs and/or proteins, *etc.*
(Supported by USPHS grant GM-34809).

Th-Pos186

CONFORMATION OF LINEAR POLYELECTROLYTES. ((C.E. Reed and W.F. Reed))Physics Department, Tulane University, New Orleans, LA 70118.

The conformation and dimensions of electrically charged biopolymers depend strongly on their charge density and the ionic strength of their milieu. The electrostatic persistence length concept provides a quantitative model for these properties. At low excluded volume, polyelectrolytes are modeled as worm-like chains with a persistence length increased by electrostatic stiffening from an intrinsic value. This implies that the average of the cosine of the angle between two parts of the polymer backbone should decrease exponentially with the contour length between the two parts of the backbone. We tested this prediction for idealized simulated polyelectrolytes, and it failed. However, an *overall* persistence length which is usually within about 30% of that predicted by Odijk can be extracted from the Monte Carlo results.

The model polymers were three-fold rotational isomeric with Debye-Hückel screening. The Monte Carlo simulation was off-lattice, non-Metropolis, and used reptation moves. Supported by NSF grant MCB9116605 and Tulane's MCB program.

Th-Pos187

NANOSECOND MOLECULAR DYNAMICS SIMULATIONS ON THE d(CGCGAATTCGCG) DOUBLE HELIX IN WATER ((K.J. McConnell, R. Nirmala, M.A. Young, G. Ravishanker and D.L. Beveridge)) Dept. of Chemistry, Wesleyan Univ., Middletown CT 06459

Three molecular dynamics computer simulations on the DNA duplex d(CGCGAATTCGCG) in water have been carried out for unprecedented run lengths ranging from several hundred picoseconds to one nanosecond. The simulations are based on the GROMOS force field, augmented with a hydrogen bond function applied to Watson-Crick base pairs. In order to test the sensitivity of the results to the choice of initial conditions, the protocols for the three simulations are identical except for the choice of starting structures: the canonical B80 fiber diffraction form, the Drew-Dickerson crystal form, and the crystal structure of the dodecamer in the Eco RI endonuclease complex. Stability and convergence behavior of the simulations are monitored via two-dimensional root-mean-square deviation maps. The dynamical structures are analyzed with respect to the time evolution of conformational and helicoidal parameters. Results indicate that all three simulations explore a common, essentially B-form dynamical state, characterized by an ensemble of structures featuring axis bending towards the major groove at or near the junctions between CG and AT tracts. The simulations demonstrate the existence of dynamical micro states in the DNA with lifetimes of 100 ps, and transient deformations in the structure which manifest themselves only on the nanosecond time scale. Comparison of the calculated results with observed crystal structure data is considered to validate the theoretical model of the solution structure of the dodecamer.

Th-Pos188

NEURAL NETWORKS TO COMPUTE MOLECULAR DYNAMICS

((L. S. Liebovitch, N. D. Arnold, and L. Y. Selector))
Center for Complex Systems
Florida Atlantic University, Boca Raton FL 33431

In present molecular dynamics computations, the forces on each atom are evaluated, the atom moved, and this procedure repeated many times. However, with the the small 10^{-15} s time steps needed, it is not possible to compute motions over long time scales.

Since neural networks share many properties with proteins (multiple energy minima, frustration, ultrametricity) they may be a much more efficient way to compute these motions. We show how to encode the spatial structure of a molecule in the values of the nodes of a network and the energy structure in the strenghts of the connections between the nodes. As the network evolves in time it therefore computes the changing structure of the molecule.

As an example of this new method, we used a Hopfield network to compute the chair to twisted boat transitions in cyclohexane.

Supported by NIH EY6234 and the Amer. Heart Assoc.

Th-Pos189

MOLECULAR DYNAMIC SIMULATIONS OF PHOSPHOLIPID BILAYERS. ((P. Huang, J. J. Perez and G. H. Loew)), Molecular Research Institute, 845 Page Mill Road, Palo Alto, CA 94304.

Molecular dynamics (MD) simulations at 37°C have been performed on three phospholipid bilayer systems composed of the lipids DLPE, DOPE, and DOPC. The model used included 24 explicit lipid molecules and a 6-8Å layer of explicit water of solvation together with constant-pressure periodic boundary conditions in three dimensions that allowed the sampling of part of a planar lattice of lipid bilayer. The dynamic behavior was characterized and the structural properties, order parameters, chain dihedral statistics, electron density profile, hydration per lipid, and water distribution along the bilayer normal have been calculated using structures stored during the MD simulations. Many of these properties are known for the three lipid systems chosen. The calculated MD behavior, chain disorder, and ratio of maximum area of hydrocarbon tails to surface area per lipid (a_t/a_h) all confirm that each of these three lipids is in the aggregation phase observed experimentally at 37°C, namely: a gel bilayer for DLPE, a hexagonal tube for DOPE, and DOPC, a liquid crystalline bilayer. Moreover, the calculated properties of the bilayers agree well with reported experimental results. The detailed effects of the *cis* unsaturated hydrocarbon chains in DOPE and DOPC compared to the fully saturated one in DLPE have been explored. Although a relatively small number of lipid molecules were explicitly included in each system, the validity of these simulations has been demonstrated by the success in reproducing experimentally measured properties for all three systems. The results of these studies demonstrate the ability of MD simulations to provide molecular level insights into the structure and properties of bilayer systems.

Th-Pos190

EXTRACTING CHANNEL KINETIC PARAMETERS USING HIDDEN MARKOV TECHNIQUES ((Feng Qin, Jialin Chen, Anthony Auerbach and Frederick Sachs)), Dept. Biophysical Sciences, SUNY at Buffalo, Buffalo, NY 14214. (Spon. by R. Spangler)

Chung et al (*P. Trans. R. Soc. Lond. 329:265*) introduced the technique of hidden Markov analysis for obtaining parameters of single channel currents. The technique was extended by Walsh and Sigworth (*Thesis, Yale University, 1992*) to deal with the effects of band limiting by analog filtering. Although complete, the latter approach is quite slow and is not readily suited to maintaining constraints on the rate constants. We have attempted to address these problems. To increase the speed we have used preprocessing to correct for bandlimiting distortion, baseline drift and harmonic interference (e.g. powerlines and computer monitors) so that these parameters need not be included in the interations over each data point. Secondly, we have approximated the corrected noise spectrum as a first order autoregressive process which is readily included in the first order Markov process. To allow contraints on the rate constants, we have used traditional variable metric optimizers rather than the Baum-Welch algorithm. To minimize the number of free parameters, the transition matrix can be automatically reduced by the constraints of detailed balance. The traditional forward-backward algorithm for calculating the likelihood is generalized to the case where the underlying noise is not white. An efficient technique was developed for analytically computing the derivative of likelihood function with respect to kinetic parameters so that the rate of optimization is increased. To further increase the rate of optimization, we begin by fitting short lengths of data to improve the initial guesses. Then progressively longer segments are analysed. We are exploring global optimization using annealing techniques. Post-analysis procedures seek to test homogeneity and stationarity by looking for drift or clustering of the kinetic parameters evaluated for individual bursts or data segments. Supported by grants from NSF, MDA, NIH, ARO (DAAL0392G0014 to FS) and SUNYAB School of Medicine and Biomedical Sciences.

Th-Pos191

INVESTIGATION OF THE KINETICS OF RAPID BIMOLECULAR REACTIONS WITHIN THE PLANE OF PHOSPHOLIPID MEMBRANES. ((S. Bergling)) Department of Biophysical Chemistry, Biocenter Basel, Klingelbergstr. 70, CH-4056 Basel, Switzerland. (Spon. by Sammy Frey) email: bergling@urz.unibas.ch

There is a general interest in the description of rapid two-dimensional kinetic processes, e.g. the kinetics of encounter-complex formation of membrane-associated or membrane-bound peptides.
The determination of rate coefficients for diffusion controlled bimolecular reactions are far more difficult in two dimensions than in three dimensions (aqueous solutions).
The well known approach of Smoluchowski fails to describe rapid two dimensional reactive systems.
Here an approach in the context of nonequilibrium statistical mechanics developed by Joel Keizer is used to determine the forward rate coefficients of diffusion controlled bimolecular reactions within the plane of membranes.
Random walk computer simulations are used to check the range of validity of Keizer's approach.
Additionally, computer simulations of two dimensional reactive systems with phospholipid membranes as solvent are used for further investigations such as the influence of membrane size on the reaction kinetics, the occurrence of particle segregation and the role of reaction products as obstacles for diminishing long range diffusion of reactants.

Th-Pos192

INTERACTION OF SMALL PEPTIDES WITH LIPID BILAYERS: MOLECULAR DYNAMICS AND FREE ENERGY SIMULATION STUDIES. ((K. V. Damodaran, Kenneth M. Merz, Jr., and Bruce Paul Gaber)) Department of Chemistry, The Pennsylvania State University, University Park, PA 16802 and Center of Bio/Molecular Science and Engineering, Naval Research Laboratory, Washington, D.C. 20375.

A 410 picosecond molecular dynamics simulation of a tripeptide Ala-Phe-Ala-O-tert-butyl interacting with a DMPC lipid bilayer with explicit water molecules is reported. The structure has been examined using probability distribution functions for various regions and their time dependences. The location of the peptide in the bilayer has been found to be in good agreement with neutron diffraction data. Comparison of the order parameter profile with NMR data shows some disagreements, which have been interpreted as due to the low concentration of the peptide in the simulated system. The perturbation of the lipid head group dynamics due to the peptide has been illustrated using time correlation functions for the head group rotational motion. The relative binding free energies of the peptide with different central residues (Phe - Leu -Ala) calculated using free energy perturbation simulations are also compared with experimental results.

Th-Pos193

THE POTENTIAL ENERGY SURFACES OF α(1-3)- AND α(1-2)-LINKED MANNOSE DIMERS IN AQUEOUS SOLUTION: CONCLUSIONS DERIVED FROM OPTICAL ROTATION. ((E.S.Stevens)) Department of Chemistry, SUNY Binghamton, P.O. Box 6000, Binghamton, NY 13902-6000.

The optical rotation of methyl 3-O-(α-D-mannopyranosyl)-α-D-mannopyranoside and of methyl 2-O-(α-D-mannopyranosyl)-α-D-mannopyranoside were calculated semiempirically as a function of the linkage dihedral angles Φ and Ψ. The observed rotations are compatible with some but not all published potential energy surfaces. The (1-3)-linked dimer is not rigid; at least two linkage conformers must be present in aqueous solution in order to account for the optical rotation. For both cases, the range of conformation population distributions compatible with the observed optical rotation is presented.

Th-Pos194

HYDROXYLATION PROFILE OF RACEMIC NORCAMPHOR BY CYTOCHROME P450cam; A MOLECULAR DYNAMICS SIMULATION PREDICTION OF REGIO PRODUCT SPECIFICITY. ((G.E. Arnold, M.D. Paulsen, and R.L. Ornstein)) MSRC, PNL, P.O. Box 999, K1-95, Richland, Washington 99352.

Previous MD simulations in our laboratory found a discrepancy between our predicted and the experimentally determined product ratios for the hydroxylation of norcamphor by cytochrome P450cam. Experimentally, a near equimolar mixture between the 5- and 6-hydroxynorcamphor products was found (45% 5-, 47% 6-, and 8% 3 hydroxynor-camphor) [W.M. Atkins and S.J. Sligar, *J. Am. Chem.* Soc., 109, 3754 (1987)]. Our simulations predicted a preponderance of the 5-hydroxynorcamphor product (from 68-88%) [M.B. Bass et al., *Proteins* 13, 26 (1992)]; our simulations were run using only D-norcamphor as the substrate, whereas the experimental results were determined from a racemic mixture of substrates. This difference could account for the discrepancy found between the theoretical and experimental product ratio. Here, we will present results of the theoretical product profile for the hydroxylation of both the L- and D-norcamphor isomers. These stereoisomers have been racemically resolved and, concurrent to our MD study, the hydroxylation profile of each enantiomer is being determined experimentally. We have no prior knowledge of the experimental results.

Th-Pos195

AB INITIO X-RAY ABSORPTION FINE STRUCTURE CALCULATIONS AND MOLECULAR MODELLING OF COBALAMIN MODEL COMPOUNDS. ((E. Scheuring,Y. Lu, M. R. Chance)) Albert Einstein College of Medicine, Bronx, N.Y.

Trans-Bis(dimethylglyoximato) cobalt complexes, commonly referred to as cobaloximes, have been extensively studied as cobalamin model compounds. Those Co(III) cobaloximes where one axial ligand is a carbon atom of an alkyl group and the other axial ligand is a nitrogen donor, such as a pyridine moiety, most closely resemble enzymatically relevant cobalamins. The four and five coordinate Co(I) and Co(II) cobaloximes are also very important as they resemble enzimatically important intermediates. In this study we show our ability to successfully simulate experimental data by theoretical methods. To simulate theoretical chi data we use the ab initio X-ray absorption fine structure code, FEFF (v. 5.05). The atomic coordinates for the FEFF input file are taken from the Cambridge Crystallographic Data Bank. Hydrogens are excluded as their scattering contributions can be ignored. In order to take into account the static and thermal disorders in the molecule the temperature and Debye-temperature parameters are introduced. Multiple scattering is taken into account. We will show the Fourier transforms of the simulated and the experimental $k^3\chi$ data and give the nonlinear least-squares fitting results. In addition, we performed modelling studies using the CHEM-X molecular modelling package to examine the dynamic nature of the axial Co-C, Co-N distances which are very important in the understanding of the enzymatic reactions. This research was supported by USDA/NRICGP-CSRS grant, #91-37200-6897.

Th-Pos196

RANDOM WALK CALCULATIONS FOR BACTERIAL MIGRATION IN A POROUS MEDIA ((Kevin Duffy, Sten Sarman , Roseanne Ford and Peter Cummings)) Department of Chemical Engineering, Thornton Hall, and the Biophysics Program, University of Virginia, Charlottesville, VA 22903-2442. (Spon. by S. Frasier-Cadoret)

Bacterial migration is important in understanding many practical problems ranging from disease pathogenesis to the bioremediation of hazardous waste in the environment. Our laboratory has been successful in quantifying bacterial migration in fluid media through experiment and the use of population balance equations and cellular level simulations that incorporate parameters based on a fundamental description of the microscopic motion of bacteria. The present work is part of our aim to extend these results to an understanding of bacterial migration in a porous media.

A random walk algorithm has been used successfully to obtain the diffusion constant for a continuum percolation problem (Tobochnik *et al.*, 1990, *Physical Review A*, 41, 3052-3058). Tobochnik *et al.* (1990) use a first-passage-time algorithm and show its efficiency in calculating diffusion coefficients in a simulated porous media.

We have generated a series of model porous media using molecular dynamics applied to a fluid of equal-sized spheres. The porosity is varied by allowing different degrees of sphere overlap. The first-passage-time algorithm is applied and the Einstein relation is used to calculate the effective bacterial diffusion coefficient. A plot of tortuosity against porosity is compared to available experimental results. Examples of simulated bacterial migration in a porous media will be discussed and computer visualizations presented.

Th-Pos197

BROWNIAN DYNAMICS SIMULATION OF THE SIEVING OF SPHERES BY GELS. ((G. A. Griess, A. Estrada, and P. Serwer)) The Univ. of Texas Health Sci. Ctr., San Antonio, TX 78284-7760

To understand empirical observations of the microscopic motion of single spheres in gels[1], a program with the following capabilities has been written for the Macintosh microcomputer: (a) A three-dimensional gel network is generated which, when projected, agrees with agarose networks observed by electron microscopy.[2] (b) Within the network, spheres execute a three-dimensional random walk that can be modified by an interaction function. (c) Projected displacements are accumulated. By using a sterically inhibited random walk, this program quantitatively simulates a recoil previously observed[1] when a high field (3 V/cm) that had driven large spheres (240 nm in radius) to steric entrapment was reduced to 0. By introducing displacements of 0 after collision with a gel fiber, simulations have shown that the empirical data for diffusion are not explained by inelastic collisions with gel fibers. Other observations[1] have shown that elastic collisons are infrequent. The data are explained by random motion damped as a function of distance from gel fibers. This function is being investigated. Supported by NSF.

1. Griess, G.A., Harris, R.A., and Serwer, P. (1993) Appl. Theor. Electrophor. 4, in press.
2. Griess, G.A., Guiseley, K.B., and Serwer, P. (1993) Biophys. J. 65, 138-148.

FOLDING AND SELF-ASSEMBLY IV: SPECTROSCOPIC AND METHODOLOGICAL STUDIES

Th-Pos198

FLUORESCENCE SPECTROSCOPY OF *Escherichia Coli* ADENYLATE KINASE MUTANTS. ((T. Bilderback[1]; T. Fulmer[1,2]; M. Glaser[1] and W. W. Mantulin[1,2])) Univ. of Illinois at Urbana-Champaign, [1]Biochemistry Dept. & [2]Laboratory for Fluorescence Dynamics, Dept. of Physics, Urbana, IL 61801.

The enzyme adenylate kinase (AK) from *Escherichia Coli* catalyzes the interconversion, synthesis and regeneration of adenosine nucleotides by the following reaction: Mg^{2+} ADP + ADP ↔ Mg^{2+} ATP + AMP. AMP and ATP binding at discrete sites is associated with large conformational changes in AK:domain movements. The reaction requires Mg^{2+} for catalysis, but not for nucleotide binding. Through site directed mutagenesis, we have expressed four tryptophan mutants (S41→W, F86→W, Y133→W, F137→W) of wild type AK, which is devoid of tryptophan. The enzymes are purified by liquid chromatography and are all active. Circular dichroic spectra suggest similar conformations for the enzymes. The spectroscopic response of the W reporter group provides information about the structure and dynamics of AK. The fluorescence spectra, intensities, lifetimes and quenching of the AK enzymes varied. For example, in the ligand free form, the emission maximum of AK86W is 325 nm, as compared to 357 nm for AK41W. The intensity averaged lifetimes are 2.95 ns and 7.23 ns, respectively. The results for AK133W and AK137W are intermediate to the other mutant AK. Placement of W reporter groups in regions of differing secondary and tertiary structure in AK is the likely source of the diversity in fluorescence response. The ultimate goal of our studies is a greater understanding of the structure-function relationship in AK.

Support: National Institutes of Health, RR03155, & American Heart Assoc., Ill. Affilliate.

Th-Pos199

VIBRATIONAL CIRCULAR DICHROISM OF PROTEINS: ADVANTAGES AND PROBLEMS.
((P. Pancoska, V.Baumruk and T.A.Keiderling)), Department of Chemistry, University of Illinois at Chicago, m/c 111, Chicago, IL 60607-7061.

Vibrational circular dichroism (VCD) spectroscopy is qualitatively sensitive to various aspects of protein structure. Measurements in both D_2O and H_2O are possible with current instrumentation. VCD also provides an advantage of multiple transition over classical electronic CD and conformationally dependent signs to IR transitions. For a set of 28 globular proteins, characteristic VCD patterns in amide I region discriminate between α, α/β ,α+β and β protein folding types. The relation between the VCD sign and frequency shows that there is not a unique relation between protein secondary structure and IR frequency as used in FTIR analyses. Neural network calculations are used to relate amide I and II VCD spectra and electronic spectra of the whole protein set to reveal their respective information content. Quantitative analyses of these CD spectra in terms of conformational fractional secondary descriptor reaches a limiting level of precision. Efforts to go beyond this by including aspects of a connectivity based supersecondary descriptor for the structure - spectra correlation are described.

Th-Pos200

PROTEIN SOLVATION CHANGES THAT ACCOMPANY SUBSTRATE BINDING AND TURNOVER. (R. P. Rand, N.L. Fuller, and C. Reid) Biological Sciences, Brock University, St. Catharines, Ontario, Canada, L2S 3A1.

Osmotic stress (OS), whereby the chemical potential of water is controlled with indifferent polymers, can be used to measure the contribution of solvation to the energetics of any system (Science1992 256:618). Yeast hexokinase (HK) has a cleft whose closure is induced by glucose binding. We have used OS to measure water's role in (HK)'s activity and conformational change. OS reduces both the dissociation constant, K_d, and the Michaelis-Menten constant, K_m, for glucose. The equilibrium data show that nearly 500 water molecules are removed as glucose binds at physiological pressures when set by osmolytes of greater than MW 2000. This suggests a large contribution by solvation to the energetics of the conformational change whereby water behaves like an inhibiting ligand. Such a large number of water molecules is difficult to reconcile with the open and closed conformations determined from the crystallographic structures. As the osmotic pressure increases this number falls continuously to about 65 waters at high pressures, a number easier to reconcile with the crystal structures. We interpret this to mean that osmotic pressure itself 'dehydrates' the protein before the substrate triggers the cleft closing. This suggests that the structure in solution may be more open than that in the crystal. Below MW 2000 the number of measured water molecules falls continuously with decreasing MW of the osmolytes, suggesting that they are excluded from ever smaller aqueous compartments around the protein. In this way we are trying to probe different aqueous spaces over the protein surface.

Th-Pos201

A CONFORMATIONAL STUDY OF *cyclo*-(Pro-Gly)$_3$ AND ITS COMPLEXES WITH CATIONS BY VIBRATIONAL CIRCULAR DICHROISM (VCD) SPECTROSCOPY ((Ping Xie and Max Diem)) Department of Chemistry, City University of New York, Hunter College, 695 Park Avenue, New York, NY 10021.

The conformation of *cyclo*-(Pro-Gly)$_3$ and several complexes with group I and II cations was studied *via* Vibrational Circular Dichroism (VCD). The conformation of this peptide depends to a great deal on the solvent, and the presence of cations, and varies from a highly symmetric structure with three γ turns to non symmetric structures. Depending on the nature, valence and concentration of the cations present, a number of different complexes can be formed. These complexes give very different VCD spectra, which can be interpreted qualitatively in terms of different solution conformations.
Supported, in part, by NIH grant GM 28619 (to MD)

Th-Pos202

AROMATIC SIDE CHAIN CONTRIBUTIONS TO THE FAR-UV CD SPECTRUM: EXPERIMENTAL STUDIES OF BPTI MUTANTS. ((H. Pan & C. Woodward)) University of Minnesota, Dept. of Biochemistry, St. Paul, MN 55108.

Circular dichroism (CD) spectroscopy is widely employed to estimate the secondary structural content of a protein with the assumption that the polypeptide backbone is the sole contributor to the far-UV spectrum. However, the CD spectrum of bovine pancreatic trypsin inhibitor (BPTI) has an unusual and pronounced negative ellipticity minimum at 202 nm, which is not explained by backbone structure. There is a suggestion from theoretical studies that aromatic side chains, especially in close proximity to each other make significant contributions in the far-UV spectrum (Manning & Woody, Biochemistry 1989, 28, 8609-8613). If this is the case, then CD can be used to monitor both tertiary and secondary structure of BPTI in partially folded species and in transient species formed during folding. We have compared far-UV CD spectra of aromatic BPTI mutants Y21A, F22A, Y23A, F45A and Y35G and of the BPTI $Cys^{14,38}$-methylated derivative. Replacement of some of these aromatic side chains does diminish the 202 nm negative ellipticity, but none eliminate it completely.

Th-Pos203

A NOVEL AND SIMPLE SPECTROSCOPIC METHOD FOR DETERMINATION OF PROTEIN TRANSITION STATES

A.A.Moosavi-Movahedi ; M.Rezaei-Tavirani and Z.Zaidi Institute of Biochemistry & Biophysics ,University of Tehran,Tehran,Iran and H.E.J.Research Institute of Chemistry,University of Karachi, Karachi,Pakistan.

A novel and simple difference spectroscopic method is presented for analyzing a set of spectra obtained from titration,to determine the transition states of protein from native to denatured states.This method is precisely formulated for two,three and four transition states.

For each individual protein,there appears to be certain specific positions in the spectrum at which there is appreciable difference in absorbance.This method was tested using Sodium n-dodecyl sulphate(SDS) as a potent denaturant and pigeon hemoglobin.Results indicate three transition states in the protein molecule upon denaturation.

Th-Pos204

THE EFFECTS OF PHOSPHOROUS METABOLITES ON THE AROMATIC AMINO ACIDS OF α-CRYSTALLIN. ((Palmisano, D.V.[1], Groth-Vasselli, B.[2] and Farnsworth, P.N.[1,2])) UMD-GSBS & NJMS, Departments of Physiology[1] and Ophthalmology[2], Newark, NJ 07103. (Spon. by P.N. Farnsworth)

Purpose. Both near UV difference and intrinsic tryptophan fluorescence spectroscopy were used to detect α-crystallin/ATP interaction, its specificity, as well as alterations of protein conformation. **Methods.** All spectra were collected at 37°C following a two hour incubation of ligand/protein in 50 mM Tris buffer, pH 7.2 at 37°C. The near UV difference spectra (240-300 nm) were generated following incubation of 1 mg/ml α-crystallin with 12.5-62.5 nM ATP, ADP, AMP, Pi or GTP. The fluorescence spectral changes (310-380 nm) were examined following incubation of 0.1 mg/ml protein with 0.05-0.4 mM of the metabolites. **Results.** With increasing concentrations of ATP, the near UV difference spectra revealed an increased intensity and a shift of the absorbance peak to shorter wavelengths. The other metabolites produced no effect. The spectral changes are indicative of increasing exposure of phenylalanine residues to the aqueous medium. The data permit the calculation of a tentative binding constant of 0.037×10^9 M^{-1} and an estimated 12 binding sites per aggregate. The fluorescence data indicate the binding of ATP and the movement of tryptophan residues to a more hydrophobic environment. No effect was seen for the other metabolites studied. **Conclusions.** The inability of other metabolites to produce spectral changes indicates the specificity of ATP effects. Also, the absence of spectral changes by other phosphorous metabolites indicates a specificity of ATP/α-crystallin binding. Spectral evidence for alterations in the environment of aromatic amino acids indicates conformational changes. Supported by NIH grant EYO 5787, UMD-GSBS and Research To Prevent Blindness.

Th-Pos205

INFRARED SPECTROSCOPIC STUDY OF CHAOTROPH-INDUCED AGGREGATION IN LYOPHILIZED CHYMOTRYPSINOGEN FORMULATIONS. ((S. Dean Allison and John F. Carpenter)), School of Pharmacy, University of Colorado Health Sciences Center, Denver, 80262.

Infrared spectroscopic examination of chymotrypsinogen freeze-dried alone showed that the protein's secondary structure in the dried solid was greatly altered relative to the native, aqueous state. However, upon rehydration the protein regained its native conformation. By adding sodium thiocyanate to the protein solution, to concentrations where there was no visible protein aggregation prior to lyophilization, we observed three levels of effects during drying. With concentrations $\leq$ 50mM, thiocyanate induced additional denaturation of chymotrypsinogen during lyophilization, but the protein still refolded upon rehydration. With 100mM thiocyanate, even more structural perturbation was indicated by the spectrum of the dried solid, and the protein aggregated when rehydrated. The spectrum of the protein dried in 250mM thiocyanate was grossly altered, resembling that of chymotrypsinogen that was aggregated in with 1M thiocyanate and then lyophilized. The appearance of a prominent band at 1618 cm^{-1}, associated with intermolecular beta-sheet formation, indicated that the protein may have already aggregated in the dried solid. Essentially complete aggregation was noted after rehydration. Taken together these results demonstrate that extent of protein aggregation after lyophilization and rehydration is directly dependent on the degree of denaturation induced by freeze-drying. Additionally, if the degree of denaturation is sufficient, then aggregation can occur prior to rehydration.

Th-Pos206

INVESTIGATING THE SECONDARY STRUCTURE OF DESIGNED AMPHIPHILIC PEPTIDES. ((M. Javadpour, C.L. Becker, S.M. Cowell, M.L. McLaughlin, M.M. Juban*, K.M. Morden*)) Department of Chemistry and *Department of Biochemistry, Louisiana State University , Baton Rouge, LA 70803.

The amphiphilic α–helix is defined as an α-helix with opposing polar and non-polar faces oriented along the axis of the helix. Three different peptides (1) (KALKALK)3, (2) (KLAKLAK)3, (3) (KLAKKLA)3 have been investigated which have the same amino acid content but differ in sequence and the angle of their polar faces. The helical content of these peptides has been investigated using CD as a function of TFE, HFIP and peptide concentration. The helical content has also been investigated in SDS micelles. (1) and (3) show CD spectra of random coil whereas (2) shows some helical characteristics at a [peptide] ~ 0.4mg/ml in 2.5 mM phosphate buffer. All of the peptides show increasing helical content with increasing concentration of TFE or HFIP. The secondary structure of these peptides in buffer changes from random coil to helix with a 100-fold increase in peptide concentration. Equilibrium centrifugation experiments on (1) show the peptide to be in a monomeric state, while for (2) a monomer/dimer equilibrium is observed. The secondary structure of the same sequence of peptides but as a 7mer, 14mer, and 28mer have also been investigated. In an attempt to relate structure to function the antibacterial activity has been determined as the M.I.C. which is the lowest concentration of antimicrobial peptide that completely inhibits growth of the organism as detected by the unaided eye. The 7mer of these peptides show no inhibitory activity. The 14 and 21mers show a range of activity from 16 to 64 micrograms/ml.

Th-Pos207

RAMAN SPECTROSCOPY OF FILAMENTOUS BACTERIOPHAGE *Ff* (*fd, f1, M13*): ASSIGNMENT AND STRUCTURAL INTERPRETATION OF COAT PROTEIN AROMATICS. ((Stacy A. Overman and George J. Thomas, Jr.)) Division of Cell Biology and Biophysics, School of Biological Sciences, University of Missouri, Kansas City, MO 64110.

Structural interpretation of the Raman spectrum of the filamentous bacteriophage *Ff* (*fd, f1, M13*) is dependent upon definitive assignments for vibrational bands of coat protein (gpVIII) subunits. Since site-specific isotope substitution allows perturbation of vibrational dynamics in a predictable manner, without altering molecular conformations of phage components, it is the method of choice for advancing Raman spectral assignments and promoting structural conclusions therefrom. Raman spectra were collected from phage *fd* incorporating gpVIII subunits with deuteriophenylalanine, deuteriotryptophan or deuteriotyrosine residues in which only the aromatic ring sites were labeled. The isotopomers of F, W and Y (F-*d5*, W-*d5* and Y-*d4*) were introduced into *fd* individually and in combination. On the basis of isotope shifts observed in Raman spectral bands, definitive assignments have been developed for all of the prominent Raman markers of the coat protein aromatic residues (F11, F42, F45, W26, Y21, Y24). These results, which constitute the first direct experimental determination of Raman fingerprints of tyrosyl and phenylalanyl side chains within hydrophobic α-helical domains, demonstrate novel and unexpected Raman frequencies and intensities for key conformation markers of the F and Y residues of gpVIII. The implications of the present and previous [Aubrey & Thomas (1991), *Biophys. J.* 60:1337-1349] assignments for the structure of the *Ff* virion will be discussed.
[Supported by NIH Grant GM50776.]

Th-Pos208

ß-STRAND STRUCTURES IN SIMULATIONS OF EMERGING POLYALANINE: THE EXCLUDED-VOLUME EFFECT. ((C.W.V. Hogue)). Dept. of Biochemistry, University of Ottawa. 451 Smyth Rd., K1H 8M5. Institute for Biological Sciences, National Research Council, Bldg. M54 Montreal Rd. Ottawa, Ont. Canada. K1A 0R6.

Studies of chaperonin-mediated protein folding suggest the DnaK family (Hsp70) of proteins bind to emerging polypeptides prior to folding, preferring ß-strands containing hydrophobic residues. Polypeptide "emergence" occurs during initial protein synthesis or after facilitated transport across membranes. Kinetic models of polymer growth provide for the addition of randomly-oriented monomers to one end of the polymer, allowing only those monomers which are not excluded by the volume of the existing polymer coil. Some question have arisen as to whether this is representative of a true random coil. Nevertheless, the kinetic model is a more precise description of the emerging polypeptide chain and its natural bias. In this work, the secondary structure of kinetic, self-avoiding, off-lattice, random walk polyalanine structures was examined. Structures were searched for simple secondary elements, e.g. turns or ß-strands using a 5-mer window. For the small structures (< = 25mers), extended polypeptides have more ß-strand segments, while compact ones have more turns, as expected. However for larger structures, (> 30mers) a constant amount of ß-strand (25% of monomers) and turns (17% of monomers) arises. This is independent of the radius of gyration; i.e. a more compact polyalanine in this simulation has the same proportions of secondary structure as an extended one. However these structures do not approach the high degree of compactness as achieved using boundary conditions (Gregoret and Cohen, 1991 J. Mol. Biol., 219:109-122.). Some of the ß-strand secondary structure is observed to arise when the kinetic walk "follows" along an existing straight segment. This process results in a considerable skewing of size distribution towards compactness. This simulation suggests that the preferential formation of these ß-strands in larger emerging polypeptides is due to the excluded-volume effect.

Th-Pos209

ZINC FINGER IDENTIFICATION IN GIARDIA LAMBLIA BY EXAFS

((J. Wu, Y. Lu, E. Scheuring, L.M. Miller, A. Xie, T.E. Nash,[#] M.R. Chance)) *Albert Einstein College of Medicine, Bronx, NY, [#]National Institutes of Health, Bethesda, MD.* (Sponsored by Gene A. Morrill)

Giardia lamblia (Giardia) is a parasite of humans and other mammals and one of the most common disease-causing protozoans worldwide. Giardia undergoes surface antigenic variation by variant-specific surface proteins (VSPs). VSPs cover the entire surface of Giardia, are rich in cysteines, and bind heavy metals, particularly zinc. To determine the quantities of zinc in Giardia, we performed x-ray microanalysis of Giardia whole cell samples. The concentrations of elements in Giardia with x-ray fluorescent emission energies ≥ 1000 eV are exhibited directly. The zinc concentration was estimated to be 0.5 mM (over 2 x iron). Subsequently, we collected EXAFS data on the Giardia preparation to analyze the ligands around zinc. It was a surprise to see the data adequately fit with a zinc sulfide model (average Zn-S distance of 2.352 ± 0.005 Å, and coordination number of 3.72-4.36). However, the best results were obtained with a two atom fit (ZnS and zinc tetraphenyl porphyrin (ZnTPP), 4S/0.5N). Those results are consistent with the bulk of zinc in Giardia coordinated to cysteinyl sulfurs in the VSPs while a small but expected fraction of zinc enzymes (typically with histidine and/or water coordination) contributes to the spectrum.

Th-Pos210

FUNCTIONAL LINEARITY OF PARAMETERS FOR EQUILIBRIUM ANALYTICAL ULTRACENTRIFUGE MODELS FROM EMPIRICAL DETERMINATION OF CONFIDENCE LIMITS. ((Ian Brooks*, Winnie Chan*, Ronald Wetzel*, Donald G. Watts+, K. Karl Soneson[#] and Preston Hensley*)) *Department of Macromolecular Sciences, SmithKline Beecham, King of Prussia, PA 19406-0939, +Department of Mathematics and Statistics, Queens University, Kingston, Ontario, Canada, K7L 3N6, #Exton, PA 19341-1730.

Equilibrium analytical ultracentrifugation is a powerful thermodynamic approach for the characterization of macromolecular assembly processes. The analysis of data in terms of subtly different models using nonlinear least squares approaches, is usually difficult, however. An important step in such analyses, is the determination of parameter confidence intervals. In contrast to linear models where these intervals may be computed directly, the confidence intervals for non-linear models must be determined empirically. Here we discuss one such approach called profile analysis. In this analysis, the conditional sum of squares is determined as each parameter is varied around its estimated best fit value. The calculations are continued until enough information is obtained to define the 99% likelihood interval upper and lower end points and parameter joint likelihood regions for all pairs of parameters. These are plotted in profile trace plots. These are convenient tools for quickly visualizing parameter correlation, parameter linearity and exact likelihood regions. As such, the plots are qualitatively and quantitatively useful in evaluation of parameter estimates. Here, we present an application of this approach in a mutational analysis of subunit interactions in the VL domain of a Bence-Jones protein, REI. The results of the computational analysis show that parameters in the various assembly models are often functionally linear. The results of this mutational analysis may have implications for the mechanism of plaque formation in certain forms of light chain amyloidosis.

Th-Pos211

PSEUDODIHEDRALS: SIMPLIFIED BACKBONE REPRESENTATION WITH KNOWLEDGE BASED ENERGY. ((R.S. DeWitte and E.I. Shakhnovich)) Chemistry Department, Harvard University, Cambridge MA. 02138.

Pair-wise contact energies[1] do not explicitly take protein secondary structure into account , and so provide an incomplete description of conformational energy. In order to construct a Hamiltonian that specifically relates to protein backbone conformations, a simplified backbone angle is introduced. The *pseudodihedral* angle (the torsion angle between planes defined by four consecutive alpha carbon atoms) provides a simplified backbone representation and continues to manifest information about secondary structure elements: the *pseudoramachandran plot* contains helical and sheet-like regions. The distribution of *pseudodihedral* angles is highly sensitive to the identity of the central pair of amino acids. Therefore, a sequence-dependent, knowledge-based potential energy was found according to the Boltzman Trick[2]. These functions form complementary additions to the contact potentials currently in use.

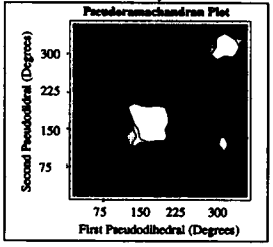

1. For example Miyazawa, S. and Jernigan, R.L., *Macromolecules*, (1985) 18 534-552.
2. Sippl, M.J., *J. Mol. Biol.* (1990) 213 859-883.

Th-Pos212

MEASUREMENTS OF SOLUBILITIES OF SICKLE HEMOGLOBIN IN SMALL SAMPLE VOLUMES ((Dan Liao and Frank A. Ferrone)) Department of Physics and Atmospheric Science, *Drexel University,* Philadelphia, PA 19104

Recently we have shown that modulated excitation can be used to observe the rate of the first ligand binding to Hb solutions which contain only a trace (1%) of CO.[1] The rate depends on the concentration of hemoglobin, so that an increase in Hb concentration can be monitored by observing the phase angle of the modulated signal. We have used this idea, in conjunction with a method for increasing the concentration of samples, to determine the solubility of HbS in volumes of a few µl. Samples are concentrated by placing them between a thin, oxygen permeable membrane of the type used in Gill cells for automated oxygenation measurements and a glass window, and passing dry N_2:CO gas over the membrane. The modulated excitation beam is scattered by the gel that is formed, and this then gives the concentration at which gelation has occured.

1. D. Liao, J. Jiang, M. Zhao and F. A. Ferrone (1993) Biophys. J. *in press*

Th-Pos213

DESCRIPTION OF KINETIC PROCESSES AND STRUCTURAL PROPERTIES OF BIOPOLYMERS USING TIME DEPENDENT LIGHT SCATTERING ((Wayne F. Reed)) Physics, Dept., Tulane University, New Orleans, La. 70118

When traditional static light scattering is adapted to an instrument capable of making simultaneous, multi-angle measurements at regular time intervals, a wealth of data can be obtained from which descriptions of both kinetic processes and structural properties of polymers can be made. Kinetic processes include aggregation, gelification, depolymerization and slow changes in conformation. For certain cases, such as random scission or uniform cleavage of mass units, exact rate constants can be found. Structural information that can be deduced includes whether the molecule is a single, double, or higher associated strand, and what types of conformational changes take place in the kinetic process. Examples are shown for such molecules as DNA, hyaluronate, proteoglycan sub-units; guar and xanthan. Supported by NSF MCB 9116605.

Th-Pos214

PHOTOPHYSICS OF 7-AZATRYPTOPHAN: EVIDENCE FOR AN EXCITED STATE REACTION. ((John D. Brennan[1] and Arthur G. Szabo[1,2*])) [1]Department of Biochemistry, University of Ottawa, Ottawa, Ontario, Canada, [2]Institute for Biological Sciences, National Research Council of Canada, Ottawa, Ontario, Canada, K1A 0R6

7-azatryptophan (7AW) is a non-natural amino acid which may be used as an intrinsic probe of protein structure and function [Négrerie *et al.*, *J. Phys. Chem.*, 95 (1991) 8663]. The interpretation of fluorescence signals from proteins and their relationship to protein structure requires that the photophysics of the intrinsic probes be fully understood. This has prompted a number of investigations of the excited-state behaviour of 7AW and its substituent chromophore 7-azaindole (7AI) over the past few years [Chen *et al.*, *J. Phys. Chem.*, 97 (1993) 1770]. There appears to be some confusion in the literature regarding the mechanism of the fluorescence decay of 7AW and the origin of the changes in decay kinetics as a function of wavelength. In another work from this lab [Houge and Szabo, *Biophys. Chem.*, (1993) in press] 7AW in a protein was shown to have a very long decay time, on the order of 10 ns. In the present study, the fluorescence spectra, intensity and decay behaviour, as well as the excitation and emission anisotropy of 7AW and 7AI were investigated. The effect of parameters such as pH, temperature, hydrogen bonding capacity of the solvent and deuteration of the solvent were examined to gain a more complete understanding of the photophysics of 7AW and 7AI. These studies revealed several interesting results which have not been reported previously. There is a clear observation that 7AI and 7AW both show a double exponential decay wherein the pre-exponential term of the shorter decay component becomes negative at wavelengths above 420 nm in H_2O, or 440 nm in D_2O. This result suggests that proton transfer occurs between the excited 7AW and water, and that this interaction significantly reduces both the fluorescence lifetime and intensity of 7AW. Decreases in solvent polarity (moving from water to alcohols to hydrophobic solvents) resulted in increases in both fluorescence intensity and lifetime. These results provide a basis for the rationalization of 7AW fluorescence data from proteins.

Th-Pos215

A CRYOGENIC CAPILLARY ELECTROPHORESIS INSTRUMENT FOR DIRECT MEASUREMENT OF POPULATIONS IN PROTEIN FOLDING/UNFOLDING TRANSITIONS.

((Vincent J. Hilser and Ernesto Freire)) Department of Biology and Biocalorimetry Center, The Johns Hopkins University, Baltimore, Maryland 21218.

A cryogenic capillary electrophoresis instrument has been developed from a commercially available instrument produced by BIORAD (BioFocus^{TM} 3000). The capillary is cooled by 100% ethanol and liquid nitrogen and is capable of maintaining a capillary temperature of < -45°C. Sample temperature is maintained with cold nitrogen gas introduced into the sample chamber and uncoated fused silica capillaries are assembled according to a modified version of the procedure provided by the manufacturer. The capability of directly measuring the populations of species present in a protein solution undergoing isomerization is investigated. A theoretical formalism using a probabilistic model is developed to provide initial estimates of the behavior of an isomerizing species. In principle, this system allows for a direct measurement of the individual population of states after thermal quenching of an experimental solution. The "frozen" equilibrium distribution from the experimental conditions can then be quantified. This type of experimental protocol provides a unique advantage over measuring a time averaged or ensemble averaged property of a solution, as no assumptions concerning the contributions of different species to an overall macroscopic property are necessary.

(Supported by NIH grants RR-04328, GM-37911, and NS-24520)

Th-Pos216

CAPILLARY ELECTROPHORESIS: A SENSITIVE TOOL FOR THE STUDY OF ISOMERIZING AND ASSOCIATING SYSTEMS.

((Vincent J. Hilser)) Department of Biology and Biocalorimetry Center, The Johns Hopkins University, Baltimore, Maryland 21218.

The spatial distribution for isomerizing species in an electrophoretic field can be defined by means of a probabilistic formalism (Mitchell, R.M. (1976) *Biopolymers* 15, 1717-1739). Here this probabilistic formalism is combined with the principles of statistical thermodynamics and linkage analysis in order to describe the temperature and ligand induced changes in the spatial distribution of isomerizing molecules in capillary electrophoresis (CE). We demonstrate that it is possible to:

1) determine the transition energetics for a two-state reversible folding/unfolding process of a protein.
2) determine the binding constant and number of binding sites for a protein/ligand interaction.
3) predict the temperature at which optimum resolution between the wild type and a mutant protein, or a protein and its degradation products will occur.

A general theoretical development is presented, and the effects of various experimental parameters on the electrophoretic profile are demonstrated by means of computer simulations, using a program developed in our laboratory (PROCZE). The assumptions and practical considerations of applying this approach to real experimental situations are also discussed.

(Supported by NIH grants RR-04328, GM-37911, and NS-24520)

Th-Pos217

AN INFRARED LASER DRIVEN ADIABATIC MICROCALORIMETER FOR THE STUDY OF STRUCTURAL TRANSITIONS IN MACROMOLECULAR SYSTEMS.

((Craig R. Johnson and Ernesto Freire)) Department of Biology and Biocalorimetry Center, The Johns Hopkins University, Baltimore MD 21218.

The thermal unfolding of macromolecules is accompanied by the absorption of heat. The total heat evolved during a transition, when normalized by the macromolecular concentration is equal to the enthalpy change. Conventional calorimeters are designed to measure this quantity. The calorimeter presented in this paper has been designed to measure the time regime of the heat absorption process as well as its magnitude. For this purpose, the temperature change in a sample solution after an instantaneous heat pulse is measured continuously as a function of time. The heat pulse is generated by an infrared laser on one side of the reaction cell and the temperature change is measured on the opossite side. The magnitude of the temperature pulses can be varied by adjusting the laser power, normally in the range of 0.01 - 0.1°C. Usually, a sequence of pulses is performed over a period of time and the data analyzed in fourier space. The small amplitude of the temperature jumps allows extensive coverage of the transition region of a protein or other macromolecule. (Supported by grants from the NIH RR-04328 and GM-37911)

Th-Pos218

INHOMOGENEITIES IN THE AGAROSE GEL MATRIX. **((N.C. Stellwagen and J. Stellwagen)) Department of Biochemistry, University of Iowa, Iowa City, IA 52242.**

Agarose gels are intrinsically birefringent; i.e., they rotate the plane of incident light. However, the sign of the intrinsic birefringence and its absolute amplitude vary randomly from one gel to another, and from one location within a gel to another, suggesting that the internal structure of the matrix is variable. The birefringence signals resulting from the orientation of agarose gels in low voltage electric fields, ranging from 1-15 V/cm, are also variable. The signs and amplitudes of the electric birefringence signals vary randomly from one gel to another, and at various locations within a single gel. If large numbers of observations are averaged together, the average absolute values of the intrinsic birefringence and the electric birefringence increase approximately linearly with agarose gel concentration. Supported in part by GM29690.

Th-Pos219

THEORETICAL AND EXPERIMENTAL STUDIES OF REPULSIVE INTERACTIONS IN 3-DIMENSIONAL MACROMOLECULAR SUSPENSIONS. ((V.A.Parsegian[1], D.C.Rau[1], J.A.Cohen[2])) [1]NIDDK & DCRT/NIH, Bethesda, MD, [2]Univ.Pacific, San Francisco, CA 94115

Interactions among macromolecules are of great biological importance, particularly in crowded intracellular environments. Yet, to date there has been no way to measure such forces in 3-dimensional suspensions, and a theoretical understanding of the energetics and 3-D organization has been lacking. As a prototype for both theory and experiment we use 0.1 μm charged latex spheres that form ordered arrays by mutual electrostatic repulsions. Our theory uses the Wigner-Seitz (WS) cell approximation, in which each unit cell of the crystalline array is an electrically neutral sphere containing the latex particle and its complement of counterions. We have developed an analytic solution equivalent to the nonlinear Poisson-Boltzmann equation, that is valid in the vicinity of the WS cell surface. This is accomplished by a superposition of two electrostatic potentials, one due to the central latex sphere and the other due to a hypothetical charged shell located just outside the WS sphere. The sum of these two potentials produces a net zero electric field on the WS cell surface. The shell charge represents the entire remaining crystal (macroions plus screening counterions) acting on the central macroion. This scheme gives analytic expressions for: (1) osmotic stress on the WS cell wall; (2) work of displacement and rms displacement of the central sphere from its equilibrium site in the WS cell; and (3) rms volume fluctuation of the WS cell itself. These analytic expressions can be compared to osmotic pressures directly measured as a function of latex-sphere concentration.

Th-Pos220

A NOVEL ACOUSTICAL APPROACH TO BIOLOGICAL THERMODYNAMICS.

((A. Sarvazyan*, T. Chalikian, and K.J. Breslauer)) Department of Chemistry, Rutgers, The State University of New Jersey, New Brunswick, NJ 08903. ((T. Funck)) Max-Planck-Institute for Biophysical Chemistry, Goettingen, FRG. *permanent address: Institute of Theoretical and Experimental Biophysics, Russian Academy of Sciences, Pushchino, Russia.

This talk will describe a novel approach which employs acoustical measurements for determining energetics of biologically relevant molecules and their interactions with small ligands (e.g., drug-biopolymer interactions). The principal thermodynamic quantites which describe biomolecular structures and interactions (ΔG^*, ΔH^*, ΔS^*, ΔCp) traditionally have been obtained indirectly by measuring the temperature dependence of some equilibrium property. A more direct approach for obtaining the relevant thermodynamic data is based on calorimetric techniques. Significantly, these thermodynamic parameters also can be derived by measuring the speed of sound, U, over a range of pressures and temperatures, since U is a function of the second derivative of the free energy over pressure. Preliminary results will be presented which illustrate how acoustic measurements allow for a thermodynamic characterization of model biomolecular systems. Advantages and complementary features of the acoustical versus calorimeric approaches for obtaining the requisite thermodynamic data will be discussed.

FOLDING AND SELF-ASSEMBLY V: (OTHER)

Th-Pos221

SPECTROSCOPIC AND ELECTROCHEMICAL PROPERTIES OF SYNTHETIC MULTIHEME PROTEINS.

((R.S. Farid, D.E. Robertson, C.C. Moser, R. Pidikiti, W.F. DeGrado, P.L. Dutton)) The Johnson Research Foundation, Department of Biochemistry and Biophysics, University of Pennsylvania, Philadelphia, PA 19104.

A series of water soluble peptides containing two parallel α-helices linked by N-terminal disulfide bonds have been synthesized that, as designed, accommodate one or two *bis*-histidine ligated heme groups (Hm-10, Hm-24). The di-α-helical peptides assemble into four-helix dimers with two or four parallel hemes (Hm-10, Hm-10', Hm-24, Hm-24') closely resembling native hemes in their distinct binding, and spectral and electrochemical properties. In all the heme-peptides studied, the α-band maxima of the reduced minus oxidized forms of Hm-10,10' and Hm-24,24' are 558.3 nm and 559.8 nm, respectively. The hemes at positions 10 and 10' are tightly bound while Hm-24 and Hm-24' are less tightly bound: K_D(Hm-10) = <0.05μM, Hm-10' = 0.8μM, Hm-24 = 0.8μM, and Hm-24' = 20μM. The electrochemical redox potentials of Hm-24, Hm-10, Hm-24', and Hm-10' are -80±5, -115±15, -190±10, and -220±10 mV vs. SHE, respectively. The binding and electrochemical properties of these multiheme proteins are consistent with primary sequence asymmetry (Arg at positions-27,27' near Hm-24,24') and heme-heme interactions (Hm-10 interacting with Hm-10' and Hm-24 with Hm-24') and are the bases for the protein structure depicted here. These properties will be exploited in electron-transfer studies aimed at elucidating the effect of protein medium on controlling all aspects of biological electron transport. (Supported by PHS GM27309)

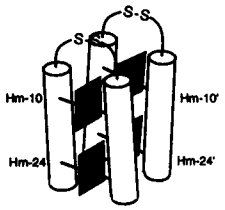

Th-Pos222

STRUCTURE AND FOLDING OF CELLULAR RETINOIC ACID BINDING PROTEIN, A PREDOMINANTLY β-SHEET PROTEIN.

((J. Rizo, Z.-P. Liu and L. M. Gierasch)) University of Texas Southwestern Medical Center, Dallas, TX 75235-9041.

Cellular retinoic acid-binding protein (CRABP) is a member of a family of β-clam proteins that bind hydrophobic ligands. To study the mechanism of ligand binding by CRABP, and understand its specificity, we are analyzing the structure and dynamics of the protein in solution using multidimensional nuclear magnetic resonance (NMR) techniques. We have completed the sequential assignment and determined the secondary structure of CRABP with and without bound retinoic acid. The NMR data indicate the presence of two 5-stranded β-sheets arranged perpendicularly, and of an N-terminal helix-turn-helix motif (residues 16-35). This architecture is analogous to that found in the crystal structures of other β-clam proteins [Jones et al. (1988) EMBO J. 7, 1597]. The distinct flexibility observed at the C-terminus of the second helix in apo-CRABP, compared to that in the holo-form, suggests that this region may serve as a hinge to allow ligand binding. We are also exploring the folding mechanism of CRABP using folding/H-D exchange competition experiments. These experiments reveal that about forty amide protons are protected early in the folding pathway, including residues of the first helix and of the C-terminus of the protein. Possible implications of the observed protection patterns for the folding mechanism of CRABP will be discussed. (Supported by NIH grant GM27616)

Th-Pos223

FAST EVENTS IN PROTEIN FOLDING: LASER T-JUMP / TIME-RESOLVED INFRARED STUDY OF THE RIBONUCLEASE *A* S-PEPTIDE

((W. H. Woodruff, R. B. Dyer, R. H. Callender, K. Paige, and T. Causgrove)) INC-14 and CLS-4, Mail Stop C-345, Los Alamos National Laboratory, NM 87545, and Dept. of Physics, City College of CUNY, NY 10031

Vibrational (Infrared and Raman) spectra are sensitive to many aspects of protein secondary and tertiary structure. Inasmuch as these spectroscopies respond to dynamics as fast as the vibrational period of a chemical bond, they have great potential for observing with structural specificity the fast events in protein folding/unfolding. In this study we employ near-IR pulsed excitation of water overtone absorbances (ν ca. 5000 cm^{-1}) to effect a temperature jump from 7°C to 37°C in 10 ns, in a solution 1 mM in the S-peptide fragment of Rnase *A*. The subsequent unfolding and refolding reactions are monitored in the mid-IR (e.g. amide I and II absorbances, ν 1400 - 1700 cm^{-1}) with instrumental time resolution of 100 ns. Results on the 10^{-7} to 10^{-3} second timescale are presented. In the amide I region we observe bleaching of the helix absorbance within the response time of the instrument, and on the same timescale positive absorption difference features characteristic of unfolded polypeptide structure appear. These transient differences return to baseline with halflives (1-2 ms) that are not the same as the relaxation halflife of the temperature jump (4 ms). Additionally, the halflives for refolding of the "random" structure(s) differ, depending upon the particular identity of the unfolded amide structure as reflected by the infrared frequencies. Differences are also seen in carboxylate and amide II absorbances. Prospects for extending the short-timescale limit of these experiments to 10^{-10} seconds will be discussed.

Th-Pos224

FAST EVENTS IN PROTEIN FOLDING INITIATED BY NANOSECOND LASER PHOTOLYSIS.

((C. M. Jones, E. R. Henry, Y. Hu, C.-K. Chan, S. D. Luck*, A. Bhuyan*, H. Roder*, J. Hofrichter and W. A. Eaton)) Laboratory of Chemical Physics, NIDDK, NIH, Bethesda, MD 20892; *Institute for Cancer Research, Fox Chase Center, Philadelphia, PA 19111.

A dramatic improvement in time resolution in kinetic studies of protein folding can be obtained by initiation with an optical trigger. We have used nanosecond photodissociation of the heme-CO complex to initiate the folding of reduced cytochrome *c*. Our optical trigger is based on the observation that under destabilizing conditions cytochrome *c* can be unfolded by preferential binding of CO to the covalently attached heme group in the unfolded state. Photodissociation of the CO thus triggers the folding reaction. Ligation events at the heme were monitored by time resolved absorption spectroscopy in the Soret region using a high precision nanosecond spectrometer. Following photodissociation of the CO there is a competition among transient binding of native and non-native ligands from the unfolded polypeptide chain, CO rebinding, and protein folding. Although rebinding of CO prevents the complete formation of the native conformation, the rapid recovery of the sample permits repetitive photolysis and therefore the acquisition of high signal-to-noise transient spectra for investigating submillisecond events. Kinetic modelling suggests that methionines 65 and 80 bind to the heme faster than histidines 26 and 33, even though the histidines are closer to the heme (which is covalently linked to the polypeptide at positions 14, 17, and 18).

Th-Pos225

PICOSECOND TEMPERATURE JUMP IN AQUEOUS PROTEIN SOLUTIONS

((C.M. Phillips, Y. Mizutani and R.M. Hochstrasser)) Department of Chemistry and Regional Laser and Biotechnology Laboratories, University of Pennsylvania; Philadelphia, PA 19104-6323

A novel, ultrafast temperature jump method for water solutions has been developed. A Nd:YAG laser based temperature jump apparatus which pumps an absorbing dye in aqueous solution has been utilized to create bulk solution T-rises in water on a 20 ps timescale. Our recent work with this technique suggest that it is a viable means of initiating protein dynamics. In addition, we have devised a sensitive thermometer for measuring the temperature change in the excited volume by means of transient IR spectroscopy (1): temperature changes induce known shifts in the water IR absorption spectrum. In other infrared regions the vibrations of the protein backbone or side chains can be observed. We are investigating the response of non-chromophore containing proteins to this ultrafast temperature rise and probing the spectral dynamics associated with conformational changes occuring on the ps to longer (ca. ms) time scales.

1. B. Locke, R. Diller and R.M. Hochstrasser, "Ultrafast Infrared Spectroscopy and Protein Dynamics", in *Biomolecular Spectroscopy: Part B*, eds. R.J.H. Clark and R.E. Hester (Wiley and Sons, New York, 1993) p. 1.

Th-Pos226

PROTEIN HYDRATION AND GLASS TRANSITION BEHAVIOR - CLUES TO THE PROTEIN FOLDING PROBLEM.

((R. B. Gregory)) Dept. of Chemistry, Kent State University, Kent Ohio 44242

Many proteins appear to be constructed from "functional domains" each consisting of a glassy, rigid "knot" embedded in a more mobile matrix. The existence of these dynamically distinct regions appears to be due to the fact that knot residues can pack very efficiently without compromising H-bond strength. In the knots, good packing and strong H-bonds are cooperatively enhanced. In matrices one tends to be sacrificed for the other. Knots have low mobilities, little or no free volume and are impermeable to water. Knot residues represent about 10-15 % of the protein and can be identified from their unusually slow proton exchange rates and low B-factors. The knot and matrix regions are characterized by different glass transition temperatures (T_g). As hydration (plasticizer content) is increased, T_g decreases. The dynamical transition observed at low hydrations (0.1 g water/g protein) at 300 K and that observed at 180 - 220 K in fully hydrated proteins thus represent a common, hydration dependent, glass transition. However, only the matrices undergo this transition. The knots remain glassy. Only on denaturation do the knots become flexible. The initial "hydrophobic collapse" of the polypeptide chain leads to a compact, but highly flexible state with no glassy regions. However, formation of the knots selects the native fold from the conformations of the compact state.

(Supported by Army Research Office grant DAAL 03-90-G-0061)

Th-Pos227

TIME VS. TEMPERATURE, KINETICS VS. THERMODYNAMICS: USING SIMPLE MODELS TO EXPLORE THE PROTEIN FOLDING PROBLEM.

((N.D. Socci and J.N. Onuchic)) Department of Physics, University of California at San Diego, La Jolla CA 92093-0319.

A detailed analysis of simple protein-like models is carried out to study several interesting aspects of the folding problem. The relationship between kinetics and thermodynamics and their respective roles in folding are explored. In particular various thermodynamic and kinetic quantities are given a precise definition and are determined in these simple models. For example the folding time (τ_f) and folding temperature (T_f) are calculated. τ_f is observed to be a non-trivial function of the temperature. We find there are two critical temperatures (T_i and T_g, $T_g < T_i$) at which the folding time changes by several orders of magnitude. The properties of the various sequences are examined to reveal which factors are important in determining whether a given sequence will fold or not. Specifically, the ways in which T_f and τ_f depend on the various sequence characteristics is investigated. From these results we conclude that an important factor in minimizing folding time is to reduce the number of energetically strong but non-native bonds made during the folding process.

* Supported by the Arnold and Mabel Beckman Foundation and the NSF (Grant# MCB9018768).

Th-Pos228

RAPID CALCULATION OF SOLVENT ACCESSIBLE AREA DERIVATIVES FOR COMPUTATION OF SURFACE FORCES.

((S. Sridharan[1], K. A. Sharp[2]))[1]Dept. of Biochemistry and Molecular Biophysics, Columbia University, [2]Dept. of Biochemistry, Univ of Pennsylvania.

Solvation models in which the energy is proportional to the solvent accessible area of the exposed atoms are increasingly being used in protein and nucleic acid modelling. To incorporate these solvation forces into molecular mechanics or dynamics requires the derivative of the solvant accessible area with respect to each atom position. We report a simple, approximate but rapid and accurate algorithm for the calculation of these derivatives: Two isolated atoms of radii a and b, whose solvent accessible surfaces (SAS) have radii A=a+c, B=b+c, where c is the solvent radius, will experience an interfacial force directed along the line joining the centers of the atoms when they are close enough that their SAS's intersect, i.e when their separation $d < A+B$. The magnitude of the force is given by $f = \pi\gamma((A-B)(A^2-B^2)+d^2(A+B))/d^2$ where γ is the surface free energy. This force is in essence generated at the circle of intersection of the two SAS's, the point at which any new area is buried upon movement of the atoms. Thus the force between the same two atoms as part of a macromolecule is given by f.p, where p is the fraction of the circle of intersection that is not contained within any other atom's SAS. The total force on an atom is the vectorial sum of the forces generated by each circle of intersection it makes. The algorithm represents the circle of intersection by a number of discrete points (n<50), which are checked for inclusion in any SAS and eliminated. p is given by the fraction of surviving points.

Th-Pos229

IDENTIFICATION AND CHARACTERIZATION OF A Ca^{2+}-INDUCED HYDROPHOBIC SITE IN CALSEQUESTRIN

((Z. He, C.A.R. Wesson, A.K. Dunker‡ & W.R. Trumble)) Dept. of Micro., Mol. Biol., & Biochem., University of Idaho, Moscow, ID 83844; Dept. of Biochem./Biophys., Washington State University., Pullman, WA 99164‡.

Calsequestrin (CSQ) is a low affinity, high capacity Ca^{2+}-binding protein found in the lumen of the terminal cisternae of the sarcoplasmic reticulum. Upon Ca^{2+} binding, CSQ folds into a more compact structure. Our previous studies demonstrated that this Ca^{2+}-induced folding is a prerequisite for subsequent CSQ aggregation, which in turn underlies the high capacity Ca^{2+} binding. Here we report studies characterizing the compact form of CSQ using a fluorescent hydrophobic probe, 8-anilino-1-naphthalene sulfonate (ANS). When associated with "unfolded" CSQ in 100mM K^+, ANS fluoresces with a blue shift and more intensity than when in buffer alone. Folding of CSQ by 1mM Ca^{2+} or 500mM K^+ leads to a further blue shift and a 5-fold increase in intensity compared to the fluorescence of ANS associated with CSQ in 100mM K^+. This suggests that the Ca^{2+}-induced folding of CSQ into the compact form is accompanied by the formation of a hydrophobic site capable of binding ANS. CSQ folded by either Ca^{2+} or K^+ exhibits a single ANS binding site with a dissociation constant near 55μM. Quenching studies suggest that this hydrophobic site is not a deep pocket, but might be similar to the nonrigidly packed hydrophobic clusters found in protein folding intermediates. This newly discovered hydrophobic binding site in folded CSQ might have physiological significance, such as binding to specific receptors in order to anchor CSQ to the terminal cisternae or playing a role in Ca^{2+}-induced CSQ aggregation.

Th-Pos230

SELF-ASSOCIATION AND MEMBRANE BINDING OF SPIN-LABELED CECROPIN AD

((Hassane S. Mchaourab, James S. Hyde, and Jimmy B. Feix)) Biophysics Research Inst., Medical College of Wisconsin, Milwaukee, WI 53226.

The cecropins are a class of antibacterial peptides found in numerous insect species. Their antibiotic activity has been associated with the ability to induce membrane damage, most likely through voltage-dependent ion channel formation. We have prepared a spin labeled derivative of the chimeric peptide, cecropin AD (CAD), modified to contain a single cysteine residue, and used EPR spectroscopy to characterize its folding behavior in helix-promoting solvent (hexafluoropropanol, HFP) and binding to model membranes. Upon addition of from 5 to 13% (v/v) HFP, spin-labeled CAD undergoes structural transitions from random coil to folded aggregate to folded monomer. The aggregate is more stable at 30° C than at 2° C, indicating an entropy-driven process; and pH titration suggests ion-pair formation involving a glutamate plays a role in stabilizing peptide self-association. Addition of spin-labeled CAD to liposomes containing negatively-charged lipids results in membrane binding, with insertion of the C-terminal helical domain into the lipid bilayer. No binding is observed with neutral bilayers, and salt titration confirms that membrane association is primarily electrostatic. Surprisingly, there is a strong dependence on membrane thickness, with binding affinity decreasing in the order DLPG > DMPG > DPPG-POPG. Binding appears to be cooperative in POPC/POPG bilayers, but no evidence for cooperativity is observed with DLPC/DLPG bilayers.

Th-Pos231

THE ROLE OF SPINODAL DEMIXING IN THE SELF-ASSEMBLY OF BOVINE SERUM ALBUMIN.

((D. Bulone, P.L. San Biagio, A. Emanuele, M.B. Palma-Vittorelli and M.U. Palma)) CNR Institute for Interdisciplinary Applications of Physics and Dept. of Physics, University of Palermo, Via Archirafi 36, I-90123 Palermo, Italy.

The present work addresses two problems: i) a philosophical one, concerning the possibility for the topological phase transition of physical gelation to occur in initially homogeneous biopolymeric solutions at concentrations remarkably lower than those predicted by random percolation theory and ii) a specific one, concerning the actual (and hitherto scarcely known) sequence of steps leading to BSA gelation. In all cases previously studied, physical gelation at very low polymer concentrations has been shown to require a preliminary symmetry-breaking step which consists in the demixing (either permanent or sufficiently long lived) of the sol as such. In the present work redundant experimental evidence shows the following time-resolved pathway for BSA gelation from aqueous solution, at concentrations below about 3% w/v: i) protein unfolding and consequent change of protein-solvent interaction (as a consequence of unfolding the solution finds itself in its region of thermodynamic instability, inaccessible in the native BSA case); ii) consequent spinodal demixing as shown by specific "signatures" such as Cahn plot, exponential growth, peaked structure function and anomalous viscoelastic behavior; iii) subsequent gelation in those regions where BSA molecules have clustered as a consequence of the symmetry-breaking process of spinodal demixing. The present experiments strongly endorse the conclusion that a symmetry break in the sol, generating protein-rich regions so as to "channel" crosslinking and percolation, is necessary for gelation at concentrations well below the random percolation threshold.

Th-Pos232

MEASUREMENT OF SICKLE HEMOGLOBIN NUCLEATION RATES BY STOCHASTIC FLUCTIUATIONS ((Zhiqui Cao and Frank A. Ferrone)), Department of Physics and Atmospheric Science, *Drexel University*, Philadelphia, PA 19104

The polymerization of sickle hemoglobin occurs by homogeneous nucleation (polymers form from monomers alone), and heterogeneous nucleation (nucleation onto pre-existing polymers). Heterogeneous nucleation creates polymer domains, and this amplification allows the homogeneous process to be observed. Since homogeneous nucleation is a molecular process, it is fundamentally stochastic, and the fluctuations in time of nucleation can be used to determine the rate of nucleation. [1,2] Previously, stochastic fluctuations have been measured in series.[1] We present a method to do this in parallel. A laser beam is broken into an array of 180 small spots by using a mesh in place of the field diaphragm in a microscope illumination system. These are focussed on a COHbS sample. Individual spots are approximately 4 μm radius, separated by 8 μm. The transmitted beam is blocked by a mask near the projective eyepiece around which scattering from the polymers can pass. This permits the stochastic method to be extended to timescales which are intractable if done in sequence.

1. J Hofrichter (1986) J. Mol. Biol. 189 553-571
2. A Szabo (1988) J. Mol. Biol. 199 539-544.

Th-Pos233

PROTEIN FOLDING STUDIED BY MODULATED EXCITATION OF CO-BOUND TO CYTOCHROME c ((Zhonglin Hu, Dan Liao, and Frank A. Ferrone)) Department of Physics and Atmospheric Science, *Drexel University*, Philadelphia, PA 19104

The heme in cytochrome c is typically liganded by protein residues at the proximal and distal side, but under denaturing conditions, the distal side is released and can bind CO. Thus the presence of CO will affect protein folding. CO can be released by laser photolysis, thereby acting as a rapid trigger for the folding transition, and this has been done by pulsed laser methods.[1,2] We have adapted modulated excitation to study this process. Modulated excitation is a perturbation method which replaces a flash of light with a continuously modulated beam. [3] The advantage of modulated excitation is that phase tuning can remove processes which may be dominant (such as ligand rebinding) but are of less interest than the processes they drive (such as protein folding.) Previously this method has been used to study allosteric change in hemoglobin.

1 W A Eaton, Abstracts of ACS meeting (Chicago, IL) 1993.
2 C M Jones, E R Henry, Y Hu, C-K Chan, A Bhuyan, H Roder, and W A Eaton, Proc. Nat Acad. Sci. USA (1993) in press
3 F A Ferrone (1991) Comments Mol. Cell. Biophys. 7 309-332.

Th-Pos234

FRAP INVESTIGATIONS ON MONTAL-MUELLER TYPE PLANAR LIPID BILAYERS. ((A. Mackie, L. Harvey, S. Ladha, D. Clark, M. Brullemans, E. Lea and H. Duclohier.)) URA 500 CNRS, Université de Rouen, 76821 Mont-Saint-Aignan (France), University of East Anglia and Institute of Food Research, Norwich, NR4 7UA (UK)

Fluorescence Recovery After Photobleaching has become an elegant way of measuring the lateral mobility of lipid and protein components of biological membranes. The lateral diffusion coefficient (D) and the degree of recovery reflect the velocity of the fluorescent probes in the plane of the membrane and the inhomogeneity of the latter. Despite earlier work (e.g. Fahey *et al.*, 1977, Science 195, 305-306) with lipid bilayers on electron microscopy grids, little efforts have been devoted with more "realistic" model membranes. The present work gives the first determinations of D on Montal-Mueller bilayers formed in a conventional manner amenable to simultaneous FRAP and conductance experiments. The lipids (POPC-DOPE, 7:3, w/w) incorporating the probe NBD-PE at 1% molar ratio were spread on top of KCl 1 M, HEPES 5 mM, pH 7.4 solutions. D for bare solvent-free lipid bilayers was in the order of $1 \cdot 10^{-7}$ $cm^2 \cdot s^{-1}$ (i.e. comparable to the values reported by Fahey *et al.*). Initial results with added cholesterol or alamethicin showed a small decrease of D. Applied voltages, especially negative ones, did slightly decrease the lateral mobility of the probe, consistent with a greater "orderliness" expected for an electrocompressed lipid bilayer.

[Supported by a Franco-British Alliance Program. M.B. acknowledges the N.S.E.R.C. (Canada) for a postdoctoral fellowship.]

Th-Pos235

ACTIN FILAMENTS AND NETWORKS: THEIR DYNAMICS, VISCOELASTICITY AND MODULATION BY TALIN AND VINCULIN. ((W.H. Goldmann, G. Isenberg and E. Sackmann)) TU Munich, Biophysics, D-85747 Garching. Germany. (Spon. by T. Feder)

High precision rheological measurements show in the regime reflecting internal chain dynamics (10^{-2} to 1 sec time domain) that filamentous actin behaves like a random-coil of the Rouse type. This contrasts with dynamic light scattering and correlation spectroscopic studies of actin filament flickering, indicating that filaments behave as semi-flexible rods. The internal chain dynamics determined by thermically stimulated bending undulations exhibit a persistence length of 0.3 - 1 μm. Evidence suggests that this discrepancy is due to a cross-over of semi-flexible rod behavior at excitation wave-lengths (Λ) below ~1 μm to random-coil behavior at $\Lambda \gg 1$ μm (expected at a frequency $\omega \sim 1$ Hz). The random coil behavior is largely determined by defects in actin filaments, leading to sharp bends of the chain, which act as hinges. Talin induces drastic effects on the time course of viscoelasticity during actin polymerization. It promotes the rapid formation of short filament fragments (~1 μm) which anneal slowly into long filaments, probably by fusion. The viscoelasticity depends on the coexistence of short and long filaments, causing a significant decrease in effective segment length and an increase in chain stiffness. Vinculin on the other hand shows no such effect.

Th-Pos236

MOLECULAR DYNAMICS STUDIES OF A DLPE MEMBRANE BILAYER AND PHOSPHOLIPASE A_2--DLPE MEMBRANE COMPLEX. ((F. Zhou and K. Schulten)) Beckman Institute, 405 N. Mathews, Urbana, IL61801

A 200 ps molecular dynamics simulation of a membrane bilayer consisting of 202 DLPE molecules and 8108 water molecules at 315 K was conducted with no cut-off of Coulomb interactions. Distribution functions of lipid groups, order parameters and other properties of the lipid bilayer were compared with experimental measurements. Water polarization profile, membrane dipole potential profile and susceptibility profile were calculated. The polarization of water was found to be determined mainly by the distribution of lipid head groups in the interfacial region. The calculated membrane dipole potential is mainly due to the ester groups linked to the glycerol backbone, while the contribution due to the PE head groups is almost completely cancelled by the contribution due to oriented water molecules. A cut-off for the Coulomb interaction increases the calculated membrane dipole potential by as much as 7 fold. The susceptibility is predicted to be around 30 for the head group--water interface and around 10 for the ester groups. The DLPE membrane was found to form stronger hydrogen bonds than the previously simulated POPC membrane. Long range correlation in the membrane surface charge densities was observed. Simulations were also carried out for the enzyme human synovial phospholipase A_2 on the DLPE membrane surface and in solution.

Th-Pos237

CHLORIDE DEPENDENT BOHR EFFECT IN HUMAN HEMOGLOBIN

Clara Fronticelli[1], Igor Pechik[2], William S. Brinigar[3], Irina Russu[4], and Gary L. Gilliland[2]. [1]Dept. Biochem., U.MD, Med. Sch., Baltimore, MD.; [2]Ctr. for Adv. Res. in Biotech., U.MD., Bethesda, MD.; [3]Dept. of Chem., Temple U., Philadelphia, PA.; [4]Dept. of Mol. Biol., Wesleyan U., Middletown, CT.

A mutant human hemoglobin, β(V1M+H2Δ), has been constructed in which β1Val was replaced by methionine and β2His was deleted. Preliminary H-NMR results suggest that the conformation of the heme pocket and the subunits interface in β(V1M+H2Δ) are similar to those of recombinant HbA. The crystal structure of the deoxy-β(V1M+H2Δ) has been determined at 2.2 Å. The results revealed differences localized to the N-termini of the β-chains. In β(V1M+H2Δ) a sulfate ion interacting with β1Val of natural hemoglobin (HbA) is replaced by two water molecules, and the N-terminal amino group of the β-chain is involved in an intrachain electrostatic interaction with β79Asp. A thermodynamic analysis indicates that at pH 8.5, in the absence of Bohr effect, the T state of β(V1M+H2Δ) is stabilized by 0.9 kcal with respect to HbA. In contrast to HbA the alkaline Bohr effect for β(V1M+H2Δ) is not modified by the addition of anions. The crystallographic and functional studies support the proposition that for HbA at physiological pH, the N-terminus of β1Val is essential for oxygen-linked chloride binding and that the observed Cl^- binding site at neutral pH is localized in the region of the β-chain N-terminus. Comparison of the thermodynamic analysis of the oxygen binding curves of HbA and β(V1M+H2Δ), indicates that in HbA the oxygen-linked Cl^- ions are released upon binding of the first oxygen molecule.

Th-Pos238

^{1}H NMR STUDY OF THE METCYANO COMPLEX OF SPERM WHALE MYOGLOBIN MUTANT H93G.

((S.M. Decatur[1], G.D. DePillis[1], D. Barrick[2], and S.G. Boxer[1])) [1]Department of Chemistry, Stanford University, Stanford, CA 94305 and [2]Institute for Molecular Biology, University of Oregon, Eugene, OR 97403.

In the sperm whale myoglobin mutant H93G(L), the proximal histidine has been replaced with glycine, leaving a cavity where a variety of proximal ligands (L) can be substituted. In the ^{1}H nmr spectrum of the paramagnetic complex H93G(L)CN, the pattern of hyperfine shifted resonances of the heme methyl groups contains information about the conformation adopted by the proximal ligand when unconstrained by covalent attachment to the protein. We have characterized the metcyano complex of H93G(Im) using 1D and 2D nmr techniques. The 1D ^{1}H nmr spectrum of H93G(Im)CN is quite different from that of the wild type protein, especially in the hyperfine shifted regions. We have assigned several protons of the heme and amino acids of the heme pocket, including the 1-Me, 8-Me and 5-Me groups of the heme. The pattern of these resonances, compared to that of wild type myoglobin, suggests that the imidazole adopts a conformation different from that of the histidyl imidazole of the native protein. Data will be presented for a variety of substituted imidazoles.

Th-Pos239

PROBING THE LIGAND BINDING PATHWAYS IN MYOGLOBIN BY RANDOM MUTAGENESIS STRATEGY

((Xiaohua Huang and Steven G. Boxer)) Department of Chemistry, Stanford University, Stanford, CA94305

A random library of single amino acid mutants of sperm whale myoglobin has been generated using a novel highly efficient random mutagenesis method in order to systematically probe the binding pathways of small diatomic ligands to myoglobin. The CO and O2 recombination kinetics of about two thousand of the mutants have been measured on ns to ms scale using a fully automated photolysis setup. A surprisingly large fraction (about 10%) of the library shows very large variations in recombination kinetics compared to the wild type. CO and O2 recombination kinetics of some of those mutants are shown in Figure 1 and Figure 2 respectively. Our results reveal that in addition to the traditional pathway (comprised primarily of residues 45, 64 and 68) single mutation of many residues far away from that pathway can profoundly affect the ligand binding kinetics, suggesting that there are many other possible ligand binding pathways. Detailed characterization of some of these pathways will be presented.

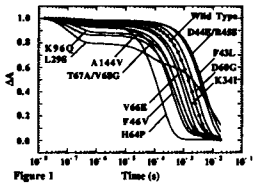

Figure 1

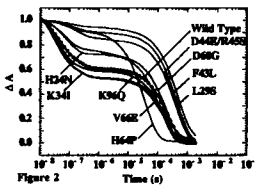

Figure 2

Th-Pos240

PROXIMAL LIGAND SUBSTITUTION IN SPERM WHALE MYOGLOBIN: EXCHANGE OF VARIOUS LIGANDS IN AND OUT OF THE CAVITY MUTANT H93G.

((G. D. DePillis[1], S. M. Decatur[1], D. Barrick[2], and S. G. Boxer[1])) [1]Department of Chemistry, Stanford University, Stanford, CA 94305 [2]Institute for Molecular Biology, University of Oregon, Eugene, OR 97403.

Expression of the sperm whale myoglobin (Mb) mutant H93G in imidazole-containing media yields a protein which is similar to WT Mb (1). We have discovered that the non-covalently attached proximal imidazole ligand can be replaced with other compounds by addition of a large excess of the desired ligand. Examples of ligands that have been subtituted into H93G(Im) by this procedure include methyl-substituted imidazoles, pyridine, furan, thiophene, phenol, ethanethiol, and thiazole. There are subtle changes in the absorption spectrum when pyridine and furan are exchanged for Im, but more dramatic changes are observed upon substitution with thiophene, ethanethiol, and phenol. On the other hand, *all* exchange mutants yield significantly altered CO recombination kinetics following flash photolysis. The figure dramatically demonstrates that exchange mutants display higher geminate yields and faster bimolecular CO recombination rates than WT or H93G(Im) Mb. The properties of the exchanged proteins will be discussed. (1) D. Barrick, Nature, submitted.

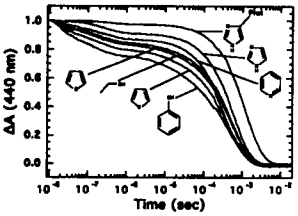

Th-Pos241

QUANTITATION OF INTRAMOLECULAR AGGREGATION AND ROTATIONAL MOBILITY OF DIPYRENYL LIPIDS WITH DIFFERENT CHAIN LENGTHS IN LIPID MEMBRANES

((K.H. Cheng, L.I. Liu, P. Somerharju and I.P. Sugar)) Texas Tech U., Lubbock, TX 79409, U. of Helsinki, Helsinki, Finland and Mount Sinai Med. Ctr., New York, NY 10029.

The state of intramolecular aggregation and rotational mobility of dipyrenyl lipids ($Dipy_nPC$ or $Dipy_nPE$) of different chain lengths (n =4 and 10) in lipid membranes have been investigated by the use nanosecond-resolved frequency-domain fluorescence intensity decay technique. Based on a classical 2-state and a new simplified 3-state model, the equilibrium constant of aggregation (K) and rotational rate (R) of the two intralipid pyrene moieties of $Dipy_nPC$ in DMPC/cholesterol and $Dipy_nPE$ in PE/PC binary mixtures were estimated from the frequency-domain data measured at the monomer (395 nm) and excimer (475 nm) emission channels. The values of K and R were sensitive to the temperature-induced gel-to-liquid crystalline phase transition of DMPC and composition-induced bilayer-to-nonbilayer transition of PE/PC mixtures. The responses of dipyrenyl lipids of short chain length (n=4) to the presence of cholesterol and the phase transitions are different from that of long chain length (n=10). Our results demonstrate the potential of using the intra-molecular excimer formation technique to separately probe the conformation and dynamics of the acyl chains at a defined depth of the lipid membranes.

Th-Pos242

ELECTROLYTE EFFECTS ON THE UV-PHOTOLYSIS OF THE OCULAR LENS PROTEIN, β-CRYSTALLIN.

((L.B. Hibbard, D. Ware, M. Tarver)) Spelman College, Atlanta, GA 30314

The effects of varying concentrations (0.0-1.0 M) of the electrolytes NaCl and $CaCl_2$ on the UV-photolysis of 1 mg/mL aqueous, buffered solutions of the bovine structural lens protein β-crystallin were studied. Protein samples were exposed to either 295 nm or 310 nm radiation from a 450-W xenon lamp with tryptophan (Trp) residue photolysis and microenvironment being monitored using steady state fluorescence and lifetime techniques. Fluorescence results showed that, though greater photolysis was evidenced at 295 nm, the presence of salt had a greater effect on photolysis of the 310 nm-exposed samples. Preliminary lifetime results, using a two component modelling system, indicated a substantial difference between the 295 nm and 310 nm irradiated samples with the longer lifetime components increasing for the 310 nm-exposed samples. The presence of salt appeared to have little effect on the Trp lifetimes of proteins irradiated at 295 nm but had a pronounced effect on the lifetimes of the samples irradiated at 310 nm, with the long lifetime component decreasing with increasing salt concentration.

Th-Pos243

APPLICATION OF HOMOTRANSFER TO CHARACTERIZE PROTEIN OLIGOMERIZATON. ((S. Scarlata and L. Runnels)) SUNY at Stony Brook, Dept. Physiol./Biophys., Stony Brook, NY 11794-8661

Traditionally, homotransfer is determined through depolarization. We measured the concentration dependence of fluorescence lifetime and anisotropy (exc. 490 nm, em. 523 nm) of several series of fluorescein samples: FITC in 80% glycerol, FITC in 100% glycerol, and fluorescein-labelled lipids in either multilayers or bilayers. Increasing fluorescein concentration produces a systematic decrease in anisotropy, that then rapidly increases as self-quenching becomes more prominent. The decrease in anisotropy can be attributed to an increasing probability of energy transfer as the separation distance between FITC molecules diminishes, with a concomitant increase in lifetime. Self-quenching dominates at higher FITC concentrations, as seen by a decreased lifetime and an increased polarization. We also examined the concentration dependence of lifetime and anisotropy with fluorescein-labelled phosphatidylethanolamine incorporated into DOPC vesicles. In these experiments, effects from rotational depolarization are far less pronounced and concentrational depolarization is more evident. We established that homotransfer between molecules can also be observed by a simple examination of excitation spectra. We observed a spectral shift of the lowest energy peak of over 1 kk with increasing FITC concentrations. The binding of 4 FITC to BSA shifted the spectra nearly 1.5 kk. This method is now being applied to monitor membrane protein oligomerization, and has been used to observe fluorescein-labelled HIV-peptide association at the surface of vesicle membranes.

Th-Pos244

KINETICS OF THE PRESSURE OSCILLATION-INDUCED LAMELLAR GEL/LAMELLAR LIQUID CRYSTALLINE TRANSITION IN HYDRATED DMPC USING TIME-RESOLVED X-RAY DIFFRACTION. ((Anchi Cheng and Martin Caffrey)) Dept. of Chemistry, The Ohio State University, Columbus, OH 43210.

We have developed an x-ray diffraction compatible pressure oscillation calorimeter and have used it to study the lamellar gel/lamellar liquid crystalline transition in 1,2-dimyristoyl-*sn*-glycero-3-phosphocholine (DMPC) / 60% (w/w) water. The position (2θ) of the lamellar (001) reflection was monitored as a measure of the degree of phase structural transformation in response to a pressure oscillation. The heat absorbed and released during the oscillation was monitored by recording the temperature change by means of a small thermistor positioned in the lipid sample. The structural and thermal response amplitude and phase shift relative to the driving pressure oscillation were analyzed with respect to perturbation frequency and mean pressure. By measuring the temperature response amplitude at a fixed temperature and at a series of fixed oscillation frequencies while varying the mean pressure, we determined the frequency-dependent heat capacity as a function of pressure. It was found that the maximal heat capacity dropped by 30-50% during a step-wise pressurization as compared to a depressurization measurement. The structure response spectrum was obtained at a mean pressure value where the heat capacity was maximal. At this point in the transition, the structure and temperature responses are linear up to oscillation amplitudes of at least ±3 bar. The data are consistent with a transition best described by the Kolmogorov-Avrami kinetic model (Ye et al. *Biophys. J.* 60: 1002-1007 (1991)) having an effective dimensionality of one and a structural relaxation time of 1.0±0.2 s. (Supported by NIH DK36849)

Th-Pos245

STRUCTURE AND DYNAMICS OF INTEGRAL MEMBRANE PROTEINS THROUGH COMPUTER MODELING AND SIMULATION
((T.R.Stouch and D.Bassolino))Bristol-Myers Squibb Pharmaceutical Research Institute, Princeton, NJ 08543-4000

We report atomic-level molecular dynamics simulations of integral membrane proteins in an explicitly represented hydrated lipid bilayer that probe the details of the structure and dynamics of these proteins. We address the intimate relationships between these proteins and the lipid components of membranes as well as the water hydrating the membranes. Current studies center around trans-membrane alpha-helices, one of the most common membrane protein motifs and target the stability, folding, and the nanosecond-scale motions (lateral diffusion and tilt) of these constructs. The differential interactions between different amino acid side chains and the other membrane components will be detailed. The effects on the helical stability of the different membrane regions (water, headgroup, hydrocarbon core) will be discussed.

Th-Pos246

THERMAL DENATURATION AND CATION-MEDIATED AGGREGATION OF β-LACTOGLOBULIN STUDIED BY ^{1}H and ^{111}Cd NMR.
((H. Li[1], C.C. Hardin[2] and E.A. Foegeding[2])) [1]Duke University, Durham, NC 27708 and [2]North Carolina State University, Raleigh, NC 27695 (USA).

Whey protein isolate contains approximately 68% β-lactoglobulin (β-LG). Important functional properties of whey proteins in foods are their ability to form gel structures. Studies of the fracture properties of these gels using scanning electron and light microscopies demonstrated different morphology-adopting influences with mono- and divalent cations. Resulting gels have progressively higher rheological shear strains at fracture when formed in Na^+, H_2O and Ca^{2+} solutions at pH 7. Thermal denaturation, aggregation and gelation of β-LG under these three ion conditions were investigated using 1 and 2D ^{1}H and ^{111}Cd NMRs. Temperature-dependence experiments showed that the oligomeric protein aggregate (octamer/dimer) dissociates to form a dimer/monomer as the temperature is increased from 10° to 25°/30°C. At temperatures above 25°/30°C the protein undergoes conformational changes which lead to denaturation, aggregation and then gelation. Calcium and Na^+ do not induce formation of different conformations in "native" β-LG at 25°C, but as the temperature is raised the unfolded proteins adopts one or a few discrete and subtly different conformations that differ in Na^+, Ca^{2+} and H_2O. $^{111}Cd^{2+}$ ions are not tightly bound to the protein. Chemical shifts suggest that divalent cations bind to the protein predominantly at carboxylate oxygen sites, and probably at hisidine nitrogens. The results show that protein aggregation and gelation occur via different mechanisms in the presence of mono- and divalent cations. Divalent cations apparently stabilize the unfolded conformation by shifting the structural equilibrium from folded to marginally unfolded and trapped by bound divalent cations, a process which accelerates the gelation rate and nucleates differently than in Na^+/H_2O and H_2O.

Th-Pos247

TEMPERATURE AND PH DEPENDENCE OF RECOMBINANT HUMAN NERVE GROWTH FACTOR DIMER DISSOCIATION
((L.R. De Young, J. Briggs, and M.F. Powell)) Department of Pharmaceutical Research and Development, Genentech, So. San Francisco, CA 94080.

The dimer dissociation rate has been determined for recombinant human nerve growth factor (rhNGF) at pH 3.5-6.5 and 15 to 37°C. RhNGF is encoded as a 120 amino acid polypeptide. C-terminal clipping of ala-arg or arg-ala-arg result in 118 and 117 amino acid variants which have different net charges. RhNGF forms a tight non-covalent dimer (Keq 10^{12} - 10^{15}) and dimers of these variants can be separated by cation exchange chromatography. Here, we mix 118/118 and 120/120 homodimers and monitor the rate of formation of the 118/120 heterodimer. The rate of formation of 118/120 is independent of the initial homodimer concentrations and the dimer distribution is random. The dissociation rate increases with a decrease in pH and an increase in temperature, similar to qualitative results reported for muNGF (Moore and Shooter, Neurobiol. 1975, 5, 369). Activation energies are approximately independent of pH and the Arrhenius A constant is strongly pH dependent. If monomer reassociation is assumed to be diffusion limited (10^{6} M^{-1} s^{-1}) dimer monomer equilibrium constants of 4 x 10^{-11} and 2 x 10^{-13} M are calculated at pH 3.5 and 6.5, respectively.

Th-Pos248

PROTEIN DYNAMICS IN CRYSTALS AND IN SOLUTION USING THE INCOHERENT QUASIELASTIC NEUTRON SCATTERING TECHNIQUE.
((H. Cao, H. E. Rorschach)) Rice University; ((C. F. Hazlewood)) Baylor College of Medicine; ((S. Shapiro, T. Thurston)) Brookhaven National Laboratory.

The incoherent quasi-elastic neutron scattering (IQNS) method makes possible motional studies of biomolecules in different forms: powder, crystalline, and solution; and at different temperatures. IQNS allows investigation of possible relaxation mechnisms of the side chains' hydrogens. We have used the IQNS technique to study the motion of the myoglobin side chains hydrogens in D_2O solution and in crystals. The scattering spectra $S(Q,\omega)$ were measured in constant-Q mode. It is found that the $S(Q,\omega)$ for myoglobin hydrogens in liquid solution are characterized by a distribution of discrete jumps of side chains' hydrogens through the broadening of the spectra, and effective-one-particle-potential with multiple wells through the anharmonic Debye-Waller factor. The motions of the side chain hydrogens is much reduced in crystals as compared to solution. In addition, we present a new approach to analyze incoherent quasielatic neutron sscattering spectra of protein in solution.

Th-Pos249

V8 PROTEOLYSIS OF RECONSTITUTED HDL PARTICLES: A CONFORMATIONAL ANALYSIS

((Erika Hayden, Linda M. Roberts and Christie G. Brouillette)) Centre College, Danville, KY 40422 and Southern Research Institute, Birmingham, AL 35205

Reconstituted HDL particles containing purified human apolipoprotein AI (apoAI) and phosphatidylcholine (POPC) in a 100:1 molar ratio of lipid to protein were prepared using detergent dialysis and purified using native gradient gel electrophoresis (GGE). Three major particles resulted from the reconstitution process with Stoke's radii of 89Å (particle 100A), 115Å (100B) and 148Å (100C). Chemical crosslinking indicates the presence of three apoAI molecules on each of the particles. Proteolysis of apoAI in the reconsituted HDL particles indicated that in all three cases, the N-terminal region of the protein (the first 40 amino acids) was the most susceptible to cleavage. Differences in the cleavage patterns of 100A and 100C were not significant. However, the cleavage pattern of 100B indicated an increased susceptibility to cleavage in the N-terminus, suggesting a more exposed conformation for this region of the protein in these particles. In marked contrast to the reconstituted particles, proteolysis of non-lipid-bound apoAI indicated a greater susceptibility to cleavage in the C-terminal region of the protein with little cleavage occurring near the N-termimus. We will present these results in terms of a model of apoAI conformation on different particle sizes and compare this to existing models of lipid-bound apoAI conformation.

Th-Pos250

CONFORMATION OF APOLIPOPROTEIN AI ON RECONSTITUTED HDL PARTICLES

((Linda M. Roberts and Christie G. Brouillette)) Centre College, Danville, KY 40422 and Southern Research Institute, Birmingham, AL 35205

Reconstituted high density lipoprotein particles (HDL) consisting of apolipoprotein AI and palmitoyl-oleoyl phosphatidylcholine (POPC) were prepared by detergent dialysis and purified by native gradient gel electrophoresis. ApoAI/POPC complexes prepared with a starting lipid-to-protein molar ratio of 40:1 yielded three major species with Stokes' radii of 81 Å (particle 40A), 85 Å (40B), and 87 Å (40C), respectively. The conformation of apoAI on each of the purified particles was studied using limited proteolysis with the serine protease chymotrypsin.

Complexes treated with a 50:1 weight-to-weight ratio of apoAI to protease produced cleavage patterns which were very similar for all three particles in terms of the kinetics of proteolysis and the size of the different fragments produced. Proteolysis of each of the particles led to the appearance of several bands similar in size to intact apoAI. After 20 minutes, most of the intact apoAI was gone whereas some of the apoAI-sized bands persisted for several hours. Complexes showed little change in size for up to 24 hours of incubation with protease as determined by electrophoresis on native gradient gels indicating that proteolyzed apoAI remained bound to the lipid. N-terminal sequencing of proteolytic fragments indicated that the apoAI in each of the three particles was most susceptible to cleavage in the N-terminal region. This is significantly different from results obtained from non-lipid-bound apoAI in which the protein is most susceptible to cleavage in the C-terminal region. The significance of these results in terms of apoAI conformation on particle surfaces and comparisons to existing models of lipid-bound apoAI structure will be discussed.

Th-Pos251

TIME-RESOLVED FLUORESCENCE OF THE SINGLE TRP IN THE ACTIVE SITE OF ERABUTOXIN A ((P. Blandin, F. Mérola, J.C. Brochon, O. Trémeau, A. Ménez)). LURE, CNRS, 91405 Orsay, France. (Spon.by M.F.Carlier-Pantaloni)

The TRF of Trp29, a central residue in the recognition site of AcChoR in snake neurotoxins, has been studied under various conditions of temperatures and pHs. The fluorescence kinetics is dominated, at 20°C and neutral pHs, by 80% of a single relaxation term, while the anisotropy decays indicate only very small amounts of ps reorientations of the Trp side chain. From 0°C to 60°C, the lifetime distributions show the same dominant component, with expected Arrhenius dependence to temperature. The Trp residue seems therefore located in a single well defined micro-environment at all time scales above the sub-ns range. The activation energy of the non-radiative quenching processes is very close to that observed for Trp derivatives. Between 70°C and 80°C, irreversible denaturation of the protein is marked by a sudden increase in ps and ns flexibilities as well as a spread of Trp fluorescence lifetimes over a very large and complex distribution. Below pH3, a fully reversible acid denaturation takes place. Above pH8 begins a progressive increase in the level of ps and ns flexibilities, which continues down to pH12.6. In the fluorescence lifetime profiles, these dynamic perturbations are paralleled by at least two detectable transitions between successive increasingly complex profiles, with approximate pKs 9.5 and 11.5. The first of these transitions is ascribed to the deprotonation of Lys27 since it is absent after selective acetylation of this residue.

Th-Pos252

QUATERNARY STRUCTURE OF TRYPTOPHANASE, NATIVE AND POINT MUTATED: TIME RESOLVED FLUORESCENCE ANISOTROPY

((A.H. Parola[1,2], P.J. Fisher[2], A. Markel[1], T. Ben-Kasus[1], S.S. Sedarous[2] and F.G. Prendergast[2])) [1]Dept. of Chemistry, Ben-Gurion University, Beer-Sheva 84105, Israel and [2]Dept. of Biochemistry and Molecular Biology, Mayo Medical School, Rochester, MN 55905.

Tryptophanase is a bacterial, pyridoxal phosphate (PLP)-dependent 208-kD tetrameric enzyme. It has two Trps and one PLP residue in each of its (identical) subunits.With its point mutated analoges, W248F and W330F (in which either one of the Trps is substituted by Phe) and their Apo- proteins, it is an inviting system for the study of subunit interactions. Nanosecond single photon counting fluorescence lifetime and anisotropy studies of Trp, PLP and the energy transfer between them reveals segmental rotational relaxation motions of these native probes. Quaternary structure can be modified by preincubating the dilute tetrameric enzymes at 4°C . Measurements were taken at various temperatures and pHs. The wild type and W248F enzymes (left and middle figures) display a unique time (ns) profile of PLP fluorescence anisotropy (ex=340nm., em=390nm) which may shed light on the enigmatic fate of PLP during catalysis: increased anisotropy following the initial decrease, may arise from reduced rotational freedom presumably due to coulombic interactions between the protonated excited PLP and negativley charged amino acids on the surface of its active site . This profile vanishes, and a classical decay profile of the W330F mutant (right) is observed. It presumably results from a transformation of the tetrameric form into a dimer. The latter was independently assessed by HPLC studies. PLP may also have a role in maintaining the tetrameric structure observed in this enzyme.*Profs. Yu. M. Torchinsky and R.S. Phillips helped in obtaining protein samples.*

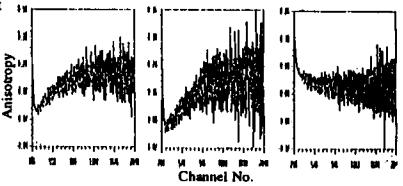

Th-Pos253

STARK EFFECT SPECTROSCOPY OF TRYPTOPHAN((Daniel W. Pierce and Steven G. Boxer))
Department of Chemistry, Stanford University,Stanford, California 94305-5080.

The difference dipole moment ($\Delta\mu$) for the transition from the ground state to the ^1L_a state of tryptophan is the key photophysical parameter for the interpretation of tryptophan fluorescence spectra in terms of static and dynamic properties of the surrounding medium. We report measurement of this parameter by means of electric field effect (Stark) spectroscopy for N-acetyl-L-tryptophanamide (NATA) in two solvents, the single-tryptophan containing peptide melittin, and 5-methoxytryptophan. The values ranged from 6.6 to 6.8±0.2 D/f for NATA and melittin, where f represents the local field correction. The ^1L_a $\Delta\mu$ was much smaller except in the case of 5-methoxytryptophan, where it was 7.0±0.2 D/f. Application of Stark spectroscopy to this chromophore required decomposition of the near-UV absorption into the ^1L_a and ^1L_b bands by measurement of the fluorescence excitation anisotropy spectrum, and represents an extension of the method to systems where band overlap would normally preclude analysis of the Stark spectrum. The results obtained for 5-methoxytryptophan point out important limitations of this method of spectral decomposition. The relevance of these results to the interpretation of steady-state and time-resolved spectroscopy of tryptophan is discussed.

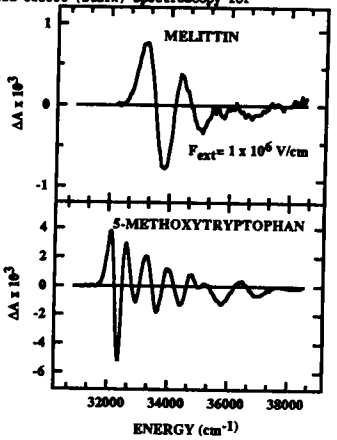

Th-Pos254

LINKED FUNCTIONS IN *E. COLI* THIOREDOXIN REDOX ACTIVITY.

((C. A. Hanson, J. A. Fuchs, C. Woodward)) Dept. of Biochemistry, University of Minnesota, St. Paul, MN 55108

E. coli thioredoxin is a small, stable, redox active globular protein that contains a single active site disulfide between Cys 32-Cys 35. In the crystal structure, the Ile75-Pro76 peptide bond is in the unusual *cis* configuration and Pro 76 is in contact with Cys 35 side chain atoms. Asp 26 is buried near the Cys 32-Cys 35 disulfide. Both are absolutely conserved. We have shown that Asp 26 titration, Ile75-Pro76 *cis-trans* isomerism and redox activity are linked functions. Previous studies of site-directed mutant D26A showed that Asp 26 has an anomalous pK of 7.4 in the wild type structure (Langsetmo, et al., Biochemistry, 1991, 30, 7603-9). To examine Asp 26 and Pro 76 in thioredoxin function, we have determined the pH dependence of the redox activity of wild type compared to that of D26A , taken as a model of the -COOH form of Asp 26, P76G, taken as the model for the Ile75-Pro76 *cis* peptide bond, and P76A, taken as a model for the *trans* peptide bond. Initial kinetic constants determined from experiments with D26A, P76G and P76A thioredoxins have, respectively, a 3 to 7-fold, 1 to 3 fold and 1.5 to 3-fold increase in Km over wild type in the pH range 7-8.5. Kcat values within this pH range increase for D26A from a 2.6 fold decrease pH 7 to a 1.1 fold decrease at pH 8.5 compared to wild type. D26A results are in contrast to P76G and P76A whose Kcat values decrease with an increase of pH from 7 to 8.5. Initial results reveal Kcat values for P76G and P76A, compared to wild type, decrease from 2.3-3.5 and 1.5-2.1, respectively with an increase in pH from 7 to 8.5

Th-Poe255

RELEASE OF Ca^{2+} BY RAPID COOLING IN SKINNED MYOCARDIUM TREATED WITH THE ANESTHETIC AGENTS HALOTHANE OR ISOFLURANE. ((FJ Julian, J Herland & DG Stephenson*)), Dept. Anesthesia, Brigham & Women's Hsp., Boston, MA & *LaTrobe U., Australia.

Rapid cooling contractures (RCCs) in which cardiac muscle is rapidly exposed to solutions cooled to less than 5°C have been used successfully to assay sarcoplasmic reticulum (SR) Ca^{2+} content, though the mechanism responsible for the cooling-induced Ca^{2+} release from the SR is not well understood. The vapor anesthetic agents are potent depressors of cardiac inotropy, but the molecular mechanisms responsible for this effect remain to be fully elucidated. A major challenge confronting a unified theory of anesthetic action is to show that these agents can exert other than non-specific actions on their target organs. Here we report results using RCCs in saponin-skinned (50µg/ml) isolated ventricular preparations from rat heart treated with halothane (0.47 & 1.89mM) or isoflurane (0.4 & 1.6mM), which can be summarized as follows. (1) A large proportion of the Ca^{2+} stored in the SR is released during an RCC in saponin-skinned preparations. (2) The amount of Ca^{2+} released by an RCC, as judged by the magnitude of the contracture force, is similar to that induced by treatment with only caffeine (0.5mM) at 23°C. (3) The magnitude of the RCC-induced contracture is a sensitive assay of SR Ca^{2+} content in saponin-skinned preparations. (4) The SR Ca pump is capable, even at low temperature (3°C), of resequestering most of the Ca^{2+} released during an RCC. (5) Isoflurane, but not halothane, inhibits the release of Ca^{2+} from the SR by an RCC in a dose-dependent manner. (6) Isoflurane does not inhibit Ca^{2+} release in muscles treated also with 0.5mM caffeine at 23°C. (7) The inhibition exerted by isoflurane in RCC-induced contractures can be fully removed by application of caffeine. Our results support a theory of selective action of vapor anesthetics because halothane and isoflurane, both small molecules with distinct chemical groupings, have significant differential effects on a key ion channel: the Ca^{2+}-release channel in cardiac SR, whose function is of great importance in modulating inotropy. Support: NIH #HL35032 (FJJ) & ARC (DGS).

Th-Poe256

CARDIAC MYOCYTE STRUCTURE AND FUNCTION DURING THE IN VITRO DIFFERENTIATION OF MOUSE EMBRYONIC STEM CELLS. ((Joseph M. Metzger, Wan-In Lin and Linda C. Samuelson)) Deptartment of Physiology, University Michigan, Ann Arbor, Michigan 48109

Pluripotent mouse embryonic stem (ES) cells differentiate *in vitro* into a variety of cell types including spontaneously contracting cardiac myocytes. Previous work has shown that differentiating ES cells express cardiac-specific contractile genes indicating that this system may represent a new model for determining the molecular and cellular mechanisms of cardiac gene expression and function *in vitro*. We have utilized this differentiation culture system to study the development of the cardiac contractile apparatus *in vitro*. Differentiation cultures were established by removing ES-D3 cells from a feeder layer of embryonic fibroblasts. Cell aggregates were formed in hanging drop cultures and plated onto gelatin coated glass cover slips. After 8-9 days in differentiation culture spontaneous contractile activity became apparent and was maintained in some myocytes for greater than 70 days. Immunofluorescence microscopy showed that myosin protein expression was discretely localized to the contracting cells. SDS-PAGE on micro-dissected samples of the contracting myocytes demonstrated the expression of β and α cardiac MHC isoforms. Functional studies on contracting cells were also conducted. Difficulties associated with the cellular heterogeneity of the ES cell culture system were overcome by developing a functional assay using cardiac myocytes mechanically isolated from differentiation cultures. Early in cardiac development *in vitro*, the contractile apparatus displayed marked sensitivity to activation by Ca^{2+}, but with prolonged time in culture Ca^{2+} sensitivity decreased and cooperatively increased. The transition in Ca^{2+} sensitivity obtained *in vitro* closely paralleled that during cardiac development *in vivo*, indicating the ES cell-derived cardiac myocytes recapitulate murine cardiogenesis. The establishment of a functional assay together with the capability of genetically manipulating contractile genes in ES cells now permits the determination of the relationship between gene expression and function during cardiogenesis *in vitro*.

Th-Poe257

INOTROPIC AND ENERGETIC EFFECTS OF NEW CALCIUM SENSITIZING AGENTS ON THE PERFUSED RAT HEART

((D.J. Grandis, P.J. DelNido, A.P. Koretsky)) Medical College of Pennsylvania, Univ. of Pittsburgh, Carnegie-Mellon Univ., Pittsburgh, PA 15213.(Sponsored By A.P. Koretsky)

ORG 30029 and EMD 57033 are new inotropic agents which are capable of increasing cardiac work without significantly affecting the calcium transient. By comparing the energetic effects of increased cardiac work by these agents to the effects of similar increases in work by dobutamine, an agent which increases calcium transients, the effect of calcium handling on cardiac energetics can be addressed. Langendorf-perfused rat hearts beat isovolumically and were paced at 5Hz. Myocardial oxygen consumption (MVO_2, µmoles/min/g dry weight) was measured with developed pressure (DevP, systolic-diastolic, mmHg) and phosphate metabolites by ^{31}P NMR. Results shown as means ± S.D. *p<.05 vs control; † vs dobutamine. Both EMD 57033 and ORG 30029 cause increased developed pressure with much

	Control	Dobutamine	EMD 57033	Dobutamine	ORG 30029
dose		67.5µg/l	2 µm/l	100µg/l	2.5 mmol/l
n	29	9	10	6	4
DevP	82±6	108±9*	106±6*	172±14*	150±12*
MVO_2	32±4	48±3*	36±2†	60±4*	38±7†

smaller changes in MVO_2 than does dobutamine. The concentrations of phosphate metabolites were unchanged from control with each agent; indicating a steady state. The differences in MVO_2 between dobutamine and the calcium sensitizing agents for similar increases in work may be due to the energetic costs of calcium handling or increased contractile efficiency.

Th-Poe258

EFFECT OF PHALLOIDIN ON Ca^{2+} REGULATION OF SKINNED CARDIAC AND SKELETAL MUSCLE FIBERS. ((A. E. Bukatina[1,3], P. W. Brandt[2] and F. Fuchs[1])) [1]Dept. Cell Biol. Physiol., University of Pittsburgh School of Medicine, Pittsburgh, PA 15261, [2]Dept. Anat., Coll. Physicians and Surgeons, Columbia University, New York, NY 10032 and [3]Inst. Theor. Exp. Biophysics, Russian Acad. Sci., Pushchino, Russia 142292.

We have studied the role of actin in Ca^{2+} regulation of striated muscle using phalloidin (PH) as an actin modifier. The effect of pre-treatment with PH on the tension-pCa relationship was studied for skinned fibers of bovine left ventricle (CM) and rabbit psoas (SM). For CM, PH pre-treatment in rigor solution was found to cause an increase in the Ca^{2+} sensitivity but no change in cooperativity of activation. The Hill equation best-fit parameters were pK=6.52±0.02, nH=1.98±0.05 (n=9) for PH pre-treated fibers and pK=6.31±0.02, nH=2.06±0.08 (n=9) for control fibers. For SM, PH pre-treatment of 1) partially activated fibers or 2) fibers in rigor resulted in increased cooperativity but little or no change in Ca^{2+} sensitivity. In the 1st case the Hill equation parameters were pK=6.18±0.03, nH=7.8±0.6 (n=6) for PH pre-treated fibers and pK=6.11±0.01, nH=5.0±0.5 (n=5) for control fibers. In the 2nd case they were pK=6.17±0.03, nH=5.7±0.3 (n=7) for PH pre-treated fibers and pK=6.17±0.03, nH=4.4±0.3 (n=7) for controls. The data are in general agreement with data on activated fiber responses to PH at different pCa and on the changes in Ca^{2+} sensitivity of myofibrillar ATPase activity (Son'kin et al., 1983; Bukatina & Fuchs, 1993). The changes in Ca^{2+} regulation induced by the PH modification could be caused via changes in actin-regulatory protein interactions and/or via changes in cross-bridge kinetics (Bremel & Weber, 1972; Brandt et al., 1980). Supported by NIH grants AR 10551and 40300.

Th-Poe259

GENETICALLY DEVELOPED CARDIAC-SKELETAL-TnC CHIMERA: LOCATION OF THE LENGTH-SENSOR IN CARDIAC TnC

((A. Babu, T. Iwazumi and J. Gulati)) Albert Einstein College of Medicine, Bronx, NY 10461

Babu et al (Science, 240, 74-76, 1988) showed that sTnC/cTnC exchange in hamster trabeculae diminished the length-dependence of pCa-force relationship similar to fast-twitch skeletal fiber, suggesting that cTnC was intrinsically a better length-sensor than sTnC. To delineate the length-sensing regions in cTnC, we have used a recently described cardiac-skeletal TnC chimeric construct (C1S) in which residues 1-40 were cardiac-type and 41-160 were skeletal-type (Gulati et al, JBC, 267, 25073-77, 1992). In skinned cardiac muscle specimens depleted of endogenous cTnC and repleted with C1S, the maximal tension response (pCa4 activation) at 2.4µm sarcomere length was 0.73±.01P_o, lower than the original P_o. This loss of tension capability was not the consequence of partial loading with C1S as further loading with cTnC caused no further improvement. The pCa-force curves are now compared at 2.4µm and 1.9µm between normal, sTnC-loaded and C1S-loaded trabeculae, and the length-induced shift was noted. This was 0.15±0.02pCa unit in the control (Pmax= 100%P_o), 0.05±0.01 in the sTnC-loaded (Pmax= 91%P_o), and 0.13±0.01 in C1S-loaded specimens (Pmax= 73%P_o). The results (1) support the earlier finding that myocardial length-dependence of Ca^{2+}-sensitivity is governed by the TnC isoform. (2) Additionally, the findings locate the intrinsic length-sensing element in cTnC within the N-terminal 1-40 residues.
Supported by NIH grant AR-33736

Th-Poe260

EFFECTS OF pH AND P_i ON MYOFIBRILLAR FORCE AND ATP TURNOVER IN RAT CARDIAC MUSCLE.

((J.P. Ebus and G.J.M. Stienen)) Laboratory for Physiology, Free University, van der Boechorststraat 7, 1081 BT Amsterdam, the Netherlands.

The effects of inorganic phosphate (P_i) and pH have been studied in maximally Ca^{2+}-activated skinned cardiac trabeculae from rat at 20°C and 2.1 µm sarcomere length. ATP turnover was determined photometrically using an enzyme-linked assay. Under control conditions (pH 7.0, no added P_i) isometric force was 51±3 kN/m^2, and ATPase activity was 0.43±0.02 mM/s, i.e. 2.6±0.1 molecules ATP per myosin head per second (n=16). When 30 mM P_i was added, isometric force gradually decreased to 31±2%, whereas isometric ATPase decreased to 87±3%. When pH was lowered to 6.2, isometric force decreased to 54±1%, and isometric ATPase decreased to 80±1%. When pH was decreased to 6.2 and 30 mM P_i was added, isometric force and ATPase were 14±1% resp. 47±3% of the control value. When square-shaped length changes (23 Hz, amplitude 2.5%) were applied, ATPase was increased while average force was decreased in comparison with the isometrical values. The effects of P_i on force and ATPase under these dynamical conditions differed only by a scaling factor from the effects during isometrical conditions. However, the effects of pH on force and ATPase differed significantly under isometrical and dynamical conditions. The combined effects of 30 mM P_i at pH 6.2 on force are not significantly different from the product obtained at pH 6.2 and at 30 mM P_i separately. This is not the case for ATPase, both under dynamic and isometric conditions. The implications of these findings for the model of crossbridge interaction in cardiac muscle will be discussed.

Th-Pos261

SIMULTANEOUS MEASUREMENT OF CYTOSOLIC pH AND ISOMETRIC TENSION IN CANINE TRABECULAE: EFFECT OF ACIDOSIS. (A. Guia, and R. Bose) Dept. of Pharmacology, Univ. of Manitoba, Winnipeg, Manitoba. Canada R3E 0W3.

Most of the studies dealing with measurement of pH_i with BCECF in cardiac muscle have reported relative changes in pH from experiments of short duration due to time-dependent changes in fluorescence. This study uses a method for correcting the calibrations of the dye's response to pH that allows the use of BCECF for measuring absolute pH in experiments of longer duration. Measurement of pH_i was verified with a 4-minute pulse of 10 mM NH_4Cl. This produced cytosolic alkalosis followed by acidosis without a change in the pH of the bathing medium (pH_O). Cardiac damage has been shown to occur during post-ischemia reperfusion. The exact reason for this is unclear although it is believed that a drop in pH_i results in sodium loading by sodium-hydrogen exchange and this sodium exchanges for calcium to cause a rise in diastolic tension. In our study, responses to changes in pCO_2, acetic acid, and lactic acid, with and without bicarbonate in the medium proved that cytosolic pH was better controlled in the presence of bicarbonate. Prolonged acidosis with addition of CO_2, acetic acid, and lactic acid for 45 minutes decreased pH_O and pH_i. Tension responses were fully reversible upon return to control pH_O. We conclude that acidosis alone does not produce cardiac tissue damage as judged by its major function—contraction. (Supported by Medical Res. Council of Canada and Canadian Heart and Stroke Foundations)

Th-Pos262

ISOMETRIC FORCE KINETICS ARE UNAFFECTED BY CA2+ IN SKINNED RAT VENTRICULAR MYOCARDIUM. ((W.O. Hancock, L.L Huntsman, D.A. Martyn and A.M. Gordon)) Ctr. for Bioengineering and Dept. of Physiol. and Biophys., Univ. of Washington, Seattle, WA 98195.

The influence of Ca^{2+} on the kinetics of isometric contraction in cardiac muscle was studied by measuring the rate constant of tension redevelopment (k_{tr}) in skinned rat ventricular myocardium at 15°C. During steady state Ca2+ activation, tension was transiently reduced by either a ramp release followed by a rapid restretch to the original length, or by a rapid 4% length step. The tension recovery was fit by an exponential function with rate constant k_{tr}. Segment length (SL) was monitored optically by attaching two foil markers to the central region of the muscle, and SL was held constant during tension redevelopment using a software controlled feedback system. The ramp release/restretch protocol caused tension to fall to approximately 60% of steady state, while the 4% SL step dropped tension to near baseline. k_{tr} obtained using either technique exhibited little dependence on the level of Ca2+ activation, decreasing slightly at maximum [Ca2+]. The average k_{tr} values from the ramp release/restretch and step methods were 6.9 sec^{-1} and 15.7 sec^{-1}, respectively. While it is not clear why the values for the two methods differ, the finding that k_{tr} does not increase at increased activation levels with either method suggests that actomyosin kinetics are independent of [Ca2+] in skinned rat myocardium. These results are consistent with those obtained from intact ferret myocardium (*Circ Res 73:603)*, and contrast with results obtained from either fast (*PNAS* **85**:3265) or slow (*Science* **247**:1088) skeletal muscle in which k_{tr} has been found to increase at higher Ca2+ activation levels. Supported by NIH Grants HL31962 and HL07403.

Th-Pos263

CARDIAC TnI IS THE DOMINANT MODIFIER OF ACIDOTIC pH-INDUCED SHIFTS OF Ca^{2+}-SENSITIVITY IN THE RAT

((X.-L. Ding, A. Babu, and J. Gulati)) Albert Einstein College of Medicine, Bronx, NY 10461

On hamster myocardium, we previously found that the exchange of endogenous cTnC with skeletal TnC left relatively unperturbed the effect of acidotic pH on pCa-tension relationship (Gulati & Babu: FEBS Letts, 1989, 245, 279). The opposite conclusion was reached recently by Metzger et al (PNAS, 1993, 90, 9036) from measurements of the pH-effect on sTnC-containing myocytes in the Parmacek-Leiden-Field transgenic mouse. Hence, we re-investigated the pH effect with TnC-exchange on rat trabeculae. The ΔpCa_{50} (i.e., pCa_{50} at pH7 - pCa_{50} at pH6.5) was 0.88±.02(9)pCa unit for the cTnC trabeculae and 0.81±.02(6) following cTnC exchange with (rabbit) sTnC4. The rat unextracted fast-twitch fiber gave a characteristic shift of 0.57±.04(3). Therefore, in the rat, analogous to the hamster, the TnC isoforms account for only a fraction (less than 30%) of the difference in the acidotic effects between skeletal and cardiac muscles. Comparable effects were also observed at pH6.2. Possibly, the Parmacek-Leiden-Field transgenic mouse is a complex construct. To elucidate the contributions of TnI, we exchanged the endogenous cardiac TnI with (rabbit) skeletal TnI, by the modified vanadate-treatment. The acidotic pH(7→6.5) induced shift in cardiac Ca^{2+}-sensitivity following sTnI+sTnC exchange was 0.62±.04(6)pCa unit compared with native 0.86±.02(9). Evidently, cTnI directs more than 70% of the pH effect. Thus, for the first time on fibers, the findings manifest a dominant role for cTnI in the acidotic effects on cardiac contractility.

Th-Pos264

OSMOTIC COMPRESSION OF SINGLE CARDIAC MYOCYTES REVERSES THE REDUCTION IN CA^{2+} SENSITIVITY OF TENSION OBSERVED AT SHORT SARCOMERE LENGTH ((K.S. McDonald and R.L. Moss)) Dept of Physiology, Univ of Wisconsin, Madison WI 53706.

Calcium sensitivity of tension increases as sarcomere length is increased in cardiac muscle. One likely explanation for this effect is a decrease in myocyte diameter and, consequently, interfilament lattice spacing as muscle length is increased. To examine this idea, we tested the hypothesis that osmotic compression of single skinned cardiac myocytes would increase Ca^{2+} sensitivity of tension at a given sarcomere length (SL). Single enzymatically isolated myocytes from rat ventricles were attached to a force transducer and piezoelectric translator. Tension-pCa relationships were obtained at short SL, at the same SL in the presence of 1, 2.5, or 5% dextran, and at long SL. The pCa for half maximal tension (i.e., pCa_{50}) increased from 5.58 ± 0.02 to 5.68 ± 0.02 ($p < 0.001$) when SL was increased approximately 0.4 μm (n = 15) i.e., Ca^{2+} sensitivity was less at short SL. Osmotic compression (5% dextran) of myocytes (n=6) at short SL increased Ca^{2+} sensitivity, shifting the tension-pCa relations to even lower Ca^{2+} concentrations (pCa_{50} = 5.80 ± 0.03) than observed at long SL. The change in Ca^{2+} sensitivity depended on both the concentration of dextran ($p < 0.001$) and dextran-induced changes in myocyte width ($r = 0.79$). These results suggest that the length dependence of Ca^{2+} sensitivity of tension in cardiac muscle arises in large part from changes in interfilament lattice spacing which accompany changes in sarcomere length. Work supported by the American Heart Association.

Th-Pos265

$[Ca^{2+}]$ AND MYOFILAMENT PHOSPHORYLATION MODULATE THE KINETICS OF TENSION DEVELOPMENT IN CARDIAC MUSCLE. ((A. Araujo and J.W. Walker)) Department of Physiology, University of Wisconsin, Madison, WI 53706

Using the technique of caged Ca^{2+} photolysis, we previously showed that the rate of tension development in skinned rat ventricular muscle is influenced by $[Ca^{2+}]$ (Biophys. J. **64**(2): A254). We now report that the rate increases by 4-fold over the range of $[Ca^{2+}]$ that supports isometric tension, with the rate changing more in the low $[Ca^{2+}]$ range. In skinned rabbit psoas fibers, variation in $[Ca^{2+}]$ results in a 20-fold increase in rate, with most of the change occurring in the high Ca^{2+} range. Neither rates nor Ca^{2+} dependency were altered after troponin C (TnC) extraction from psoas fibers (to 0-5% P_o) and reconstitution with the cardiac TnC (to 78 ± 8% P_o). Observed differences between cardiac and skeletal muscle do not appear to be due solely to different TnC isoforms. Protein kinase A resulted in phosphorylation of C-protein and TnI (measured by ^{32}P-autoradiography/SDS-PAGE) and caused a shift of the tension-pCa relationship to higher $[Ca^{2+}]$ by 0.17 pCa units. Protein kinase A increased the rate of tension development by 50% at all levels of tension. Myosin light chain kinase (MLCK; kind gift from Prof. M. Ikebe) resulted in phosphorylation of myosin light chain 2 and shifted the tension-pCa relationship to lower $[Ca^{2+}]$ by 0.13 pCa units. MLCK increased the rate of tension development by 70% at all levels of tension. Tension development rates in mammalian cardiac muscle appear to be regulated by $[Ca^{2+}]$ and by phosphorylation of specific regulatory subunits on the myofilament.

Th-Pos266

BETA-ADRENERGIC STIMULATION DOES NOT SHIFT CALCIUM SENSITIVITY OF TENSION IN IMMATURE RAT SKINNED CARDIAC MYOCYTES. ((S.H. Buck, K.T. Strang, and R.L. Moss)) Depts of Pediatrics and Physiology, Univ of Wisconsin, Madison WI 53706

During cardiac development, there is a switch in TnI isoform population from slow skeletal TnI (ssTnI) to cardiac TnI. Previous work indicated ssTnI lacks phosphorylatable serine residues believed to be responsible for the rightward shift of calcium sensitivity of mature cardiac myocytes following β-adrenergic stimulation. We tested the hypothesis that β-adrenergic stimulation does not affect myofilament calcium sensitivity in developing heart by comparing the tension-pCa relationship of mechanically isolated single skinned ventricular myocytes from 14 day-old rats before and after treatment with PKA. To directly determine if ssTnI is a substrate for PKA phosphorylation, control and PKA-treated myocytes were incubated with ^{32}P-ATP followed by autoradiography to determine ^{32}P-labelling of proteins. In contrast to mature cardiac myocytes which exhibit a significant rightward shift of the tension-pCa relationship following incubation with PKA, no such shift to the right was evident in immature myocytes following PKA incubation. Autoradiograms of control and PKA-treated immature cardiac myocytes which predominantly expressed the ssTnI isoform did not differ in the region of ssTnI. This confirms ssTnI is not a substrate of PKA phosphorylation. These direct observations support the hypothesis that β-adrenergic mediated phosphorylation of ssTnI in developing heart does not occur which most likely accounts for the lack of rightward shift of calcium sensitivity in immature heart.

Th-Poa267

α_1-ADRENERGIC STIMULATION DECREASES MAXIMUM SHORTENING VELOCITY (V_0) OF RAT SKINNED VENTRICULAR MYOCYTES.

((K.T. Strang and R.L. Moss)) Dept of Physiology, Univ of Wisconsin, Madison, WI 53706

α_1-adrenergic receptor stimulation decreases maximal Ca^{2+}-activated actomyosin MgATPase in rat myocardium by a mechanism involving phosphorylation of myofilament proteins (Venema and Kuo, J Biol Chem 268:2705,1993). Although this suggests that α_1-adrenergic stimulation might influence maximum shortening velocity, no such effect has been reported. To investigate this possiblity we compared V_0 between control cells and cells treated with phenylephrine in the presence of propranolol. Single ventricular myocytes were enzymatically isolated, agonist-treated, and rapidly skinned with Triton-X100, thus preserving the phosphorylation of myofibrillar proteins (Puceat, et al, Circ Res 67:517,1990). V_0 was measured during maximal activation (pCa 4.5) using the slack test method, and Ca^{2+}-sensitivity of tension was also assessed by determining the isometric tension-pCa relationship for each cell. V_0 was reduced to 68±8% of control in α_1-stimulated cells (n=8), but we detected no difference in Ca^{2+} sensitivity of tension. We conclude that α_1-adrenergic stimulation decreases the rate of cross-bridge detachment during unloaded shortening, an effect that may be mediated by phosphorylation of TnI and/or TnT. (Supported by HL25861 and AHA-Wis.)

Th-Poa268

ENDOTHELIN SECRETION AS A CARDIOREGULATORY MECHANISM.

((G. McClellan, A. Weisberg, D. Rose and S. Winegrad)) Dept. of Physiol, School of Medicine, Univ. of Penna, Phila, PA 19104-6085.

The contractility of mammalian cardiac muscle is regulated by substances added to the coronary circulation by vascular endothelial cells (Circ. Res. 72: 1044, 1993). The regulation is sensitive to the rate of coronary flow, presumably through shear stress on the endothelial cells, and tissue oxygen tension with the cardiac myocytes acting as oxygen sensors and releasing substances that modify the function of the endothelial cells. This study was carried out to determine whether endothelin is the up regulating substance and how the rate of coronary flow and oxygen tension influence the secretion of the up regulating factor. The coronary venous effluent from an isolated perfused working heart was collected, reoxygenated and assayed for contractility-modifying activity on an isolated cardiac trabecula in which the endocardial endothelium had been damaged by a 1 second exposure to Triton X-100. The vascular endothelium in the perfused heart was then disrupted by a brief exposure to an elevated perfusion pressure, and the diffusible contents of the endothelial cells were collected and assayed for cardioregulatory activity. The results show that: 1) the concentration of endothelin correlated very well with extent of up regulating activity; and 2) the increase in contractility from a given concentration of endothelin in the coronary effluent or endothelial contents was very similar to the amount of up regulation from the same amount of endothelin added to standard Krebs solution. Endothelin can account for all of the up regulating activity in endothelial cells. The rate of coronary flow appeared to determine the amount of endothelin in the endothelial cells but not the rate of secretion. Tissue oxygen tension appeared to regulate the rate of secretion through factors released by the cardiac myocytes. This cardiac myocyte-endothelial cell loop has the capacity to balance the work performed by and energy supplied to the contractile cells. (Supported by grants from N.I.H and the Mary Smith Charitable Lead Trust.)

Th-Poa269

THE EXTENT OF ENDOTHELIN REGULATION OF CARDIAC CONTRACTILITY IN MAMMALIAN HEARTS.

((A. Weisberg, G. McClellan, and S. Winegrad)) Dept. of Physiol., School of Medicine, Univ. of Penna, Phila, PA 19104-6085.

The level of contractility of cardiac muscle is regulated by endothelin and a down regulating factor, as yet unidentified, that are released into the coronary circulation by coronary vascular endothelial cells (Circ. Res. 72: 1044, 1993 and adjacent abstract). The importance of endothelin in setting the level of contractility was determined in a series of isolated cardiac trabeculae by measuring the effect on contractility of adding endothelin or BQ-123, a specific antagonist of endothelin-1, to the bathing medium. Isolated trabeculae were bathed in standard Krebs solution for different lengths of time after dissection to achieve different degrees of stabilization of the level of contractility. During this period of partial or complete stabilization, peak tension developed during a contraction declines. The increase in peak tension with added endothelin and the decrease with added BQ-123 were determined as a function of the extent of decline in force during the period of partial or complete stabilization. The greater the decline in force prior to addition of endothelin, the greater was the increase in force produced by added endothelin. Endothelin addition raised the peak developed tension to approximately 80% of maximum regardless of the value before addition of endothelin, which varied between 20 and 85% of peak tension. BQ-123 reduced force by up to 50% and the degree to which BQ-123 lowered force was related to the degree to which contractility had fallen during stabilization. The reduction in peak force produced by BQ-123 was decreased almost 80% by damaging the endocardial endothelium by a 1 sec exposure to Triton X-100. These results indicate that endothelin is an important regulator of cardiac contractility *in vivo* and they support the suggestion (PNAS 89: 4033, 1992) that an important component of stabilization of contractility in isolated cardiac tissue is the washout of endothelial derived regulatory factors. (Supported by grant from N.I.H.)

Th-Poa270

α_{1B}-ADRENOCEPTOR-MEDIATED POSITIVE INOTROPIC RESPONSE IN RAT HEART ELICITED VIA PKC-DEPENDENT ACTIVATION OF Na/H EXCHANGE

((A.P. Williamson, E. Seifen, J.P. Lindemann and R.H. Kennedy)) UAMS, Little Rock, AR 72205

The role of protein kinase C (PKC) and Na/H exchange in the inotropic response to α_{1A}- and α_{1B}-adrenoceptor (AR) stimulation were studied in rat atrial and ventricular myocardium. Phenylephrine (10 μM), a nonselective α_1-AR agonist, elicited a monophasic positive inotropic response in isolated left atria (LA), and a triphasic inotropic action in isolated papillary muscle (PM) consisting of transient positive, then negative inotropic components preceding a sustained positive inotropic response. The positive inotropic response in LA and the sustained positive inotropic response in PM were antagonized in a concentration-dependent manner by a Na/H exchange inhibitor, ethylisopropylamiloride (EIPA; 3, 10 and 30 μM), and by an inhibitor of PKC, staurosporine (100 nM). EIPA also concentration-dependently antagonized the transient positive inotropic component in PM. Following a 30 min pretreatment with (and subsequent washout of) 300 μM chloroethylclonidine, an irreversible α_{1B}-AR antagonist, 30 μM EIPA had no effect on the sustained positive inotropic response in LA or PM. In the presence of 100 nM staurosporine, 30 μM EIPA further antagonized the sustained positive inotropic response in PM, but had no effect in LA. These data indicate that stimulation of α_{1B}-ARs elicit sustained positive inotropic responses in rat atrial and ventricular myocardium via PKC-dependent activation of Na/H exchange. In addition, these data suggest that α_{1B}-ARs may mediate a non-PKC-dependent activation of Na/H exchange in rat ventricular myocardium, or possibly reflect a difference in the concentration-dependence of staurosporine in rat atrial and ventricular myocardium. (Supported by VA Merit Review to JPL)

Th-Poa271

ADENOSINE ANTAGONIZES ß-ADRENERGIC INDUCED DECREASE IN CA^{2+} SENSITIVITY OF ISOMETRIC TENSION IN SKINNED SINGLE CARDIAC MYOCYTES.

((J.W. Lester, K.F. Gannaway & P.A. Hofmann)) Department of Physiology, University of Tennessee, Memphis, TN 38163.

In ventricular myocytes adenosine antagonizes effects of ß-adrenergic stimulation through inhibition of adenylate cyclase activity (Romano et al, *Am J Physiol* 257:1088, 1989) or activation of a phospholamban specific phosphatase (Gupta et al, *Circ Res* 72:65, 1993). We hypothesized if adenosine inhibits adenylate cyclase activity, then the ß adrenergic - adenylate cyclase - PKA dependent decrease in myofilament Ca^{2+} sensitivity should be inhibited by adenosine stimulation. To test this hypothesis rat single ventricular myocytes were enzymatically isolated, agonist treated and rapidly skinned with Triton X-100 (Puceat et al, *Circ Res* 67:517, 1990). This technique preserves phosphorylated myofilament proteins while allowing control of intracellular $[Ca^{2+}]$. Isometric tension was measured as a function of $[Ca^{2+}]$ and the $[Ca^{2+}]$ of half maximum tension, i.e. pCa_{50}, determined. The pCa_{50} values were 5.87 ± 0.06 for control myocytes (n=9), 5.69 ± 0.04 for myocytes stimulated with isoproterenol (n=13; 30 nM ISO), and 5.93 ± 0.05 for myocytes treated with ISO and the A_1 adenosine agonist R-phenylisopropyladenosine (n=8; 30 nM ISO plus 100 μM R-PIA). Sarcomere length, maximum isometric tension, and slope of the tension-pCa relationships were not significantly different between control and agonist treated myocytes. We conclude adenosine inhibits the ß-adrenergic induced decrease in Ca^{2+} sensitivity of isometric tension in rat ventricular myocytes. This suggests antiandrenergic effects of adenosine are mediated, in part, through inhibition of adenylate cyclase activity. (Supported by HL48839.)

Th-Poa272

ALTERED CA^{++}-REGULATION IN THE HUMAN HEARTS DURING IDIOPATHIC DILATED CARDIOMYOPATHY.

((S.S. Margossian, A. Malhotra, J.B. Caulfield, and P. Norton)) Div. Mol. & Cell. Med., Albany Med. Col., Albany, N.Y. 12208; Montefiore Med. Ctr., Bronx, N.Y. 10467 and Dept. Pathology, U. Alabama, Birmingham, AL 35294.

The effectiveness of the calcium switch in human myocardium was investigated during idiopathic dilated cardiomyopathy (IDC). Four out of the five cases analyzed exhibited some degree of dysfunctional Ca^{++}-regulation as indicated by myofibrillar Mg^{++}-ATPase assays in the presence and absence of calcium. The extent of ATPase inhibition by EGTA varied from 60% to none, i.e., no regulation at all. Earlier we had demonstrated the presence of an active protease in IDC hearts. It was therefor postulated that the cause for reduced calcium sensitivity was the proteolysis of TnT and to a lesser extent of TnI thus eliminating binding of troponin to tropomyosin and/or the troponin-mediated inhibition of MgATPase by EGTA. Western blots of myofibrillar preparations demonstrated that the level of TnT (and TnI in certain cases) was either 40-60% of that in the controls or that it was totally absent which would also account for the absence of regulation in these cases.

Th-Pos273

TROPONIN T MODIFICATIONS IN HYPERTROPHIED FAILING GUINEA PIG HEARTS. ((J. Gulati, A. Babu, S.D. Nikolic, V. Starc, E.H. Sonnenblick, and F.M. Siri)) Albert Einstein College of Medicine, Bronx, N.Y. 10461.

Biventricular hypertrophy and congestive heart failure develop in guinea pigs subjected to gradual left ventricular pressure overload induced by early banding of their ascending aortas. This is associated with impaired unloaded shortening of isolated myocytes and, in the intact heart, with depressed slope of the Starling relation. To investigate the possibility that at least part of this contractile depression may be due to altered expression of a particular subunit of troponin, we analyzed Western blots of ventricular samples using a commercial TnT antibody. Four distinct bands, designated here as T1,T2,T3, and T4 (higher to lower molecular weight) were seen in right and left ventricular samples from three controls (C) and from four guinea pigs with heart failure (HF). HF was associated with decreases in T1 and T2 coupled with increases in T3 and T4. The ratio: (T1+T2)/(T3+T4) decreased with increasing right (circles) or left (squares) ventricular weight expressed as percent change from the respective means for C. (Figure: C, open symbols; HF, filled symbols. R= -0.65, P < 0.02). These observations suggest that isoformic shifts in troponin T may modify the Starling length-sensing operation of troponin C in this model of heart failure.

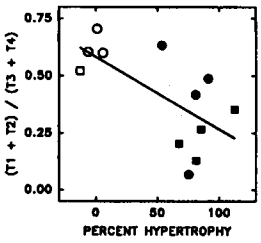

Th-Pos274

STIFFNESS-FORCE-LENGTH RELATIONS IN RIGOR AND RELAXED ISOLATED RAT CARDIAC MYOCYTES. ((A.J. Brady, H.L.M. Granzier and K. Wang)) Dept. Chem&Biochem, University of Texas at Austin,Austin,TX 78712.

Force and stiffness were measured in collagenase isolated detergent skinned rat cardiac myocytes by attachment to Cell_Tak-coated suction micropipettes. Myocytes were perfused with an ATP-free (rigor) or 3 mM Mg-ATP, pCa=8 (relaxing) solution. Stiffness was determined from the oscillatory force induced by a 1 % length perturbation from a piezoelectric driver over a frequency range of 0.06 to 160 Hz. Cell length was varied over a 5% range in rigor and a 30% range in relaxation. Resting force increased almost linearly in both the rigor (10 ug/% length change) and relaxed cells (0.5ug/% length change). The slope of the resting force/length curve declined at about 125% rest length in the relaxed cell suggesting a yield point (J Gen Physiol 101:235,1993; Biophys J 64:1161, 1993). Subsequent stretch and release cycles showed lower slopes and higher slack lengths. These observations imply that passive stress-bearing filament structures undergo some irreversible extension (yield) under these conditions. The rigor complex stiffness/force relation was nearly linear as reported in insect direct flight muscle (J Gen Physiol 101:235,1993. The noise level limited complex stiffness analysis in relaxed cells.

Th-Pos275

THE PASSIVE STIFFNESS PROPERTIES OF SINGLE SKINNED CARDIAC MYOCYTES FROM HYPERTENSIVE RATS.
((Roy E. Palmer, Allan J. Brady and Kenneth P. Roos)) Cardiovascular Research Lab., UCLA School of Medicine, Los Angeles, CA 90024-1760

There is an increased resistance to diastolic filling in the hypertrophied heart. The source of this increased stiffness may be either extracellular (e.g. collagen), intracellular (e.g. titin, microtubules, contractile apparatus), or both. We have investigated the intracellular component using detergent skinned myocytes from control (Wistar Kyoto) and spontaneously hypertensive rats (SHR). Single cells were attached at both ends using a newly developed low mass double-barreled pipette attachment system, which induced little deformation of the cell. We examined the resting stiffness properties of the single myocytes during a period of controlled stretch. In phase stiffness was calculated at 100 Hz. The sarcomere length was calculated using a video analysis system. There was a rise in stiffness which began at sarcomere lengths above approximately 2.3 μm and began to plateau at lengths above 2.8 μm in both types of animal. The myocytes from SHR (> 6 months) showed an increased stiffness modulus, compared to the age-matched controls. Cells from young SHR (< 6 weeks), which did not yet show hypertension, did not show an increased stiffness compared to the control. The data supports the suggestion that the increased diastolic stiffness in the SHR, is at least in part due to intracellular changes, independent of any extracellular component. Supported by NIH HL-47065 (KPR)

Th-Pos276

PASSIVE VISCOELASTIC PROPERTIES OF RAT CARDIAC TRABECULAE.
((M. Scarabello & H.E.D.J. ter Keurs)) University of Calgary, Calgary, AB Canada

Passive cardiac muscle behaves as an elastic element in parallel with the combination of a viscous element in series with an elastic structure. The passive viscosity is sufficient to limit shortening velocity of the sarcomeres. The present study was designed to test whether the series elastic element was located within the sarcomere. Hearts of rat were rapidly excised under ether anaesthesia and trabeculae were dissected from the right ventricle. Trabeculae were studied in Krebs-Henseleit solution at 25°C in the presence of 1.5 mM $[Ca^{++}]_o$. Force was measured by silicon strain gauge attached via a remnant of the tricuspid valve to the trabecula. Sarcomere length (SL) was measured by laser diffraction. SL was increased from 1.95 to 2.15 μm at velocities ranging from 3 to 15 μm/s using either muscle length control or SL control by a servo motor. With both methods, force showed viscoelastic characteristics after correction for the contribution of the parallel elastic force. Under muscle length control, the viscoelastic force increased exponentially with a time constant of 3-5 ms and was proportional to the sarcomere velocity of stretch (0.2% of maximal twitch force per μm/s). Under SL control, the viscoelastic force rose with a similar time constant, by 0.1-0.2% of maximal twitch force per μm/s. Fixation of the valve with 2.5% gluteraldehyde did not change the force response to sarcomere stretch. We conclude that the valve contributes to part, but not all, of the elasticity in series with the viscous term. We hypothesize that there is an additional series elastic term inside the sarcomere, possibly titin.

Th-Pos277

ATPASE ACTIVITY AND ISOMETRIC FORCE GENERATED BY SINGLE SKELETAL MYOFIBERS IN HYPERTROPHIC CARDIOMYOPATHY ASSOCIATED WITH ß-MYOSIN HEAVY CHAIN GENE MUTATIONS. ((S. Chaen, R. Horowits, R.J. Podolsky, N.D. Epstein, and L. Fananapazir)) NIH Bethesda MD 20892

In about 30% of kindreds with hypertrophic cardiomyopathy (HCM), the disease is caused by missense mutations in the ß-myosin heavy chain (ß-MHC) gene. Although considered a primary cardiac disease, it has been shown that mutant ß-MHC message and protein are expressed in slow skeletal muscle of HCM patients, and that mutant ß-myosin purified from skeletal muscle translocates actin with reduced velocity. In this study, we simultaneously recorded ATPase activity (NADH fluorescence method) and isometric force of single chemically skinned myofibers obtained from soleus muscle. Slow muscle fibers were identified by SDS-PAGE gel analysis of MHC isoforms. Two missense ß-MHC mutations were studied: a 741 (Gly to Arg) and a 908 (Leu to Val). T=23°C.

	Normal (mean ± SD)	741 (mean ± SD)	908 (mean ± SD)
ATPase(sec^{-1}-$head^{-1}$)	0.31 ± 0.09 (n=20)	0.41 ± 0.16 (n=9)	0.34 ± 0.20 (n=16)
Force (Kg/cm^2)	1.10± 0.41 (n=20)	1.00± 0.90 (n=9)	0.70 ± 0.41 (n=16)

The myosin content measured by densitometric scanning of the MHC band on SDS-PAGE gels was used to calculate both values, assuming that myosin comprised 5.3 % of the fiber volume by weight. No statistical differences (P<0.05) in the ATPase activity between normal and mutant were found. However, isometric force of the 908 mutant was decreased by ~30% (P<0.05). The present results suggest that these two distinct ß-MHC mutations do not influence the rate limiting processes that dominate the ATPase activity during isometric contraction.

Th-Pos278

BIOCHEMICAL AND MECHANICAL EFFECTS OF N-PHENYLMALEIMIDE LABELING OF MYOSIN IN GLYCERINATED RABBIT PSOAS FIBERS
((Vincent A. Barnett†, Cheryl A. Miller† & Mark Schoenberg‡)) †Dept. of Physiology, University of Minnesota Medical School, Minneapolis, MN 55455 and ‡Laboratory of Physical Biology, NIAMS, NIH Bethesda, MD 20892.

We have previously shown that treatment of relaxed chemically skinned rabbit psoas muscle fibers with N-phenylmaleimide (NPM) stabilized an ATP-independent conformation of myosin analogous to the weakly-binding rapid-equilibrium M•ATP crossbridge found in untreated relaxed muscle fibers (Barnett et al., 1991). This was demonstrated by the nearly identical profiles of the stiffness vs duration of stretch for the treated fibers in rigor when compared with untreated relaxed fibers. In the current study we examine the underlying biochemical effects that correlate with this NPM-induced change in stiffness. We measured the K\EDTA- and Ca^{++}\$K^+$-ATPase of glycerinated rabbit psoas fibers that were treated with NPM using the same conditions as the stiffness measurements. The timecourse for the decline in K^+\EDTA-ATPase and the fall of rigor stiffness after NPM treatment are similar. There is a small initial rise in the Ca^{++}\$K^+$-ATPase activity profile followed by an decline to zero. The results are consistent with the labeling of SH_1 and SH_2 by NPM in relaxed muscle being responsible for the production of ATP-insensitive weakly binding myosin crossbridges.

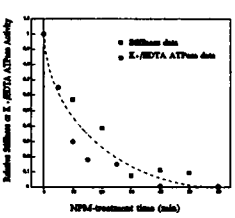

Th-Pos279

CAN MYOSIN HEADS WEAKLY-BOUND TO ACTIN EXERT A DRAG ON FILAMENT VELOCITY? YES AND NO. ((E. Pate, M. Bhimani, G. Wilson, and R. Cooke)) Dept. Math., WSU, Dept. of Biochem. and CVRI, UCSF, and Dept. Anatomy, Univ. Sydney.

We have investigated the effects of vanadate (Vi) on maximum shortening velocity (Vm) in chemically-skinned rabbit psoas fibers as a function of temperature (T). Attached cross-bridges bound to Vi are thought to be an analog of the weakly-bound A•M•D•Pi state. Using new temperature-jump experimental protocols which allow reproducible data to be obtained from fibers activated at high temperature, we have reexamined the effect of increased [Vi] on Vm for T≤30°C. We find that for T≤20°C, increasing [Vi] inhibits Vm; for T≥25°C, increasing [Vi] does not inhibit Vm. Thus our results reconcile the reported differences on the effects of Vi on Vm in the studies of Wilson et al, 1990 (no effect, 25°C) and Chase et al, 1993 (inhibition, 10-13°C). The data suggest that the weakly-bound state can inhibit Vm at low temperature, but not at high temperature. We have also investigated the effects of pH on Vm at 30°C. Previous reports by ourselves and others (T≤15°C) indicate that decreasing pH decreases Vm. At 30°C, however, we find that decreasing pH does not inhibit Vm. Thus pH may be functioning in a manner similar to Vi, populating a weakly-bound state. Additionally, the data at more physiological temperature indicate that previous assertions from studies with glycerinated fibers implicating decreasing pH in the inhibition of Vm during muscle fatigue would appear inapplicable at in vivo temperatures. Supported by NIH grants HL32145 (RC) and AR39643 (EP), a grant from the Muscular Dystrophy Association (RC). EP is an American Heart Association Established Investigator.

SMOOTH MUSCLE PHYSIOLOGY II

Th-Pos280

CHARACTERIZATION OF SMOOTH MUSCLE MYOSIN LIGHT CHAIN (LC) PHOSPHORYLATION, & INTRACELLULAR Ca^{2+} ($[Ca^{2+}]_i$), IN ISOTONIC & ISOMETRIC CONTRACTION. ((He Jiang)) Dept of Physiol, Univ of Manitoba, Winnipeg, MB R3E 0W3 CANADA

We investigated the temporal relationships of $[Ca^{2+}]_i$, LC phosphorylation, isometric force development and isotonic shortening stimulated with electrical (EFS), K^+, and acetylcholine (Ach). Phosphorylation of LC increased rapidly upon EFS (isometric) and peaked at about 4.5 ± 0.7 s. The isotonic LC level showed smaller peak values; a spontaneous elevation in the relaxation phase was seen. The level of $[Ca^{2+}]_i$ (fura-2) and mechanical properties were monitored simultaneously. The intervals between increase in $[Ca^{2+}]_i$ and onset of contraction were 0.8 ± 0.17 for EFS, 2.6 ± 0.54 for K^+, and 1.75 ± 0.3 s for Ach, respectively. The time for the onset of isotonic shortening after increase in $[Ca^{2+}]_i$ was 1.57 ± 0.3 s greater than that for isometric. The levels of $[Ca^{2+}]_i$ peaked by 3.1 ± 0.6 for EFS, 17.46 ± 3.7 for K^+, and 6.49 ± 1.9 s for Ach, respectively. In most cases, force returned to basal level prior to $[Ca^{2+}]_i$, which showed either a sustained submaximal level or a biphasic transient in the late phase of contraction. Isotonic $[Ca^{2+}]_i$ was also less than isometric and a spontaneous increase late in relaxation was noticed in the former. We conclude that LC phosphorylation is very sensitive to small increase in $[Ca^{2+}]_i$ early in both types of contractions. The time between $[Ca^{2+}]_i$ increase and onset of contraction is much faster when Ca^{2+} is released from intracellular source compared to that from extracellular. Furthermore, isotonic shortening is associated with reduced activation of smooth muscle while late in isotonic relaxation spontaneous reactivation develops. (Supported by a grant and a fellowship (H.J.) from Med Res Council, Canada)

Th-Pos281

COMPUTER STOCHASTIC SIMULATION OF SMOOTH MUSCLE CONTRACTION. ((Jizhong Wang* and Newman L. Stephens)) Dept. of Physiol., Univ. of Manitoba, Winnipeg, Canada R3E 0W3

Many investigators have shown that the mechanical properties of various smooth muscles are quite similar to those of striated muscle, which indicates smooth muscle most likely has the same or comparable force generation mechanisms as striated muscle. Little doubt now remains about the applicability of the sliding filament/crossbridge theory to smooth muscle contraction the ambiguity of the cyto-skeletal structure of the smooth muscle cell notwithstanding. In this study, we added a weakly-binding state, under the rationale that weakly-binding crossbridges would act as internal resistances and contribute to muscle stiffness during muscle contraction, to Hai's (1988) four state model to form a more flexible and complete five state, strain-dependent model. To avoid laborious analytical parameter finding, we used Brokaw's (1976) stochastic procedure and modified it to fit our particular needs. Our model allowed us to simulate most if not all of the mechanical properties of an activated smooth muscle. Thus we found: (1) The recovery time of the force transient to quick release was longer than that for quick stretch. (2) Two fast force transients followed by a slow transient on quick release were observed with some variability due to stochastic fluctuations arising from our model simulations. (3) The force-velocity relation obtained by both isovelocity and isotonic shortening methods exhibited the conventional shape. (4) Muscle stiffness preceded force development by 10-30 ms by taking into account the weakly binding state, which offered another possible explanation for the force lag. (5) Finally, myosin light chain phosphorylation increased as did Ca^{+2} concentration in the early phase of contraction; these gradually dropped to a lower level in the later phase, during which force increased and was then maintained at a plateau value. (Supported by the Manitoba Heart and Stroke Foundation, Canada; J.Wang is the recipient of a studentship from the Medical Research Council of Canada).

Th-Pos282

KINETICS OF CONTRACTIONS ELICITED BY PHOTOCHEMICAL INACTIVATION OF THE CALCIUM ENTRY BLOCKER NIFEDIPINE IN DEPOLARISED SMOOTH MUSCLE ((U. Malmqvist and A. Arner)) Dept Physiology and Biophysics, Lund University, Lund Sweden. (Spon. by H. Westerblad)

The kinetics of contractile protein activation and force development was investigated in guinea-pig taena coli smooth muscle using photochemical inactivation of the calcium entry blocker Nifedipine. This compound looses its channel blocking activity after illumination and has previously been used to study the excitation contraction coupling in cardiac muscle by Morad et al. 1983 (Nature 304: 635). Contractions were elicited with 60 or 120 mM K^+ in the presence of Ca^{2+}. Addition of Nifedipine (10^{-9} M) inhibited force to about 20% in the depolarising K^+ solution in the presence of calcium. Illumination with an ultraviolet light flash induced a rapid contraction to almost 100% of the force during the K^+ induced contractions. The force development started after a delay of 300 ms. The delay was independent of extracellular $CaCl_2$. The rate of force development was 0.139 s^{-1} at 60 mM K^+ and 2.5 mM extra cellular $CaCl_2$. At 0.4 mM $CaCl_2$, force was decreased to about 40% and the rate to 0.095 s^{-1}. At 120 mM K^+ and 2.5 mM $CaCl_2$ the rate and force amplitude were similar to those obtained at 0.8 mM $CaCl_2$ at 60 mM K^+. The calcium and K^+ dependence of the rate of contractions reflects modulation of the rate of calcium influx or of the level of intracellular calcium reached after the light flash.

Th-Pos283

MECHANISM OF AGONIST-INDUCED CALPONIN REDISTRIBUTION IN VASCULAR SMOOTH MUSCLE CELLS.
((C.A. Parker+, K. Takahashi**, T. Tao*, and K.G. Morgan+)) +Harvard Medical School, Beth Israel Hospital, Boston, MA 02215; *Boston Biomedical Research Institute, Boston, MA 02214; **Center For Adult Diseases, Osaka, Osaka 537 Japan. (Spon. by D.R. Rigney)

We have reported that agonist stimulation of smooth muscle cells causes redistribution of the thin filament associated protein calponin (CaN). CaN appears homogeneously distributed in resting cells, but in stimulated cells there is a loss of immunoreactive calponin in the core of the cell giving a "donut-like" appearance on cross-section. We have now investigated the mechanism of this redistribution by determining the kinetics and the effect of PKC antagonism. In the presence of 1 μM calphostin, a relatively selective protein kinase C (PKC) inhibitor, the redistribution was inhibited by 44%. The half-time for redistribution of CaN was 3.4 minutes. This is shorter than the half-time for the PKC-associated contraction, 6.4 minutes. The time course of CaN redistribution overlaps with that of PKC translocation. Studies were attempted to identify the structural basis of the donut-like appearance of CaN immunofluorescence in the stimulated cells. CaN distribution was compared to that of actin, myosin and desmin in resting and stimulated cells. Agonist stimulation caused no detectable redistribution of any of these filaments. CaN was distributed similarly to actin and myosin at rest, but differently from that of all three populations of filaments after stimulation. These results suggest a model whereby CaN regulates vascular tone via a PKC-dependent pathway. (Support: NIH HL-42293 and AR-41637)